CHIRALITY 20:63–68 (2008)

Chiral HPLC Analysis of Milnacipran and Its FMOC-Derivative on Cellulose-Based Stationary Phases

ANGELA PATTI,* SONIA PEDOTTI, AND CLAUDIA SANFILIPPO
Istituto di Chimica Biomolecolare del CNR, Via del Santuario 110, I-95028 Valverde CT, Italy

ABSTRACT The HPLC enantioseparation of the last generation antidepressive drug milnacipran (±)-**1** was investigated on different cellulose-based chiral stationary phases (CSPs). On carbamate-type columns, Chiralcel OD and OD-H (±)-**1** could be separated with α value about 1.20 but the resolution was quite low because of the tailing of the peaks. Direct determination of (±)-**1** with high selectivity and resolution was obtained on Chiralcel OJ in normal phase mode elution. Precolumn derivatization of milnacipran with Fmoc-Cl gave compound (±)-**2** which was enantioseparated on all the investigated CSPs and allowed enhanced UV or fluorimetric detection. The Chiralpak IB, that could be considered the immobilized version of Chiralcel OD-H, was found completely ineffective in the chiral recognition of (±)-**1** and moderately efficient in the separation of (±)-**2**. *Chirality 20:63–68, 2008.*

KEY WORDS: milnacipran; chiral drug; enantioselective HPLC; cellulose-based chiral stationary phase; Fmoc-derivative

INTRODUCTION

Milnacipran [(±)-*Z*-diethylaminocarbonyl-2-aminomethyl-1-phenylcyclopropane, (±)-**1**] is an antidepressive drug, belonging to the class of selective serotonin reuptake inhibitors, developed and marketed as the racemic hydrochloride salt by Pierre Fabre Medicament (Ixel®, Dalcipran®). It shows an equipotent inhibitory action on serotonin and noradrenaline neuronal reuptake systems[1] and a total lack of affinity for neurotransmitter receptors, thus giving a similar efficacy to the triciclic antidepressant in the treatment of clinical depression but with fewer side effects.[2] The therapeutical potential of (±)-**1** could be related to its activity as *N*-methyl-D-aspartate receptor antagonist,[3] and recently it has also been found effective in relieving the chronic pain associated with fibromyalgia.[4]

Although some synthetic methodologies for the preparation of enantiomerically enriched **1** have been reported,[5–8] pharmacokinetic and bioavailability studies of milnacipran have been mainly carried out on the racemic form.[9] The importance of pharmacokinetic studies on the separate enantiomers of a chiral drug, also in cases where a given drug is marketed as racemate, is well documented[10,11] and there is a continuous demand for the development of suitable enantioselective analytical and/or preparative methods.[12,13]

The achiral determination of milnacipran in plasma has been previously carried out by reversed-phase HPLC analyses on C_{18} columns using UV or fluorimetric detection[14–16] or by micellar electrokinetic capillary chromatography.[17] In some articles dealing with the asymmetric synthesis of milnacipran, the optical purity of the target product has been indirectly determined from chiral HPLC analysis of its lactone precursor.[6,8] To date, the only reported enantioselective separation of (±)-**1** has been obtained by capillary electrophoresis[18] and we decided to develop a chiral HPLC method as a useful alternative.

The present article deals with the investigation of the direct enantioseparation of (±)-**1** as well as its Fmoc-derivative, (±)-**2** (Figure 1), on different cellulose-based chiral stationary phases (CSPs). Beyond the analysis of biological samples from patients (or animals) administered with the drug, this study can be useful in all the cases where it is necessary to check the optical purity of milnacipran (e.g., asymmetric synthesis, analysis of enriched formulation of the drug) or for semipreparative purpose.

EXPERIMENTAL PROCEDURES

Chromatographic Conditions and Procedures

Chromatography was performed on a Dionex Summit HPLC equipped with a P680A LPG/4 pump, a UVD 170U UV/Vis 4-channel detector, a TCC-thermostatted column compartment, and ASI-100 autosampler. Typical injection volume was 20 μl. The analyses were carried out at constant temperature of 25°C with simultaneous detection at λ = 220, 235, 250, and 266 nm and the chromatographic

Contract grant sponsor: POR Sicilia 2000–2006, misura 3.15 (Tecnologie sensoristiche e sistemi automatici intelligenti per l'innalzamento competitivo delle attività produttive)
*Correspondence to: Angela Patti, Istituto di Chimica Biomolecolare del CNR, Via del Santuario 110, I-95028 Valverde CT, Italy.
E-mail: angela.patti@icb.cnr.it
Received for publication 13 June 2007; Accepted 5 October 2007
DOI: 10.1002/chir.20496
Published online 13 November 2007 in Wiley InterScience (www.interscience.wiley.com).

data were collected on a computer running Chromeleon CHM-1 version 6.7 software. The Chiralcel OJ and Chiralcel OD (both 250 × 4.6 mm I.D., 10 μm) columns and Chiralcel OD-H and Chiralpak IB (both 250 × 4.4 mm I.D., 5 μm) columns were purchased from Daicel Chemical Industries (Tokyo, Japan).

The dead time (t_0) was obtained from the elution time of the unretained 1,3,5-tri-*iso*-propylbenzene and the retention factor was determined as $k_i = (t_{Ri} - t_0)/t_0$. The resolution was calculated from the USP formula $R_s = 2(t_{R2} - t_{R1})/(w_2 + w_1)$ where t_{Ri} and w_i are the retention time and the baseline width of each enantiomer. A conditioning time of 90 min at least, applied whenever the eluent composition or the temperature were changed, was found essential to obtain data reproducibility. Retention times were mean values of three replicate determinations.

On Chiralcel OJ, eluting with *n*-hexane:EtOH 90:10 at flow rate 1.0 ml/min, the linearity of the response was assessed in the range 1.5 μg/ml−1.0 mg/ml concentration of each enantiomer using nine different concentrations and three replicates for each point. The limit of detection (LOD) and quantification (LOQ) were determined by calibration curve method.[19] Solutions containing each enantiomer in the range 0.5–1.0 μg/ml were analyzed in triplicate and the average areas plotted against concentration. The slope S of the obtained curve and the calculated residual variance σ due to the regression were then applied in the equations: $LOD = 3.3 \times \sigma/S$ and $LOQ = 10 \times \sigma/S$.

Precision of the method was determined as injection repeatability at three assay concentrations (30,125, and 500 μg/ml of each enantiomer).

For the percentage recovery determination, samples of human plasma were spiked with known amounts of (±)-**1** hydrochloride on three concentration levels and extracted according to a procedure specifically described for milnacipran.[16]

Sample Preparation

In a mortar, tablets of the pharmaceutical product were pulverized and the powder suspended in 2 N NaOH aqueous solution and stirred for 30 min. The suspension was then extracted with AcOEt and the organic phase dried on Na_2SO_4. After filtration, the solution was taken to dryness to give (±)-**1** as pale yellow oil, with analytical purity 95%. Purity >98% was achieved after column chromatography on silica gel (AcOEt:MeOH 1:1). Standard solutions, prepared by dissolving 3–5 mg of analyte in 10 ml of chromatographic eluent, were filtered through a 0.45 μm membrane filter before the injection.

The extraction of (±)-**1** hydrocloride, required to spike human plasma samples in the recovery experiments, was carried out by suspending the pulverized tablets of the pharmaceutical product in MeOH, stirring the suspension for 30 min, and removing the solid by filtration. The solution was then taken to dryness affording (±)-**1** hydrocloride as white solid with >95% purity.

For the derivatization with 9-fluorenyl-methoxycarbonyl chloride (Fmoc-Cl), a sample of (±)-**1** (1.0 mg, 4 μmol) was dissolved in 200 μl of a 2:1 v/v mixture dioxane: saturated $NaHCO_3$ aqueous solution and the reagent (1.2 mg, 4.4 μmol) was added. The immediate formation of a white precipitate was observed and after 5 min the mixture was diluted with saturated NH_4Cl and extracted with AcOEt (3 × 1.0 ml). The organic phase was collected and dried over Na_2SO_4. The solvent was then removed under a stream of nitrogen and the residue dissolved in the HPLC eluent.

In a separate batch, (±)-**2** was purified on silica gel column (*n*-hexane:AcOEt 7:3) and its identity confirmed by ^{1}H-NMR (400.13 MHz, $CDCl_3$): δ 0.85 (3H, t, J = 7.2 Hz), 1.14 (4H, bt), 1.54 (1H, m), 1.59 (1H, m), 2.84 (1H, ddd, J = 3.2, 8.9 and 14.2 Hz), 3.33 (2H, m), 3.49 (2H, m), 3.86 (1H, ddd, J = 4.5, 8.7 and 14.2 Hz), 4.24 (1H, m), 4.36 (2H, m), 6.21 (1H, bd), 7.22–7.40 (9H, m), 7.63 (2H, m), 7.76 (2H, d, J = 8.0 Hz).^{13}C-NMR (100.03 MHz, $CDCl_3$): δ 12.42 (CH_3), 12.97 (CH_3), 17.55 (CH_2), 28.85 (CH), 33.99 (C), 39.36 (CH_2), 41.80 (CH_2), 42.98 (CH_2), 47.29 (CH), 66.68 (CH_2), 119.83 (CH), 125.18 (CH), 125.65 (CH), 126.59 (CH), 126.96 (CH), 127.52 (CH), 128.73 (CH), 140.45 (C), 141.24 (C), 144.08 (C), 156.54 (CO), 170.38 (CO).

RESULTS AND DISCUSSION

Direct Enantioseparation of (±)-1

Milnacipran (±)-**1** was extracted as free base from the commercial drug formulation, and its identity and purity were checked by ^{1}H- and ^{13}C-NMR analyses. Among the commercially available cellulose-based CSPs, the tris-(3,5-dimethylphenylcarbamate)cellulose derivative (Chiralcel OD) and the tris-(4-methylbenzoate)cellulose-derivative (Chiralcel OJ), both coated with silica gel, are the leader chiral selectors allowing the resolution of a large variety of racemic samples. The recently marketed Chiralpak IB, where the same polymer of Chiralcel OD is chemically bonded to a silica support, has also been included in this study to compare the performances of these two CSPs and gain information on the recognition mechanism. Furthermore, due to the polysaccharide immobilization, on Chiralpak IB it is possible to use a broader range of solvents as mobile phases thereby introducing additional parameters for the optimization of the enantioseparation.[20]

On Chiralcel OD column, the elution with *n*-hexane:2-PrOH mixtures gave a partial separation of milnacipran enantiomers with concomitant low resolution due to the tailing of the peaks, which was found unaffected by the increase in the flow rate and variation of temperature. Changing the alcohol modifier in the mobile phase with EtOH was detrimental for the separation since (±)-**1** was eluted as a very broad single peak. (Table 1, entries 1–2).

Comparable unsatisfactory results were also achieved on Chiralcel OD-H column with *n*-hexane:2-PrOH mixture, despite of the smaller (5 μm) particle size with respect to Chiralcel OD (entry 3). The use of diethylamine (DEA) up to 0.2% as additive in the eluent to suppress the strong interaction of the analyte with the CSP did not improve the separation and resolution (entries 4–5). Furthermore, higher concentration of a basic additive in the eluent was not allowed due to the sensible increase in the background level which led to severe limitation in the detection of the analyte, which has low UV absorption at λ > 220 nm.

TABLE 1. Chromatographic parameters for the separation of (±)-1 on cellulose-based CSPs[a]

Entry	Column	Eluent	Flow	k_1	α	R_s
1	Chiralcel OD	*n*-hexane:2-PrOH 90:10	0.7	3.91	1.20	0.63
2		*n*-hexane:EtOH 90:10	0.7	2.29	1.00	–
3	Chiralcel OD-H	*n*-hexane:2-PrOH 90:10	0.7	3.85	1.23	0.97
4		*n*-hexane:2-PrOH 90:10 (+0.1% DEA)	0.7	3.94	1.21	0.83
5		*n*-hexane:2-PrOH 90:10 (+0.2% DEA)	0.7	4.05	1.22	0.84
6		*n*-hexane:EtOH 98:2	1.0	15.09	1.26	0.98
7		*n*-hexane:EtOH 98:2	1.5	12.54	1.24	1.32
8	Chiralcel OJ	*n*-hexane:2-PrOH 90:10	1.0	1.42	3.43	5.97
9		*n*-hexane:EtOH 90:10	1.0	1.12	2.65	6.39
10		*n*-hexane:2-PrOH 95:5	1.0	3.55	3.76	7.11
11		*n*-hexane:EtOH 95:5	1.0	2.53	3.03	7.51

[a]All the analyses were carried out at 25°C and the UV detection set at 220 nm.

However, on the Chiralcel OD-H column using EtOH as alcohol modifier a separation of (±)-**1** was obtained and more symmetrical peaks were observed. The separation profile was found sensitive to changes in the flow rate and good performances were obtained with *n*-hexane:EtOH 98:2 at 1.5 ml/min flow rate (Table 1, entries 6–7).

On the immobilized carbamate-type CSP Chiralpak IB (±)-**1** was highly retained, so that a 20% at least alcohol concentration in the mobile phase was required, without selectivity; a single broad peak was observed in all the tested conditions using *n*-hexane/alcohol (2-PrOH or EtOH) eluents. Since in both Chiralcel OD, Chiralcel OD-H, and Chiralpak IB the cellulose is derivatized with the same carbamate group, the hydrogen-bond interactions between the selectand and the selector, that are considered the main factor in determining the analyte enantiodifferentiation,[21] should be the same and give a comparable selectivity. However, it is evident that other factors, not easily understood due to the unknown exact chemical structure of the immobilized selector, are responsible for the observed differences in selectivity.

Nonconventional solvent mixtures of 20% EtOH with *tert*-butyl methyl ether or chloroform as well as the recently developed polar-mode elution[22] were also unsuccessful in the enantioseparation of (±)-**1** on Chiralpak IB. Furthermore, some eluent mixtures developed high back pressure in the column giving some limitation in the allowable flow rate.

Large values of selectivity and resolution were found on the benzoate-type CSP Chiralcel OJ and the separation profiles were influenced by the nature of the alcohol in the mobile phase; higher selectivities were obtained using 2-PrOH whereas better resolution values were measured with EtOH, which is more efficient in suppressing the peak tailing (Table 1, compare entries 8–9 and 10–11). The absolute configuration (1*R*, 2*S*) of the first eluting enantiomer (−)-**1** was determined by collecting single enantiomers and measuring their optical activity.[5]

The enantioseparation of (±)-**1** on Chiralcel OJ was found linear in the range 1.5 μg/ml − 1 mg/ml concentration of each enantiomer, the calibration curves showing excellent linearity for both (+)-**1** and (–)-**1** with correlation coefficient (R^2) >0.999. LOD = 0.21 and 0.23 μg/ml and LOQ = 0.64 and 0.70 μg/ml were determined for (−)-**1** and (+)-**1** respectively. Since the analyses were carried out with a 20 μl injection volume, the found LOQs correspond to 13 ng for (−)-**1** and 14 ng for (+)-**1** as absolute amount. Precision (% RSD) of injection repeatability was 0.31 for (–)-**1** and 0.41 for (+)-**1**.

The averaged extraction recovery from human plasma was found 75% for both enantiomers of milnacipran, confirming the data obtained in the achiral quantification of this drug.[16]

Representative chromatograms of the different retention behavior of (±)-**1** on the four CSPs here investigated are shown in Figure 2.

Enantioseparation of (±)-2

Because of the high values of α and R_s observed on Chiralcel OJ an easy scale up of the direct separation of

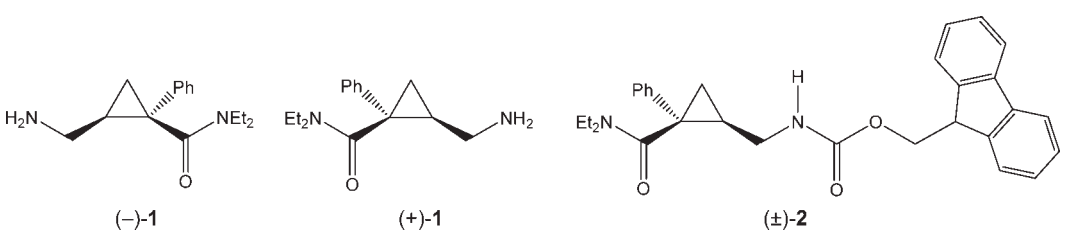

Fig. 1. Chemical structures of milnacipran enantiomers and the Fmoc-derivative.

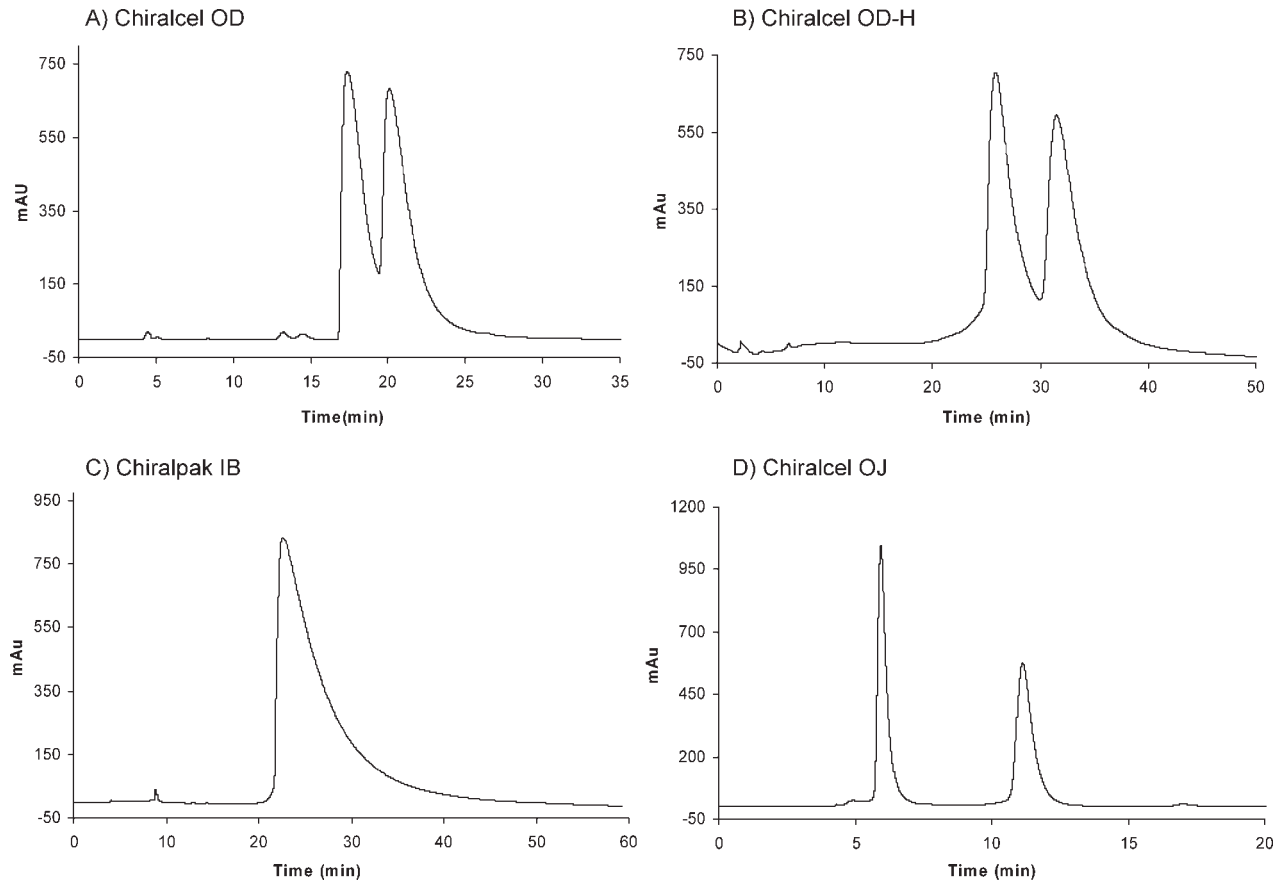

Fig. 2. HPLC chromatograms of the analysis of **(±)-1** on different columns. (**A**) *n*-hexane:2-PrOH 90:10, flow rate 0.7 ml/min; (**B**) *n*-hexane:EtOH 98:2, flow rate 1.5 ml/min; (**C**) *n*-hexane:EtOH 80:20, flow rate 0.7 ml/min; (**D**) *n*-hexane:EtOH 90:10, flow rate 1.0 ml/min.

(±)-**1** on a semipreparative column seems reasonable; on the contrary quantitative detection of the milnacipran enantiomers in biological samples, as required in the pharmacokinetic studies, could be limited by the UV absorption features of the analyte.

The precolumn derivatization of primary amines to give a fluorescent compound is a well established protocol in liquid chromatography to enhance the detection limit. Derivatization of (±)-**1** also appeared as a useful means for improving the determination of this drug on the carbamate-type CSP here investigated, whose low-selective interaction with the analyte could be due to the free aminic group present in (±)-**1**. So, although we did not have a fluorimetric detector, the enantioseparation of the Fmoc derivative of milnacipran, the compound (±)-**2**, was evaluated using UV-detection.

Our choice was based on the good stability of (±)-**2** in organic solvent and the hypothesis that the conversion of an aminic group into a carbamate one, structurally able to form complementary hydrogen-bonds with the carbamate-derivatized cellulose, should give a more enantiodifferentiated analyte on this CSP.

Indeed, a baseline separation of the enantiomers of (±)-**2** was obtained on all the tested columns with *n*-hexane:EtOH mixtures in the optimized conditions reported in Table 2 and a remarkable increase in selectivity and resolution was observed on Chiralcel OD changing the alcohol modifier with 2-PrOH. However, also in this case the immobilized carbamate-type Chiralpak IB was found to be sensibly less efficient with respect to the coated analogue Chiralcel OD (see Fig. 3).

Compound (±)-**2** was quantitatively formed in 5 min reaction and the excess of reagent as well as the side product Fmoc-OH did not interfere in the determination of milnacipran.

To date, there is only one report describing the enantiomer resolution of some Fmoc-α-aminoacids derivatives on Chiralcel columns.[23]

TABLE 2. Chromatographic parameters for the separation of (±)-2 on cellulose-based CSPs

Column	Eluent	k_1	α	R_s
Chiralcel OD	*n*-hexane:2-PrOH 80:20[a]	12.95	1.51	4.52
	n-hexane:EtOH 80:20[a]	4.50	1.13	1.59
Chiralpak IB	*n*-hexane:EtOH 80:20[b]	3.23	1.07	1.30
Chiralcel OJ	*n*-hexane:EtOH 90:10[b]	3.87	1.57	3.11

[a]Flow rate 0.7 ml/min.
[b]Flow rate 1.0 ml/min.

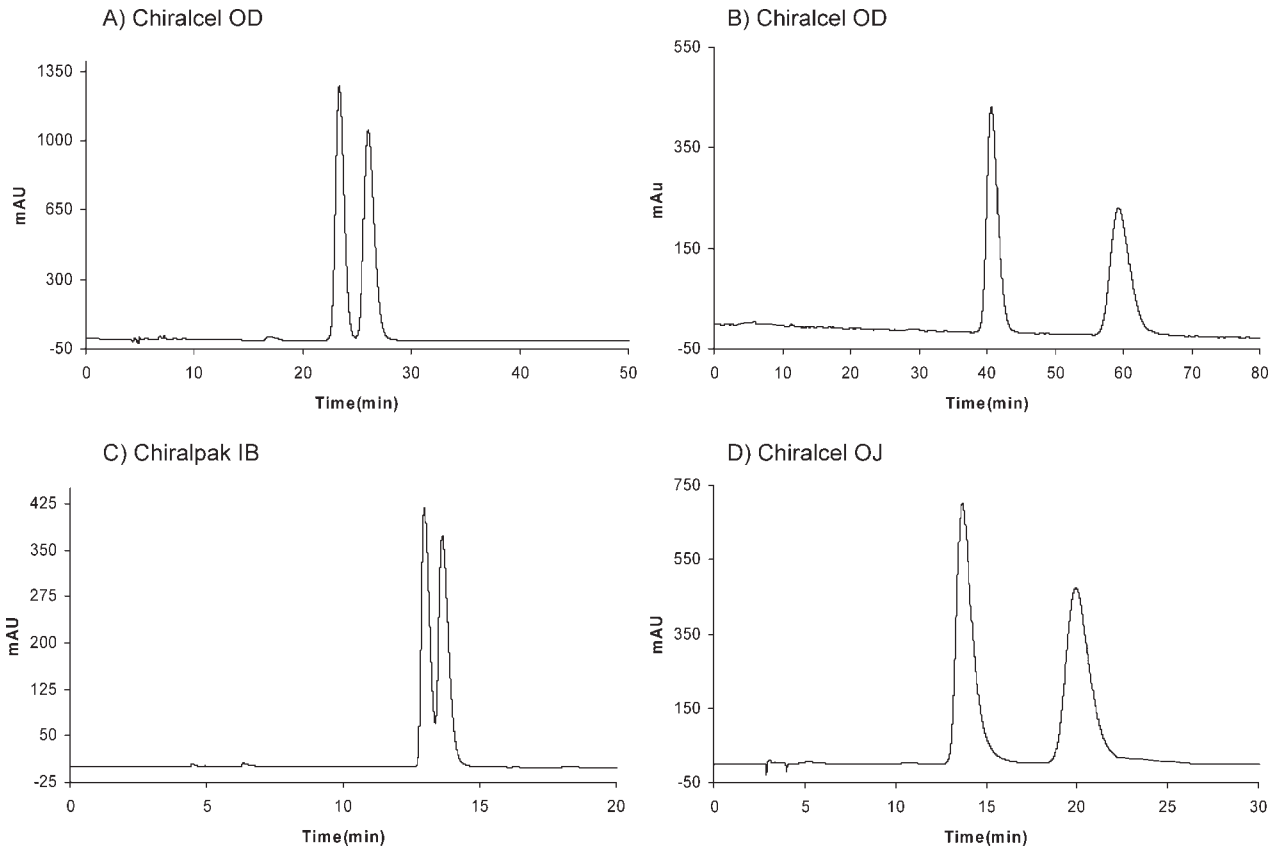

Fig. 3. HPLC chromatograms of the enantioseparation of (±)-**2** on different columns. **(A)** *n*-hexane:EtOH 80:20, flow rate 0.7 ml/min; **(B)** *n*-hexane:2-PrOH 80:20, flow rate 0.7 ml/min; **(C)** *n*-hexane:EtOH 80:20, flow rate 0.7 ml/min; **(D)** *n*-hexane:EtOH 90:10, flow rate 1.0 ml/min.

Although maximum sensitivity in the determination of (±)-**2** could be obtained via fluorimetric detection, from the comparison of the UV spectra of (±)-**1** and (±)-**2** reported in Figure 4, it seems evident that the analysis of milnacipran as Fmoc-derivative can be advantageously carried out also by UV-detection at $\lambda = 220$ nm, with about a two-fold increase of the molar extinction coefficient, or $\lambda = 266$ nm where interferences of biological matrix should be minimized.

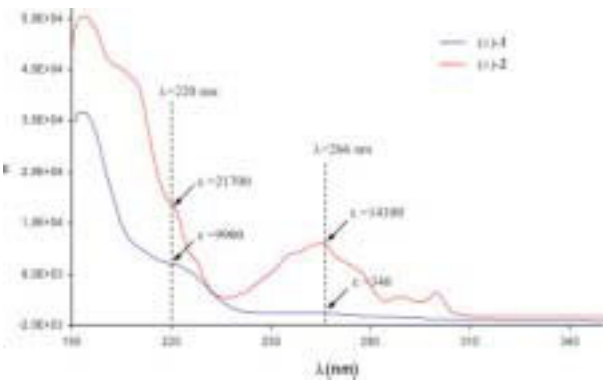

Fig. 4. UV spectra of milnacipran (±)-**1** and its Fmoc-derivative (±)-**2**. [Color figure can be viewed in the online issue, which is available at www.interscience.wiley.com.]

CONCLUSIONS

The first enantioselective HPLC method for the direct determination of the enantiomers of the antidepressive drug milnacipran can be considered developed. On Chiralcel OJ column, eluting with *n*-hexane-alcohol mixtures without any basic additive, high selectivity and resolution were obtained in short analysis time and the method was found simple, linear, and precise.

Precolumn derivatization of (±)-**1** with Fmoc-Cl and subsequent analysis shows advantageous enhanced sensitivity of the assay with UV- or fluorescence detection and allows good enantioseparation also on carbamate-type Chiralcel columns, which were ineffective in the direct determination of (+)- and (−)-**1**. The structural features of the Fmoc group could be generally exploited for the enantioseparation of amines without any additive addition in the mobile phase.

LITERATURE CITED

1. Moret C, Charveron M, Finberg JP, Briley M. Biochemical profile of midalcipran (F 2207), 1-phenyl-1-diethylaminocarbonyl-2-aminomethylcyclopropane (Z) hydrochloride, a potential fourth generation antidepressant drug. Neuropharmacology 1985;24:1211–1219.
2. Briley M. Milnacipran, a well-tolerated specific serotonin and norepinephrine reuptake inhibiting antidepressant. CNS Drug Rev 1998;4:137–148.

3. Shuto S, Takada H, Mochizuki D, Tsujita R, Hase Y, Ono S, Shibuya N, Matsuda A. (±)-(*Z*)-2-(aminomethyl)-1-phenylcyclopropanecarboxamide derivatives as a new prototype of NMDA receptor antagonists. J Med Chem 1995;38:2964–2968.
4. Leo RJ, Brooks V. Clinical potential of milnacipran, a serotonin and norepinephrine reuptake inhibitor, in pain. Curr Opin Invest Drugs 2006;7:637–642.
5. Shuto S, Ono S, Hase Y, Kamiyama N, Matsuda A. Synthesis of (+)- and (−)-milnaciprans and their conformationally restricted analogs. Tetrahedron Lett 1996;37:641–644.
6. Doyle MP, Hu W. A new enantioselective synthesis of milnacipran and an analogue by catalytic asymmetric cyclopropanation. Adv Synth Catal 2001;343:299–302.
7. Zhang M-X, Eaton PE. BuMgN-*iso*-Pr_2: a new base for stoichiometric, position-selective deprotonation of cyclopropanecarboxamides and other weak CH acids. Angew Chem Int Ed Engl 2002;41:2169–2171.
8. Roggen H, Kehler J, Stensbøl TB, Hansen T. Synthesis of enantiomerically pure milnacipran analogs and inhibition of dopamine, serotonin, and norepinephrine transportes. Bioorg Med Chem Lett 2007;17:2834–2837.
9. Puozzo C, Panconi E, Deprez D. Pharmacology and pharmacokinetics of milnacipran. Int Clin Psychopharmacol 2002:17;25S–35S.
10. Baker GB, Prior TI. Stereochemistry and drug efficacy and development: relevance of chirality to antidepressant and antipsychotic drugs. Ann Med 2002;34:537–543.
11. Marzo A, Heftmann E. Enantioselective analytical methods in pharmacokinetics with specific reference to genetic polymorphic metabolism. J Biochem Biophys Methods 2002;54:57–70.
12. Rentsch KM. The importance of stereoselective determination of drugs in the clinical laboratory. J Biochem Biophys Methods 2002; 54:1–9.
13. Andersson S, Allenmark SG. Preparative chiral chromatographic resolution of enantiomers in drug discovery. J Biochem Biophys Methods 2002;54:11–23.
14. Lacassie E, Gaulier J-M, Parquet P, Rabatel J-F, Lachatre G. Methods for the determination of seven selective serotonin reuptake inhibitors and three active metabolites in human serum using high-performance liquid chromatography and gas chromatography. J Chromatogr B 2000;742:229–238.
15. Tournel G, Houdret N, Hédouin V, Deveaux M, Gosset D, Lhermitte M. High-performance liquid chromatographic method to screen and quantitate seven selective serotonin reuptake inhibitors in human serum. J Chromatogr B 2001;761:147–158.
16. Puozzo C, Filaquier C, Zorza G. Determination of milnacipran, a serotonin and noradrenaline reuptake inhibitor, in human plasma using liquid chromatography with spectrofluorimetric detection. J Chromatogr B 2004;806:221–228.
17. Labat L, Deveaux M, Dallet P, Dubost JP. Separation of new antidepressants and their metabolites by micellar electrokinetic capillary chromatography. J Chromatogr B 2002;773:17–23.
18. Grard S, Morin P, Dreux M, Ribet J.-P. Enhancement of second-migrating enantiomer peak symmetry of basic drugs by using dual-cyclodextrin system in capillary electrophoresis. Electrophoresis 2000;21:3028–3034.
19. Q2B Validation of Analytical Procedures, ICH Sectretariat, November 1996 http://www.fda.gov/cder/guidance/1320fnl.pdf
20. Zhang T, Nguyen D, Franco P, Murakami T, Ohnishi A, Kurosawa H. Cellulose 3,5-dimethylphenylcarbamate immobilized on silica. A new chiral stationary phase for the analysis of enantiomers. Anal Chim Acta 2006;557:221–228.
21. Okamoto Y. Yashima E. Polysaccharide derivatives for cromatographic separation of enantiomers. Angew Chem Int Ed Engl 1998;37:1020–1043.
22. Matthijs N, Maftou M, Vander Heyden Y. Screening approach for chiral separation of pharmaceuticals. IV. Polar organic solvent chromatography. J Chromatogr A 2006;1111:48–61.
23. Jin JY, Lee W, Park JH, Ryoo JJ. Covalently bonded and coated chiral stationary phases derived from polysaccharide derivatives for enantiomer separation of *N*-fluorenylmethoxycarbonyl α-amino acids with fluorescence detection. J Liq Chromtogr Rel Technol 2006;29:1793–1801.

CHIRALITY 20:69–74 (2008)

The Resolution of Five Racemic α-Lactams by HPLC

HUI YU†, KYU HUR†, ISTVÁN LENGYEL, AND VICTOR CESARE*
Department of Chemistry, St. John's University, Jamaica, New York

ABSTRACT The resolution of five racemic α-lactams (**1a-d,g**) using HPLC is reported. Five different Pirkle-type stationary phases were tested. The enantiomers of α-lactams containing the trityl group (**1a-d**) were separated (selectivity factors ranging from 1.08 to 1.20) using a mobile phase of hexane/2-propanol:98/2 and a stationary phase consisting of the 3,5-dinitroaniline derivative of (*S*)-valine with a urea linkage. Among the dialkyl-substituted α-lactams (**1e-g**), only 1,3-di-*tert*-butylaziridinone (**1g**) could be resolved, but only partially (selectivity factor = 1.07), with a mobile phase of hexane/1,2-dichloroethane:95/5 and the stationary phase consisting of the 3,5-dinitrobenzoic acid derivative of (*R*)-1-naphthylglycine. *Chirality 20:69–74, 2008.* © 2007 Wiley-Liss, Inc.

KEY WORDS: aziridinone; racemate; chiral; stationary phase; enantiomers

INTRODUCTION

α-Lactams (aziridinones, **1**) are three-membered cyclic amides. The structural requirements for all stable, isolable α-lactams are a tertiary alkyl substituent on the nitrogen atom (e.g. *tert*-butyl, 1-adamantyl, or trityl) and at least one tertiary alkyl group at the C-3 position.[1] They undergo thermal fragmentation to an aldehyde or ketone and an isocyanide and react with nucleophiles via attack at either the C-2 or C-3 position (see Fig. 1). Several excellent reviews of α-lactams describing their synthesis, thermal stability, and synthetic utility have been published.[1–5]

Recently, a better understanding of the ring-opening reactions of α-lactams has begun to emerge[6–9] and their usefulness as synthons[4,10] has been recognized. To further develop the synthetic utility of α-lactams, the stereochemistry of these highly strained rings needs to be explored since most stable α-lactams contain a chiral center at position 3 of the ring. To date, only one chiral non-racemic α-lactam, (*R*)-1,3-di-*tert*-butylaziridinone, has been reported[11] and its optical purity (91%) was determined by gas chromatography (GC). However, the general use of GC to determine the optical purity of other stable α-lactams can be problematic since many of them will thermally rearrange at elevated temperatures. Separation of α-lactam enantiomers by HPLC is an attractive alternative.

This research was undertaken to determine if any of the stable α-lactams could be resolved by HPLC, a necessary step in the further development of α-lactams as useful synthetic compounds. Specifically, the resolution of seven racemic and one non-racemic α-lactam using five different chiral stationary phases under normal phase conditions were attempted.

MATERIALS AND METHODS

The Waters HPLC system used in this study consisted of a Model 515 pump with a Model 2487 UV detector (λ = 254 and 238) or a PDR Advanced Laser Polarimeter detector. The data obtained were analyzed by Waters Millenium software. Chiral columns (4.6 mm × 50 mm) were purchased from Phenomenex (Torrance, CA): Chirex 3005 (Column A), 3010 (Column B), 3014 (Column C), 3020 (Column D), and Chirex 3010 (Column B, 4.6 mm × 250 mm); and Regis Technologies (Morton Grove, IL): Pirkle Chiral HPLC column 731041 (Column E, 4.6 mm × 250 mm). All solvents used in the mobile phases and all chemicals used in the synthesis of α-lactams **1a-g** were purchased from Sigma-Aldrich (Milwaukee, WI) and used without further purification. Flash chromatographic purification of the precursors used to synthesize the α-lactams were performed using silica gel (JT Baker, Phillipsburg, NJ, 40 μm) as the stationary phase.

Synthesis

Racemic α-lactams (1a-g). The seven racemic α-lactams (**1a-g**) were synthesized according to a published procedure[12] and all physical and spectral data were in agreement with previously reported values. The synthesis of non-racemic α-lactam (**(−)-1g**) and its precursors are described below:

Racemic 2-bromo-3,3-dimethylbutanoic acid((−)-3). A solution of 3,3-dimethylbutanoic acid (**2**) (23.23 g, 0.200 mol), $SOCl_2$ (95.18 g, 0.80 mol), and CCl_4 (20 ml) was heated to 65°C for 30 min. After cooling to room temperature (RT), finely powdered *N*-bromosuccinimide (NBS) (42.72 g, 0.240 mol), CCl_4 (20 ml), and seven drops of 48% HBr were added to the reaction mixture and it was heated between 70 and 75°C for 90 min.[13,14] After cooling

*Correspondence to: Victor Cesare, Department of Chemistry, St. John's University, Jamaica, New York. E-mail: cesarev@stjohns.edu
†These two authors are co-first authors.
Received for publication 20 June 2007; Accepted 13 October 2007
DOI: 10.1002/chir.20499
Published online 3 December 2007 in Wiley InterScience (www.interscience.wiley.com).

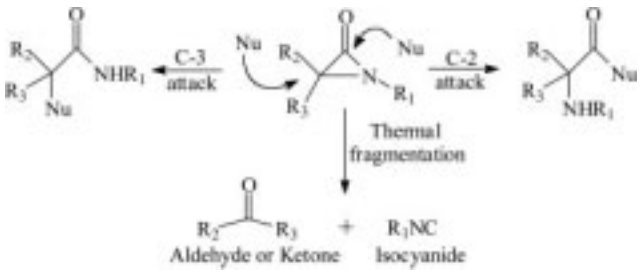

Fig. 1. Nucleophilic (Nu) attack and thermal fragmentation of α-lactams.

to RT, the CCl_4 and excess $SOCl_2$ were removed by reduced pressure, CCl_4 (50 ml) was added and the resulting mixture was filtered. The solid succinimide was washed three times with CCl_4 (15 ml) and all filtrates were combined. The CCl_4 was removed under reduced pressure and the remaining liquid was vacuum distilled to afford 2-bromo-3,3-dimethylbutanoyl chloride (32.82 g, 76.9%, bp = 72°C/19 mm Hg; lit.[15] 93–97°C/37 mm Hg, ^{1}H-NMR ($CDCl_3$): δ = 1.20(s, 9H), 4.40 (s, 1H)). The resulting α-bromoacid chloride (16.59g, 0.0777 mol) was dissolved in tetrahydrofuran (THF) (35 ml) and distilled water (7 ml) was slowly added at RT with stirring. After stirring overnight, the THF was removed under reduced pressure and the remaining aqueous layer was washed twice with ethyl acetate (50 ml). The organic layer was dried with Na_2SO_4 and the ethyl acetate removed under reduced pressure to obtain racemic 2-bromo-3,3-dimethylbutanoic acid[3] (7.37 g, 48.4%, mp = 70–72°C; lit.[15] 72–73°C, IR (KBr): 3200 (O—H), 2972 (C—H), 1716 cm^{-1} (C=O), ^{1}H-NMR ($CDCl_3$): δ = 1.18(s, 9H), 4.13 (s, 1H), 8.86 (bs, 1H)).

(−)-2-Bromo-3,3-dimethylbutanoic acid ((−)-3). Optically pure (−)-2-bromo-3,3-dimethylbutanoic acid **((−)-3)** was obtained following the resolution procedure of Suzuki et al.[16] Thus, racemic 2-bromo-3,3-dimethylbutanoic acid (4.70 g, 0.0241 mol) was added to a solution of 80% ethanol/20% water (4 ml). (*S*)-(−)-phenylethylamine (2.92 g, 0.0241 mol) was added and the mixture was warmed until a solution was obtained. After cooling for 90 min, the precipitate was filtered and recrystallized from a solution of 80% ethanol/20% water to obtain 0.62 g of salt, $[\alpha]_D = -20.4°$, ethyl alcohol. The ratio of the ^{1}H-NMR CHBr (δ = 3.84 and 3.87) signals of the two diastereomeric salts was used to determine the amount of each stereoisomer present. The salt was hydrolyzed by the addition of 1 M HCl at 0°C and after extraction of the aqueous layer by the addition of CH_2Cl_2, drying the organic layer with Na_2SO_4, and removing the CH_2Cl_2 under reduced pressure, optically pure acid **(−)-3** was obtained, 0.37g, $[\alpha]_D = -12.5°$, $CHCl_3$, lit.[16] $[\alpha]_D = -12.3°$, $CHCl_3$).

Non-racemic *N*-trityl-2-bromo-3,3-dimethylbutanamide ((−)-4). Acid **(−)-3** (1.95 g, 0.01 mol), $SOCl_2$ (4.76 g, 0.04 mol), and CCl_4 (5 ml) were heated to 65°C for 30 min and then stirred at RT for 12 h. The solvent and excess $SOCl_2$ were removed under reduced pressure to obtain crude 2-bromo-3,3-dimethylbutanoyl chloride (2.14 g, 100%), which was used without further purification. A solution of crude α-bromo acid chloride (2.13 g, 0.01 mol) in CH_2Cl_2 (20 ml) was dropwise added to a solution of tritylamine (3.63 g, 0.014 mol) and triethylamine (1.45 g, 0.014 mol) in CH_2Cl_2 (20 ml) at 0°C. After the addition was complete, the reaction mixture stirred at RT for 12 h. It was then washed with 2 M HCl (50 ml) and twice with distilled water (80 ml). The organic layer was dried with Na_2SO_4 and the solvent removed under reduced pressure to obtain crude **(−)-4** (4.10 g, 94%). After column chromatography using a mobile phase of hexane/ethyl acetate: 90/10, pure non-racemic **(−)-4** (2.2 g, 45.9%, $[\alpha]_D = +1.8°$ ($CHCl_3$), was obtained. The enantiomeric excess (ee) was determined to be 13.5 using column **E** with a mobile phase of hexane/2-propanol:98/2.

Non-racemic (−)-3-*tert*-butyl-1-tritylaziridinone ((−)-1d). A mixture of CH_2Cl_2 (3 ml), sodium hydride (0.022 g, 0.55 mmol), and 15-crown-5 ether (0.066 g, 0.3 mmol) stirred for 30 min at RT and then non-racemic amide **(−)-4** (0.131 g, 0.3 mmol) was added. After stirring for 2 h, distilled water (10 ml) was slowly added with stirring and the organic layer was separated and washed twice with distilled water (10 ml). The organic layer was dried with Na_2SO_4 and the solvent removed under reduced pressure to obtain crude α-lactam **(−)-1d** (0.18 g, 88.2%). An analytical sample of pure **(−)-1d** was obtained after column chromatography using a mobile phase of hexane/ethyl acetate:90/10 $[\alpha] = -17.2°$ ($CHCl_3$), IR (CCl_4): 1840 cm^{-1} (C=O) ^{1}H-NMR ($CDCl_3$): δ = 0.95 (s, 9H), 2.12 (s, 1H), 7.35 (m, 15H).

HPLC

Approximately 10 mg of α-lactams **1a-g** were dissolved in 10 ml of *n*-hexane/2-propanol:98/2 and 10 μl of these solutions were injected through columns **A-D** (4.6 mm × 50 mm) and columns **B** and **E** (4.6 mm × 250 mm). A dual λ UV absorbance detector was used with the 250 mm columns while a PDR chiral detector was used to monitor the resolution of enantiomers with the 50 mm columns. Mobile phases consisting of hexane/1,2-dichloroethane or hexane/2-propanol (95/5, 98/2, or 100/0) were used at a flow rate of 0.5 ml/min for the 50 mm columns or 1.0 ml/min for the 250 mm columns. Results are shown in Tables 1 and 2, and Figures 5 and 6.

TABLE 1. Resolution of α-lactams 1a-g using column B (4.6 mm × 50 mm)

α-Lactam	α[a]
1a	1.07(+)
1b	1.17(+)
1c	1.0
1d	1.06(+)
1e	1.0
1f	1.0
1g	1.0

[a]Selectivity factor with mobile phase of hexane/2-propanol:98/2 and a flow rate of 0.5 mL/min. The (+) indicates that the (+)-enantiomer eluted first. Both the UV and polarimeter detectors were used.

TABLE 2. Resolution of α-lactams 1a-g using column B (4.6 mm × 250 mm) and UV detection

α-Lactam	RT-1 (min)	RT-2 (min)	α[a]
1a	9.77	10.28	1.08
1b	8.12	9.03	1.20
1c	9.76	10.28	1.08
1d	7.00	7.52	1.15
1e	8.93		1.0
1f	8.60		1.0
1g			#

RT-1, retention time of the first peak; RT-2, retention time of the second peak.
[a]Selectivity factor with mobile phase of hexane/2-propanol:98/2 and a flow rate of 1.0 mL/min; #, not detectable with UV detection.

RESULTS AND DISCUSSION

The HPLC resolution of α-lactams offers unique challenges due to their instability and susceptibility to nucleophilic attack. Therefore, seven relatively stable α-lactams were chosen for this study. Previously, Pirkle-type columns[17,18] have been reported for the resolution of β- and γ-lactams. Therefore, four Pirkle-type stationary phases (columns **A-D**, 4.6 mm × 50 mm) were chosen for the initial part of this study. These four columns (**A-D**) were purchased as an HPLC method development kit and their purpose was to determine the best chromatographic conditions that would eventually lead to baseline resolution using a larger column (the chiral column kit was purchased from Phenomenex®, Torrance, CA). Their structural features are shown in Figure 2. The main reason for selecting this chiral column kit was because it provides the three general types of Pirkle stationary phases: π-electron acceptor/π-electron donor (column **A**), π-electron acceptor (column **B**), and π-electron donor (column **C** and **D**). Besides π-π interactions, factors such as hydrogen bonding and steric crowding have been reported for enantiomeric separation when using Pirkle-type stationary phases and it was reasoned that these same factors could be used to resolve racemic α-lactams. In addition to columns **A-D**, the Whelk-O1 column (Regis Technologies, Morton Grove, IL), which is one of the more widely applicable Pirkle-type stationary phases, was also considered. However, since the stationary phases of the Whelk-O1 and column **A** provided in the chiral kit both possess the π-electron acceptor dinitrophenyl moiety and π-electron donor naphthyl group (see Fig. 2), the decision was made to test the Whelk-O1 column only if column **A** demonstrated superior resolution of α-lactams compared with columns **B-D**. An excellent review discussing the development and general principles of Pirkle stationary phases has been published.[19]

Normal phase conditions were chosen so that relatively non-polar mobile phases could be used. It was concluded that the use of water and or methanol in a reverse phase system should be avoided since it has been reported[1] that these nucleophilic solvents readily react with some α-lactams resulting in ring-opening products.

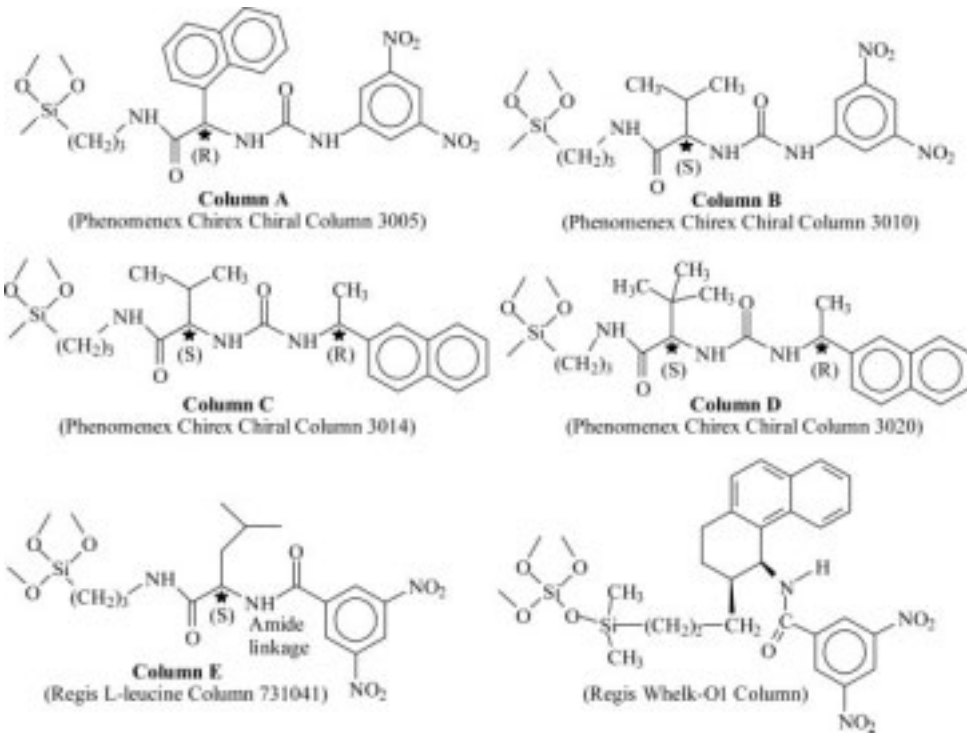

Fig. 2. The stationary phases of chiral columns **A-E** and the Whelk-O1 column.

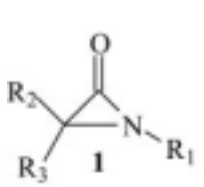

	R_1	R_2	R_3
1a	Ad	H	Tr
1b	Tr	H	Ad
1c	*t*-Bu	H	Tr
1d	Tr	H	*t*-Bu
1e	Ad	H	*t*-Bu
1f	*t*-Bu	H	Ad
1g	*t*-Bu	H	*t*-Bu

Fig. 3. α-Lactams used in this study (Ad, 1-adamantyl; *t*-Bu, *tert*-butyl; Tr, trityl).

Columns **A-D** were evaluated for their resolving power toward seven different racemic α-lactams (see Fig. 3): 1-(1-adamantyl)-3-tritylaziridinone (**1a**),[20] 3-(1-adamantyl)-1-tritylaziridinone (**1b**),[20] 1-*tert*-butyl-3-tritylaziridinone (**1c**),[20] 3-*tert*-butyl-1-tritylaziridinone (**1d**),[14] 1-(1-adamantyl)-3-*tert*-butylaziridinone (**1e**),[21] 1-*tert*-butyl-3-(1-adamantyl)-aziridinone (**1f**),[22] and 1,3-di-*tert*-butylaziridinone (**1g**).[23] In addition, one non-racemic α-lactam, (−)-3-*tert*-butyl-1-tritylaziridinone (**(−)-1d**) was also synthesized and used in this study. These α-lactams (**1a-g**) were chosen for their relative stability and because the three sets of isomers (**1a-b**, **1c-d**, and **1e-f**) might offer some insight into the resolution mechanism.

Since non-racemic α-lactam **(−)-1d** has not been previously reported, the synthetic pathway used to obtain it is shown in Figure 4.

The step used to introduce chirality in the synthesis of **(−)-1d** was the resolution of 2-bromo-3,3-dimethylbutanoic acid[3] via its diastereomeric salt formation with (*S*)-1-phenylethylamine. The progress of this key step was easily monitored by ^{1}H-NMR (see experimental) and optically pure acid **(−)-3** was obtained after hydrolysis of the salt. Using acid **(−)-3**, non-racemic 1-(1-adamantyl)-3-*tert*-butylaziridinone (**(−)-1d**) was then synthesized by the same procedure[12,14] used to synthesize racemic **1d** and the other α-lactams. Since α-bromoacid **(−)-3** was optically pure, yet the enantiomeric excess for amide **(−)-4** was only 13.5, partial racemization must have occurred during the amide synthesis. Attempts to couple acid **(−)-3** with tritylamine under milder conditions at RT, using dicyclohexylcarbodiimide or *N*-ethyl-5-phenylisoxazolium-3′-sulfonate (Woodward's K reagent) as the coupling reagents were not successful. However, the purpose of the synthesis of **(−)-1d** was to determine if an HPLC method could be developed to calculate the enantiomeric excess of a non-racemic α-lactam.

Two mobile phase systems (hexane/2-propanol or hexane/1,2-dichloroethane) at three different concentrations (95/5, 98/2, and 100/0) were tested. These two mobile phase systems were chosen mainly because there would be little chance that they would react with any of the α-lactams. The best results using the 50 mm columns **A-D** were obtained with column **B** and a mobile phase consisting of hexane/2-propanol:98/2. The results using column **B**, which are summarized in Table 1, indicates that only the enantiomers of α-lactams containing the trityl group (**1a,b,d**) could be partially separated and that the (+)-enantiomer eluted first. This would indicate that the π-π interaction between the π-acidic dinitrophenyl group of the stationary phase of Column **B** and the trityl moiety of the α-lactams, which are acting as a π-basic group, is important to achieve separation of these trityl containing α-lactams. When the concentration of the 2-propanol was increased to 5%, only the enantiomers of α-lactam **1b** showed a slight separation (α = 1.02). The α-lactams failed to elute when the mobile phase was changed to 100% hexane. No resolution of any α-lactam was observed with columns **A**, **C**, or **D** using hexane/2-propanol as the mobile phase. The only difference between columns B and A is that the isopropyl group is replaced by the π-basic naphthyl moiety. Therefore, it appears that the second discriminating factor is steric in nature since the α-lactams that were partially resolved by column **B** all contain the bulky adamantyl or *tert*-butyl group. A third resolving factor of column **B** is most likely the potential hydrogen bonding that can occur between the N—H groups of the urea linkage of the stationary phase and the amide functional group of the α-lactam.

When the mobile phase was changed to hexane/1,2-dichloroethane:95/5, Column **A** showed partial resolution of α-lactam enantiomers **1b** (α = 1.03) and **1c** (α = 1.07), with the (−)-enantiomer eluting first in each case. However, varying the percentages of hexane to 1,2-dichloroethane and/or the flow rate did not improve the separation.

Since column **B** with hexane/2-propanol:98/2 gave the best results, all the α-lactams (**1a-g**) were tested using column **B** with dimensions of 4.6 mm × 250 mm and the results are summarized in Table 2.

Essentially, baseline resolution was achieved for all trityl containing α-lactams (**1a-d**), including **1c** which had an α = 1.08 even though it showed no resolution on the smaller column. When the trityl moiety is at the N-1 position of the α-lactam ring (**1b,d**), better separation was achieved than the isomeric α-lactams (**1a,c**), where the trityl group is at the C-3 position. The bulkier adamantyl group (**1b**) versus the *tert*-butyl group (**1d**) at position 3 lead to the best separation of enantiomers, α = 1.20 for **1b** (see Fig. 5), which is further evidence that steric factors are important in the resolution process.

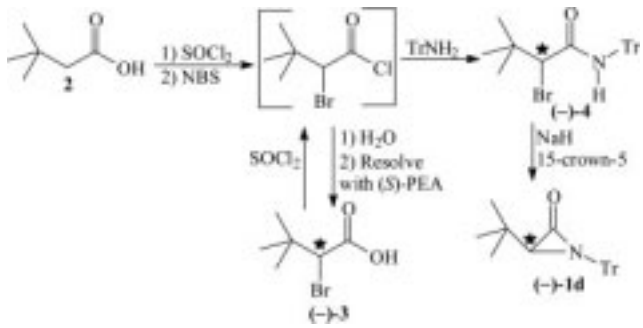

Fig. 4. The synthesis of non-racemic α-lactam **(−)-1d**, NBS, *N*-bromosuccinimide; PEA, 1-phenylethylamine; Tr, trityl.

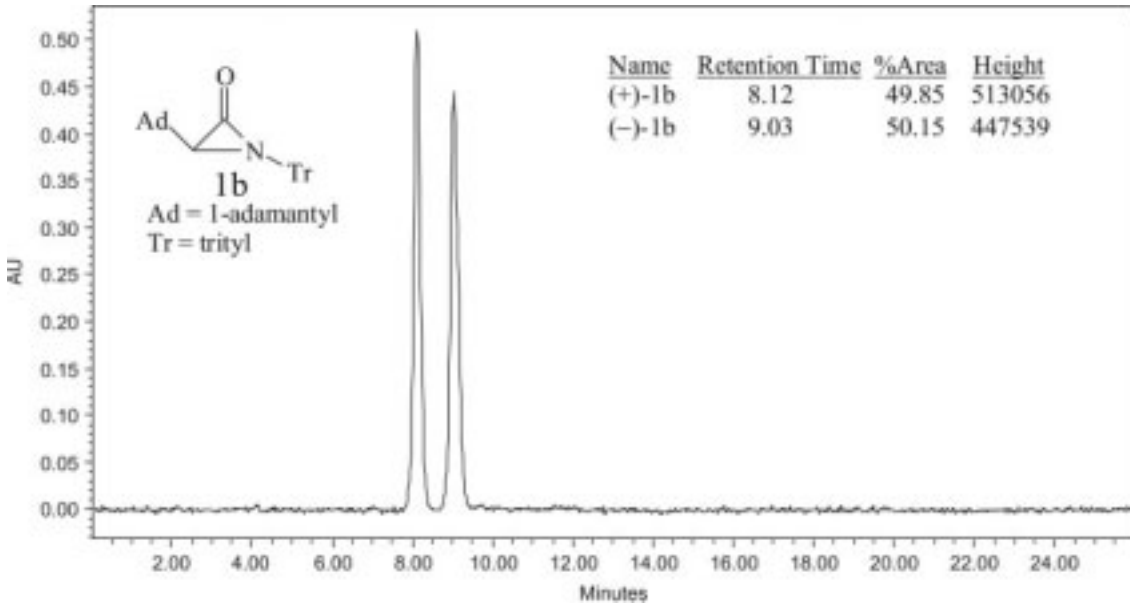

Fig. 5. The resolution of 1-trityl-3-(1-adamantyl)-aziridinone (**1b**) using column **B** with a mobile phase of hexane/2-propanol:98/2 and a flow rate of 1 ml/min.

To ascertain that this method could be used to determine the enantiomeric excess for a non-racemic α-lactam, **(−)-1d** was resolved using column **B** with a mobile phase of hexane/2-propanol:98/2. The chromatogram of non-racemic **(−)-1d** is shown in Figure 6 and the enantiomeric excess was easily determined (ee = *10*).

Since better separation of α-lactam **1b** was achieved using column **B** compared with column **A**, the Whelk-O1 column initially under consideration for use in this study was not tested. Instead, resources were used to test a new stationary phase (column **E**) that is similar in structure to column **B**. Both columns **B** and **E** (see Fig. 2) contain the π-acidic dinitrophenyl group, which appears to be a necessary structural feature to resolve α-lactam **1b**. However, column **E** contains the following structural differences from column **B** which might lead to better separation of α-lactam **1b** or a better understanding of the resolution mechanism:

1. a bulkier isobutyl group compared with the isopropyl substituent of column **B**;
2. an amide linkage between the dinitrophenyl group and the chiral center compared with the urea linkage of column **B**. The amide linkage alters the spatial separation

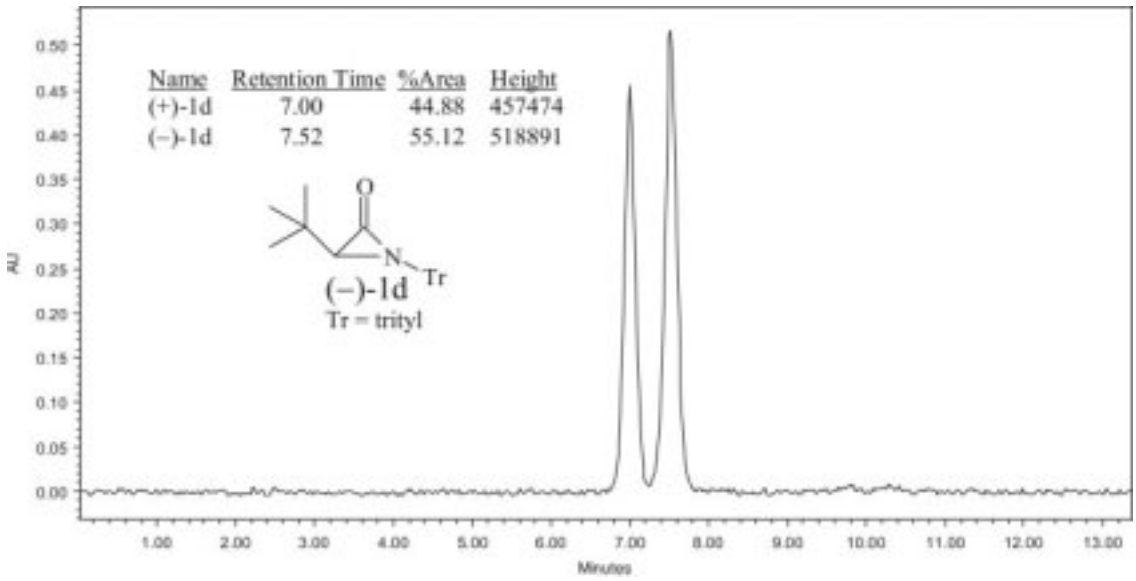

Fig. 6. The resolution of non-racemic 1-trityl-3-*tert*-butylaziridinone (**(−)-1d**) using column **B** with a mobile phase of hexane/2-propanol:98/2 and a flow rate of 1 ml/min.

between the chiral center and the dinitrophenyl group and only provides one N—H hydrogen bonding site.

While column **B** resolved α-lactam **1b** with a separation factor of 1.20, column **E** showed no separation (α = 1.0) using a mobile phase of hexane/2-propanol:98/2. Therefore, for α-lactam **1b**, the additional N—H group provided by the urea linkage in the stationary phase or it proximity to the chiral center and/or the π-acidic dinitrophenyl group's position relative to the chiral center of column **B** appears to be a crucial separation factor.

CONCLUSION

In summary, it is possible to separate the enantiomers of trityl-containing α-lactams (**1a-d**) using a stationary phase consisting of a 3,5-dinitroaniline derivative of (*S*)-valine with a hexane/2-propanol (98/2) mobile phase. These highly strained α-lactams are stable to the normal phase conditions used in the present study. In addition, the enantiomeric excess of the non-racemic α-lactam **(−)-1d** can be determined. The π-acidic dinitrophenyl group and the bulky isopropyl group provided by the stationary phase of column **B** appear to be important chiral recognition features for the resolution of the trityl substituted α-lactams.

LITERATURE CITED

1. Lengyel I, Sheehan JC. α-lactams (Aziridinones). Angew Chem Int Ed Engl 1968;7:25–36.
2. L'abbe G. Heterocyclic analogs of methylenecyclopropanes. Angew Chem Int Ed Engl 1980;19:277–290.
3. Backes J. 2-Oxo-aziridine (α-lactame) und deren derivate. In: Klamann D, editor. Houben-Weyl, Methoden der Organischen Chemie, Vierte Auflage, Band E16b. Stuttgart: Georg Thieme Verlag; 1991. p 1–19.
4. Hoffman RV. Stereospecificity in the α-lactam (aziridinone) synthon. In: Greenberg A, Breneman C, Liebman J, editors. The amide linkage: selected structural aspects in chemistry, biochemistry, and material science. New York: Wiley; 2000. p 137–155.
5. Hoffman RV, Cesare V, α-Lactams. In: Shinkai I, Weinreb S, editors. Science of synthesis, Houben-Weyl methods of molecular transformations, Vol. 21, Chapter 8. Stuttgart: Georg Thieme Verlag; 2005. p 591–608.
6. Cesare V, Taldone T, Lengyel I. About the factors that govern the ring-opening of α-lactams with primary amines. II. The relative basicity of the amine. Heterocycles 2002;57:1851–1868.
7. Lengyel I, Cesare V, Chen S, Taldone T. About the factors that govern the ring-opening of α-lactams with benzylamine. I. The relative stability of the α-lactam and the subtituent on nitrogen. Heterocycles 2002; 57:677–695.
8. Hoffman RV, Zhao Z, Costales A, Clarke D. Origins of regioslectivity in the reactions of α-lactams with nucleophiles. Two distinct acid-catalyzed pathways involving O- and N-protonation. J Org Chem 2002; 67:5284–5294.
9. Talaty ER, Yusoff MM. Regioselectivity in nucleophilic ring-opening of ariridinones. Chem Commun 1998;985–986.
10. Lengyel I, Cesare V, Taldone T. A direct link between the Passerini reaction and α-lactams. Tetrahedron 2002;60:1107–1124.
11. Quast H, Leybach H. Synthese eines chiralen, nicht-racemischen aziridinons (α-lactams). Chem Ber 1991;124:849–859.
12. Cesare V, Lyons TM, Lengyel I. A high-yielding general synthesis of α-lactams. Synthesis 2002;12:1716–1720.
13. Harpp ND, Bao LQ, Black CJ, Gleason JG, Smith RA. An efficient α-halogenation of acyl chlorides by *N*-bromosuccinimide, and molecular iodine. J Org Chem 1975;40:3420–3427.
14. Lengyel I, Cesare V, Karram H, Taldone T. About 1-triphenylmethyl-3-*tert*-butylaziridinone and some of its reactions. J Heterocyclic Chem 2001;38:997–1002.
15. Homeyer HA, Whitmore FC, Wallingford VH. Preparation of *tert*-butylacetic acid and its derivatives. J Am Chem Soc 1933;55:4209–4214.
16. Suzuki Y, Kirino O, Hashimoto S, Matsumoto K, Oshio H. Japanese Patent 63,211,248 (1988), C.A. # 110:59936c.
17. Pirkle WH, Spence PL. Chiral recognition of phthalides and lactams. Chirality 1998;10:430–433.
18. Pirkle WH, Tsipouras A, Hyun MH, Hart DJ, Lee C. Use of chiral stationary phases for the chromatographic determination of enantiomeric purity and absolute configuration of some β-lactams. J Chromatogr 1986;358:377–384.
19. Welch CJ. Evolution of chiral stationary phase design in the Pirkle laboratories. J Chromatogr A 1994;666:3–26.
20. Lengyel I, Cesare V, Adam I, Taldone T. About four new trityl-substituted α-lactams. Heterocycles 2002;57:73–95.
21. Bott K. Synthesis of α-chloro-1-adamantaneacetic acids and α-chloro-2-norbornaneacetic acid by means of trichloroethylene. Agnew Chem Int Ed 1967;6:946–947.
22. Lengyel I, Uliss DB. The synthesis and spectral properties of a new stable α-lactam: 1-(1-adamantyl)-3-*t*-butylaziridinone. Chem Commun 1968;1621–1622.
23. Sheehan JC, Beeson JH. α-lactams IV, a stable α-lactam, 1,3-di-*t*-butylaziridinone. J Am Chem Soc 1967;89:362–366.

CHIRALITY 20:75–83 (2008)

Synthesis of Chiral Vicinal Diols and Analysis of Them by Capillary Zone Electrophoresis

PENG LIU, WEI HE, YAN ZHAO, PING-AN WANG, XIAO-LI SUN, XIAO-YE LI, AND SHENG-YONG ZHANG*
Research Center for Chirotechnology, Fourth Military Medical University, X'ian, Shaanxi, China

ABSTRACT This paper describes an improved access to 1,4-bis (9-*O*-quininyl) phthalazine [$(QN)_2PHAL$], a very useful chiral ligand for catalytic asymmetric dihydroxylation (AD), by using CaH_2 as acid-binding reagent in a high yield under mild conditions. The application of $(QN)_2PHAL$ to the AD reactions of eight olefins exhibited excellent enantioselectivity and activity with corresponding chiral vicinal diols. Furthermore, a capillary zone electrophoresis method was developed to separate the aforementioned chiral vicinal diols by using of neutral β-cyclodextrin (β-CD) as chiral selector and borate as running buffer. High resolution was achieved under the optimal conditions of β-CD 2.2% (w/v), pH 10, 200 mM borate buffer at 15 kV, and 20°C within 15 min. The relative standard deviations of the corrected peak areas and migration time were less than 3.9% and 1.3%, respectively. In addition, the developed method was successfully applied to the determination of the purity and the enantiomeric excesses value (%ee) of the AD reaction products. *Chirality 20:75–83, 2008.*

KEY WORDS: chiral ligand; enantiomer separation; capillary electrophoresis; vicinal diols; β-cyclodextrin; borate complexation

INTRODUCTION

Undoubtedly, chiral vicinal diols have a prominent role in fine chemicals and pharmaceuticals because of their versatile utilities.[1-3] As we know, the catalytic asymmetric dihydroxylation (AD) of olefins provides a highly effective method for the preparation of various chiral vicinal diols.[4] In order to obtain high yields and enantioselectivities of chiral vicinal diols, the design and synthesis of chiral ligands for the AD reaction have drawn much attention of organic chemists over past two decades.[5] A lot of new and efficient ligands have been successfully developed and used in the AD reaction.[5-7] 1,4-Bis(9-*O*-quininyl)phthalazine [$(QN)_2PHAL$] **2**, an efficient chiral ligand for AD reaction, was first synthesized by Song et al.,[8] and then, Jiang et al. improved this synthetic method to furnish **2** in good yield.[9] In the present study, we further developed a convenient access to **2** in excellent yield under mild conditions by using CaH_2 as an acid-binding reagent. The chiral ligand **2** was then used to catalyze the AD reactions of eight olefins to afford corresponding chiral vicinal diols in excellent yields and enantioselectivities.

With the fast development of the AD reaction in organic synthesis and industrial application, an efficient and convenient enantioseparation and quantitative analysis of the chiral vicinal diols are badly needed. Among many analytic techniques, capillary electrophoresis (CE) has been widely used in enantioseparation because of its high efficiency, rapid method development, short analysis time, and low consumption of reagents.[10-14] In CE, borate as background electrolyte with vicinal hydroxyl of carbohydrates, nucleosides, and 1,2-diols to form negative complexes has been extensively studied.[15-17] To the best of our knowledge, there have been only a few reports on the enantioseparation of the chiral vicinal diols with β-CD as chiral selector and borate as running buffer.[18-21] In this study, we systematically optimized enantioseparation conditions of eight synthetic vicinal diols enantiomers (±)-I–(±)-VIII by using neutral β-CD as chiral selector in the presence of borate buffer, and first investigated the enantioseparation of (±)-II–(±)-VIII by capillary zone electrophoresis (CZE). Additionally, we used the optimal CZE method to monitor the process of the AD reaction and to determine the purity and the enantiomeric excesses value (%ee) of the AD reaction products.

EXPERIMENTAL

Apparatus and Reagents

All the CZE analysis was performed with Beckman P/ACE™ MDQ CE system equipped with a diode array detector (Beckman Coulter, Fullerton, CA). The operation was controlled by an integrated 32 karat software (version 5.0) package. Uncoated fused-silica capillary columns of

Contract grant sponsor: National Natural Science Foundation of China.
Contract grant sponsor: Shaanxi Province; Contract grant numbers: 20572131, 2007K12-02.
*Correspondence to: Sheng-Yong Zhang, Research Center for Chirotechnology, Fourth Military Medical University, Xi'an, Shaanxi, China.
E-mail: syzhang@fmmu.edu.cn
Received for publication 7 May 2007; Accepted 10 October 2007
DOI: 10.1002/chir.20500
Published online 3 December 2007 in Wiley InterScience (www.interscience.wiley.com).

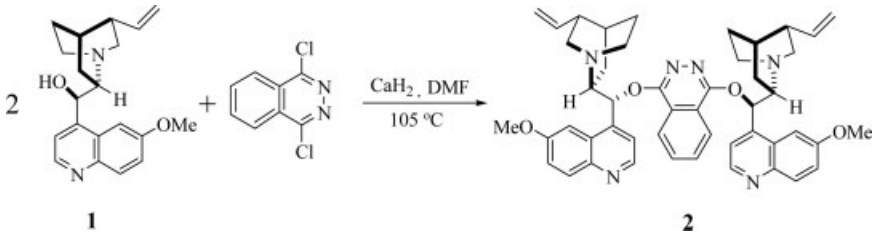

1 2

Scheme 1. Synthesis of chiral ligand **2**.

75 μm i.d. × 375 μm o.d., with a total length of 48.5 cm and effective length of 38.5 cm, were used as the separation capillary (Yongnian Optical Fiber, Hebei Province, China). The temperature of the cartridge holding the capillary column was set at 20°C and maintained by the liquid cooling system. All pH measurements were made with a Delta 320-S pH meter (Metter Toledo, Shanghai, China). ^{1}H NMR spectra was recorded on a Bruker AV-300 NMR spectrometer (300 MHz) (Bruker, Karlsruhe, Germany), with $CDCl_3$ as solvent and TMS as internal reference. High performance liquid chromatography (HPLC) was performed by Agilent 1100 (Agilent Technologies, Wilmington, DE) interfaced to an HP 71 series computer workstation with Daicel Chiralcel OJ-H chiral column (Daicel Chemical Industries, Japan). Optical rotation values were measured at 25°C on a PerkinElmer 343 polarimeter (PerkinElmer Bodenseewerk, Überlingen, Germany). Melting points were uncorrected and expressed in degree celsius.

HPLC grade methanol and acetonitrile were purchased from Tedia (Fairfield, OH). β-Cyclodextrin hydrate (β-CD) was purchased from Acros Organics (Geel, Belgium). Boric acid and sodium hydroxide were obtained from Sigma (St. Louis, MO). 1,4-Dichlorophthalazine was prepared according to literature procedure[22] [m.p. 163.5–164.5°C (lit.[22] m.p. 164°C)]. Water for the experiments was purified by Milli-Q system (Millipore, Bedford, MA). All other chemicals used were of analytical grade.

Section 1: Organic Synthesis

Preparation of 2. A 100 ml three-necked round-bottomed flask was charged with 1,4-dichlorophthalazine (2.04 g, 10.3 mmol), quinine **1** (7.35 g, 22.66 mmol), and anhydrous DMF (50 ml) under nitrogen. The reaction mixtures were stirred until all the quinine dissolved. CaH_2 (4.22 g, 100.3 mmol) was then added in small portions, and the reaction mixtures were heated gradually to 105°C and stirred until TLC indicated that **1** had disappeared. A light brown reaction mixture was allowed to cool to room temperature and was filtrated through Celite, and the cake was washed with CH_2Cl_2. The organic layers were combined, washed with water and brine, and dried over anhydrous $MgSO_4$. The solvent was evaporated under reduced pressure to give a crude product as a light yellow solid, which was then recrystallized with EtOAc to give **2** (7.49 g, 94% total recrystallized yields); m.p. 160–161°C (lit.[8] m.p. 159–160°C). The structure was also established by ^{1}H NMR and ^{13}C NMR (Scheme 1).

AD of Olefins

Synthesis of enantiomerically pure vicinal diols. $K_3Fe(CN)_6$ (1.96 g, 6.0 mmol), K_2CO_3 (0.82 g, 6.0 mmol), and ligand **2** (15.6 mg, 0.02 mmol) were dissolved in ^{t}BuOH/H_2O (v/v = 1:1, 24 ml) at room temperature, followed by addition of $K_2OsO_2(OH)_4$ (1.47 mg, 0.004 mmol) and $CH_3SO_2NH_2$ (190 mg, 2.0 mmol). After stirring for 5 min, olefin (2.0 mmol) was added. The solution was cooled to 0°C. The mixture was stirred vigorously at 0°C until TLC showed no olefins. Na_2SO_3 (1.5 g) was then added, and the mixture was allowed to warm to room temperature and stirred for 30 min. AcOEt (20 ml) was added to the reaction mixture, and the aqueous phase was further extracted with AcOEt (15 ml × 3) after separation of the layers. The combined organic layers were washed with 2 M NaOH (20 ml), and were then washed with water to neutral, dried over anhydrous $MgSO_4$, and evaporated to dryness under reduced pressure to obtain a crude product, which was purified by a flash column chromatography (*n*-hexane/EtOAc, 7:3) to afford enantiomerically pure vicinal diols (I–VIII).

I: δ 7.35–7.26(m, 5H, Ar-H), 4.98–4.96(d, J = 2.46 Hz, 1H, *CH), 4.33–4.31 (d, J = 2.87 Hz, 1H, *CH), 3.80 (s, 3H, CH_3), 2.91 (br, 2H, OH). II: δ 7.20 (m, 2H, Ar-H), 6.91 (m, 2H, Ar-H), 5.10 (d, J = 2.76 Hz, 1H, *CH), 4.46 (d, J = 2.74 Hz, 1H, *CH), 3.81 (s, 3H, CH_3), 2.92 (br, 2H, OH). III: δ 7.33 (m, 4H, Ar-H), 4.98 (d, J = 2.75, 1H, *CH), 4.32 (d, J = 2.74 Hz, 1H, *CH), 3.81 (s, 3H, CH_3), 2.91 (br, 2H, OH). IV: δ 7.29–7.26 (d, J = 7.75 Hz, 2H, Ar-H),7.18–7.16 (d, J = 7.78 Hz, 2H, Ar-H), 4.98 (d, J = 1.43 Hz, 1H, *CH), 4.34 (d, J = 2.07 Hz, 1H, *CH), 3.80 (s, 3H, CH_3), 2.83 (br, 2H, OH), 2.34 (s,3H, CH_3). V: δ 7.33 (d, J = 8.51 Hz, 2H, Ar-H), 6.90 (d, J = 8.55 Hz, 2H, Ar-H), 4.96 (d, J = 2.67 Hz, 1H, *CH), 4.34 (d, J = 2.79 Hz, 1H, *CH), 3.81 (s, 3H, CH_3), 3.79 (s, 3H, CH_3), 2.75 (br, 2H, OH). VI: δ 7.32 (d, J = 8.19 Hz, 2H, Ar-H),6.89(d, J = 8.19 Hz, 2H, Ar-H), 4.95 (s, 1H, *CH), 4.33 (s, 1H, *CH), 3.80 (s, 3H, CH_3), 3.78 (s, 3H, CH_3), 2.80 (br, 2H, OH). VII: δ 7.57–7.20 (m, 10H, Ar-H), 4.98 (s, 1H, *CH), 2.80 (br, 2H, OH), 1.60 (s, 3H, CH_3). VIII: δ 7.69–7.66 (m, 2H, Ar-H), 7.45–7.10 (m, 6H, Ar-H), 5.30 (br, 2H, *CH), 2.78 (br, 2H, OH).

Synthesis of racemic vicinal diols. Racemic vicinal diols were prepared with *trans*-1,2-disubstituted olefins according to literature procedures.[23]

Section 2: Analysis by CZE

Buffer preparation and electrophoretic procedures. Borate buffers (200 mM) were prepared in purified water

TABLE 1. Asymmetric dihydroxylation of olefins using 2 as the chiral ligand

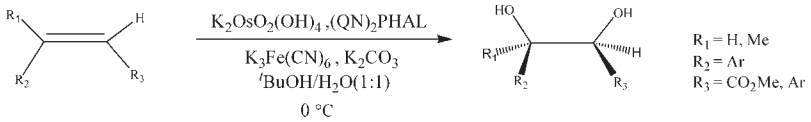

Entry	Olefins	Chiral vicinal diols	Yield[a] (%)	%ee[b]	%ee[c]	$[\alpha]_D^{25}$ [d]	m.p. (°C)	Config.[e]
1	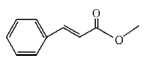	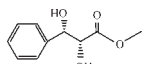 I	75.1	99.74	99.57	+10.4	84.5–85.5	2*R*,3*S*
2	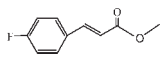	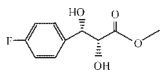 II	86.7	99.56	99.53	+9.1	61.5–62.5	2*R*,3*S*
3	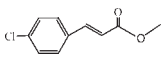	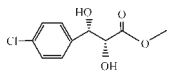 III	91.8	99.06	99.55	+15.8	117–118	2*R*,3*S*
4	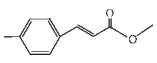	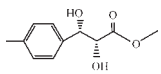 IV	90.3	99.80	99.84	+6.3	97.5–99	2*R*,3*S*
5	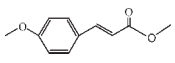	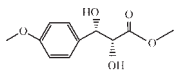 V	75.6	99.90	99.60	+5.5	106–107	2*R*,3*S*
6	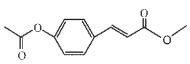	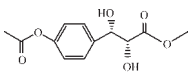 VI	83.1	99.19	99.54	+5.8	105–106	2*R*,3*S*
7	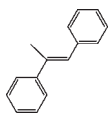	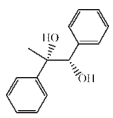 VII	85.7	97.70	97.97	+39.2	83.5–84.5	1*S*,2*S*
8	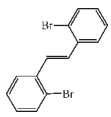	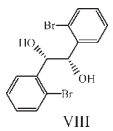 VIII	89.6	99.80	99.65	−2.6	107–108	1*S*,2*S*

[a]Isolated yields by column chromatography.
[b]The ee values were determined by HPLC analysis of the diols (See page footnote for details).*
[c]The ee values were determined by CZE analysis of the diols.
[d]$[\alpha]_D^{25}$ values measured in ethanol, 1.0×10^{-2} g/ml (diol of I measured in $CHCl_3$).
[e]The absolute configurations of diols were determined by comparison of their optical rotations with literature values.

*I: Daicel Chiralcel OJ, *n*-hexane/^{i}PrOH = 90:10, flow rate 1.0 ml/min, t_R (min) = 26.9(major), 39.5 (minor).

II: Daicel Chiralcel OJ, *n*-hexane/^{i}PrOH = 90:10, flow rate 1.0 ml/min, t_R (min) = 19.8(major), 24.1 (minor).

III: Daicel Chiralcel OJ, *n*-hexane/^{i}PrOH = 90:10, flow rate 1.0 ml/min, t_R (min) = 20.3 (major), 22.7 (minor).

IV: Daicel Chiralcel OJ, *n*-hexane/^{i}PrOH = 90:10, flow rate 1.0 ml/min, t_R (min) = 22.7 (major), 26.7 (minor).

V: Daicel Chiralcel OJ, *n*-hexane/^{i}PrOH = 85:15, flow rate 1.0 ml/min, t_R (min) = 31.2 (major), 35.6 (minor).

VI: Daicel Chiralcel OJ, *n*-hexane/^{i}PrOH = 85:15, flow rate 1.0 ml/min, t_R (min) = 33.1 (major), 38.6 (minor).

VII: Daicel Chiralcel OJ, *n*-hexane/^{i}PrOH = 93:7, flow rate 1.0 ml/min, t_R (min) = 27.4 (major), 30.5 (minor).

VIII: Daicel Chiralcel OJ, *n*-hexane/^{i}PrOH = 92:8, flow rate 0.6 ml/min, t_R (min) = 50.4 (major), 54.9 (minor).

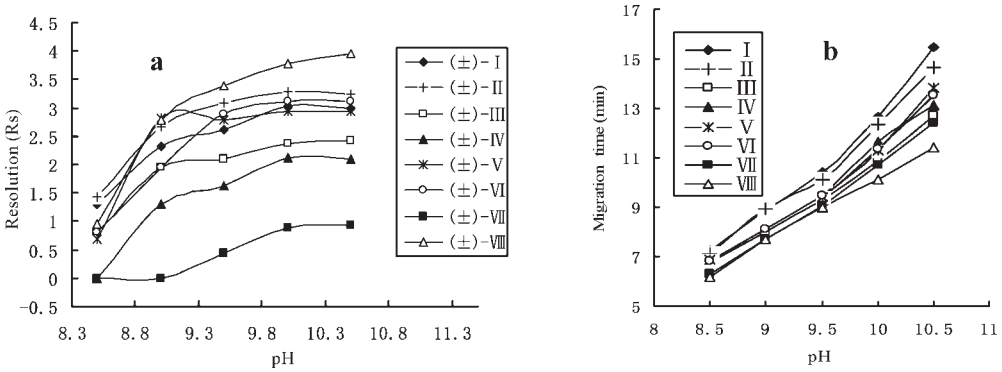

Fig. 1. Effect of pH on resolution (**a**) and migration time (**b**) of chiral vicinal diols. Separation conditions: fused-silica capillary, 58.5 cm (48.5 cm effective length) ×75 μm i.d.; BGE, 200 mM borate buffer, 2.2% (w/v) β-CD; temperature, 20°C; applied voltage, 15 kV; UV detection at 214 nm.

and the pH was adjusted with sodium hydroxide. β-CD was dissolved in each background electrolyte (BGE) for appropriate concentration after adjusting to the desired pH values. Sample solutions were prepared by dissolving vicinal diols in a mixture of water solution containing 20% methanol. The running buffers and sample solutions were filtered through a 0.22 μm syringe filter and were degassed by using an ultrasonic bath for 5 min prior to use. All the solutions were stored in the refrigerator at 4°C for later use. New capillary column was flushed with 1.0 M NaOH for 30 min, followed by flushing with water for 30 min, then flushed with 0.1 M HCl for 10 min, and again with water for 10 min. At the start and end of each working day, the capillary was washed with water for 3 min, 0.1 M NaOH for 3 min, and again with water for 3 min. Prior to every run, the capillary was rinsed with 0.1 M NaOH, then water, followed by the running buffer, each for 3 min at 20 psi pressure. Sample solution was introduced into the capillary with a pressure of 0.5 psi for 5 sec. The electrophoretic separation was performed at an applied voltage of 15 kV unless stated otherwise, with the injection end at the anode. Methanol was used as the electroosmotic flow (EOF) marker.

Calculation. The enantiomeric resolution values were calculated according to the method via the built-in 32 Karat software program. The resolution (*R*s) between the two enantiomers was calculated by using the following formula:

$$Rs = 2\frac{t_2 - t_1}{w_1 + w_2}$$

where t is the enantiomer migration time and w is the width of peak at the baseline.

Enantiomeric excess was defined as the excess of one enantiomer in a pair of enantiomers and was calculated according to the following formula:

$$\text{ee}(\%) = \left[\frac{A_1 - A_2}{A_1 + A_2}\right] \times 100$$

where A is the corrected peak area of enantiomer (dividing the area of each peak with its corresponding migration time, A/t). Logically an ee value of 100 stands for an enantiomerically pure substance and an ee value of 0 for a racemate.

RESULTS AND DISCUSSION

Preparation of Chiral Ligand 2

Although the synthesis of **2** was previously reported by Song et al.[8] and Jiang et al.,[9] these two procedures were not satisfactory enough for large-scale preparation. For our improved method, by using CaH_2 as an acid-binding reagent, the chiral ligand **2** was obtained under mild reaction conditions in 94% yield (22% and 9% higher than literature data,[8,9] respectively). Moreover, mono-cinchona alkaloid ligand or bis-cinchona alkaloid ligand could be yielded by controlling the reaction time. The ligand was purified by simple crystallization (from EtOAc).

Synthesis of Enantiomerically Pure Vicinal Diols

Eight enantiomerically pure vicinal diols were obtained via the AD reactions of olefins with **2** as the chiral ligand, exhibiting an excellent enantioselectivity and activity (Table 1).

Method Optimization for the Vicinal Diols Separation by CZE

Effect of borate buffer pH. The running buffer pH, as an important parameter, affects chiral discrimination and migration time, because it can affect the mobility of analyte and EOF by changing the dissociation degree of the analytes and Si—OH groups in the inner wall of the capillary. Experiments were performed using 200 mM borate buffer at different pH values in the range from pH 8.5 to 10.5. As shown in Figure 1, the resolution of all the enantiomers of vicinal diols was poor at pH 8.5. When the buffer pH increased from 8.5 to 10.0, except for compound (±)-VII, the resolution of all other analytes was higher than 1.6. When the pH was higher than 10.0, compounds (±)-III, (±)-V, and (±)-VIII kept increasing in resolution, whereas compounds (±)-I, (±)-II and (±)-IV were decreasing. Moreover, the baseline worsened, and the sensitivity also decreased when the pH was higher than 10.0. Based on the earlier results, as a compromise, pH 10.0 was chosen

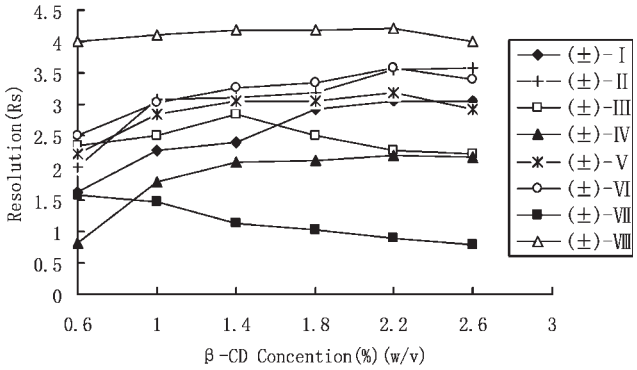

Fig. 2. Effect of β-CD concentration on resolution of chiral vicinal diols. Separation conditions: fused-silica capillary, 58.5 cm (48.5 cm effective length) ×75 μm i.d.; BGE, 200 mM borate buffer, pH, 10.0; temperature, 20°C; applied voltage, 15 kV; UV detection at 214 nm.

as the optimal acidity of the borate buffer for subsequent studies.

Effect of β-CD concentration. With β-CD playing a key role in the process of chiral discrimination for racemic vicinal diols, β-CD concentration is considered to be very important. Wren and Rowe[24-26] developed a theoretical model, suggesting that the degree of separation depends on the concentration of chiral selector, and an optimal concentration exists for the chiral selector. In addition, Jira et al.[18] proposed a dual chiral recognition mechanism that both inclusion of the aromatic moiety into the chiral cavity of the CD and the formation of borate complex with diol groups are assumed to be responsible for chiral recognition. Thus, higher β-CD concentration leads to better resolution, because much more inclusion complexes between enantiomers and β-CD are formed, but when the β-CD concentration was up to a certain degree, the complex between the enantiomers and β-CD is in dynamic equilibrium, and the resolution will not be promoted even by increasing β-CD concentration. In this study, under 200 mM borate buffer at pH 10.0, the influence of β-CD concentration in the range of 0.6–2.6% (w/v) on the enantioseparation of the chiral vicinal diols was investigated. As can be seen from Figure 2, raising the β-CD concentration from 0.6 to 2.2% (w/v) resulted in an improvement in the separation of all analytes, except for (±)-VII. When β-CD concentration was 2.2% (w/v), a maximum resolution for (±)-IV, (±)-V, (±)-VI, and (±)-VIII was achieved. With the concentration up to 2.6% (w/v), the resolution for (±)-I and (±)-II increased slightly, whereas the resolution for other chiral vicinal diols decreased. Hence, a β-CD concentration of 2.2% (w/v) was selected for the final method and was found to provide a good resolution and a suitable run time.

Effect of borate concentration. Borate acts as BGE for CZE, and forms tertiary inclusion complex with β-CD and vicinal diols. The buffer concentration affects the baseline stability, peak shape, and separation selectivity. With the increase of the concentration of borate, the ion strength and the hydrophobic interaction between β-CD and enantiomers are also increased, and sharp peaks can be obtained. At the same time, the zeta potential and EOF were decreased; consequently, the migration time was prolonged and the minor distinction of mobility was enlarged, which promoted the separation efficiency. As borate can provide the excellent baseline enantioseparation for the chiral vicinal diols within 15 min, we used borate as buffer solution. However, when the concentration of borate was above a certain value (>300 mM), some side effects can be observed, such as lower reproducibility, distortional peak shape, serious baseline drift, and long migration time. The borate concentration was investigated in the range of 50–300 mM in the presence of 2.2% (w/v) β-CD at pH 10.0 (Fig. 3). When the borate concentration increased from 50 to 200 mM, the separation of all the analytes was substantially improved. When borate concentration increased in the range from 200 to 300 mM, only a slight increase in the separation was observed. Meanwhile, there was also a slight increase in migration time due to a decrease in the EOF. Therefore, a 200 mM borate concentration was selected as the optimal enantioseparation method.

Effect of temperature and applied voltage. Temperature leads to different effects on chiral resolution. In addition to a decrease of running buffer viscosity and enhancement of the diffusional band broadening, an increase in temperature contributes to a decrease in the stability of

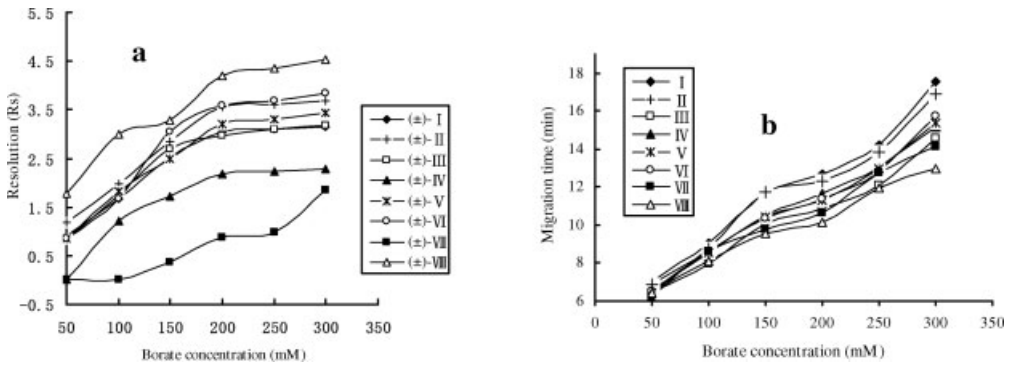

Fig. 3. Effect of borate buffer concentration on resolution (**a**) and migration time (**b**) of the chiral vicinal diols. Separation conditions: fused-silica capillary, 58.5 cm (48.5 cm effective length) ×75 μm i.d.; 2.2% (w/v) β-CD; pH, 10.0; temperature, 20°C; applied voltage, 15 kV; UV detection at 214 nm.

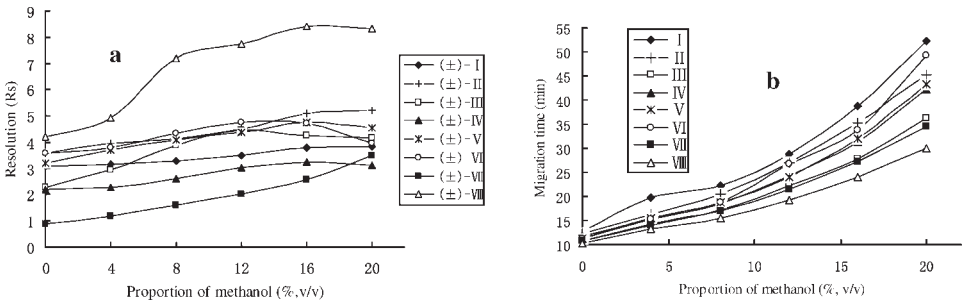

Fig. 4. Effect of proportion of methanol additive (%, v/v) on resolution (**a**) and migration times (**b**) of the chiral vicinal diols. Separation conditions: fused-silica capillary, 58.5 cm (48.5 cm effective length) ×75 μm i.d.; BGE, 200 mM borate buffer, 2.2% (w/v) β-CD; pH, 10.0; temperature, 20°C; applied voltage, 15 kV; UV detection at 214 nm.

the solute-CD inclusion complexes. The experimental results showed that higher resolution and lower sensitivity were obtained at lower temperature. When the temperature was higher than 25°C, the baseline deteriorated because the higher current caused excessive Joule heating and then increased EOF. As a result, a temperature of 20°C was finally chosen as capillary temperature.

As the applied voltage directly affects the migration time and the resolution, the effect of the applied voltage between 9 and 27 kV on the separation of the analytes was investigated. The results indicated that increasing the voltage shortened migration time for all the analytes, whereas the resolution and the peak areas of the analytes decreased. When the applied voltage was higher than 27 kV, the currents were above 280 μA, which generated excessive Joule heating. In addition, the prolonged analysis time and severe peak broadening were observed when the separation voltage was below 9 kV. For our experiments, 15.0 kV was selected as the optimal applied voltage to accomplish a good compromise.

Effect of the organic modifier on separation behavior. The addition of organic modifier to the BGE can cause a considerable increase in separation of the enantiomers. In fact, the organic modifier may influence several parameters, such as binding constants of enantiomer-CD inclusion complexes, viscosity of the BGE, EOF, analysis time, conductivity of buffer, solubility of enantiomers or CD.[25] Two organic modifiers, methanol and acetonitrile, were added to the BGE within a 0–20% (v/v) range. As shown in Figures 4 and 5, with increase in the proportion of methanol or acetonitrile, the vicinal diols resolution was improved. However, at higher proportion of methanol or acetonitrile, the migration time of the analytes was prolonged. At 5% (v/v) acetonitrile or 8% (v/v) methanol, all the enantiomers of vicinal diols were more effectively separated. Finally, 8% methanol or 5% acetonitrile was chosen as the suitable proportion of organic modifier to give a compromise between resolution and the migration time.

Optimum conditions of enantioseparation. According to the factors mentioned earlier, the optimal condition was obtained with running electrolyte containing 200 mM borate, pH 10.0, 2.2% (w/v) β-CD [0.6% (w/v (±)-VII], 20°C temperature, and 15 kV applied voltage. All the eight chiral vicinal diols were well separated within 15 min. Electropherograms obtained under the optimized conditions are presented in Figure 6.

Relatively high resolution (Rs > 1.6) was obtained without organic modifier in running buffer, and there was a slight decrease in the repeatability observed because of the volatilization of methanol or acetonitrile in buffer. Thus, the optimal CZE conditions were established without organic modifier.

Repeatability, linearity, and sensitivity. Evaluation of repeatability, linearity, and sensitivity was performed with V, VII, and VIII as samples. Enantiomerically pure vicinal diols solution of 60.0 μg/ml was analyzed five times to

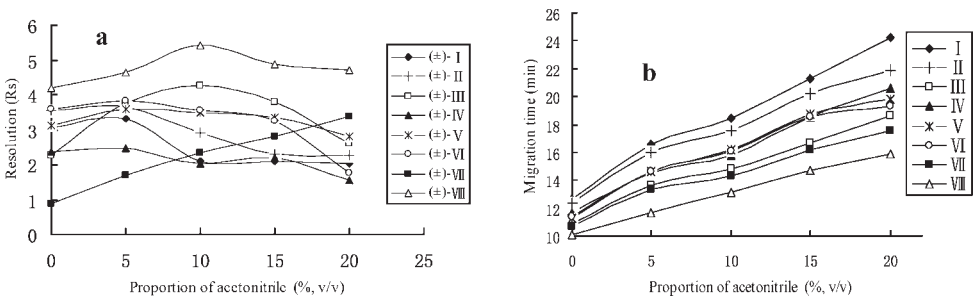

Fig. 5. Effect of proportion of acetonitrile additive (%, v/v) on resolution (**a**) and migration times (**b**) of the chiral vicinal diols. Separation conditions: fused-silica capillary, 58.5 cm (48.5 cm effective length) ×75 μm i.d.; BGE, 200 mM borate buffer, 2.2% (w/v) β-CD; pH, 10.0; temperature, 20°C; applied voltage, 15 kV; UV detection at 214 nm.

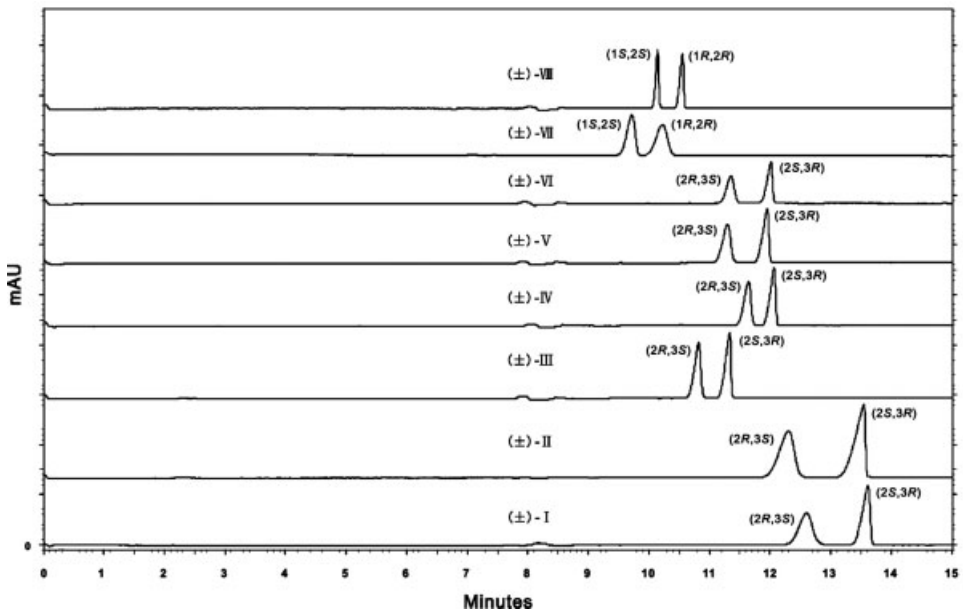

Fig. 6. Electropherograms of the eight chiral vicinal diols under optimal conditions. Separation conditions: fused-silica capillary, 58.5 cm (48.5 cm effective length) ×75 μm i.d.; BGE, 200 mM borate buffer, pH, 10.0, 2.2% (w/v) β-CD [0.6% (w/v) (±)-VII]; temperature, 20°C; applied voltage, 15 kV; UV detection at 214 nm.

determine the repeatability of the corrected peak area (A/t) and migration time for all analytes under the optimal conditions. The results indicate a good repeatability of the method, both for the corrected peak areas (RSD < 3.9%) and migration times (RSD < 1.3%). In order to evaluate the signal linearity, a series of the calibration solutions of concentrations ranging from 2.5 to 500.0 μg/ml were investigated. The calibration curves between Y (the corrected peak area) and X (the concentration of samples, μg/ml) were indicative of good linear correlations, since the correlation coefficient (r) was in the range of 0.9990–0.9993, while the coefficient of determination (R^2) was 0.9980–0.9986. The limit of detection (LOD) and limit of quantification (LOQ) values were in the range of 1.1–2.5 μg/ml and 5.0–10.0μg/ml, respectively (Table 2). LOD was based on the lowest detectable peak with a signal-to-noise ratio of 3, and LOQ was 10 times the signal-to-noise ratio. Therefore, repeatability, linearity, and sensitivity of the method were suitable for the determination of the main product content of the AD reaction.

Accuracy and precision. Under the optimized CZE conditions, the accuracy and precision was investigated by measuring the analytes recovery (V, VII, VIII) at three different concentrations: 10.0, 25.0, and 60.0 μg /ml. Each concentration was performed for six determinations. Accurately adding 10.0, 25.0, and 60.0 μg/ml of enantiomerically pure vicinal diols (V, VII, VIII) into 60.0 μg/ml corresponding racemic diols [(±)-V,(±)-VII,(±)-VIII] gave these enantiomerically pure vicinal diols a final concentration in the range of 40.0–90.0 μg /ml. The results showed that recoveries of the added enantiomerically pure vicinal diols were in the range of 97.3–103% and the precision expressed as relative standard deviation was found to be less than 4.9% (Table 3). Moreover, the validity of the method was corroborated by using the peak-purity capability of the diode array detector, which enables detection and identification of vicinal diols in the samples. Thus, the accuracy and precision of the method was well suited to the quantitative analysis of real samples.

Analysis of Synthetic Samples

Determination of the vicinal diols content. The purity of three real synthetic vicinal diols (V, VII, and VIII) was determined by the aforementioned method of the optimal CZE conditions, and the purity was 99.16%, 97.52%,

TABLE 2. Linearity and sensitivity of the method for the determination of the main product content of the AD reaction (n = 5)

Analytes	Regression equation	Linear range(μg/ml)	r	R^2	LOD(μg/ml)	LOQ(μg/ml)
V	$Y = 41.8037X + 230.44$	10.0–450.0	0.9990	0.9980	2.5	8.0
VII	$Y = 28.7539X + 255.47$	12.5–400.0	0.9993	0.9986	2.0	10.0
VIII	$Y = 36.8411X + 295.67$	7.5–370.0	0.9992	0.9984	1.1	5.0

Conditions: fused-silica capillary, 58.5 cm (48.5 cm effective length) ×75 μm i.d.; BGE, 200 mM borate buffer, pH 10.0, 2.2% (w/v) β-CD [0.6% (w/v) (±)-VII]; temperature, 20°C; applied voltage, 15 kV; UV detection at 214 nm.

TABLE 3. Recovery of the enantiomerically pure vicinial diols ($n = 6$)

Analytes	Added (μg/ml)	Recovered (μg/ml)	Recovery±RSD (%) (n=6)
V	10.0	9.8±0.4	98.2±4.5
	25.0	24.9±0.7	99.6±2.9
	60.0	58.4±2.6	97.3±4.5
VII	10.0	10.3±0.5	103.2±4.9
	25.0	24.8±0.9	99.2±3.8
	60.0	58.8±1.5	98.0±2.5
VIII	10.0	9.8±0.4	97.8±4.2
	25.0	25.3±0.9	101.2±3.6
	60.0	59.9±0.6	99.8±1.0

Experimental conditions as in Table 2.

and 99.25%, respectively. This method was also used to efficiently monitor the process of the AD reactions.

Determination of enantiomeric excesses (%ee). Eight synthetic samples of the AD reactions at the concentration of about 2.2 mg/ml were assayed to determine the enantiomeric excesses value (%ee) by the optimized method. The baseline separation of the enantiomers was still observed at excessively high concentration level. The results are shown in Table 1. It was found that the enantiomeric excess value (%ee) determined by the CZE method was in accordance with that by HPLC, indicating that the proposed method is suitable for the determination of %ee value of the AD reaction samples. Typical electropherograms of %ee determination are shown in Figure 7.

CONCLUSION

Synthesis of chiral ligand $(QN)_2PHAL$ **2** was improved under mild conditions in an easier procedure and in high yield. It provided a practical way to synthesize the chiral ligand in a large scale. The chiral ligand showed high chemical yields and excellent enantioseletivity in AD of olefins. Furthermore, the utility of β-CD-modifed CE method for the fast and efficient enantioseparation of eight chiral vicinal diols was demonstrated. Under the optimal operation conditions, an efficient separation of the diols was obtained within 15 min. The developed method proved to be a simple and rapid technique for monitoring the process of the AD reaction as well as determining the purity and the enantiomeric excesses value (%ee) of the AD reaction products.

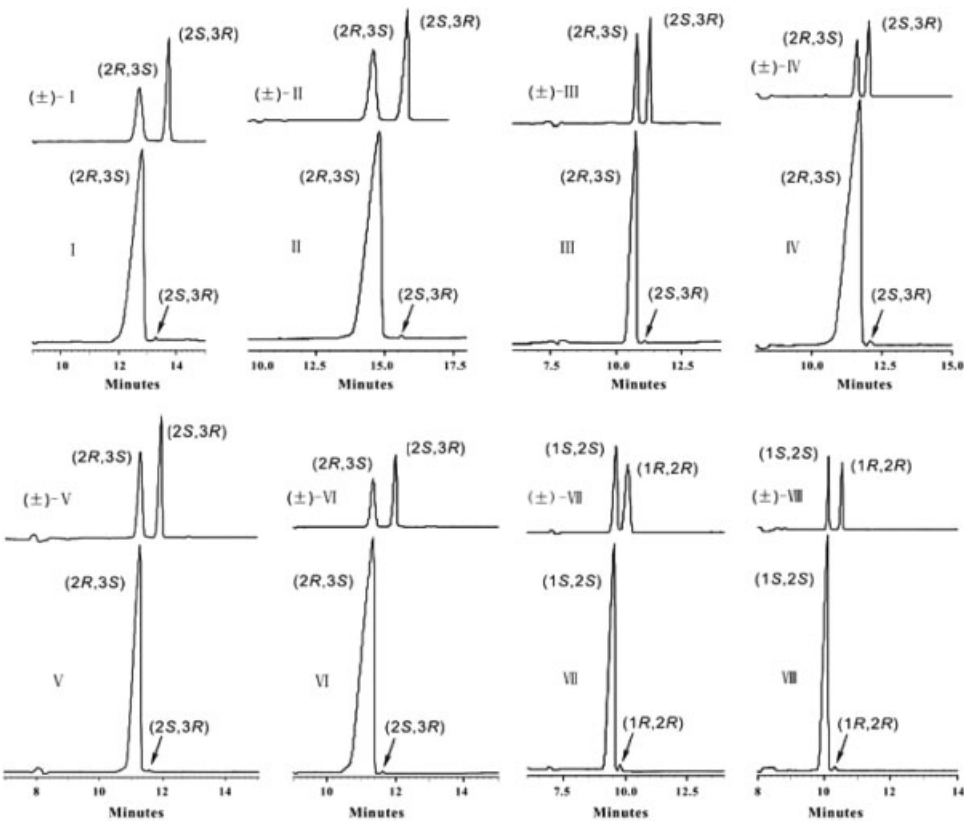

Fig. 7. Typical electropherograms of %ee determination. Separation conditions: fused-silica capillary, 58.5 cm (48.5 cm effective length) ×75 μm i.d.; BGE, 200 mM borate buffer; pH, 10.0, 2.2% (w/v) β-CD [0.6% (w/v) (±)-VII]; temperature, 20°C; applied voltage, 15 kV; UV detection at 214 nm.

LITERATURE CITED

1. Kim NS, Choi JR, Cha JK. A concise, enantioselective synthesis of castanospermine. J Org Chem 1993;58:7096–7099.
2. Kobayashi Y, William AD, Tokoro Y. Sharpless asymmetric dihydroxylation of *trans*-propenylphosphonate by using a modified AD-mix-α and the synthesis of fosfomycin. J Org Chem 2001;66:7903–7906.
3. Beller M, Sharpless KB. Diols via catalytic dihydroxylation. In: Cornils B, Herrmann WA, editors. Applied homogeneous catalysis with organometallic compounds, 2nd ed. Weinheim: Wiley-VCH; 2002. Vol. 3. p 1149–1159.
4. Kolb HC, VanNieuwenhze MS, Sharpless KB. Catalytic asymmetric dihydroxylation. Chem Rev 1994;94:2483–2547.
5. Zaitsev AB, Adolfsson H. Recent developments in asymmetric dihydroxylations. Synthesis 2006;11:1725–1756.
6. Motorina I, Crudden CM. Asymmetric dihydroxylation of olefins using cinchona alkaloids on highly ordered inorganic supports. Org Lett 2001;3:2325–2328.
7. Bolm C, Maischak A. Asymmetric dihydroxylations using immobilized alkaloids with an anthraquinone core. Synlett 2001;1:93–95.
8. Song CE, Yang JW, Ha HJ, Lee S. Efficient and practical polymeric catalysts for heterogeneous asymmetric dihydroxylation of olefins. Tetrahedron Asymmetry 1996;7:645–648.
9. Jiang R, Kuang YQ, Sun XL, Zhang SY. An improved catalytic system for recycling OsO_4 and chiral ligands in the asymmetric dihydroxylation of olefins. Tetrahedron Asymmetry 2004;15:743–746.
10. Gong Y, Lee HK. Application of cyclam-capped β-cyclodextrin-bonded silica particles as a chiral stationary phase in capillary electrochromatography for enantiomeric separations. Anal Chem 2003;75:1348–1354.
11. Verleysen K, Sandra P. Separation of chiral compounds by capillary electrophoresis. Electrophoresis 1998;19:2798–2833.
12. Rizzi A. Fundamental aspects of chiral separations by capillary electrophoresis. Electrophoresis 2001;22:3079–3106.
13. Fanali S. Enantioselective determination by capillary electrophoresis with cyclodextrins as chiral selectors. J Chromatogr A 2000;875:89–122.
14. Hernández-Borges J, Frías-Garcíaa S, Cifuentes A, Rodríguez-Delgado MA. Pesticide analysis by capillary electrophoresis. J Sep Sci 2004;27:947–963.
15. Hoffstetter-Kuhn S, Paulus A, Gassmann E, Widmer HM. Influence of borate complexation on the electrophoretic behavior of carbohydrates in capillary electrophoresis. Anal Chem 1991;63:1541–1547.
16. Landers JP, Oda RP, Schuchard MD. Separation of boron-complexed diol compounds using high-performance capillary electrophoresis. Anal Chem 1992;64:2846–2851.
17. Oefner PJ, Vorndran AE, Grill E, Huber C, Bonn GK. Capillary zone electrophoretic analysis of carbohydrates by direct and indirect UV detection. Chromatographia 1992;34:308–316.
18. Jira T, Bunke A, Schmid MG, Gübitz G. Chiral resolution of diols by capillary electrophoresis using borate-cyclodextrin complexation. J Chromatogr A 1997;761:269–275.
19. Schmid MG, Wirnsberger K, Jira T, Bunke A, Gübitz G. Capillary electrophoretic chiral resolution of vicinal diols by complexation with borate and cyclodextrin: comparative studies on different cyclodextrin derivatives. Chirality 1997;9:153–156.
20. Lin CE, Lin SL, Liao WS, Liu YC. Enantioseparation of benzoins and eenantiomer migration reversal of hydrobenzoin in capillary zone electrophoresis with dual cyclodextrin systems and borate complexation. J Chromatogr A 2004;1032:227–235.
21. Zhao Y, Yang XB, Sun YL, Jiang R, Zhang SY. Enantiomeric separation of synthetic 2,3-dihydroxy-3-phenylpropionate compounds by β-cyclodextrin-modified capillary electrophoresis. J Chromatogr A 2006;1108:258–262.
22. Amberg W, Bennani YL, Chadha RK, Crispino GA, Davis WD, Hartung J, Jeong KS, Ogino Y, Shibata T, Sharpless KB. Syntheses and crystal structures of the cinchona alkaloid derivatives used as ligands in the osmium-catalyzed asymmetric dihydroxylation of olefins. J Org Chem 1993;58:844–849.
23. Minato M, Yamamoto K, Tsuji J. Osmium tetraoxide catalyzed vicinal hydroxylation of higher olefins by using hexacyanoferrate(III) ion as a cooxidant. J Org Chem 1990;55:766–768.
24. Wren SAC, Rowe RC. Theoretical aspects of chiral separation in capillary electrophoresis. I. Initial evaluation of a model. J Chromatogr 1992;603:235–241.
25. Wren SAC, Rowe RC. Theoretical aspects of chiral separation in capillary electrophoresis. II. The role of organic solvent. J Chromatogr 1992;609:363–367.
26. Wren SAC. Theory of chiral separation in capillary electrophoresis. J Chromatogr 1993;636:57–62.

CHIRALITY 20:84–95 (2008)

Molecular Homochirality and the Parity-Violating Energy Difference. A Critique with New Proposals

SOSALE CHANDRASEKHAR*

Department of Chemistry, Middle East Technical University, 06531 Ankara, Turkey

ABSTRACT Previous proposals for the origin of molecular homochirality, based on the effect of the weak neutral current (WNC) on enantiomers, and the amplification of the resultant parity-violating energy difference (PVED), are possibly flawed. The additive amplification of PVED in crystals and polymers ("Yamagata hypothesis") cannot lead to detectable levels of optical activity, the original theory apparently overestimating PVED by a factor equal to Avogadro's number. An alternative theory based on the irreversible and spontaneous evolution of a dynamically fluctuating system is apparently impractical. However, the nonlinear amplification of PVED via autocatalytic polymerization may be possible as indicated by a simplified physico-chemical approach. This may also occur during crystallization and melting, and form the basis of the second order asymmetric transformation. (Thus, reported differences in the melting points of enantiomers in several cases may well be real). Also, the preponderance of racemic compounds over conglomerates may be based on the destabilization of the conglomerate by the action of the WNC on the crystalline lattice. The WNC may also be involved in the anomalous scattering of X-rays, which possibly arises from their circular polarization: the current theory would need to be revised accordingly. *Chirality 20:84–95, 2008.*

KEY WORDS: anomalous X ray scattering; autocatalytic polymerization; circular polarization; conglomerate; crystallization; origin of chirality; origin of life; racemic compound; weak neutral current

INTRODUCTION

Homochirality and the Origin of Life

The search for the origin of life is a fundamental quest at the frontiers of modern science, but one that is predicated on the question of the origin of molecular chirality. This is because the overwhelmingly homochiral nature of the present biosphere strongly suggests that homochirality is a prerequisite for the emergence and sustenance of life.[1–4]

The question of the origins of molecular homochirality forms a part of the larger question of the origins of organic molecules and their evolution, first into the early macromolecules and thence to the primitive life forms.[1] It is currently believed that prebiotic chemical evolution began with the synthesis of the simpler hydroxy and amino acids, by the action of lightning on the reducing atomosphere of the early earth. These conditions also afforded the purine and pyrimidine bases of the nucleic acids via a Fischer–Tropsch type process. The early sugars are believed to have formed from formaldehyde and lime (the "formose reaction"). Subsequent chemical events would form the nucleotides and their polymers, leading to the emergence of autocatalytic and self-replicating systems (the "RNA world").[5] The evolution of molecular homochirality would have to fit into this scheme at an appropriate stage.

The origin of molecular homochirality has (understandably) been the subject of much speculation and inquiry in recent decades. Fundamentally, the essentially homochiral nature of the biosphere raises the intriguing question of a possible universal chiral influence that predated the emergence of the first organic molecules. The possible prior existence of such an essentially nonchemical chiral force, perhaps dating back to the origins of the universe itself, is of considerable philosophic allure, as it indicates that the drive towards homochirality—and the subsequent emergence of life—were predestined (Pasteur had reportedly speculated upon this possibility[3,6]).

Indeed, theories of the origin of optical activity in nature are apparently subject to the philosophic dichotomy of chance and determinism. A particularly fascinating deterministic theory proposes that the weak neutral current (WNC), a minuscule chiral force binding the atomic nucleus together,[2] is manifest in chemical compounds, and

Sosale Chandrasekhar while on Sabbatical leave from Department of Organic Chemistry, Indian Institute of Science, Bangalore 560012, India
*Correspondence to: Sosale Chandrasekhar, Department of Organic Chemistry, Indian Institute of Science, Bangalore 560012, India.
E-mail: sosale@orgchem.iisc.ernet.in
Received for publication 22 January 2007; Accepted 17 October 2007
DOI: 10.1002/chir.20502
Published online 3 December 2007 in Wiley InterScience (www.interscience.wiley.com).

was somehow amplified over evolutionary time to the present levels of homochirality.[3]

Other deterministic theories have involved a chiral physical force of some sort, notably circularly polarized light,[4] which possibly affected the stabilities or reactivities of chiral molecules differentially, thus leading to an excess of one of the enantiomers. Among the chance theories, accidental crystallization phenomena related to the second order asymmetric transformation, have been seriously considered.

The deterministic theories are apparently rather more reasonable, considering that chance cannot satisfactorily explain the uniformity and the ubiquity of the chiral bias of the biosphere. (Thus, the D-sugars and the L-amino acids predominate overwhelmingly in all parts of the world.) However, it must not be assumed that "chance" implies that the same accidental event happened at different locations (with the same chiral bias). It is possible that the accidental production of an enantiomerically enriched chiral chemical species gradually evolved into the early life forms at a particular location. These primitive species—perhaps even the "twilight zone molecules" such as early RNA—could have catalyzed their own further growth, thus simultaneously propagating molecular homochirality and life.

It is also noteworthy that there is a school of thought that strongly believes that the origins of molecular homochirality are extra-terrestrial.[7,8] This is because of the minuscule magnitude of WNC and the inherent difficulty of its amplification under terrestrial conditions. Accordingly, it has been proposed that molecular homochirality first arose under the extreme conditions prevalent in outer space, e.g., in supernovae, and was transmitted to (prebiotic) earth via meteorites, comets, etc.

In view of the fundamental importance of the question of the origin of optical activity in nature (as briefly discussed earlier), this area of scientific enquiry has been fertile ground for both imaginative speculation and ingenious experimentation. The area is also well served by several excellent reviews and monographs, written by workers active in the area, who are thus able to provide contemporary and authoritative accounts of the developments.[1–4]

This selective review is focused on a particular aspect concerning the effects of the WNC, briefly aforementioned. The WNC is a manifestation of a general "parity violation" in nature, which renders the enantiomers of a chiral molecule energetically nonequivalent. The possible amplification of this infinitesimally small effect—the "Yamagata hypothesis"—has been proposed to account for the origin of natural optical activity.[9,10] This proposal is critically evaluated in this article, and an alternative viable mechanism, based on autocatalytic polymerization, is proposed to explain biomolecular homochirality.

In fact, it is possible that the WNC lurks in several stereochemical phenomena without being implicated (possibly because of its controversial and esoteric nature). Particularly intriguing is the possibility that it is the basis of the anomalous scattering technique of X-ray crystallography, which is employed to assign the absolute configurations of enantiomers.[11] This is explored in some detail later in this article.

Also explored is a possible extension of the effect of the WNC on the stability of crystalline enantiomers, which might bear upon the relative stabilities of the two types of crystalline racemate—conglomerates and racemic compounds. The fact that the vast majority of racemates exist as racemic compounds rather than as conglomerates remains intriguing.[4,12] A possible mechanism to explain this relative preponderance based on the WNC is presented herein. (Also discussed in passing are a few recent proposals that implicate the WNC to explain certain experimental observations, but apparently without justification).

The essential problem in linking the WNC with chemical phenomena is its minuscule magnitude ($\sim 10^{-20}$ per molecule), which renders it beyond the limits of detection with the usual experimental techniques. Clearly, amplification mechanisms would need to be enormously efficient to bring the WNC into the normal range of detection. Further details of the nature of previous attempts at accomplishing this and of the present proposals are to be found in the discussion below.

DISCUSSION

Current State of the Art—a Brief Review of Previous Approaches

Parity violation and its linear amplification. An interesting deterministic theory is based on the effect of the WNC, which primarily binds the components of the atomic nucleus together. The WNC has a chirality associated with it, which can be transmitted to a molecular framework from the component atoms, via the electrons of the chemical bonds. If the molecular framework is chiral, the corresponding enantiomers would then have different energies: this is the molecular equivalent of "Parity Violation," which was originally applied to the case of electron spin. The differing energies of a pair of enantiomers is termed the "parity violating energy difference" (PVED).

Although it is tempting to consider PVED as the origin of molecular homochirality, a fundamental stumbling block is the very small magnitude of the effect of the WNC (the "electroweak effect"). The electroweak effect, in fact, has been estimated to be as low as 10^{-20} E_h, so that it is normally undetectable. However, it has been postulated that it can be amplified to levels that permit detection by conventional experimental techniques.

An early theory by Yamagata was based on the "accumulation principle," according to which the PVED was amplified to detectable levels via a linearly additive process, during the polymerization of enantiomeric monomers (e.g., nucleotides).[9] This theory was later extended to the case of crystallization, in which the amplification was believed to occur during the sequential addition of enantiomeric unit cells, leading to enantiomorphic crystals.[10] In both these processes, the ratio of enantiomeric products r was believed to be related to the "advantage factor" ε (as shown in eqs. 1 and 2, n being the number of cycles of polymerization or addition of unit cells (in the case of crystallization). (ΔE_{pv} is the PVED in terms of Gibbs free energy, k_B is Boltzmann's constant and T the absolute temperature.)

However, there are a number of problems with this simplistic approach, as discussed below (these arguments have been presented in preliminary form[13]).

$$r = e^{n\varepsilon} \cong 1 + n\varepsilon \quad (1)$$

$$\varepsilon = \Delta E_{pv}/k_B T \quad (2)$$

Assuming a value for ε of $\sim 10^{-17}$, n should be $\geq 10^{17}$ for r (a measure of the enantiomeric excess in eq. 1) to be detectable.[10] Even if the reaction were to be performed on a nanomolar scale, this would require 10^8 moles of monomer.

Another problem concerns yields. Even assuming a yield of 99% in each step of the polymerization cycle, the final yield after 10^{17} cycles would be practically 0%: the detailed calculation shows that the amount of monomer needed to carry out the above scheme would then exceed a trillion powers of ten (in tons).* (The mass of the earth is $\sim 10^{19}$ tons!) These arguments also imply that the Yamagata scheme cannot lead to even a single molecule of the polymer with 10^{17} monomer units.*

Furthermore, it is noteworthy that the correct expression for ε would employ R (the gas constant) rather than k_B (Boltzmann's constant), as in eq. 3. This follows the usual convention for relating the rate constant to the corresponding free energy of activation via the Eyring equation.[14] In eq. 3, $\Delta E'_{pv}$ is the PVED in J mol^{-1} and is related to ΔE_{pv} (eq. 2) as in eq. 4 (N_A is Avogadro's number). The PVED per molecule would then be ΔE_{pv}, and the corresponding "advantage factor" would be ε' (eq. 5).

$$\varepsilon = \Delta E'_{pv}/RT \quad (3)$$

$$\Delta E'_{pv} = \Delta E_{pv} N_A \quad (4)$$

$$\varepsilon' = \varepsilon N_A^{-1} = (\Delta E'_{pv} N_A^{-1})/RT = \Delta E_{pv}/RT \quad (5)$$

In fact, the original Yamagata scheme employed $\varepsilon \sim 10^{-7}$ and implied the sequential polymerization of $\sim 10^8$ molecules of monomer. (Note that this would produce only a single molecule of the polymer. These assumptions were not explicitly stated, but neither were the earlier discussed problems of scale mentioned.) In such a case, the appropriate "advantage factor" (cf. eq. 1) would be ε' rather than ε. With (now revised) $\varepsilon \sim 10^{-17}$, and hence $\varepsilon' \sim 10^{-40}$, the scheme would require the polymerization of $\geq 10^{40}$ molecules of monomer, or $\sim 10^{17}$ moles (a prohibitively large amount). Thus, the scheme appeared viable because of the enormous overestimation of either ε or n.

These arguments similarly invalidate the crystallization analog of the Yamagata process.[10] Crystal growth involves the linear and sequential addition of individual unit cells, so the appropriate "advantage factor" would be ε' (not ε). Thus, giant crystals consisting of $\sim 10^{40}$ unit cells (representing 10^{17} moles) would need to be grown, for PVED to be manifest. Again, these large numbers indicate prohibitive quantities of materials, to say the least. The following thermodynamic argument is also illuminating.

In the Yamagata proposal, the "accumulation" is believed to accrue during the linear and sequential addition of monomer units. This essentially implies that the PVEDs between the (enantiomeric) transition states add up (linearly) over n cycles. The process may be envisaged as occurring at either a macroscopic level or a (hypothetical) microscopic level. The macroscopic reaction would involve a mole of material, or some fraction thereof. The microscopic reaction would involve the growth of a single molecule of each enantiomeric polymer. The PVED for each cycle of the macroscopic reaction would be N_A times that of the microscopic reaction (1 mole being employed). Assuming a PVED of 10^{-11} J mol^{-1}, the most "daring" recent estimate,[2] and to obtain a detectable level of accumulation, say 1 J, the macroscopic process would need to occur over 10^{11} cycles of 1 mol each (total of 10^{11} moles, assuming 100% yields at each step). For the microscopic process, the corresponding PVED would be $\sim 10^{-34}$ J/cycle; in order to obtain a detectable level of accumulation (1 J), the process would need to occur over 10^{34} cycles (total of 10^{34} molecules or 10^{11} moles). Thus, although the macroscopic and microscopic processes are distinct, both are invalidated by the same problems of scale.

Yet another problem with the Yamagata approach is that a grossly oversimplified kinetic scheme was employed to represent the growth of a polymer. Thus, the overall enantiomer ratio was represented as the product of the enantiomer ratio of each step of the polymerization process. However, a rigorous approach would apply the methods employed for treating consecutive reactions, which (apparently) would be very complex for the case of polymerization. However, this is of no consequence in view of the above fundamental invalidation of the Yamagata approach. Similar comments apply to the criticism by Bonner that the Yamagata approach overlooks the formation of diastereomers.[15] It appears that earlier treatments not only overestimated the amplification of PVED by a factor of N_A, but also misinterpreted the significance of the number of growth cycles.[9,10]

Clearly, the above linearly-additive amplification mechanisms cannot lead to detectable optical activity, without involving prohibitive quantities of material.

PVED control of the irreversible evolution of a randomly fluctuating (racemic) state: "Anticatalysis."[16,17] An interesting mechanism for PVED amplifi-

*The reasoning is as follows: the yield (%) at the end of m polymerization cycles would be $100 \times (0.99)^m$; for $m = 10^{17}$ this would be $\sim 10^{-p}$ where $p = 10^{14}$. Thus, 10^p moles of monomer would finally yield 1 mole of polymer; note that this is in addition to the 10^{16} moles that would be added along the way! A single molecule of polymer would require $\sim 10^p \times 10^{-23}$ moles of monomer, still an astronomical quantity. The following argument is more straightforward and illuminating: even assuming 100% yield at each step, if 1 g of monomer is added at each step, the total amount of monomer required for 10^{17} steps is 10^{17} g.

cation that has been seriously reconsidered in recent times, is based on an earlier (1953) mechanism based on autocatalysis.[16] This proposal depends on the idea that a particular enantiomeric product in a reaction can be a catalyst for its own production, and an "anticatalyst" for the production of its opposite enantiomer. This mechanism has been resuscitated in recent years with the incorporation of advanced nonequilibrium kinetic models and sophisticated computer simulations.[17]

The proposal is based on a model chemical system which autocatalytically produces enantiomeric species from achiral precursors. With an unrestricted supply of precursors the system drifts away from equilibrium and approaches a randomly fluctuating metastable state in which both chiral products are being produced. At this stage ("bifurcation point") a small perturbation suffices to tilt the system, which then produces only one of the enantiomeric products. The system thence evolves irreversibly under the influence of the perturbation, which may be as weak as the electroweak effect. For a detectable level of amplification, however, the system needs to evolve over a relatively long period of time.

$$S + T \rightleftharpoons X_{\mathrm{L(D)}} \tag{6}$$

$$S + T + X_{\mathrm{L(D)}} \rightleftharpoons 2X_{\mathrm{L(D)}} \tag{7}$$

$$X_{\mathrm{L}} + X_{\mathrm{D}} \rightarrow P \tag{8}$$

The model considered is shown in eqs. 6–8, wherein S and T are the achiral precursors, $X_{\mathrm{L(D)}}$ are the enantiomeric products, and P is the *meso* product of a cross-reaction between the enantiomers $X_{\mathrm{L(D)}}$. Note that the final formation of P (eq. 8) is irreversible, whereas the initial formation of $X_{\mathrm{L(D)}}$ (eq. 6) and its further autocatalytic production (eq. 7) are reversible.

The original 1953 proposal was based on the concept of "anticatalysis,"[16] which seems clearly unviable in the light of transition state theory for solution state processes.[14] "Anticatalysis" apparently implies that the formation of a transition state can be suppressed in some way, but this is generally impossible. The recent version replaces the anticatalysis idea with that of "mutual destruction," by which the enantiomers effectively destroy each other by forming the *meso* cross-product (eq. 8).[17] This is apparently a key requirement in the above scheme, as it results in the irreversible removal of the PVED-disfavored enantiomer: this apparently leaves behind a trace excess of the PVED-favored enantiomer for further autocatalytic renewal.

This nonequilibrium kinetic scheme is reinforced by computer simulations, and is apparently compelling. However, it is practically impossible to test experimentally (because of the reaction period of several thousand years), although, of course, this does not disprove it. Importantly, it apparently suffers from critical problems of scale, which render its status uncertain. Thus, a simple calculation indicates the formation of millions of tons of the cross-product P.* In the early stages, apparently, P would be the major product, although the PVED-favored enantiomer $X_{\mathrm{L(D)}}$ is expected to accumulate gradually. Thenceforth, the process as a whole, and (in particular) the formation of the PVED-favored enantiomer, would be accelerated (presumably enormously) by autocatalysis (eq. 7). This stage may well involve the turnover of prohibitively large quantities of material.

Another problem with the scheme is the finding that even the minuscule electroweak effect can tilt the "precarious balance" at the bifurcation point. Since other minor chiral fluctuations of the same order would be generally present in chemical systems, the spontaneous generation of optical activity should be much more common than observed. The chiral fluctuations would involve production of a minuscule excess of one enantiomer in a reaction, etc. This was possibly present in the prebiotic scene, and would be in the present biosphere, which is predominantly homochiral.

Some recent reports. Intriguingly, the Yamagata and related linear amplification mechanisms continue to form the backdrop for investigations into the origins of biomolecular chirality.[18,19] Thus, crystallization of tris(1,2-ethanediamine)Co(III) and tris(1,2-ethanediamine)Ir(III) reportedly led to enantiomerically enriched material, which was explained on the basis that the PVED was proportional to the sixth power of the atomic number.[18] Thus, the possibility of observing PVED is greater in the cases involving heavier elements (Co and Ir in this case). Although the experimental results are of interest, the Yamagata mechanism (as the crystallization analog) was invoked as explanation.

Another interesting recent study reports that the enthalpy changes in the helix-to-coil transitions of D- and L-polyglutamic acid are consistently different (by ~10%).[20] An intriguing nonconventional explanation, involving the PVED-based preferential affinity of *ortho*-H_2O for the L-polyamide, that was also amplified autocatalytically during the helix-coil transition, was proposed. This is almost certainly invalid for two reasons. Firstly, *ortho*-H_2O is an achiral molecule and there is no reason why it should preferentially stabilize one of the enantiomeric polymers (but see later). Secondly (and more importantly), autocatalytic amplification provides only a kinetic pathway, and cannot explain the observed thermodynamic differences. These most likely arise from impurities as the study employed commercial samples of the enantiomeric polymers without further purification. The observed solvent isotope effect in D_2O may also be thus explained. In fact, the authors base

*The reasoning is as follows. The reactions are considered to occur in a volume (V) $\sim 10^9$ l, with reactant concentrations of $\sim 10^{-3}$ M. The bimolecular rate constant (k) for the irreversible formation of the cross-product P (eq. 8) is 10^{-3} M^{-1} s^{-1}. Assuming a steady supply of $X_{\mathrm{L(D)}}$, the rate of formation (v) of P would be: $v = k[X_{\mathrm{L}}][X_{\mathrm{D}}] = 10^{-9}$ M s^{-1}. If the reaction occurs over a period t and a volume V, the amount of product P formed = vVt moles. With $t = 15 \times 10^3$ y, $V = 10^9$ l, and $v = 10^{-9}$ M s^{-1}, $> 10^{11}$ moles of P would be formed. If the molecular weight of P $\sim 10^2$, this indicates that $\sim 10^7$ tons of P would be formed. This does not take into account the (possible) increase in [X] because of autocatalysis (eq. 7).

their explanation on their hypothesis of "magnetic correspondence,"[21] according to which the L-enantiomeric polymer has a higher PVED-induced magnetism, thus preferentially interacting with the magnetic field of *ortho*-H_2O. The status of this proposal is unclear, and would largely depend on whether the diamagnetic susceptibilities of enantiomers are measurably different. In any case, however, the broad conclusions of the study seem unlikely for the aforementioned reasons.

A very recent article by Lahav et al.,[22] apart from offering a timely and critical evaluation of the current status of the debate on PVED amplification, focuses on an earlier report by Shinitzky et al. that claimed the differential growth and dissolution of crystalline L- and D-tyrosine.[23] Lahav et al. attribute these observations to artifacts deriving from unidentified impurities. They based this conclusion on their own detailed investigations, involving the growth and dissolution of crystals in the presence of intentionally added impurities. Importantly, they draw attention to the effect of microscopic chiral impurities (e.g., dust) in the environment on crystal growth, a view shared by this author on the basis of results from his own laboratories.[24]

These results indeed introduce a fundamental and general caveat that applies to all experimental studies of the origin of chirality: as the biosphere (including the atmosphere) is laden with chiral matter, the contamination of any experimental set-up by chiral dust, pollen, etc., can never be entirely ruled out. Viewed in this light, the experimental search for the origin of molecular chirality is doomed to uncertainty and skepticism. It is indeed sobering—if not depressing—to consider the fact that, to the extent that a firm answer to the question of the origin of molecular chirality does not emerge, the origin of life will remain a mystery. Evolutionary studies would then be confined to arriving at a set of most probable scenarios, based on sound theorizing and supported by appropriate experimentation. An element of doubt, however, will always attach to the results—defining, apparently, a fundamental limit of experimental science.

New Proposals Involving PVED: Autocatalytic Polymerization; Anomalous Scattering of X-rays; Conglomerates Versus Racemic Compounds

PVED amplification via autocatalytic polymerization. As has been elaborated in the previous section, linearly-additive amplification of PVED as represented by the Yamagata and analogous schemes is practically unviable. Therefore, alternative strategies need to be explored for a viable mechanism for PVED amplification to be developed. Interestingly, in view of the enormous levels of amplification needed to bring PVED (possibly) into the range of detection, autocatalytic systems which are characterized by exponential growth rates seem to offer some promise.[25–27] The following treatment is intended to explore the scope and demonstrate the feasibility of this approach (but is not to be construed as "conclusive proof").

For the simple autocatalytic reaction shown in eq. 9, the rate of growth of the product is represented by eq. 10 (based on the treatment of Atkins[25]). $([A]_0$ and $[P]_0$ are the initial concentrations of reactant and product respectively, x is the increment in $[P]$ at time t, and k is the rate constant.) An analogous equation would apply for the (noncompetitive) conversion of A to a different product P', and the ratio $[x]/[x']$ would be given by eq. 11; (a' and b' are analogs of a and b respectively). This can be simplified to eq. 12 if it be assumed that $b \sim b' \sim 0$, which is reasonable if $[P]_0 \sim 0$, and a and a' are not "excessively" large. Equation 12 again simplifies to eq. 13 if $at \sim a't > 0$. Now, suppose that k and k' are the rate constants for the formation of enantiomeric products P and P' from an achiral precursor, and that their free energies of activation differ by PVED. It then follows that $k \sim k'$, so that $[x]/[x'] = 1$ for all practical purposes. Thus, a simple autocatalytic system apparently fails to show any detectable levels of PVED amplification.

$$A + P = 2P \tag{9}$$

$$x/[P_0] = (e^{at} - 1)/(1 + be^{at})$$
$$a = ([A_0] + [P_0])k; \quad b = [P_0]/[A_0] \tag{10}$$

$$x/x' = (e^{at} - 1)(1 + b'e^{a't})/(1 + be^{at})(e^{a't} - 1) \tag{11}$$

$$x/x' \sim (e^{at} - 1)/(e^{a't} - 1) \tag{12}$$

$$x/x' \sim e^{(a-a')t} \quad (a - a') = ([A_0] + [P_0])(k - k') \tag{13}$$

The above treatment, however, leads to interesting results upon extension to the case of autocatalytic polymerization. A formal treatment of the kinetics of autocatalytic polymerization would be mathematically complex and beyond the scope of this review,[28–31] but the simplified approach described below is useful in the present context. In fact, the possibility that terrestrial homochirality originated in autocatalytic polymerization has been explored in a few recent articles,[28,29] but apparently inconclusively at least *vis-à-vis* PVED amplification. These mathematical treatments apparently extend earlier approaches, and it remains to be seen whether or not they bear fruit practically. The simplified physico-chemical approach presented below, however, is apparently valid at least under the conditions described herein.

Consider the polymerization sequence shown in Scheme 1, involving the successive addition of Y n times to A, leading finally to the polymer P_n via the corresponding intermediates B, C, etc. The kinetics of this process can be approached with the help of the steady state approximation to arrive at eq. 14 (the details of the deriva-

Scheme 1.

tion are to be found in the Appendix). The key simplifying assumptions are: (i) there is a steady input of Y into the system, so $[Y]$ remains essentially constant; (ii) reversibility of all intermediate steps is negligible, and the final formation of P_n is totally irreversible (the reaction is thus thermodynamically driven); the rate constants of all the steps are nearly identical. Under these conditions the reaction is approximately a pseudo first order process (cf. eq. 14), with κ being a "pseudo rate constant" derived from the steady state treatment.

$$\mathrm{d}[P_n]/\mathrm{d}t = \kappa^{\mathrm{n}}[A] \tag{14}$$

$$x_n(d)/x_n(l) \sim \mathrm{e}^{(a-a')t}$$

$$(a - a') = ([A_0] + [(P_n)_0])[(\kappa_\mathrm{d})^n - (\kappa_\mathrm{l})^n)] \tag{15}$$

$$x_n(d)/x_n(l) \sim \exp[([A_0])t(\kappa_\mathrm{d})^n(n\varepsilon)] \tag{16}$$

Furthermore, consider the possibility that the final product P_n catalyzes its own sequential formation, so the above kinetic treatment can (possibly) be applied (cf. eqs. 9–13). Also consider that two enantiomeric sequences operate to produce the enantiomeric products $P_n(d)$ and $P_n(l)$. Their relative rates of growth would then be represented by eq. 15 via analogs of eqs. 10–13. Furthermore, if the free energies of activation corresponding to the sequential rate constants for the formation of $P_n(d)$ and $P_n(l)$ differ by PVED, eq. 16 follows (details being in the Appendix). This shows that very high levels of optical activity would arise even for low levels of polymerization: with $\varepsilon \sim 10^{-40}$, $n = 40$, $\kappa_\mathrm{d} \sim 10$, $t[A]_0 \sim 10^{-1}$ (with appropriate units) the relative growth rate would be $\sim e^4$.

Key to the success of this scheme is the factor $(\kappa_\mathrm{d})^n$ which largely overcomes the low value of ε. $(\kappa_\mathrm{d})^n$ derives from the sequential polymerization process, which is, therefore, critically important for the success of the proposed scheme. In this scheme the chiral selectivity, $x_n(d)/x_n(l)$, depends exponentially on the chain length n (eq. 16), as opposed to the linear dependence in the Yamagata scheme (eq. 1). Therefore, the chiral selectivity can be large even when n is relatively small.

Note that a value of $\varepsilon \sim 10^{-40}$ (corresponding to ε', cf. eq. 5) has been employed, to indicate the growth of a single molecule of the polymer. The aforementioned chain length of $n = 40$ implies the uptake of 40 moles of monomer for every mole of polymer. To reiterate, therefore, the factor of $(\kappa_\mathrm{d})^n$ resulting from the autocatalytic polymerization sequence, obviates the need for prohibitive quantities of material, as was the case with the Yamagata and related schemes.

Therefore, the possibility that autocatalytic polymerization can amplify PVED to detectable levels of enantiomeric excess is worth further consideration, both experimentally and theoretically. Possible examples would include the polymerization of amino acids and nucleotides, this also indicating that PVED amplification possibly occurred during molecular evolution synchronously with the arrival of the first biopolymers. (The process in the case of RNA has been explored in a recent paper.[31]) It is noteworthy that complex biopolymers remain catalysts par excellence to this day, thus reinforcing the above autocatalysis proposal.

Crystallizations. A possible analog of autocatalytic polymerization is crystallization, in which the surface of the crystal acts as a template for its own further growth. Interestingly, there are several claims of PVED amplification involving crystallization, and in the light of the above proposal, it is possible that some of these may be valid. Unfortunately, however, it is also true that crystallization is highly sensitive to trace (chiral) impurities. It is not the intention here to slight investigators or pass judgement on their work; as discussed at the end of the previous section, all such studies are subject to the caveat of chiral contamination. The article by Lahav et al. offers a comprehensive and critical summary of the state of the art,[22] and should be consulted in this regard.

Two studies from this author's laboratories exemplify the above arguments. In one, an apparent PVED amplification during the formation of inclusion compounds between urea and racemic long chain esters, was proved to be possibly due to chiral dust.[24] In another study, a consistent difference in the melting points of the enantiomeric asparagines was apparently confirmed.[32] (Pasteur resolution of the conglomerate led to the pure enantiomers, possible chiral contamination with auxiliaries being thus avoided.) Interestingly, melting may be viewed as the reverse of crystallization and possibly as autocatalyzed, in the sense that the liquid melt hastens the further melting of the crystal.

Therefore, the possibility that crystallization processes can be considered as autocatalytic systems apparently needs to be explored further, both theoretically and experimentally. A better understanding of such processes would indicate whether or not PVED amplification via crystallization can be considered part of a likely scenario for the emergence of life.

Second order asymmetric transformations. Interestingly, the above ideas can be extended to the case of crystallization-induced spontaneous generation of optical activity, more often termed "second order asymmetric transformation (SAT)."[33,34] An SAT process occurs when the enantiomers of a chiral compound interconvert relatively rapidly in solution during a concomitant crystallization: if one of the enantiomers begins to crystallize out it shifts the solution state equilibrium between the enantiomers, so that the resulting crystals are enantiomerically enriched. A conglomerate is usually required for the process to be feasible. It is currently believed that the initial crystallization is a chance event, possibly deriving from accidental nucleation of one of the enantiomers. This is apparently supported by the observation that either of the two enantiomers may result from the process, which is thus beyond experimental control *vis-à-vis* the chirality of the crystallized product.

A problem with the above explanation is that chance is not meaningful at the molecular level, as molecular phenomena involve an extremely large number of discrete events occurring randomly and rapidly. In such a case, the

probability of any particular event being selected in preference to an "opposite" event is practically zero. In other words, during an SAT process, not only is the probability of initial nucleation identical for the two enantiomers, but also the nucleation of one of them should be rapidly followed by the nucleation of the other.

An alternative explanation for SAT involves the preferred nucleation of the PVED stabilized enantiomer, that is autocatalytically amplified during crystallization (*vide supra*). "Nucleation" has a broad reference here, and could also mean the formation of a precrystalline aggregate. However, although this explains the spontaneous generation of optical activity, it does not explain the fact that the PVED destabilized enantiomer may also be obtained, apparently with nearly equal probability. (Although a bias towards one of the enantiomers is often observed during SAT, the statistical significance of this is unclear. As always, the problem of chiral contaminants remains.)

An interesting and possible explanation for the above, is that the PVED destabilized enantiomer is obtained if the solution becomes supersaturated in the PVED stabilized enantiomer. "Supersaturation" is a general term referring to a case in which the thermodynamically stable phase does not separate out of a mixture.[35] In the case of SAT it is conceivable that the precrystalline aggregates of both the enantiomers are formed competitively, and that crystallization is initiated by the collapse of the PVED stabilized aggregate. Supersaturation corresponds to the state when the latter event is slow, thus allowing the PVED destabilized enantiomer to collapse to a crystal.

It should be noted that in the early stages of crystallization PVED amplification would be minimal, resulting in a fine balance between chance and determinate mechanisms. The formation and subsequent collapse of precrystalline aggregates, however, appears fundamentally different from simple nucleation, which is statistically far more random in principle. It is plausible that the collapse of the aggregate initiates rapid autocatalytic growth and the destruction of the (opposite) enantiomeric aggregate. (The enantiomeric aggregates are presumed to be in equilibrium during an SAT.) The formation of precrystalline aggregates, therefore, apparently offers a window of opportunity for a determinate mechanism to operate. The above tentative proposals, of course, await further work and developments.

Conglomerates versus racemic compounds. Crystalline racemates are of two forms: "racemic compounds" and "conglomerates."[4,12] In the former both enantiomers are present (generally) in the same centrosymmetric crystal lattice; in conglomerates the enantiomers crystallize separately in enantiomeric crystal lattices (hence "spontaneous resolution"). Intriguingly, it has been known for long that the number of racemic compounds far exceeds that of conglomerates.

A thermodynamic basis for this has also been inferred from Wallach's rule,[36] which states that the density of a racemic compound is generally greater than that of its corresponding chiral crystal (i.e., conglomerate form). This led to a belief that the presence of opposite enantiomeric pairs in a crystalline lattice leads to better packing. It was also proposed that the lattice of a racemic compound benefits from the entropy of mixing,[12] because of the presence of both enantiomers, and is hence thermodynamically preferred over the corresponding conglomerate form.

However, it has also been argued that any listing of racemic comounds and corresponding conglomerates would be statistically biased in favor of the former,[36] as such a list can only be drawn up when the racemic compound is more stable, the corresponding chiral forms then being obtained via resolution. (In other words, chiral crystals, i.e., conglomerates, may be obtained regardless of their stability, whereas racemic compounds may be obtained only when they are more stable.) It should be noted, however, that this argument applies only to the simultaneous listing of racemic compounds and conglomerates, and thus only in the context of Wallach's rule. Therefore, the general validity of this objection may not be assumed.

In other words, the general experimental observation that racemic compounds are generally encountered far more often than conglomerates cannot be ignored. This is highly likely to have a general thermodynamic basis. The argument based on the entropy of mixing is also an intriguing one (*vide supra*), and apparently only applies to the case of single crystals of racemic compounds and corresponding chiral forms. In a collection of such crystals, however, the entropy of mixing for both forms would appear to be identical as they include both the enantiomers.[36]

On the other hand, it is unclear whether the entropy of mixing should be considered at the molecular or crystalline level, in these cases. In the formation of a conglomerate, spontaneous resolution has occurred and the enantiomers are located in separate lattices, separated in space. The individual crystal would then need to be considered as the chiral object, and not the molecule. In other words, the chiral crystals are mixed but not the molecules. The entropy of mixing would then be far less at the level of the crystals as these are far fewer in number than molecules.

This is apparently a conceptual gray area at present, and a resolution of the paradox must await further work. To this writer, it appears that the entropy of mixing of a conglomerate should lie between the values for the homochiral and racemic compound forms, i.e., 0 and $Rln2$ respectively. The exact value may also depend on the state of crystalline subdivision, as this will determine the number of chiral crystals present (*vide supra*). Thus, a collection of relatively small crystals would possess greater entropy (per mole), which would approach the limiting value of $Rln2$ as the crystalline size decreases. This implies that conglomerates would tend to produce smaller crystals, but crystal size is determined by a variety of factors.

It is also noteworthy that the entropy of mixing ($=Rln2$) amounts to <2 kJ/mol in terms of Gibbs free energy at normal temperatures. Although this is not insubstantial, the enthalpic difference between a racemic compound and its conglomerate form may well be larger than this, and thus outweigh the entropic effect. It seems unlikely, therefore, that entropic effects would explain the preferred formation of racemic compounds. Intriguingly, in fact, it is possible that PVED has a role to play, as discussed below.

Possible role of PVED. The manifestation of the WNC in chemical compounds is believed to occur via a mechanism akin (but not identical) to that involved in the coupling of nuclear spins through the intervening chemical bonds.[2,3] It is thus that the WNC is transmitted to the molecular skeleton. It is interesting to consider an extension of this mechanism to the multitude of weak interactions that compose a crystalline lattice. These are usually van der Waals and related forces, hydrogen bonding, π stacking, etc., that are evidenced by the short contacts obtained from X-ray diffraction analysis.[37] Interestingly, the operation of the WNC through these weak "bonds" would (possibly) permit the PVED to manifest itself at the level of the entire lattice, overlaid over the normal molecular level PVED, which would be identical for racemic compound and conglomerate.

Furthermore, the effect of such an operation of the WNC at the lattice level would be different for racemic compounds and conglomerates. In the case of a racemic compound there would be no PVED as the lattice is (generally) centrosymmetric. In the case of the conglomerate, however, the WNC would destabilize one of the enantiomeric lattices, and with it the overall conglomerate form. The autocatalytic amplification of this relative destabilization during crystallization would ensure that the racemic compound forms preferentially.

The key assumption in the above argument is that the PVED arises from the destabilization of the "wrong" enantiomer rather than the stabilization of the other. In principle, the PVED may arise either from the stabilization of one enantiomer or the destabilization of the other (or, of course, both). If the WNC generally stabilizes a molecular skeleton, its effect at the lattice level would be similar both on the racemic compound and one enantiomer; however, the "wrong" enantiomer would be less stabilized, and (overall) the conglomerate form would be relatively destabilized. These possibilities are shown in Figure 1.

An interesting question that now arises is why conglomerates form in some cases. A possible answer may be that the molecular and lattice level PVEDs may not always support each other, so the overall destabilization is nullified; alternatively, the lattice level PVED may be negligible *per se*: in all such cases conglomerates may be preferred on the basis of other lattice packing considerations.

The general preponderance of racemic compounds *vis-à-vis* conglomerates is an intriguing phenomenon that is not easily rationalized. Earlier explanations based on the effects of symmetry on crystal packing (cf. Wallach's rule), entropy, etc., seem unlikely to be generally valid. The above explanation based on the lattice level PVED represents a conceptual departure from earlier approaches, and offers a fundamental deterministic basis for the phenomenon. Again, however, these tentative proposals await further developments in our understanding of the WNC and its chemical manifestation.

Anomalous scattering of X-rays. An important extension of the X-ray crystallographic method of structure determination is the technique based on anomalous scattering (or dispersion). This enables the direct determination of the absolute configuration of a chiral molecule and has come to play a key role in modern stereochemistry.[11,38–41]

The current theory is apparently based on a breakdown of Friedel's law when X-ray scattering by electrons occurs via absorption (hence "anomalous"). This resonance condition occurs when the frequency of the X-rays corresponds with the energy required to excite the valence electrons of the scattering atom (scattering occurring at the "absorption edge"). This is believed to alter the atomic structure factors in such a way as to include real and imaginary dispersion corrections.

The theory is then developed with the help of vector diagrams, and apparently hinges critically on the assumption that the normal imaginary corrections, but not the anomalous ones, are inverted for two enantiomerically related lattices. This results in a nonzero "Bijvoet difference" leading finally to the breakdown of Friedel's law, which essentially implies that the scattering factors are different for the enantiomeric lattices: $F(hkl) \neq F(\bar{h}\bar{k}\bar{l})$. (The assignment of the absolute configuration involves an extension of this approach, and is also briefly discussed further below.)

To those schooled in the traditional concepts of organic stereochemistry, however, the above treatment appears unconvincing. It is a fundamental tenet of stereochemistry that the discrimination of enantiomeric systems (molecules, crystalline lattices, etc.), is only feasible by the imposition of an additional or external chiral agency, such as a chiral auxiliary (chemical agency), circularly polarized radiation (physical agency), etc. The current theory of anomalous dispersion, however, attempts to discriminate between enantiomeric crystalline lattices without involving any external chiral agency (X-rays are considered to be achiral). As the experimental observations themselves are not in doubt, i.e., the anomalous dispersion effects are real, their current theoretical treatment may not be rigorously valid.

Interestingly, it is possible that anomalous dispersion of X-rays involves parity violation in some manner. The simplest explanation would be that X-rays are circularly polarized during their generation because of the weak nuclear current (WNC). X-rays are generated by bombarding heavy metals with high energy electrons; the resulting electronic excitation and subsequent relaxation generates X-rays.[38–41] Although the WNC is primarily a nuclear force, its effect on the valence electrons of a metal atom may be considerable and possibly exceed that proposed for the case of molecules (cf., discussion on PVED amplification above). Also, the above effects are observed only upon anomalous dispersion possibly because anomalous dispersion involves a more intimate interaction between X-rays and the lattice (*vide supra*).

Thus, the WNC would impart chirality to a metal atom, which is otherwise achiral, so the PVED and its amplification are irrelevant. Also, as the WNC is invariant, it would impart the same chirality to the generated X-rays in all cases, i.e., either right or left circularly polarized. However, the degree of circular polarization will be small, as the WNC is minuscule, which is apparently evidenced by

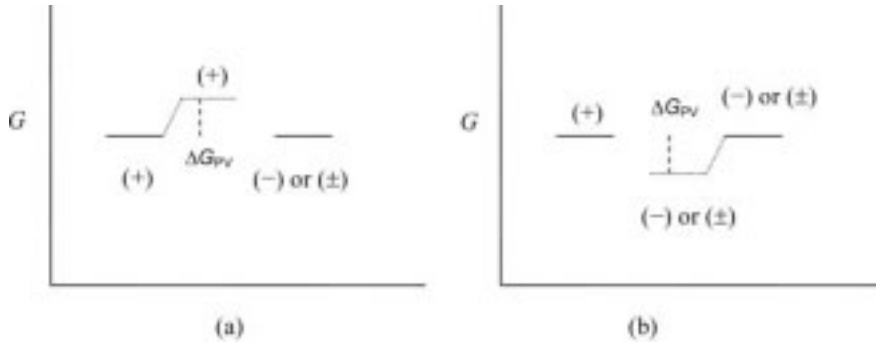

Fig. 1. Representation of the possible effect of the WNC on enantiomers (arbitrarily denoted by + and −) giving rise to the PVED, in terms of the Gibbs free energy (*G*): (**a**) the (+) enantiomer is destabilized but the (−) enantiomer and the racemic compound (±) are essentially unchanged; (**b**) the (+) enantiomer is essentially unchanged but the (−) enantiomer and the racemic compound (±) are stabilized. The dotted lines represent the altered energy states. The dashed line indicates the PVED (ΔG_{PV}). The operation of either of these modes at the level of the crystal lattice would destabilize the conglomerate form relative to the racemic compound. (This is possibly manifested via amplification during crystal growth.)

the weakness of the observed effect. (A heavy atom is required for the anomalous dispersion technique to be applied.*)

It is noteworthy that the circular polarization of X-rays would represent the first direct experimental evidence in support of the WNC as manifested in atomic and molecular phenomena.

Davankov has recently proposed that chirality is "an inherent general property" of matter because of the parity violating effects of the WNC.[42] While this is incontestable, the problem remains that the WNC is a very weak force, and its thermodynamic effect on the equilibrium between left- and right-handed forms of matter and radiation must perforce be marginal. The WNC is also largely localized in the atomic nucleus. All these indicate that it will only be manifested upon enormous kinetic amplification.

It is noteworthy that the theory of anomalous dispersion was developed before parity violation was well established. The vectorial approach, although ingenious, would now appear to be a convenient artifice. Admittedly, however, the anomalous dispersion method leads consistently to the correct stereochemical configuration, insofar as can be correlated by chemical methods. This is clearly intriguing and a possible explanation is presented later.

It must be recognized that the current theory of anomalous dispersion is based on assumptions that are tantamount to introducing an external chiral influence: in fact, the breakdown of Friedel's law is an assumption that is introduced via the hypothesis that the normal and anomalous corrections are different (*vide supra*). Therefore, the theory cryptically involves an "external influence" of a consistent and determined chirality, whose interaction with a chiral lattice is predictable *vis-à-vis* its enantiomeric counterpart. The external influence is proposed to be circularly polarized X-rays. The new proposals may then be summarized as follows.

The scattering of X-rays results in a phase shift, because of which the structure factors are represented as complex quantities involving real and imaginary parts. In normal scattering, the structure factors for a given lattice and its enantiomeric pair are inverted with respect to the vectors for both the real and imaginary parts, so Friedel's law is obeyed. In the case of anomalous scattering a correction is applied to the structure factors, which also includes both real and imaginary parts. However, the above inversion applies to the normal (nonanomalous) part as also to the real part of the anomalous correction, but not to the imaginary part of the anomalous correction. Accordingly, Friedel's law is not obeyed.

The reason for the anomalous imaginary correction being exempted from the vectorial inversion has so far been unclear. It is now suggested that this is a consequence of the differential interaction between circularly polarized X-rays and the Friedel pairs: i.e., the diastereomeric interaction between the chiral X-rays and the enantiomeric lattices is represented by the fact that the anomalous imaginary correction is vectorially unaltered. This resolves—in a way—the above conundrum on the breakdown of Friedel's law, and explains the success of the Bijvoet approach in assigning absolute configurations.

Possible experimental tests of this proposal would involve the intentional generation of X-rays possessing a high degree of circular polarization, as these would lead to an enhanced anomalous dispersion effect. Clearly, however, further theoretical and experimental approaches are indicated in order to arrive at a satisfactory final explanation for the phenomenon.

CONCLUSIONS

The possibility that there is a fundamental deterministic basis for biomolecular homochirality has tantalized theo-

*An alternative explanation would be that X-rays are not circularly polarized but that anomalous scattering effects arise from PVED between the enantiomeric lattices; the problem here, of course, is that of amplification, as PVED *per se* is too small to manifest a detectable difference in the scattering.

retical and experimental researchers alike, and inspired efforts that have increased in sophistication over several decades. At stake is no less than the origin of life itself, as this most fundamental of all scientific riddles cannot be approached without first understanding the origin of biomolecular chirality. The possible manifestations of the chiral weak nuclear force at the molecular level, and the amplification of the resulting parity violating energy difference (PVED) in the case of enantiomers, form the dominant backdrop to both experimental and theoretical work.

A fundamental problem is the minuscule magnitude of the WNC, which makes the PVED practically undetectable. Early theories for the amplification of the PVED to detectable levels were based on a linearly additive process, which was believed to occur during competitive polymerization and crystallization processes. However, these were fundamentally flawed as they employed grossly overestimated values for PVED and consequently need to be abandoned. It seems possible, however, that autocatalytic polymerization processes can amplify PVED to practical levels. As crystallization and related processes are possibly autocatalytic, these offer a window of opportunity for PVED amplification, and could explain the origin of biomolecular homochirality.

Thus, the reported cases of the spontaneous generation of optical activity during crystallization may well be genuine. However, these are predicated on a general caveat: as the biosphere is overwhelmingly chiral, the possibility of chiral contamination can never entirely be ruled out in any experimental study; in fact, this may well define an important limit of experimental science in its approach to the origin of life.

It seems possible that the WNC may be the basis for a broad range of stereochemical phenomena, although this is generally unrecognized because of the minuscule magnitude and esoteric nature of the WNC. Several crystallization phenomena, particularly involving second order asymmetric transformations, may be based on PVED amplification. This could also explain the observed general preponderance of racemic compounds over conglomerates, via the action of the WNC at the lattice level, current explanations based in conventional thermodynamics being unsatisfactory. Particularly intriguingly, the current theory of anomalous X-ray diffraction, a technique widely employed in stereochemistry to assign absolute configurations, may need to be revised: it is possible that it arises from the circular polarization of X-rays, itself a consequence of the WNC.

ACKNOWLEDGMENTS

The author is grateful to the referees for constructive suggestions, including relevant references, that greatly aided in the preparation of the final manuscript.

LITERATURE CITED

1. Mason SF. Chemical evolution, Chapter 14. Oxford: Clarendon Press; 1991.
2. Quack M. How important is parity violation for molecular and biomolecular chirality? Angew Chem Int Ed Engl 2002;41:4618–4630.
3. McDermott AJ, Tranter GE. Electroweak bioenantioselection. Croat Chem Acta 1989;62:165–187.
4. Eliel EL, Wilen SH, Mander LN. Stereochemistry of organic compounds. New York: John Wiley; 1994. pp 159, 298.
5. Eschenmoser A. The TNA-family of nucleic acid systems: properties and prospects. Orig Life Evol Biosph 2004;34:277–306.
6. Pasteur L. Dissymétrie moléculaire. In: Vallery-Radot P, editor. Oeuvres de Pasteur,Vol. 1. Paris: Masson et Cie; 1922. p 369.
7. Cline DB. On the physical origin of the homochirality of life. Eur Rev 2005;13 (Suppl 2):49–59.
8. Bonner WA, Rubenstein E, Brown GS. Extraterrestrial handedness: a reply. Orig Life Evol Biosph 1999;29:329–332.
9. Yamagata Y. A hypothesis for the asymmetric appearance of biomolecules on earth. J Theor Biol 1966;11:495–498.
10. Tranter GE. Parity violating energy differences of chiral minerals and the origin of biomolecular homochirality. Nature (London) 1985;318:172–173.
11. Eliel EL, Wilen SH, Mander LN. Stereochemistry of organic compounds. New York: John Wiley; 1994. p 113–115.
12. Jacques J, Collet A, Wilen S. Enantiomers, racemates and resolutions. New York: John Wiley; 1981. p 43–81.
13. Chandrasekhar S. Chemistry preprint archive, Vol. 2004, Issue 5 (May 2004), p 64–76, accessible via http://www.sciencedirect.com/preprintarchive.
14. Hammett LP. Physical organic chemistry, 2nd ed. New York: McGraw Hill; 1970. p 101–145.
15. Bonner WA. Chirality amplification—the accumulation principle revisited. Orig Life Evol Biosph 1999;29:615–623.
16. Frank FC. On spontaneous asymmetric synthesis. Biochim Biophys Acta 1953;11:459–463.
17. Kondepudi DK, Nelson GW. Weak neutral currents and the origin of biomolecular chirality. Nature (London) 1985;314:438–441.
18. Szabó-Nagy A, Keszthelyi L. Determination of the parity-violating energy difference between enantiomers. Proc Natl Acad Sci USA 1999;96:4252–4255.
19. Keszthelyi L. Homochirality of biomolecules: counter-arguments against critical notes. Orig Life Evol Biosph 2001;31:249–256.
20. Scolnik Y, Portnaya I, Cogan U, Tal S, Haimovitz R, Fridkin M, Elitzur AC, Deamer DW, Shinitzky M. Subtle differences in structural transitions between poly-L- and poly-D-amino acids of equal length in water. Phys Chem Chem Phys 2006;8:333–339.
21. Shinitzky M, Elitzur AC. *Ortho–para* spin isomers of the protons in the methylene group—possible implications for protein structure. Chirality 2006;18:754–756.
22. Lahav M, Weissbuch I, Shavit E, Reiner C, Nicholson GJ, Schurig V. Parity violating energetic difference and enantiomorphous crystals—caveats; reinvestigation of tyrosine crystallization. Orig Life Evol Biosph 2006;36:151–170.
23. Shinitzky M, Nudelman F, Barda Y, Haimovitz R, Chen E, Deamer DW. Unexpected differences between D- and L-tyrosine lead to chiral enhancement in racemic mixtures. Orig Life Evol Biosph 2002;32:285–297.
24. Chandrasekhar S, Kausar A. Spontaneous generation of optical activity in urea inclusion compounds *vis-a-vis* current theories. J Chem Res (S) 1998;440–441.
25. Atkins PW. Physical chemistry, 6th ed. Oxford: Oxford University Press; 1998. p 808.
26. Steinfeld JI, Francisco JS, Hase WL. Chemical kinetics and dynamics, 2nd ed. Upper Saddle River: Prentice Hall; 1999. p 151–154.
27. Blackmond DG. Asymmetric autocatalysis and its implications for the origin of homochirality. Proc Natl Acad Sci USA 2004;101:5732–5736.
28. Sambeth R, Baumgaertner A. Autocatalytic polymerization generates persistent random walk of crawling cells. Phys Rev Lett 2001;86:5196–5199.
29. Nilsson M, Brandenburg A, Andersen AC, Höfner S. Unidirectional polymerization leading to homochirality in the RNA world. Int J Astrobiol 2005;4:1–7.

30. Gleiser M. Asymmetric spatiotemporal evolution of prebiotic homochirality. Orig Life Evol Biosph 2007;37:235–251.
31. da Silva L, Mundim KC, Tsallis C. Effect of cross-links on the autocatalytic polymerization of RNA-like chains. Physica A 1998;259:415–429.
32. Hota R. Enantiomerism and physical properties: melting point. The case of D and L asparagine. In: Novel studies in organic stereochemistry. Ph.D. thesis, Indian Institute of Science, Bangalore, September 2005. p 64–71.
33. Eliel EL, Wilen SH, Mander LN. Stereochemistry of organic compounds. New York: John Wiley; 1994. p 315–322.
34. Jacques J, Collet A, Wilen S. Enantiomers, racemates and resolutions. New York: John Wiley; 1981. p 371–373.
35. Atkins PW. Physical chemistry, 6th ed. Oxford: Oxford University Press; 1998. p 156.
36. Brock CP, Schweizer WB, Dunitz JD. On the validity of Wallach's rule: on the density and stability of racemic crystals compared with their chiral counterparts. J Am Chem Soc 1991;113:9811–9820.
37. Rohrer GS. Structure and bonding in crystalline materials. Cambridge: Cambridge University Press; 2001. p 263–285.
38. Atkins PW. Physical chemistry, 6th ed. Oxford: Oxford University Press; 1998. p 639–641.
39. Woolfson MM. An introduction to X-ray crystallography, 2nd ed. Cambridge: Cambridge University Press; 1997. p 179–189.
40. Massa W. Crystal structure determination. Berlin: Springer-Verlag; 1999. p 129–133.
41. Giacovazzo C. The diffraction of X-rays by crystals. In: Giacovazzo C, Monaco HL, Artioli G, Viterbo D, Ferraris G, Gilli G, Zanotti G, Catti M, editors. Fundamentals of crystallography. Oxford: Oxford University Press; 2002. p 180–185.
42. Davankov V. Chirality as an inherent general property of matter. Chirality 2006;18:459–461.
43. Steinfeld JI, Francisco JS, Hase WL. Chemical kinetics and dynamics, 2nd ed. Upper Saddle River: Prentice Hall; 1999. p 37–40.
44. Lide DR, editor. Handbook of chemistry and physics, 84th ed. Boca Raton: CRC Press; 2003. p A85.

APPENDIX
Autocatalytic Polymerization: Derivation of Equations 14–16

Derivation of eq. 14. The steady state approximation[43] is applied to the reaction sequence in Scheme 1. The rates of formation and disappearance of the penultimate product P_{n-1} are thus equated, to arrive at eq. A1, which leads to eq. A2 (k_{n-1} is the rate constant for the conversion of P_{n-1} to P_n and k^r_{n-1} that for the reverse process, P_{n-2}, k_{n-2} and k^r_{n-2} having an analogous significance.)

$$k_{n-2}[P_{n-2}][Y] + k^{\mathrm{r}}_{n-1}[P_n] = k^{\mathrm{r}}_{n-2}[\mathrm{P}_{n-1}] + k_{n-1}[P_{n-1}][Y] \tag{A1}$$

$$[P_{n-1}] = \{k_{\mathrm{n}-2}[P_{n-2}][Y] + k^{\mathrm{r}}_{n-1}[P_n]\}/\{k^{\mathrm{r}}_{n-2} + k_{n-1}[Y]\} \tag{A2}$$

The rate of formation of P_n may then be represented by eq. A3 noting that, as there is a steady and constant input of Y into the system, $[Y]$ is constant; combining eqs. A2 and A3 then leads to eq. A4 for the rate of formation of P_n:

$$\mathrm{d}[P_n]/\mathrm{d}t = k_{n-1}[P_{n-1}][Y] = k'_{n-1}[P_{n-1}], \text{ where } k'_{n-1} = k_{n-1}[Y] \tag{A3}$$

$$\mathrm{d}[P_n]/\mathrm{d}t = k'_{n-1}\{k_{n-2}[P_{n-2}][Y] + k^{\mathrm{r}}_{n-1}[P_n]\}/(k^{\mathrm{r}}_{n-2} + k'_{n-1}) \tag{A4}$$

Equation A4 simplifies to eq. A5 as the formation of P_n is irreversible, i.e. $k^r_{n-1}\ [P_n] = 0$:

$$\begin{aligned}\mathrm{d}[P_n]/\mathrm{d}t &= \{k'_{n-1}k_{n-2}[P_{n-2}][Y]\}/(k^{\mathrm{r}}_{n-2} + k'_{n-1}) \\ &= k'_{n-1}k'_{n-2}[P_{n-2}]/(k^{\mathrm{r}}_{n-2} + k'_{n-1}) = \kappa_n[P_{n-2}]\end{aligned} \tag{A5}$$

where, $k'_{n-2} = k_{n-2}[Y]$ and $\kappa_n = k'_{n-1}k'_{n-2}/(k^{\mathrm{r}}_{n-2} + k'_{n-1})$

$[P_{n-2}]$ can be represented by eq. A6, the analog of eq. A2:

$$[P_{n-2}] = \{k_{n-3}[P_{n-3}][Y] + k^{\mathrm{r}}_{n-2}[P_{n-1}]\}/\{k^{\mathrm{r}}_{n-3} + k_{n-2}[Y]\} \tag{A6}$$

This simplifies to eq. A7 if it is assumed that the formation of P_{n-1} is irreversible, i.e., $k^r_{n-2}\ [P_{n-1}] = 0$, and noting that $k_{n-2}[Y] = k'_{n-2}$ and $k_{n-3}\ [Y] = k'_{n-3}$:

$$[P_{n-2}] = k'_{n-3}[P_{n-3}]/(k^{\mathrm{r}}_{n-3} + k'_{n-2}) = \kappa_{n-1}[P_{n-3}] \tag{A7}$$

where $\kappa_{n-1} = k'_{n-3}/(k^r_{n-3} + k'_{n-2})$; note also that $k^r_{n-2}[P_{n-1}]$ is neglected but not k^r_{n-2} and k^r_{n-3} as $[P_{n-1}]$ is presumed to be $\ll 1$ (by the steady state approximation).

Combining eqs. A5 and A7, leads to eq. A8 for the rate of formation of P_n:

$$\mathrm{d}[P_n]/\mathrm{d}t = \kappa_n[P_{n-2}] = \kappa_n\kappa_{n-1}[P_{n-3}] \tag{A8}$$

Clearly, the above protocol may be repeated until original substrate A is reached, to obtain eq. A9, leading to eq. A10 if it is assumed that $\kappa_n \sim \kappa_{n-1} \sim \kappa_{n-2} \sim \ldots \kappa_{n-m} \ldots \sim \kappa_1 = \kappa$:

$$\mathrm{d}[P_n]/\mathrm{d}t = \kappa_n\kappa_{n-1}.....\kappa_1[A] \tag{A9}$$

$$\mathrm{d}[P_n]/\mathrm{d}t = \kappa^n[A] \tag{A10}$$

Equation A10 is identical to eq. 14, noting that the polymerization is overall pseudo first order and κ^n a pseudo first order rate constant. It should also be noted that, in general, κ_{n-m} are dimensionless except for κ_n which possesses the dimensions of a pseudo first order rate

constant, bearing in mind that [*Y*] is kept constant in all the cases. Thus, κ^n also may be treated as a pseudo first order rate constant. (Note: more rigorously, a standard state of 1 M may be assigned to [*Y*]; the overall autocatalytic process would be a second order reaction, cf. eq. 9, the above comments pertaining to the uncatalyzed process, which should be first order in [*A*] for the above treatment to be applied.)

Derivation of eqs. 15 and 16. As the polymerization reaction in Scheme 1 is a pseudo first order process, eq. 10 may be applied to eq. 14 to obtain eq. A11, κ^n being substituted for *k*:

$$x/[P_0] = (e^{at} - 1)/(1 + be^{at})$$
$$a = ([A_0] + [P_0])\kappa^n; \quad b = [P_0]/[A_0] \quad \text{(A11)}$$

Equation 15 is analogous to eq. 13, *x* referring to $x_n(d)$ and x' to $x_n(l)$, the incremental increase in the concentrations of the right and left handed final polymer products. [$(\kappa_d)^n$ and $(\kappa_l)^n$ are the pseudo first order rate constants for the formation of the enantiomeric polymers.] Equation 16 then follows by applying the Eyring equation to κ_d and κ_l, thus relating these pseudo rate constants to their respective free energies of activation, $\Delta G_d^{\ddagger}$ and $\Delta G_1^{\ddagger}$ (eqs. A12 and A13, the symbols having the usual significance):

$$x/x' \sim e^{(a-a')t}$$
$$(a - a') = ([A_0] + [P_0])(k - k') \quad \text{(13)}$$

$$x_n(d)/x_n(l) \sim e^{(a-a')t}$$
$$(a - a') = ([A_0] + [(P_n)_0])[(\kappa_d)^n - (\kappa_1)^n)] \quad \text{(15)}$$

$$\kappa_d = (k_B T/h)\ \exp(-\Delta G_d^{\ddagger}/RT) \quad \text{(A12)}$$

$$\kappa_1 = (k_B T/h)\ \exp(-\Delta G_1^{\ddagger}/RT) \quad \text{(A13)}$$

The difference $[(\kappa_d)^n - (\kappa_1)^n)]$ in eq. 15 may be estimated as follows:

$$[(\kappa_d)^n - (\kappa_1)^n)] = (\kappa_d)^n[1 - (\kappa_1)^n/(\kappa_d)^n)] \quad \text{(A14)}$$

Also, $(\kappa_1)^n/(\kappa_d)^n = (\kappa_1/\kappa_d)^n$, and from eqs. A12 and A13,

$$(\kappa_1/\kappa_d) = \exp[\Delta G_d^{\ddagger} - \Delta G_1^{\ddagger})/RT] = e^{\varepsilon} \quad \text{(A15)}$$

$$(\kappa_1/\kappa_d)^n = e^{n\varepsilon} \quad \text{(A16)}$$

where $\varepsilon = (\Delta G_d^{\ddagger} - \Delta G_1^{\ddagger})$, assuming that the difference in the free energies of activation for the individual steps of the polymerization sequence is of the order of PVED (ε). Equation A14 then reduces to eq. A17, via the approximation ($e^x \sim 1 + x$) for $x \ll 1$ (the absolute value $|n\varepsilon|$ is considered as $[(\kappa_d)^n - (\kappa_1)^n)]$ is defined arbitrarily with respect to the enantiomers):[44]

$$[(\kappa_d)^n - (\kappa_1)^n)] = (\kappa_d)^n(1 - e^{n\varepsilon}) = (\kappa_d)^n n\varepsilon \quad \text{(A17)}$$

From eqs. 15 and A17 follows eq. A18:

$$(a - a') = ([A_0] + [(P_n)_0])[(\kappa_d)^n - (\kappa_1)^n)]$$
$$= ([A_0] + [(P_n)_0])(\kappa_d)^n n\varepsilon \quad \text{(A18)}$$

If the initial concentration of the final polymer product $[P_n]_0 \sim 0$:

$$(a - a') = ([A_0])(\kappa_d)^n n\varepsilon \quad \text{(A19)}$$

Introducing eq. A19 into eq. 15 leads to eq. 16:

$$x_n(d)/x_n(l) \sim \exp[([A_0])t(\kappa_d)^n(n\varepsilon)] \quad \text{(16)}$$

CHIRALITY 20:96–102 (2008)

The Chiral Pyrethroid Cycloprothrin: Stereoisomer Synthesis and Separation and Stereoselective Insecticidal Activity

BIAO JIANG,* HUA WANG, QUN-MEI FU, AND ZHU-YI LI

Shanghai Institute of Organic Chemistry, Chinese Academy of Sciences, Shanghai 200032, China

ABSTRACT The synthesis and separation of the isomers of the pesticide cycloprothrin have been realized for the first time. Complete separation was achieved on a DAICEL CHIRALCEL® OJ-H column (25 × 0.46 cm) for (1*R*, α*)-cycloprothrin isomers and on a DAICEL CHIRALCEL OD-H column (25 × 0.46 cm) for (1*S*, α*)-cycloprothrin isomers. The insecticidal activity of (1*R*, α*R*)-cycloprothrin for the larvae of *Mythimaseparata* and *Aphismedicagini* was found to be about six times and four times higher, respectively, than that of racemic cycloprothrin. *Chirality 20:96–102, 2008.* © 2007 Wiley-Liss, Inc.

KEY WORDS: pyrethroid; chiral cycloprothrin; chiral separation; insecticidal activity

INTRODUCTION

Chirality is an important concept in the pharmaceutical and life sciences. Its significance was long recognized in relation to the relative biological activity of the individual enantiopure isomers of natural compounds and synthetic drugs.[1–3] Chiral pesticides currently constitute about 25% of all pesticides used and this ratio has been continuously increasing, as more complex structures are introduced.[4,5] For economic reasons, chiral pesticides are primarily used as mixtures of enantiomers, or racemates.[6] However, enantiomers usually differ in their biological properties as a result of their interaction with enzymes or other naturally occurring chiral molecules. Enantioselectivity plays an important role in the environmental fate and ecological risks of a chiral compound, as many biologically mediated environmental processes are enantioselective. Chirality occurs widely in synthetic pyrethroids and organophosphates, which are the mainstay of modern insecticides. For example, studies have shown that enantiomers of synthetic pyrethroids, such as permethrin, behave significantly differently in terms of their bioaccumulation and biodegradation in the environment.[7,8] Earlier synthetic pyrethroids were usually prepared from a natural product such as chrysanthemic acid, pyrethrolone etc.[9] However, more recently, novel synthetic pyrethroids have been prepared without using natural product precursors but were nevertheless enantiopure. Because of the presence of multiple asymmetric carbon positions, many pyrethroids contain four or eight optical isomers. Cycloprothrin (Fig. 1), a synthetic pyrethroid, is used in controlling insects and acaroids of crops. Each year these pests destroy an estimated 15% of agricultural crops in the United States and even more in developing countries. Despite the great public concern associated with the use of the insecticides, the biological and environmental significance of the Chirality of cycloprothrin is poorly understood. In this study, we asymmetrically synthesized and resolved isomers of cycloprothrin on chiral columns, and evaluated the enantioselectivity of their insecticidal activity. Dramatic differences of the isomers were observed in their acute toxicity to *Mythimaseparata, Aphismedicagini*. The insecticidal activity of (1*R*, α*R*)-cycloprothrin towards the larvae of *Mythimaseparata* and *Aphismedicagini*, respectively, was about six times and four times higher than that of racemic cycloprothrin.

MATERIALS AND METHODS

^{1}H NMR and ^{13}C NMR spectra were recorded at 300 MHz using a Varian EM-360A spectrometer in $CDCl_3$ solution with TMS as the internal standard. Chemical shift (δ) values are given in ppm. MS were recorded with HP-5989A spectrometer using the EI or ESI method. Melting points were determined on an SGW X-4 melting point apparatus and are uncorrected. Optical rotations were obtained with a Perkin-Elmer 341 Polarimeter.

Racemic Cycloprothrin

Racemic cycloprothrin (Scheme 1) was synthesized as the literature described[10] and identified by ^{1}H NMR spectroscopy.

(+)-S-2,2-Dichloro-1-(4-ethoxyphenyl) Cyclopropanecarboxylic Acid (S-(4))

The racemic acid **4** (3.0 g) and (−)-α-methylbenzylamine (1.5 ml) in ethyl acetate (25 ml) was heated to 40°C and then left standing for 4 days at room temperature. The precipitated salt was collected and recrystallized twice

Contract grant sponsor: Shanghai Byelen Chemical Co. Ltd.
*Correspondence to: Biao Jiang, Shanghai Institute of Organic Chemistry, Chinese Academy of Sciences, Shanghai 200032, China.
E-mail: Jiangb@mail.sioc.ac.cn
Received for publication 15 May 2007; Accepted 19 October 2007
DOI: 10.1002/chir.20508
Published online 10 December 2007 in Wiley InterScience (www.interscience.wiley.com).

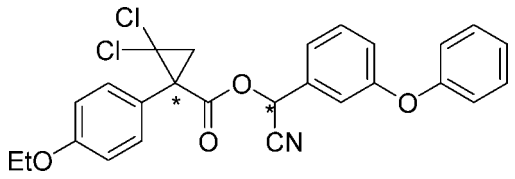

Fig. 1. Chemical structure of synthetic cycloprothrin with (*) indicating chiral positions.

from ethyl acetate and then from acetone, yielding colorless needles of the salt. The salt was dissolved in ethanol and acidified with HCl (2 N). The crystals were collected after 24 h and washed with water and aqueous ethanol to give *S*-(**4**) (1.35 g, 45%). ^{1}H NMR($CDCl_3$, 300 MHz) δ = 7.42 (d, *J* = 10.8 Hz, 2H), 6.94 (d, *J* = 12.0 Hz, 2H), 4.09 (q, *J* = 6.9 Hz, 2H), 2.65 (d, *J* = 7.5 Hz, 1H), 2.11 (d, *J* = 7.8 Hz, 1H), 1.47 (t, *J* = 7.2Hz, 3H); $[\alpha]_D^{24}$ = 66.56 (*c* 1.0, $CHCl_3$); ee = 99%.

*(−)-*R*-2,2-Dichloro-1-(4-ethoxyphenyl) Cyclopropanecarboxylic Acid (*R*-(4))*

The reaction was carried as described for *S*-(**4**) above using (+)-α-methylbenzylamine to give *R*-(**4**) in 46% yield. ^{1}H NMR($CDCl_3$, 300 MHz) δ = 7.42 (d, *J* = 10.8 Hz, 2H), 6.94 (d, *J* = 12.0 Hz, 2H), 4.09 (q, *J* = 6.9 Hz, 2H), 2.65 (d, *J* = 7.5 Hz, 1H), 2.11 (d, *J* = 7.8 Hz, 1H), 1.47 (t, *J* = 7.2Hz, 3H); $[\alpha]_D^{23}$ = −67.40 (*c* 1.0, $CHCl_3$); ee = 99%.

(1S, α)-Cycloprothrin*

A solution of the carboxylic acid *S*-(**4**) (1.1 mmol), 4-(*N,N*-dimethylamino)pyridine (DMAP) (1.0 mmol), and 2-hydroxy-2-(3-phenoxyphenyl) acetonitrile (**5**) (2.2 mmol) in dried methylene chloride (20 ml) was stirred in an ice bath. l-Ethyl-3-[3-(dimethylamino)propyl]carbodiimide hydrochloride (EDCI, 2.0 mmol) was added, and the reaction mixture was stirred at 0°C for 2 h and left at room temperature overnight. The solvent was removed in vacuo, and the product purified by flash chromatography on silica gel (hexane: EtOAc = 20:1) to give (1*S*, α*)-cycloprothrin as a yellow oil; yield: 88%. ^{1}H NMR($CDCl_3$, 300 MHz) δ = 7.43–6.30 (m, 13H), 6.31 (d, *J* = 7.5 Hz, 1H), 4.01 (q, *J* = 6.9 Hz, 2H), 2.62 (d, *J* = 7.5 Hz, 1H), 2.09 (d, *J* = 7.5 Hz, 1H), 1.41 (t, *J* = 6.9 Hz, 3H); MS (EI) *m/e* 445 (M^+-HCl, 1.91), 384 (14.0), 355 (12.1), 302 (10.0), 273 (99.3), 245 (100); HRMS(EI) calcd for $C_{26}H_{21}NO_4Cl$: 446.1159. Found: 446.1146. $[\alpha]_D^{24}$ = +23.9 (*c* 1.0, EA).

(1R, α)-Cycloprothrin*

The procedure was carried out as described for (1*S*, α*)-cycloprothrin using *R*-(**4**). Yield 88% ^{1}H NMR($CDCl_3$, 300 MHz) δ = 7.40–6.83 (m, 13H), 6.31 (d, *J* = 8.1 Hz, 1H), 4.01 (q, *J* = 7.2 Hz, 2H), 2.61 (d, *J* = 7.5 Hz, 1H), 2.09 (d, *J* = 7.5 Hz, 1H), 1.41 (t, *J* = 6.9 Hz, 3H); MS (EI) *m/e* 445 (M^+-HCl, 1.91), 384 (14.0), 355 (12.1), 302 (10.0), 273 (99.3), 245 (100); HRMS (EI) calcd for $C_{26}H_{21}NO_4Cl$: 446.1159. Found: 446.1173. $[\alpha]_D^{25}$ = −22.2 (*c* 1.0, EA).

Synthesis of (1S, αS)-Cycloprothrin and (1R, αS)-Cycloprothrin

2-Cyano-(3-phenoxyphenyl) methyl acetate (**6**) (277.2 mg, 1.04 mmol), butanol (38.5 mg), lipase from *Pseudomonas* sp. (19 mg, 22 units/mg) and diisopropyl ether (22 ml) were mixed and heated at 35°C. After 7 h, the reaction mixture was divided into two equal parts. One part was treated with *S*-(**4**) (71.4 mg, 0.26 mmol) and the other was treated with *R*-(**4**) (71.4 mg, 0.26 mmol) following the procedure for (1*S*, α*)-cycloprothrin to yield (1*S*, α*S*)-cycloprothrin and (1*R*, α*S*)-cycloprothrin, respectively, in 64% yield.

Chromatographic Separation and Peak Identification (Fig. 2)

Separation of individual enantiomers was carried out on a Daicel Chiralcel® OD-H column (25 × 0.46 cm) for (1*S*,

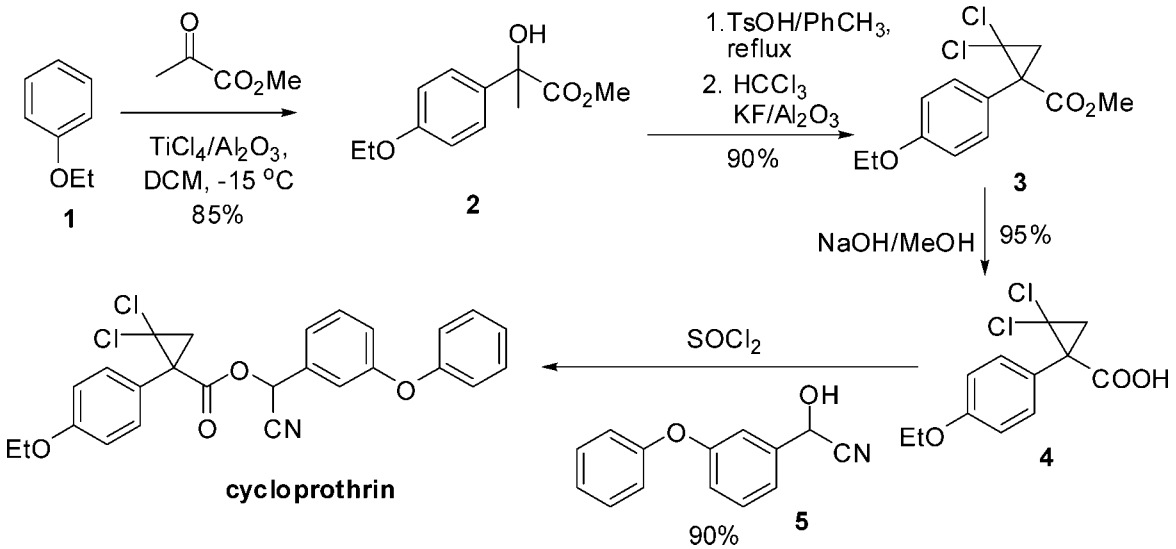

Scheme 1. Synthesis of racemic cycloprothrin.

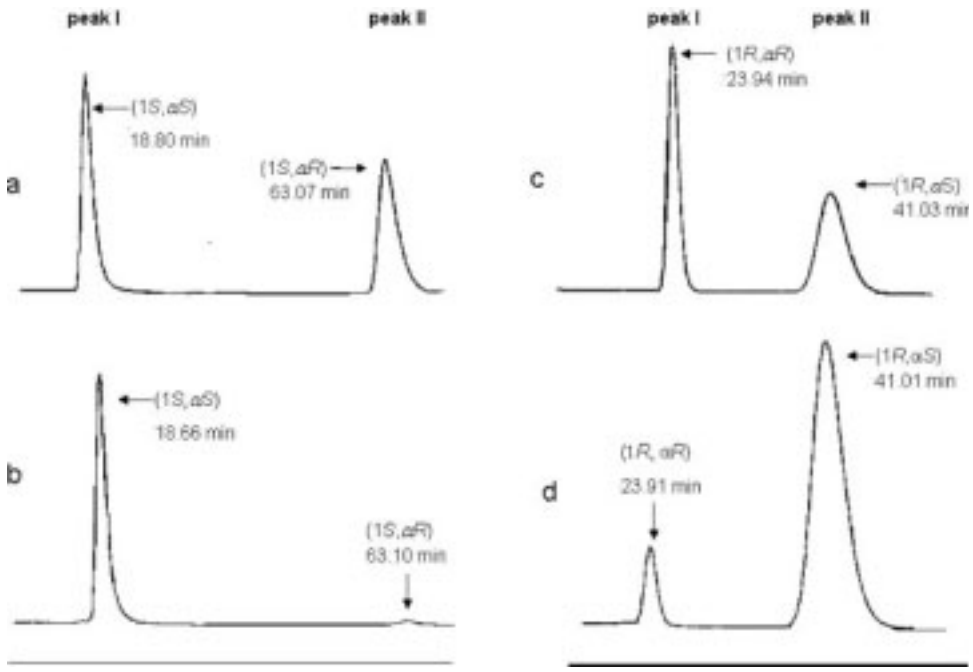

Fig. 2. Chromatographic separation by chiral HPLC and peak identification: (**a**) separation of (1*S*, α*)-cycloprothrin on the Chiralcel® OD-H column; (**b**) separation of (1*S*, α*S*)-cycloprothrin on the Chiralcel® OD-H column; (**c**) separation of (1*R*, α*)-cycloprothrin on the Chiralcel® OJ-H column; (**d**) separation of (1*R*, α*S*)-cycloprothrin on the Chiralcel® OJ-H column.

α*)-cycloprothrin isomers using hexane/IPA (9:1 by volume) as the mobile phase and on a Daicel Chiralcel OJ-H column (25 × 0.46 cm) for the (1*R,* α*)-cycloprothrin isomers with hexane/IPA (7:3 by volume) as mobile phase, flow rate: 1 ml/min, detection wavelength: 254 nm and column temperature: 35°C. Assignment of absolute configurations to the resolved peaks was made by comparing chromatograms from enantiopure samples and racemates using peak retention time as the evaluation criterion. To obtain the individual enantiomers used for bioassays and spectroscopic analysis, the resolved isomers were manually collected into glass vials. The fractions were evaporated to dryness under a stream of nitrogen. The spectral data for the four isomers are as follows:

(1*S*, α*R*)-Cycloprothrin. ^{1}H NMR($CDCl_3$, 300 MHz) δ = 7.34–6.78 (m, 13H), 6.24 (s, 1H), 3.94 (q, *J* = 6.9 Hz, 2H), 2.56 (d, *J* = 7.5 Hz, 1H), 2.03 (d, *J* = 7.5 Hz, 1H), 1.34 (t, *J* = 7.2 Hz, 3H); ^{13}C NMR ($CDCl_3$, 75 MHz) δ = 166.1, 159.3, 158.0, 156.2, 132.7, 131.8, 130.5, 129.9, 124.6, 124.0, 121.7, 120.3, 119.1, 117.3, 115.2, 114.3, 63.7, 63.4, 61.4, 43.8, 30.6, 29.6, 14.7; MS (ESI) *m/e* 481 (M^+); HRMS(MALDI) calcd for $C_{26}H_{21}NO_4Cl_2Na+1$: 504.07399. Found: 504.0754. ee = 98%. $[\alpha]_D^{25}$ = 64.99 (*c* 1.0, EA).

(1*S*, α*S*)-Cycloprothrin. ^{1}H NMR($CDCl_3$, 300 MHz) δ = 7.34–6.78 (m, 13H), 6.27 (s, 1H), 3.94 (q, *J* = 6.9 Hz, 2H), 2.56 (d, *J* = 7.5 Hz, 1H), 2.03 (d, *J* = 7.5 Hz, 1H), 1.34 (t, *J* = 7.2 Hz, 3H); ^{13}C NMR ($CDCl_3$, 75 MHz) δ = 166.1, 159.3, 158.0, 156.2, 132.7, 131.8, 130.5, 129.9, 124.6, 124.0, 121.7, 120.3, 119.1, 117.3, 115.2, 114.3, 63.7, 63.4, 61.4, 43.8, 30.6, 29.6,14.7; MS (EI) *m/e* 445 (M^+-HCl, 1.91), 384 (14.0), 355 (12.1), 302 (10.0), 273 (99.3), 245 (100); HRMS (EI) calcd for $C_{26}H_{21}NO_4Cl$: 446.1159. Found: 446.1167. ee = 98%. $[\alpha]_D^{25}$ = +5.47 (*c* 1.0, EA).

(1*R*, α*R*)-Cycloprothrin. ^{1}H NMR($CDCl_3$, 300 MHz) δ = 7.34-6.78 (m, 13H), 6.34 (s, 1H), 3.94 (q, *J* = 6.9 Hz, 2H), 2.56 (d, *J* = 7.5 Hz, 1H), 2.03 (d, *J* = 7.5 Hz, 1H), 1.34 (t, *J* = 7.2 Hz, 3H); ^{13}C NMR ($CDCl_3$, 75 MHz) δ = 166.1, 159.3, 158.0, 156.2, 132.7, 131.8, 130.5, 129.9, 124.6, 124.0, 121.7, 120.3, 119.1, 117.3, 115.2, 114.3, 63.7, 63.4, 61.4, 43.8, 30.6, 29.6, 14.7; MS (EI) *m/e* 445 (M^+-HCl, 1.91), 384 (14.0), 355 (12.1), 302 (10.0), 273 (99.3), 245(100); HRMS (EI) calcd for $C_{26}H_{21}NO_4Cl$: 446.1159. Found: 446.1173. ee = 83%. $[\alpha]_D^{25}$ = −6.30 (*c* 1.0, EA).

(1*R*, α*S*)-Cycloprothrin. ^{1}H NMR($CDCl_3$, 300 MHz) δ = 7.34–6.78 (m, 13H), 6.29 (s, 1H), 3.94 (q, *J* = 6.9 Hz, 2H), 2.56 (d, *J* = 7.5 Hz, 1H), 2.03 (d, *J* = 7.5 Hz, 1H), 1.34 (t, *J* = 7.2 Hz, 3H); ^{13}C NMR ($CDCl_3$, 75 MHz) δ = 166.1, 159.3, 158.0, 156.2, 132.7, 131.8, 130.5, 129.9, 124.6, 124.0, 121.7, 120.3, 119.1, 117.3, 115.2, 114.3, 63.7, 63.4, 61.4, 43.8, 30.6, 29.6, 14.7; MS (ESI) *m/e* 481 (M^+); HRMS(MALDI) calcd for $C_{26}H_{22}NO_4Cl_2$: 482.09204. Found: 482.0919. ee = 94%. $[\alpha]_D^{25}$ = −31.9 (*c* 1.0, EA).

Bioassay of Insecticidal Activities (Table 1)

Newly hatched larvae of *Tetranychus cinnabarnus* and *Aphismedicagini* laid by female adults 24 h before bioassay and third instar larvae of *Nilaparvatalegen* and *Mythimase-*

TABLE 1. The insecticidal activity for cycloprothrin and its stereoisomers[a]

	Mortality (%)							
	Ni[b] (mg/l)	Tc[c] (mg/l)	Ap[d] (mg/l)			My[e] (mg/l)		
Compounds	500	250	250	100	20	250	100	20
Racemic cycloprothrin	0	0	98	83	77	100	100	90
(1*R*, α*)-Cycloprothrin	0	0	98	93	69	100	100	99
(1*R*, α*R*)-Cycloprothrin	0	0	100	99	84	100	100	100
(1*R*, α*S*)-Cycloprothrin	0	0	100	78	66	100	100	33
(1*S*, α*)-Cycloprothrin	0	0	52	2	0	10	22	0
(1*S*, α*S*)-Cycloprothrin	0	0	0	0	0	0	0	0
(1*S*, α*R*)-Cycloprothrin	0	0	0	–	–	0	–	–
Untreated	0	0	0	–	–	0	–	–

[a]Method of bioassay is described in materials and methods.
[b]Ni: *Nilaparvatalegen*
[c]Tc: *Tetranychus cinnabarnus*.
[d]Ap: *Aphismedicagini*.
[e]My: *Mythimaseparata*.

parata were reared in laboratory at (27 ± 1)°C. In the first screen, the compounds were tested for insecticidal activity by Potter Tower spraying methods[11] at concentrations of 250 or 500 mg/l. For the second screen, the compounds in food media were tested for killing *Mythimaseparata* and *Aphismedicagini* larvae. Two to three replicates of each test were performed and the mortality assessed after 24 h for *Aphismedicagini* larvae and 72 h for *Nilaparvatalegen* larvae. Control group insects, reared in food media were treated with water only.

Toxicity Test

The compounds were tested for killing *Mythimaseparata* and *Aphismedicagini* larvae with food media by dipping poison methods[11] at different concentrations. Two to three replicates of each test were performed and mortality was assessed after 24 h for *Aphismedicagini* larvae and 72 h for *Nilaparvatalegen* larvae. The insecticidal effects and toxicity were determined by counting survivors at the end of the exposure period. The control morality was adjusted by using Abbot's formula. Toxicity is expressed as a media concentration (LC_{50}). All tests were carried out in accordance with SOP guidance.[11]

RESULTS AND DISCUSSION

Synthesis of Racemate and Isomers

Recently, we have reported an efficient synthesis (Scheme 1) of the racemate methyl 2-(4-ethoxyphenyl)-2-hydroxypropanic acid[10] via highly regioselective Friedel-Crafts reactions of 1-ethoxybenzene with pyruvate ester promoted by $TiCl_4$ in the presence of basic Al_2O_3 for 3 h at −15°C. This is followed by dehydration simply by heating in toluene with a catalytic amount of *p*-toluenesulfonic acid and dichlorocyclopropanation with chloroform in the presence of KF/Al_2O_3 in acetonitrile at room temperature. Hydrolysis of the ester afforded racemic 2,2-dichloro-1-(4-ethoxyphenyl)cyclopropane carboxylic acid in 95% yield. The racemic cycloprothrin was prepared by esterification of its acid chloride with 2-hydroxy-2-(3-phenoxyphenyl) acetonitrile in 90% yield.

The Chirality of cycloprothrin arises from the acid and/or the alcohol moieties. Racemic acids are commonly resolved into their enantioisomers by fractional crystallization of diastereoisomeric salts formed with a suitable optically active amine. Thus, 2,2-dichloro-1-(4-ethoxyphenyl) cyclopropanecarboxylic acid (**4**) was treated with (+) and/or (−)-α-methylbenzylamine in ethyl acetate, followed by acidification with hydrogen chloride in ethanol to remove the amine. The precipitated free acid was recrystallized from ethanol twice to afford the pure antipodes (*R*)-**4** ($[\alpha]_D^{22.6} = -67.4$ (*c* 1.0, $CHCl_3$) and ee 99%) and (*S*)-**4** ($[\alpha]_D^{24.3} = 66.6$ (*c* 1.0, $CHCl_3$), ee 99%)[12,13] (Scheme 2).

The chiral pyrethroids, having an alcohol moiety of (α*S*)-cyano-3-phenoxybenzyl alcohol ((*S*)-CPBA) usually shows higher bioactivity than its (*R*)-enantiomer.[9] Many methodologies have been developed for synthesis of (*S*)-CPBA, among which the chemo-enzymatic process provided an efficient process for preparation (*S*)-CPBA in high enantiomer excess.[14–17] Racemic CPBA was converted into α-cyano-(3-phenoxyphenyl)-methyl acetate (**6**). Finally, the transesterification resolution of the racemic ester by a highly enantioselective lipase from *Pseudomonas sp*. afforded (*S*)-CPBA in 43.4% yield with 95% ee[16] (Scheme 2).

The insecticidal activity and configuration of each isomer of cycloprothrin could now be individually assessed. With (*R/S*)-acid **4** and alcohol (*S*)-CPBA-**5** in hand, diastereoisomers of cycloprothrins were prepared. The classical esterification procedure by the reaction of acid chloride with alcohol **5** was found to give racemic cycloprothrin because of the racemization of the acid **4** when it was treated with thionyl choride. However, the ester formation was carried out by treatment of the (*R/S*)-acid **4** with racemic CPBA **5** in presence of l-ethyl-3-[3-(dimethylamino)-

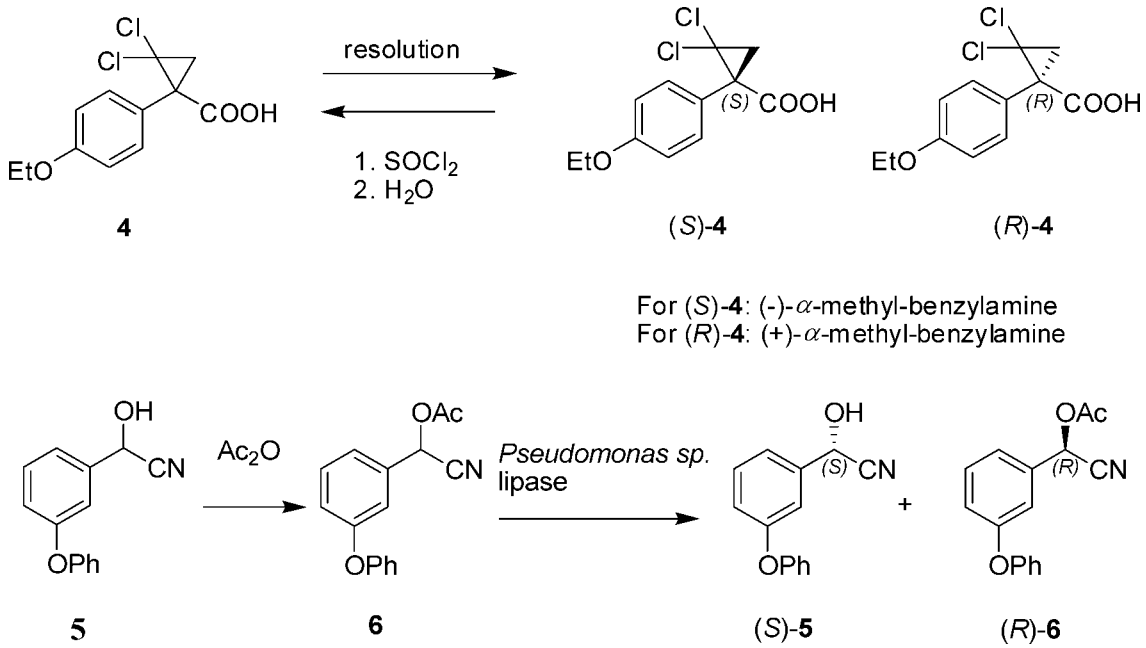

4 (S)-4 (R)-4

5 6 (S)-5 (R)-6

Scheme 2. Resolution of chiral acid **4** and preparation of (*S*)-CPBA **5.**

propyl] carbodiimide hydrochloride (EDCI) and 4-(*N,N*-dimethylamino)pyridine (DMAP) in CH_2Cl_2 to give (1*R,* α*)/(1*S,* α*)-cyloprothrin in high yields without racemization (Scheme 3).[18] The most insecticidally active isomer of the respective compound in this synthetic pyrethroid group had an absolute configuration that corresponded to the (1*R*)-configuration of chrysanthemic acid.[10] In synthetic pyrethroids such as (2*S*,α*S*)-fenvalerate, (2*S*)-flucythrinate and (2*S*)-fluvalinate, those with a (1*S*)-phenylalkonoic acid moiety have higher insecticidal activity than those racemates that were developed and marketed.[18] Taking these reported results into consideration, the two isomers (1*R,* α*S*)- and (1*S,* α*S*)-cyloprothrin were synthesized directly by the reaction of (*R*)-acid **4** or (*S*)-acid **4,** respectively, with (*S*)-CPBA **5** (Scheme 3).

Isomer Separation, Analysis, and Peak Identification

Chiral separation by HPLC has advanced to become the most powerful method not only for analyzing enantiomers,[19] but also for obtaining them in significant amount of the pure form for bioassay.[20] Separation of racemic cycloprothrin could not be effectively achieved using a variety of chiral HPLC columns. However, complete separation was achieved on a Chiralcel OD-H column (25 × 0.46 cm) for (1*S,* α*)-cycloprothrin isomers and a Chiralcel OJ-H column (25 × 0.46 cm) for (1*R,* α*)-cycloprothrin isomers (Figs. 2a and 2c). The effective preparative separation of (1*S,* α*)-cycloprothrin on a Chiralcel OD-H column (25 × 0.46 cm) gave two peaks with retention times of 18.8 min (peak I) and 63.1 min (peak II) with hexane/IPA = 9:1 (flow rate: 1 ml/min). The elution of a known sample of (1*S,* α*S*)-cycloprothrin under the same conditions gave a major peak at 18.6 min, indicating that peak I corresponded to (1*S,* α*S*)-cycloprothrin; therefore, the second peak II was (*1S,* α*R*)-cycloprothrin (Figs. 2a and 2b). Running (1*R,* α*)-cycloprothrin on Chiralcel OJ-H column (25 × 0.46 cm) gave two peaks with retention time of 23.9 min (peak I) and 41.0 min (peak II) with hexane/IPA = 7:3 (flow rate: 1 ml/min). The retention time of authentic (1*R,* α*S*)-cycloprothrin was 41.0 min, indicating that peak I is (1*R,* α*R*)-cycloprothrin and peak II is (1*R,* α*S*)-cycloprothrin (Figs. 2c and 2d). The adequate resolution allowed individual isomers to be recovered for use in bioassays.

Stereostructure-Activity Relationship for Insecticidal Activity

The insecticidal activity of the racemates and four stereoisomers of cycloprothrin were assessed against the larvae of *Tetranychus cinnabarnus*, *Nilaparvatalegen*, *Mythimaseparata,* and *Aphismedicagini*. As listed in Table 1, in a primary screen, the compounds were tested for insecticidal activity by the Potter Tower spraying method[11] at concentrations of 250 or 500 mg/l. Cycloprothrins proved to be toxic to the larvae of *Mythimaseparata* and *Aphismedicagini*, but not to larvae of *Tetranychus cinnabarnus* or *Nilaparvatalegen*. Cycloprothrins with the *R*-acid moiety had much higher insecticidal activity than those with the *S*-acid moiety. The (1*R,* α*R*)-cycloprothrin showed the highest insecticidal activities against larvae of *Mythimaseparata* and *Aphismedicagini*. The second screen tests were carried out with different concentration (20–100 mg/l) for larvae of *Aphismedicagini* and *Mythimaseparata* with food media by dipping poison methods.[20] Racemic cycloprothrin had 100% mortality to *Mythimaseparata* larvae at a concentration of 20 mg/l, and (1*R,* α*R*)-cycloprothrin had 90% mortality at the very low concentration of 2.25 mg/l.

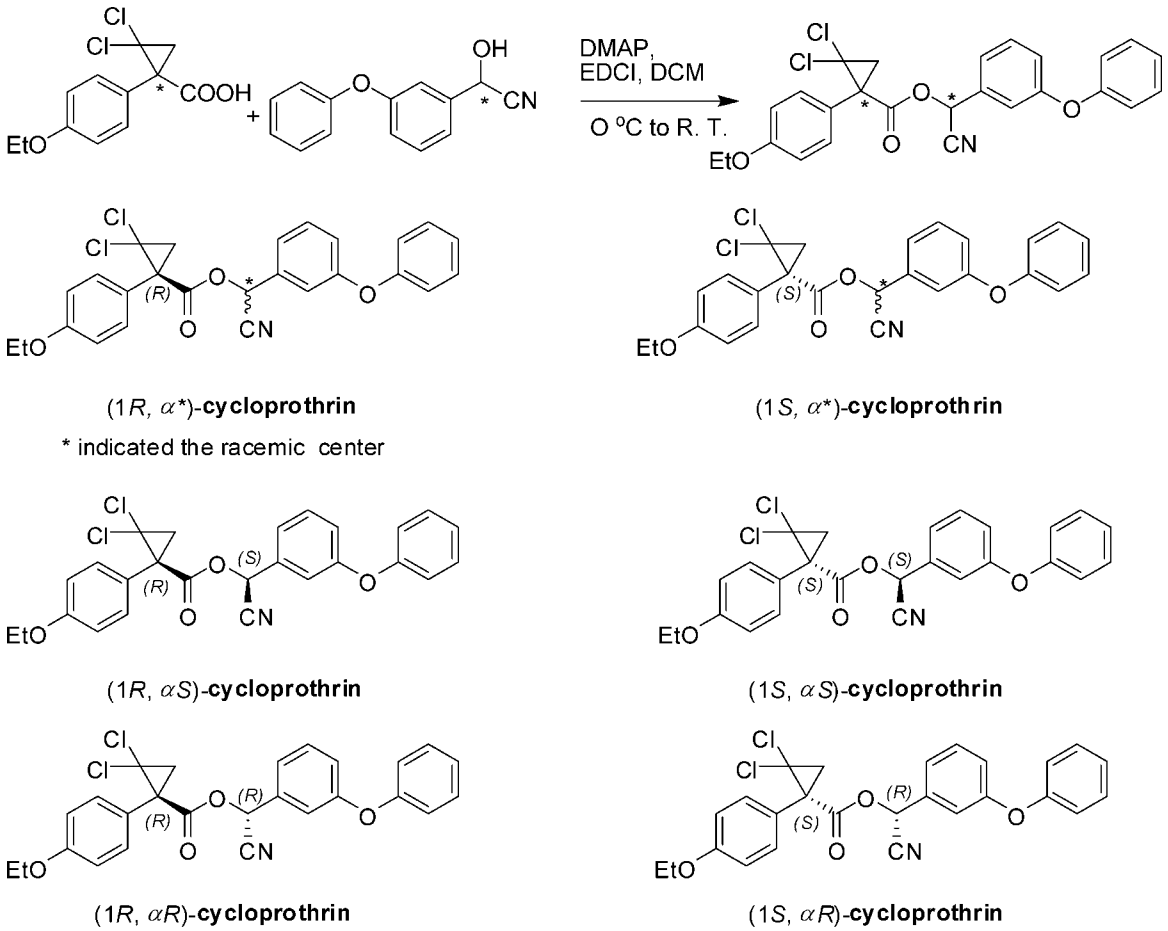

Scheme 3. Synthesis of isomers of cycloprothrin.

Furthermore, racemic cycloprothrin had 98% mortality to *Aphismedicagini* larvae at a concentration of 250 mg/l, and (1*R*, α*R*)-cycloprothrin had 84% mortality at 20 mg/l. Neither (1*S*, α*)-, (1*S*, α*S*)- nor (1*S*, α*R*)-cycloprothrin showed any insecticidal activity at a concentration of 20 mg/l towards larvae of *Aphismedicagini* and *Mythimaseparata*.

On the basis of the above primary results of mortality tests, one of the isomers, (1*R*, α*R*)-cycloprothrin was chosen for toxicity testing in comparision with racemic cycloprothrin.[11] The toxicity test against the third instar larvae of *Mythimaseparata* showed that this organism was the most susceptible to (1*R*, α*R*)-cycloprothrin (LC_{50} 0.64 mg/l) compared with racemic cycloprothrin (LC_{50} 3.66 mg/l). The insecticidal activity of (1*R*, α*R*)-cycloprothrin for this larvae is thus about six times higher than that of racemic cycloprothrin. Toxicity tests against newly hatched larvae of *Aphismedicagini* showed that the (1*R*, α*R*)-cycloprothrin again had a higher activity (LC_{50} 3.71 mg/L) with racemic cycloprothrin some four times less active (LC_{50} 15.15 mg/l).

LITERATURE CITED

1. Lewis DL, Garrison AW, Wommack KE, Whittemore A, Steudler P, Melillo J. Influence of environmental changes on degradation of chiral pollutants in soils. Nature 1999;401:898–901.
2. Koeller KM, Wong CH. Enzymes for chemical synthesis. Nature 2001;409:232–240.
3. Yoon TP, Jacobsen EN. Privileged chiral catalysts. Science 2003; 299:1691–1693.
4. Garrison AW. Probing the enantioselectivity of chiral pesticides. Environ Sci Technol 2006;40:16–23.
5. Committee on the Future Role of Pesticides in US Agriculture, Board on Agriculture and Natural Resources, Board on Environmental Studies and Toxicology, National Research Council. The future role of pesticides in US agriculture, Washington, D. C.: National Academy Press; 2000.
6. Williams A. Opportunities for chiral agrochemicals. Pestic Sci 1996; 46:3–9.
7. Liu W, Gan J, Schlenk D, Jury WA. Enantioselectivity in environmental safety of current chiral insecticides. Proc Natl Acad Sci 2005; 102:701–706.
8. Hegeman WJM, Laane RWPM. Review of enantiomeric enrichment of chiral pesticides in the environment. Environ Contam Toxicol 2002; 173:85–116.
9. Naumann K. Synthetic pyrethroid insecticides: structure and properties. Berlin: Springer-Verlag; 1990.
10. Si YG, Jiang B. Highly regioselective Friedel-Crafts reactions of electron-rich aromatic compounds with pyruvate catalyzed by Lewis acid-base: efficient synthesis of pesticide cycloprothrin. Adv Synth Catal 2006;348:898–904.
11. Chen CN. Biological measuring technology of pesticides. Beijing: Beijing Agricultural University Press, 1992.
12. Holan G, Walser R. Process of making phenylacrylic esters. U.S. Patent 4,309,350, 1982.

13. Duke CC, Wells RJ. Investigation of readily available chiral compounds for preparative scale resolutions. Aust J Chem 1987;40:1641–1654.
14. Casas J, Baeza A, Sansano JM, Carmen N, Jose MS. Enantioselective cyanoformylation of aldehydes mediated by BINOLAM-$AlCl_3$ as a monometallic bifunctional catalyst. Tetrahedron: Asymmetry 2003; 14:197–200.
15. Casas J, Baeza A, Sansano JM, Carmen N, Jose MS. Enantioselective addition of trimethylsilyl cyanide to aldehydes catalysed by bifunctional BINOLAM-$AlCl_3$ versus monofunctional BINOL-$AlCl_3$ complexes. Tetrahedron 2004;60:10487–10496.
16. Inagaki M, Hiratake J, Nishioka T, Oda J. Lipase-catalyzed kinetic resolution with in situ racemization: one-pot synthesis of optically active cyanohydrin acetates from aldehydes. J Am Chem Soc 1991;113:9360–9361.
17. Hatch CE, Baum JS, Takashima T, Kondo K. Stereospecific total synthesis of the potent synthetic pyrethroid NRDC 182. J Org Chem 1980;45:3281–3285.
18. Kurihara N, Miyamoto J, Paulson GD, Zeeh B, Skidmore MW, Hollingworth RM, Kuiper HA. Chirality in synthetic agrochemicals: bioactivity and safety consideration. Pure Appl Chem 1997;69:1335–1348.
19. Allenmark S. Chromatographic enatioseparation methods and application, 2nd ed. New York: EllisHorwood; 1991.
20. Liu W, Gan JJ, Qin S. Separation and aquatic toxicity of enantiomers of synthetic pyrethroid insecticides. Chirality 2005;17:S127–S133.

CHIRALITY 20:103–109 (2008)

Review Article

Stereochemical Comparison of Nebivolol with other β-Blockers

CARSTEN D. SIEBERT,[1]* ANDRÉ HÄNSICKE,[2] AND THOMAS NAGEL[2]
[1]*Johann Wolfgang Goethe-Universität, Frankfurt/Main, Germany*
[2]*Berlin-Chemie AG, Glienicker Weg 125, Berlin, Germany*

ABSTRACT β-Blockers are widely used in the treatment of cardiovascular disease and act by antagonizing the effects of adrenaline (epinephrine) and noradrenaline (norepinephrine) on β-adrenergic receptors. All β-blockers currently used in the treatment of cardiovascular disease contain at least one chiral center and, while most are marketed as racemates, their cardiac antihypertensive activity generally resides in the *S*-enantiomer. Nebivolol is a third generation β-blocker that is highly selective for the β_1-adrenoceptor. The nebivolol molecule contains four chiral centers and is marketed as a racemate of (+)-nebivolol (*SRRR*-configuration) and (−)-nebivolol (*RSSS*-configuration). Nebivolol differs from all other β-blockers with a hydroxypropanolamine substructure in that its cardiac antihypertensive activity resides in the *R*-enantiomer at the hydroxy group, whereas all other β-blockers have antihypertensive activity in the *S*-enantiomer. Two of the four chiral centers in nebivolol are part of a ring structure and the increased rigidity of this structure may be related to nebivolol's divergence from the standard pharmacophore model of β-blockers. *Chirality 20:103–109, 2008.*

KEY WORDS: β-blockers; hydroxypropanolamine structure; enantiomer; eutomer; racemate

INTRODUCTION

Nebivolol (Nebilet®) is a racemic mixture of (+)-nebivolol, which has selective β_1-receptor blocking activity, and (−)-nebivolol, which causes vasodilation. The nebivolol molecule contains four chiral centers; (+)-nebivolol has the *SRRR*-configuration whereas its enantiomer (−)-nebivolol has the *RSSS*-configuration. The constitution of nebivolol is fundamentally different from the typical first generation β-blockers.[1] In this article, the absolute configuration of nebivolol and that of the hydroxypropanolamine substructure is discussed with regard to propranolol and the native enantiomerically pure neurotransmitters adrenaline (epinephrine) and noradrenaline (norepinephrine).

β-BLOCKERS: STEREOCHEMICAL CONSIDERATIONS

β-Blockers are used widely in the treatment of cardiovascular conditions including angina, hypertension, and arrhythmias. These agents act by antagonizing the actions of adrenaline (epinephrine) and noradrenaline (norepinephrine) on β-adrenoceptors. All currently available β-blockers contain at least one chiral center in their structure, and interaction of β-blockers with β-adrenoceptors is highly stereoselective[2]; the binding pocket of these receptors is a good example of chiral recognition.

Propranolol, the first successful β-blocker to be developed, is a nonselective β-adrenoceptor antagonist that blocks β_1- and β_2-receptors to similar extents. Like many β-blockers used in the treatment of cardiovascular disease, propranolol is marketed as a racemic mixture consisting of the *R*- and *S*-enantiomers in a fixed 1:1 ratio. Remarkably, the stereoisomer of propranolol with *R*-configuration at the hydroxy group (dexpropranolol; Fig. 1A) has no pharmaceutical importance and it is the *S*-enantiomer that accounts for the cardiac β-blocking effects of propranolol (Fig. 1B); a phenomenon that has been observed with other β-blockers.[3] In fact, certain β-blockers used for the treatment of hypertension are produced as enantiomerically pure compounds containing only the enantiomer which is more active (that is, the eutomer), including timolol (Dispatim®), levobunolol (Vistagan®), penbutolol (Betapressin®), and esatenolol (Atpure®).

A feature common to the chemical structure of β-blockers is the presence of at least one aromatic residue attached to a side alkyl chain that possesses hydroxy and amine functional groups; in all cases β-blockers contain one or more chiral centers, one of which is always a carbon atom in the alkyl chain directly attached to a hydroxy group.[2] The neurotransmitters adrenaline (Fig. 1C) and noradrenaline (Fig. 1D), which exert β-sympathomimetic activity in the body, contain just such a chiral center for

*Correspondence to: Carsten D. Siebert, Eltviller Straße 4, D-65936 Frankfurt/Main, Germany. E-mail: dr.cdsiebert@web.de
Received for publication 11 May 2007; Accepted 19 October 2007
DOI: 10.1002/chir.20509
Published online 10 December 2007 in Wiley InterScience (www.interscience.wiley.com).

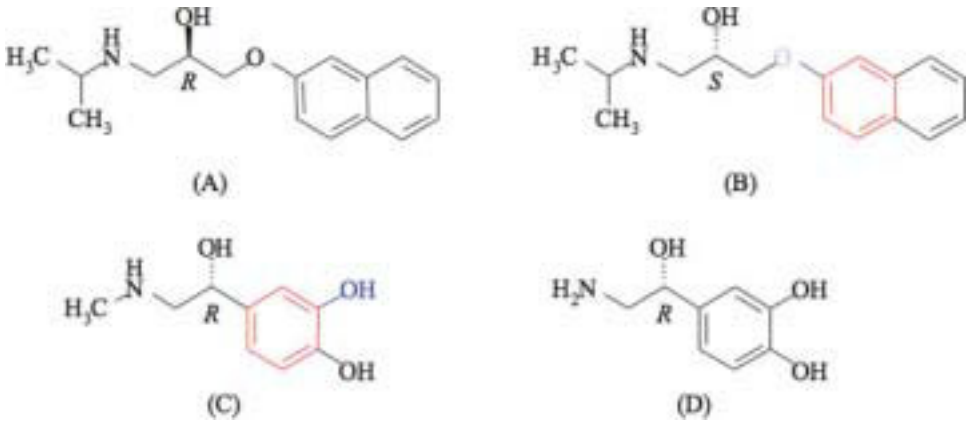

Fig. 1. Dexpropranolol (*R*-configuration) (**A**) is less potent than the *S*-enantiomer of propranolol (**B**). The neurotransmitters adrenaline (**C**) and noradrenaline (**D**) contain OH groups with *R*-configuration. Adrenaline (C) and *S*-propranolol (B) have different absolute configuration but the same spatial orientation (highlighted in color). [Color figure can be viewed in the online issue, which is available at www.interscience.wiley.com.]

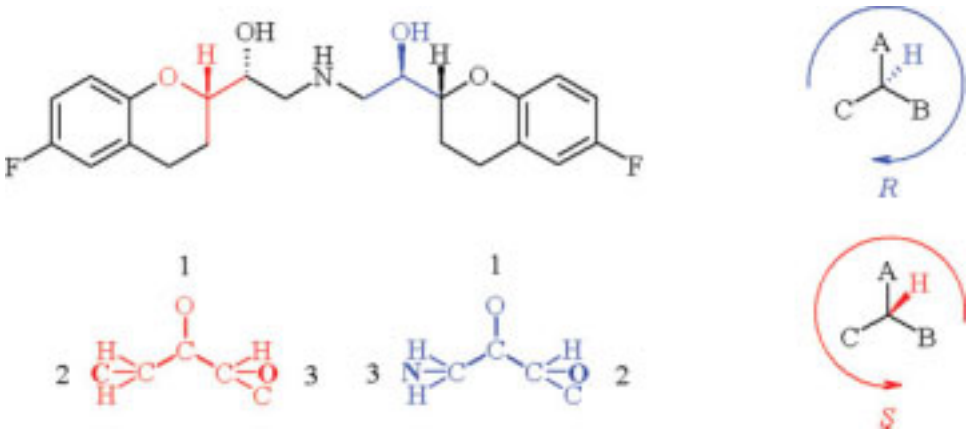

Fig. 2. (+)-Nebivolol is the *SRRR*-eutomer of racemic nebivolol. The absolute configuration of (+)-nebivolol is determined by digraphs. [Color figure can be viewed in the online issue, which is available at www.interscience.wiley.com.]

which the absolute configuration has been determined to be *R*.

Binding at the β-adrenoceptor binding site requires hydrogen bonds, ionic, and π–π interactions. A comparison of adrenaline and propranolol reveals a distinct spatial orientation of the hydroxy group, the amino group, and the aromatic residue that is essential for binding at the adrenoceptors. Reversal of the hydroxybenzene moiety in adrenaline (Fig. 1C) as, for example, is seen in propranolol (Fig. 1B) leads to an antagonistic effect upon binding at the binding site of the receptor.[4]

As illustrated in Figure 1, the absolute configuration of adrenaline and *S*-propranolol is contrary although their spatial orientation is similar. This difference in absolute configuration (*R* vs. *S*) depends on the Cahn-Ingold-Prelog (CIP) rules for describing a chiral center. The spatial orientation of the ligand is critical to eliciting sympatholytic and sympathomimetic activity at the β-adrenoceptor.

Some types of β-blocker have more than one chiral center. Labetalol, although not a propanolamino-type β-blocker, has two chiral centers and is marketed as a racemate of four stereoisomers. Its *RR*-stereoisomer accounts for most of its β-blocking activity, whereas the *SR*-stereoisomer is responsible for most of its α-blocking activity.[5]

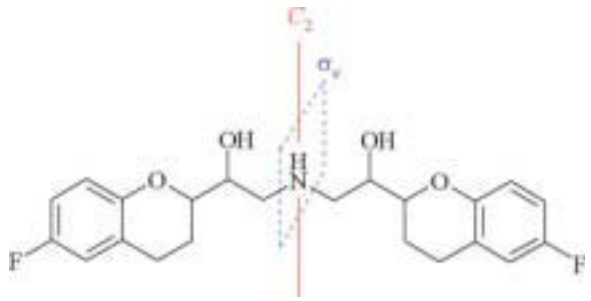

Fig. 3. The constitution (not the configuration) of nebivolol. [Color figure can be viewed in the online issue, which is available at www.interscience.wiley.com.]

When labetalol was tested in anaesthetized dogs, the isomer (−)-2-hydroxy-5-[(*R*)-1-hydroxy-2-((*R*)-1-methyl-3-phenylpropylamino)ethyl]benzamide (dilevalol) showed nonselective β-antagonism, 2-hydroxy-5-[(*S*)-1-hydroxy-2-((*R*)-1-methyl-3-phenylpropylamino)ethyl]benzamide was the most potent antagonist at α_1-adrenoceptors, whereas the enantiomer of dilevalol, (+)-2-hydroxy-5-[(*S*)-1-hydroxy-2-((*S*)-1-methyl-3-phenylpropylamino)ethyl]benzamide, showed weak activity at both adrenoceptors.[5] This example shows that the influence of stereoisomers is not limited to nebivolol, but the topology of the most active labetalol stereoisomer is the same as in adrenaline and noradrenaline. In both molecules the hydroxy group has *R*-configuration. Comparison of a 50:50 mixture of the *RR* and *SR* stereoisomers with racemic labetalol (*RR*, *RS*, *SR*, *SS*) in rats confirmed that these two labetalol isomers are responsible for the treatment effects in systemic hypertension.[5,6] Nevertheless, dilevalol was withdrawn from the market due to liver toxicity.

THE β-BLOCKER NEBIVOLOL

Unlike racemic propranolol, which shows no selectivity for β_1- over β_2-adrenergic receptors, nebivolol is highly selective for β_1-adrenergic receptors[7] and is not associated with β_2-mediated bronchoconstrictive effects. Nebivolol is at present the only β-blocker which differs fundamentally from the structure derived from propranolol. For all other β-blockers with a hydroxypropanolamine substructure, the *S*-configuration at the chirality center (i.e. at the chiral carbon attached to the hydroxy group) is responsible for the molecule's antihypertensive effect, with the *S*-enantiomers generally having about 100-fold greater cardiac β-blocking activity than the *R*-enantiomers.[2] To understand the unique properties of nebivolol, the precise orientation of the four chirality centers must be considered (Fig. 2).

To investigate the stereochemical properties of nebivolol, all possible stereoisomers were synthesized by enantioselective reactions.[8,9] The starting materials were (*R*)-6-fluorochroman-2-carboxylic acid and (*S*)-6-fluorochroman-2-carboxylic acid, respectively.[9] In the next step, the carboxylic acid was reduced to yield the aldehyde,[10] which was converted into 6-fluoro-2-oxiranylchroman. The four 6-fluoro-2-oxiranylchroman key intermediates were prepared in the desired stereochemical configuration: (*R*,*R*), (*R*,*S*), (*S*,*R*), and (*S*,*S*). These compounds were separated by reverse-phase liquid chromatography. Subsequent ring-opening of two building blocks with benzylamine delivered 2-{benzyl-[2-(6-fluorochroman-2-yl)-2-hydroxyethyl]amino}-1-(6-fluorochroman-2-yl)ethanol, the *N*-protected (±)-nebivolol, and its stereoisomers. After debenzylation, all isomers were purified by chiral chromatography (preparative chiral chromatography on a Chiralpak AD column using MeOH [0.1% *N*,*N*-diisopropylethylamine] as the eluent)[11] and isolated as hydrochloride salts. The stereochemical purity of all isomers is shown in Table 1; impurities of more than 1% were analyzed to exclude the existence of constitutional byproducts. Single crystals were prepared and the unit cells were investigated by X-ray crystallography,[12] additionally ^{1}H and ^{13}C NMR data confirmed the structures. The spatial orientation of all isomers was found to correlate with the four chirality centers and the crystallized compounds demonstrated definite differences in extension. Notably, (±)-nebivolol is less flexible than other stereoisomers and the two aromatic moieties are approximately coplanar. To understand the geometric properties a stereochemical consideration is helpful.

TABLE 1. Stereochemical purity of nebivolol isomers

Stereoisomer	Stereochemical purity (area %)	Impurities (area %)
SRRS	99.7	–
RSSR	99.9	–
RSRS	99.0	–
RRRS	99.9	–
RSSS	99.9	–
RRRR	99.9	–
RRSR	97.0	1.6 *RSSS*, 1.3 *SRSS*
SRSS	99.0	–
RRSS	99.2	–
SSSS	96.7	3.3 *RRSS*

STEREOCHEMICAL RESEARCH

The constitution of nebivolol is symmetric in that the two substituents on nitrogen have the same constitution (although not the same configuration). The absolute configuration of both enantiomers leads to C_1-symmetry in the molecule. A C_2-axis and a mirror plane σ_v do not exist. In Figure 3 the two elements of symmetry are drawn in the constitution formula.

The number of possible stereoisomers for a chiral organic compound with *unsymmetric* constitution is determined by $N_r = 2^n$ stereoisomers (N_r = real number of stereoisomers, n = number of chirality centers). Figure 4 shows all 16 of the theoretically possible stereoisomers of nebivolol. Reflecting the images on the mirror planes σ_x and σ_y reduces the number of stereoisomers from eight enantiomeric pairs (16 compounds) to 10 compounds (Table 2). It is important to realize that reflection on σ_x and σ_y gives the same result (Fig. 5). This theoretical treatment is sufficient and drawing of all stereoisomers is not necessary—this is very useful if a number of compounds with many stereogenic units are of interest.

Thus, nebivolol (1-(6-fluorochroman-2-yl)-2-[2-(6-fluorochroman-2-yl)-2-hydroxyethylamino]ethanol), with its four chiral centers, exists as only 10 possible stereoisomers. Two of them are meso-compounds (i.e. they have an intramolecular mirror plane) and the others are enantiomeric pairs. All other relationships between the stereoisomers are diastereomeric. All actual stereoisomers are listed in Table 2. Only two of them have intrinsic activity: (+)-nebi-

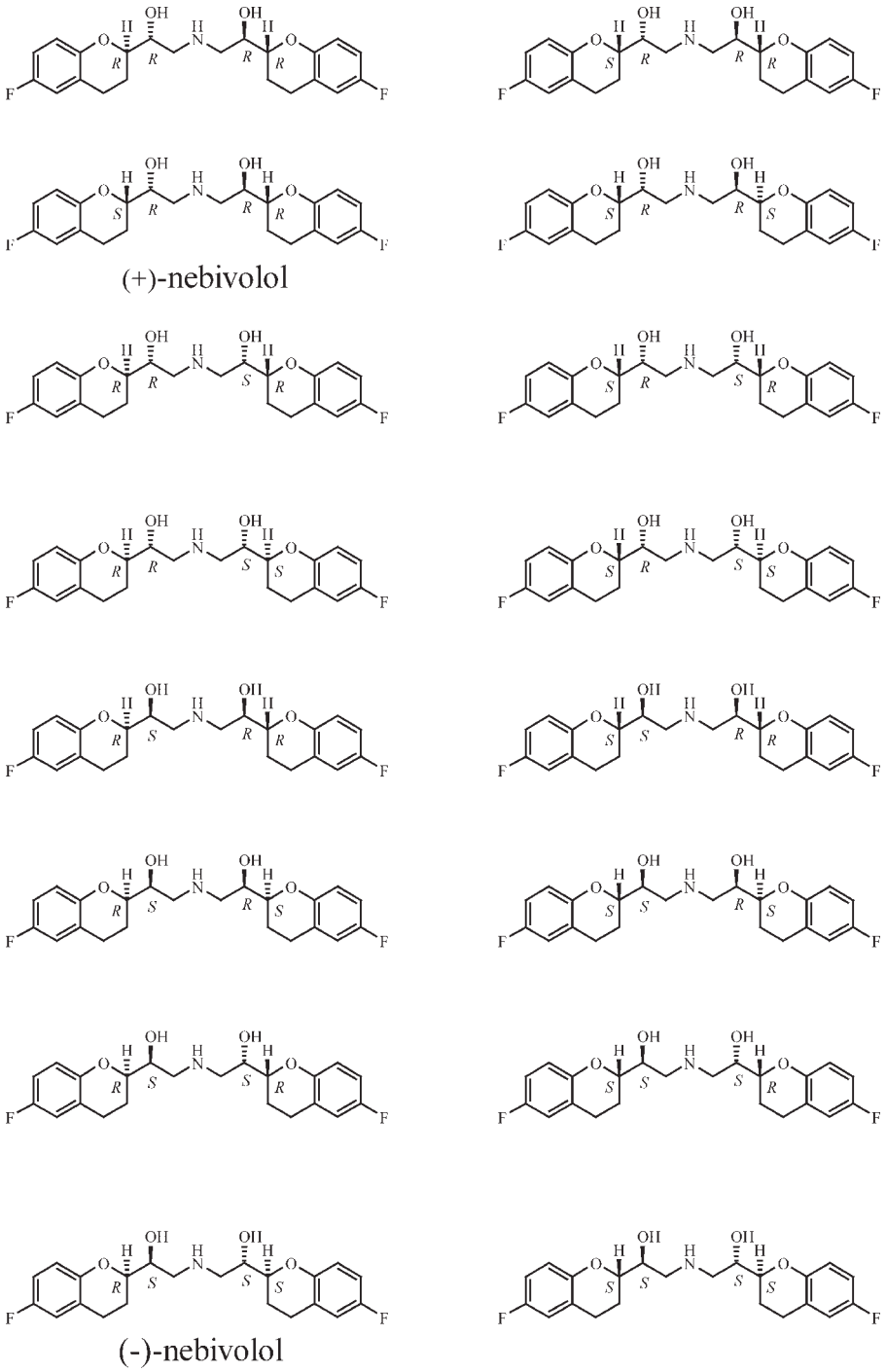

Fig. 4. Sixteen theoretically possible stereoisomers of nebivolol.

volol (*SRRR*) and (−)-nebivolol (*SSSR*). The term intrinsic activity is used to denote that a ligand–receptor complex shows a desired effect in the organism, in this instance antihypertensive activity; the assumption is that this results from the binding of a drug molecule at its receptor.

The number of actual stereoisomers ($n = 10$) is less than the number of possible stereoisomers ($2^4 = 16$) because the constitution of nebivolol is symmetric. The identical sets of stereodescriptors are named in Table 3. Now it becomes much clearer that (+)-nebivolol can be described stereochemically by two sets of stereodescriptors: *SRRR* and *RRRS*. This knowledge is helpful when searching and reading scientific literature: for chiral molecules with symmetric constitutions, pairs of molecules are

TABLE 2. Actual stereoisomers of nebivolol

Image	Reflected image	Isomeric relationship	Point group	Σ = 10
RRRR	*SSSS*	Enantiomeric	C_2	2
RRSR	*SRSS*	Enantiomeric	C_1	2
SRRR [(+)-nebivolol]	*SSSR* [(−)-nebivolol]	Enantiomeric	C_1	2
RRSS	*RRSS*	Meso-compounds	C_s	1
RSRS	*RSRS*	Meso-compounds	C_s	1
RSSR	*SRRS*	Enantiomeric	C_2	2

identical when the sequence of stereodescriptors for one is exactly the reverse of another, e.g. an *RRRS*-configuration is identical with an *SRRR*-configuration. Reading forward or backward is allowed.[4]

To help elucidate the stereochemistry at the hydroxy group, the configuration of the enantiomerically pure β-blockers timolol, penbutolol, levobunolol, and esatenolol is shown in Figure 6. Levobunolol is an ingredient of racemic bunolol and esatenolol is the *S*-enantiomer of atenolol (Atehexal®).

It can be seen from Figure 6 that the hydroxy group is always in the *S*-configuration to get an antihypertensive systemic effect (excepting ophthalmic use[13]). Conversely, the pure *R*-configuration enantiomer dexpropranolol (Fig. 1A) has no pharmacological relevance. Nevertheless, most of the more than 100 agents with β-blocking activity are administered as racemates.

The determination of the absolute configuration of nebivolol is described in detail in Figure 2. The CIP rules for the determination of priority are applied to specify the configuration of a chiral center. The substituents are ranked and the position of the hydrogen atom which is above or below the plane of the paper must be considered. A clockwise numbering with hydrogen (the substituent of lowest priority) below the plane of the paper results is deemed the *R*-configuration. An anticlockwise counting is deemed the *S*-configuration.

Fig. 5. Nebivolol contains 10 possible stereoisomers instead of the $n = 2^4 = 16$ stereoisomers. For nebivolol pairs of isomers are identical when the sequence of stereodescriptors for one is exactly the reverse of another, e.g. the *RRRS*-configuration is identical with an *SRRR*-configuration. This simple rule allows elimination of identical stereoisomers without the necessity of drawing all 16 compounds by reflection on σ_x and σ_y. [Color figure can be viewed in the online issue, which is available at www.interscience.wiley.com.]

Comparison of the first generation β-blockers and nebivolol indicates that the orientation of the hydroxy group relative to the neighboring aryl residue is important (*R*-configuration in nebivolol and *S*-configuration in enantiomerically pure aryloxyaminopropanol derivatives). The topology of these structural elements is not comparable although their intrinsic activity (i.e. cardiac antihypertensive activity) is comparable.

The binding of (+)-nebivolol, (−)-nebivolol and the eight stereoisomers to β_1-adrenoceptors from rabbit lung membrane preparations was tested in an in vitro assay.[14] The IC_{50} values of the stereoisomers are listed in order of decreasing potency in Table 4. The binding of the *SSSS*-stereoisomer was about 1200-fold weaker than that of (+)-nebivolol, and binding of the *RSSS*-stereoisomer, (−)-nebivolol, was 175-fold weaker than that of (+)-nebivolol. Most of the stereoisomers with a hydroxy group in the *S*-configuration had weak binding affinities. Both symmetric meso-compounds showed only high nanomolar activity. All enantiomeric couples had very different binding affinities. It is obvious from these findings that a relationship between configuration at the chirality centers and binding affinity is not simple.

It is surprising that (+)-nebivolol (*SRRR*) is about 175 times more active than (−)-nebivolol (*RSSS*). It is difficult to reconcile this finding with the stereochemistry of other β_1-selective blocking agents; that is, the orientation of the hydroxy group and the neighboring bicyclic system is not in accordance with that observed in all other β-blockers. Obviously, the established pharmacophore

TABLE 3. *SRRR* and *RRRS* are identical because the sequence for one stereodescriptor is exactly the reverse of another

Stereo-descriptor 1	Stereo-descriptor 2	Isomeric relationship	Point group	Σ = 6
RSSS	*SSSR* [(−)-nebivolol]	Identical	C_1	1
SRSS	*SSRS*	Identical	C_1	1
RRSS	*SSRR*	Identical	C_s	1
RSRS	*SRSR*	Identical	C_s	1
SRRR [(+)-nebivolol]	*RRRS*	Identical	C_1	1
RSRR	*RRSR*	Identical	C_1	1

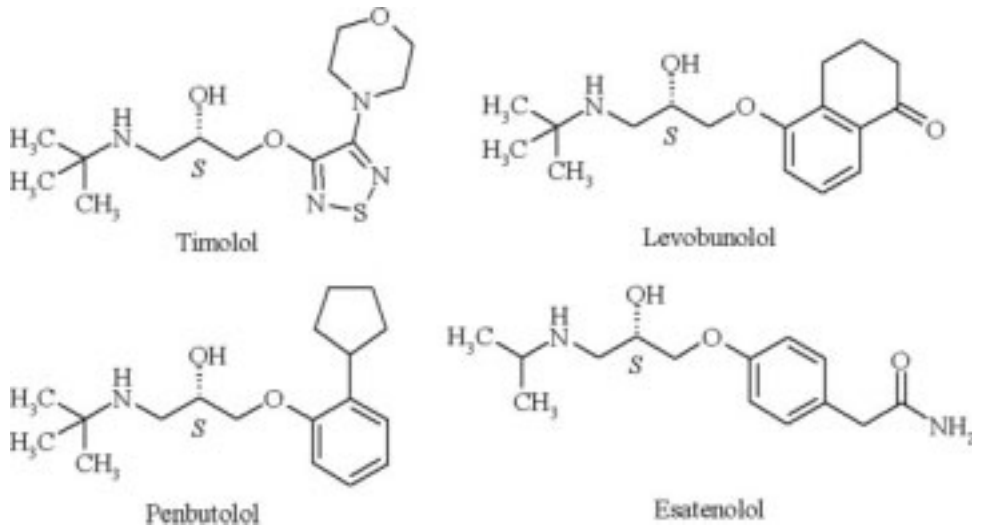

Fig. 6. β-Blockers marketed as pure enantiomers.

model for the interaction of ligands at the receptor binding site must be extended. All other sympatholytics contain only 1 or 2 chiral centers and have more degrees of freedom because of their linear carbon chains. In the case of nebivolol, in which two chirality centers are part of a ring structure, increased rigidity seems to be important for this deviation from the standard pharmacophore model of β-blockers.

Nebivolol is a β-blocker with an unusual constitution and configuration and has an interesting pharmaceutical profile. Racemic nebivolol differs from all other β-blockers and its antihypertensive properties and beneficial effects on left ventricular function result from the combined and synergistic actions of both enantiomers. The (+)-enantiomer shows β_1-blocking activity and the (−)-enantiomer acts as a vasodilator.[13–17] Vasodilation may be achieved by NO release, as indicated by studies in animal models and in humans, with possible mechanisms including an increase in NO synthase and stimulation of P2Y-purinoceptor-mediated NO release.[18] Consideration of stereochemical properties and the application of modern analytic methods delivers deeper insights into the antihypertensive profile of nebivolol.

TABLE 4. IC_{50} values in a rabbit lung β_1-adrenoceptor binding assay[14]

Stereoisomer	IC_{50} (nM)
SRRR [(+)-nebivolol]	0.8
SRRS	2.7
RRSR	3.8
RRRR	11
SRSS	30
SRSR	38
RSSR	84
RRSS	133
RSSS [(−)-nebivolol]	140
SSSS	945

LITERATURE CITED

1. Siebert CD. Spatial view and description of nebivolol. Pharmazie Unserer Zeit 2004;33:450–454.
2. Mehvar R, Brocks DR. Stereospecific pharmacokinetics and pharmacodynamics of β-adrenergic blockers in humans. J Pharm Pharm Sci 2001;4:185–200.
3. Stoschitzky K, Lindner W. Specific and nonspecific effects of β-receptor blockers: stereoselectively different properties exemplified by (*R*)- and (*S*)-propranolol. Wien Med Wochenschr 1990;140:156–162.
4. Siebert CD, Tampe N. Stereoisomers of compounds with symmetric constitutions. Arch Pharm (Weinheim) 2005;338:534–8.
5. Brittain RT, Drew GM, Levy GP. The α- and β-adrenoceptor blocking activities of labetalol and its individual stereoisomers in anaesthetized dogs and in isolated tissues. Br J Pharmacol 1982;77:105–114.
6. Riva E, Mennini T, Latini R. The α- and β-adrenoceptor blocking activities of labetalol and its RR-SR (50:50) stereoisomers. Br J Pharmacol 1991;104:823–828.
7. Brixius K, Bundkirchen A, Bolck B, Mehlhorn U, Schwinger RH. Nebivolol, bucindolol, metoprolol and carvedilol are devoid of intrinsic sympathomimetic activity in human myocardium. Br J Pharmacol 2001;133:1330–1338.
8. Chandrasekhar S, Venkat Reddy M. Enantioselective total synthesis of the antihypertensive agent (*S*,*R*,*R*,*R*)-nebivolol. Tetrahedron 2000;56:6339–6344.
9. Van Lommen G, De Bruyn M, Schroven M. Synthesis and pharmacological properties of nebivolol, a new antihypertensive compound. J Pharm Belg 1990;45:355–360.
10. Zakharkin LI, Khorlina IM. Reduction of esters of carboxylic acids into aldehydes with diisobutylaluminum hydride. Tetrahedron Lett 1962;14:619–620.
11. Aboul-Enein HY, Ali I. HPLC enantiomeric resolution of nebivolol on normal and reversed amylose based chiral phases. Pharmazie 2001;56:214–216.
12. Tuchalski G, Emmerling F, Gröger K, Hänsicke A, Nagel T, Reck G. X-ray investigations of nebivolol and its isomers. J Mol Struct 2006;800:28–44.

13. Steinhilber D, Schubert-Zsilavecz M, Roth HJ. *Medizinische Chemie—Targets und Arzneistoffe* [Medicinal Chemistry—Targets and Drugs]. Germany: Deutscher Apotheker Verlag Stuttgart; 2005. p 209–216.
14. Pauwels PJ, Gommeren W, Van Lommen G, Janssen PA, Leysen JE. The receptor binding profile of the new antihypertensive agent nebivolol and its stereoisomers compared with various beta-adrenergic blockers. Mol Pharmacol 1988;34:843–851.
15. Johannes CW, Visser MS, Weatherhead GS, Hoveyda AH. Zr-catalyzed kinetic resolution of allylic ethers and mo-catalyzed chromene formation in synthesis. Enantioselective total synthesis of the antihypertensive agent (*S,R,R,R)*-nebivolol. J Am Chem Soc 1998;120:8340–8347.
16. Stoleru L, Wijns W, van Eyll C, Bouvy T, Van Nueten L, Pouleur H. Effects of D-nebivolol and L-nebivolol on left ventricular systolic and diastolic function: comparison with DL-nebivolol and atenolol. J Cardiovasc Pharmacol 1993;22:183–190.
17. Van Peer A, Snoeck E, Woestenborghs R, Van De Velde V, Mannens G, Meuldermans W, Heykants J. Clinical pharmacokinetics on nebivolol. A review. Drug Invest 1991;3 (Suppl 1):25–30.
18. Bakris GL. Pharmacological augmentation of endothelium-derived nitric oxide synthesis. J Manag Care Pharm 2007;13 (5 Suppl):S9–S12.

CHIRALITY 20:110–114 (2008)

Synthesis of a New C_2-Symmetric Chiral Catalyst and Its Application in the Catalytic Asymmetric Borane Reduction of Prochiral Ketones

YAN ZHOU, WEN-HUA WANG, WEI DOU, XIAO-LIANG TANG, AND WEI-SHENG LIU*

College of Chemistry and Chemical Engineering, State Key Laboratory of Applied Organic Chemistry, Lanzhou University, Lanzhou 730000, People's Republic of China

ABSTRACT A new C_2-symmetric chiral catalyst 3,5-bis[(2*S*)-(hydroxy-diphenylmethyl)- pyrrolidin-1-ylmethyl]-1,3,4-oxadiazole was successfully synthesized by the reaction of 2,5-dichloromethyl-1,3,4-oxadiazole with (*S*)-α,α-diphenyl-2-pyrrolidinemethanol, and applied to the catalytic asymmetric reduction of prochiral ketones with borane. When the catalyst loading was 1 mol %, enantiomeric excesses of up to 86.8% and 94.5% were observed in reduction of aromatic and α-halo ketones, respectively. *Chirality 20:110–114, 2008.*

KEY WORDS: C_2-symmetric; amino alcohol; enantioselectivity; asymmetric reduction; ketones

INTRODUCTION

The borane-mediated asymmetric reduction of prochiral ketones has attracted considerable attention owing to its usefulness in preparing enantiomerically enriched secondary alcohols.[1–3] After the reports by Itsuno and coworkers[4] and Corey et al.[5,6] using chiral 1,3,2-oxazaborolidines as catalysts in the enantioselective borane reduction of prochiral ketones, considerable efforts have been directed to develop more effective catalysts derived from prolinols.[7–14] C_2-symmetric catalysts have also received much attention and have been used in many reactions,[15–19] as it has been suggested that the C_2 ligands enhance the enantioselectivity of the reaction by reducing the number of competing diasteromeric parthways due to the homotopic nature of the remaining coordination sites of the complexes formed by the ligand.[20] Du and coworkers[7] used **1** and **2** as catalysts in the borane reduction of prochiral ketones. Their results demonstrated that catalyst containing a monoprolinol **1** was better than the C_2-symmetric ligand **2** (Fig. 1). To further understand the structural effect of the catalysts on their catalytic activity, we designed and synthesized a modified ligand **3** based on the mechanism proposed by Du and coworkers.[7] Two major structural changes were made compared to catalyst **2**: (1) a more highly coordinated N atom; and (2) expanded space between two prolinol parts. Ligand **3** was employed as a catalyst in the reduction to examine whether these changes would be beneficial for the improvement of the enantiosectivity. Its crystal structure [Crystal data for 2,5-bis[(2*S*)-(hydroxydiphenylmethyl)-pyrrolidin-1-ylmethyl]-1,3,4-oxadiazole. $CHCl_3$: Empirical formula: $C_{39}H_{41}Cl_3N_4O_3$, formula weight: 720.11, monoclinic, space group $P2_1$(No. 4), a = 13.6651(3), b = 10.8796(3), c = 13.6653(3) Å, α = 90°, β = 116.5180(10) °, γ = 90°, V = 1817.89(8) Å^3, Z = 2, D_c = 1.316 g cm^{-1}, μ = 0.295 mm^{-1}, λ(MoK$_\alpha$) = 0.71073 Å, F(000) = 756.0, crystal size 0.3 × 0.27 × 0.2 mm^3, $R(I > 2s_1)$ = 0.0541, wR^2 = 0.1409. Detailed X-ray crystallographic data are available from the Cambridge Crystallographic Data Center, 12 Union Road, Cambridge CB2 1EZ, UK (CCDC No646244)] was also confirmed by X-ray analysis. It was obtained as an air-stable, colorless single crystal upon slow evaporation in acetate-chloroform. A perspective view of it is shown in Figure 2.

EXPERIMENTAL SECTION

General Methods

Melting points were taken on an X-6 melting point apparatus and the data were uncorrected. FT-IR spectra were obtained on a Nicolet FT-170SX spectrometer with KBr disc. ^{1}H NMR spectra were recorded on a DRX-300 MHz spectrometer with tetramethylsilane (TMS) serving as internal standard. Electron ionization mass spectra were obtained on a Hewlett-Packard HP5988A mass spectrometer. ESI-MS was recorded on a Mariner® biospectrometer. Optical rotations were measured on a Perkin–Elmer 341 Polarimeter spectrometer. Elemental analyses were carried out on an Elementar Vario EL instrument. The ee value determination was carried out using chiral HPLC on a Daicel Chiracel® OB-H (or OJ-H) columns on Waters® with a 996 UV-detector or on a Daicel Chiracel® OD-H col-

Contract grant sponsor: NSFC; Contract grant numbers: 20431010, 20621091, J0630962
Contract grant sponsor: Lanzhou University, China
*Correspondence to: Wei-Sheng Liu, College of Chemistry, Chemical Engineering and State Key Laboratory of Applied Organic Chemistry, Lanzhou University, Lanzhou 730000, People's Republic of China.
E-mail: liuws@lzu.edu.cn
Received for publication 24 August 2007; Accepted 19 October 2007
DOI: 10.1002/chir.20503
Published online 11 December 2007 in Wiley InterScience (www.interscience.wiley.com).

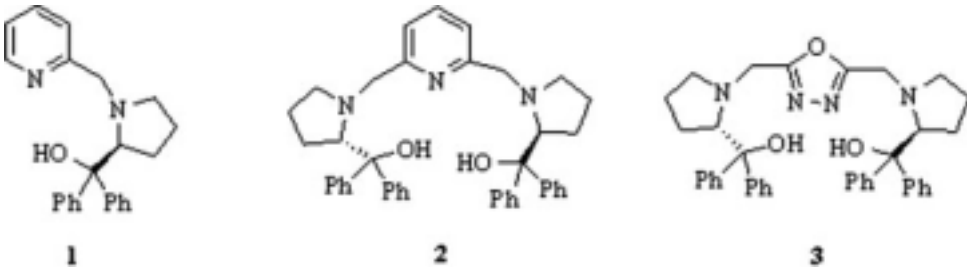

Fig. 1. Structures of **1**, **2** and **3**.

umn on Varian® with a UV detector. The absolute configuration of the major enantiomer was assigned according to the sign of the specific rotation. All reactions were carried out under an argon atmosphere. THF and toluene was dried over sodium and freshly distilled before use. Borane-dimethyl sulfide was obtained from Acros.

Preparation of the Chiral Ligand 3

2,5-Dichloromethyl-1,3,4-oxadiazole **4**: Compound **4** was prepared according to the literature[21] as a colorless liquid in 42% yield; IR (KBr): υ3030, 2970, 1583, 1567, 1429, 1384, 1235, 992, 786, 763, 721, 657 cm^{-1}; ^1H NMR (300 MHz, $CDCl_3$): δ 4.70(s, 4 H); ^{13}C NMR (75 MHz, $CDCl_3$): 32.58, 163.55; MS (EI): *m/z*: 167.8$[M+1]^+$, 116.8, 130.9, 165.8; Anal. Calcd for $C_4H_4Cl_2N_2O$: C, 28.77; H, 2.41; N, 16.78; Found: C, 28.64; H, 2.21; N, 16.70.

(*S*)-α,α-Diphenyl-2-pyrrolidinemethanol 5: Compound 5 was prepared according to a literature procedure[22] in 65% overall yield as a colorless solid. $[\alpha]_D^{20}$= –55 (*c* 0.33, CH_3OH) [lit.[23] $[\alpha]_D^{21}$= –54.3 (*c* 0.261, CH_3OH)]; Mp 76.4–78.6°C [lit.[23] Mp 79–79.5°C]; IR (KBr): υ 3600–3100 (br), 3060, 2957, 2886, 1491, 1450, 1400, 1181, 753, 706, 635 cm^{-1}; ^1H NMR (300 MHz, $CDCl_3$): δ 1.54–1.67(m, 2H), 1.69–1.79(m, 2H), 2.91–3.07(m, 2H), 4.26(t, *J* = 7.5 Hz, 1H), 7.14–7.19(m, 2H), 7.25–7.32(m, 4H), 7.50(d, *J* = 8.1 Hz, 2H), 7.58(d, *J* = 8.1 Hz, 2H); MS (ESI): *m/z*: 254.2$[M+1]^+$; Anal. Calcd for $C_{17}H_{19}NO$: C, 80.60; H, 7.56; N, 5.53; Found: C, 80.36; H, 7.60; N, 5.27.

2,5-bis[(2*S*)-(hydroxy-diphenylmethyl)-pyrrolidin-1-yl-methyl]-1,3,4-oxadiazole **3:** To a solution of 2,5-dichloromethyl-1,3,4-oxadiazole **4** (1 mmol) in absolute ethanol was added anhydrous potassium carbonate (2 mmol) and KI (5 mg). The solution was stirred at 40°C for 0.5 h and then (*S*)-α,α-diphenyl-2-pyrrolidinemethanol **5** (2 mmol) was added. The reaction was stirred and refluxed. After the completion of the reaction as indicated by TLC, the mixture was filtered and the solvent was removed under reduced pressure. The crude product was purified by column chromatography (petroleum ether-ethyl acetate 10:1) and recrystallization from ethyl acetate/chloroform (5:1) to afford a colorless solid 590 mg in 82% yield. $[\alpha]_D^{20}$ = +18 (*c* 0.26, $CHCl_3$); Mp 109.2-111.4°C; IR (KBr): υ 3408, 3333, 2817, 1577, 1491, 1446, 1364, 1216, 1169, 1121, 1032, 983 cm^{-1}; ^1H NMR (300MHz, $CDCl_3$): δ 1.66–1.82(m, 6H), 1.89–2.00(m, 2H), 2.63–2.71(m, 2H), 3.06–3.11(m, 2H), 3.31, 3.39(AB system, *J* = 15.6Hz, 4H), 4.22–4.27(dd, *J* = 4.2, 8.7 Hz, 2H), 4.44(br s, 2H), 7.13–7.34(m, 12H), 7.60(d, *J* = 7.5 Hz, 4H), 7.70(d, *J* = 7.8 Hz, 4H); ^{13}C NMR (75 MHz, $CDCl_3$): 22.74, 29.89, 48.36, 55.67, 69.10, 78.18, 125.76, 125.79, 126.74, 126.90, 128.43, 128.55, 146.10, 147.66, 164.59; MS (ESI): *m/z*: 601.5$[M+1]^+$; Anal. Calcd for $C_{39}H_{41}Cl_3N_4O_3$: C, 65.05; H, 5.74; N, 7.78; Found: C, 65.14; H, 5.80; N, 7.61.

Typical Procedure for the Reduction of Prochiral Ketones

To a stirred solution of **3** (0.005 mmol) in dry THF (3 mL) was added $BH_3{\cdot}Me_2S$ (0.3 mL, 2M) under argon at 0°C. The resulting solution was heated to reflux and then stirred at refluxing temperature for 3 h. A solution of the ketone (0.5 mmol) in dry THF (3 mL) was added dropwise

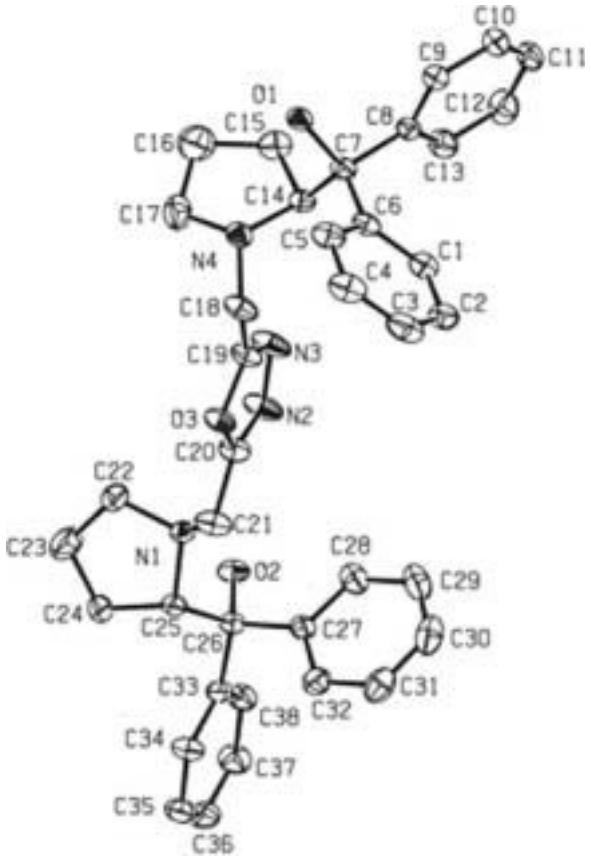

Fig. 2. ORTEP diagram of catalyst **3**.

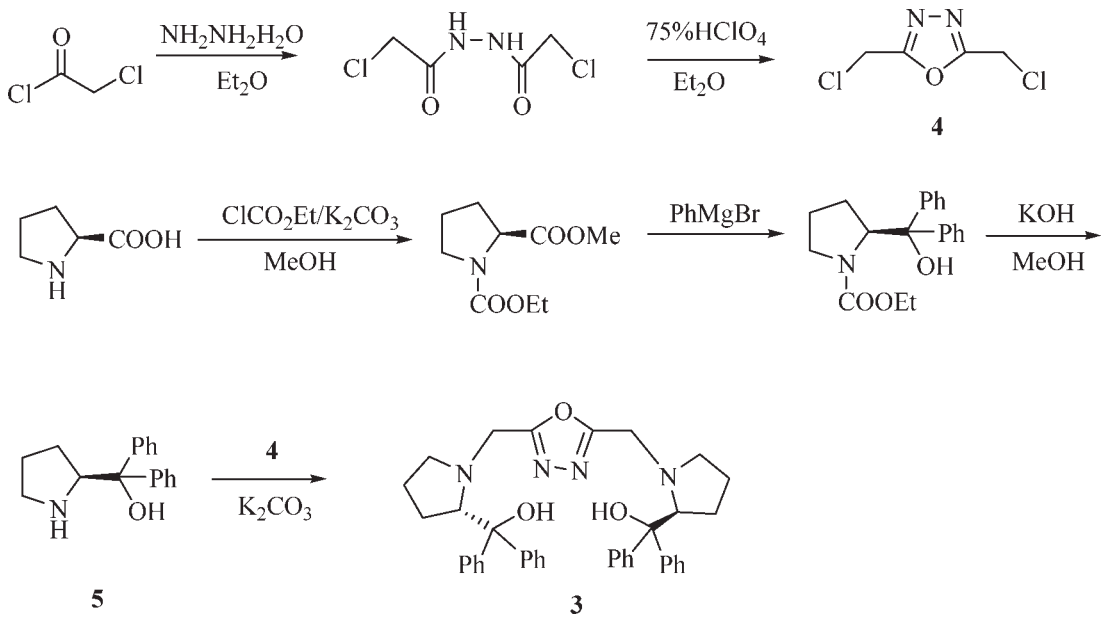

Scheme 1. Synthesis of catalyst **3**.

over a period of 1 h at refluxing temperature. After refluxing for a further 1 h, the reaction mixture was cooled and decomposed by dropwise addition of aqueous HCl (2N, 2 mL). When gas emission ceased, the alcohol product was extracted into ethyl acetate (10 mL × 3). The organic extract was washed with brine and dried over anhydrous sodium sulfate. After concentrated by rotatory evaporation, the product was purified by column chromatography on silica gel (petroleum ether/ethyl acetate 8:1) to afford the corresponding secondary alcohol. The enantiomeric excess was determined by HPLC with chiral columns.

RESULTS AND DISCUSSION

The new chiral C_2-symmetric prolinol derivative 3,5-bis[(2*S*)-(hydroxy- diphenylmethyl)-pyrrolidin-1-ylmethyl]-1,3,4-oxadiazole **3** was first synthesized from *N*-alkylation of (*S*)-α,α-diphenyl-2-pyrrolidinemethanol **5** with 2,5-dichloromethyl-1,3,4-oxadiazole **4**. Compound **4** was obtained in 42% yield from inexpensive and commercially available chloroacetyl chloride and hydrazine hydrate by a known procedure[21] (Scheme 1).

The C_2-symmetric chiral ligand **3** was first evaluated in the catalytic enantioselective borane reduction of acetophenone under various experimental conditions to find the optimum reaction conditions. The results were summarized in Table 1. It was found that the enantiomeric purity of the secondary alcohol product was greatly affected by the reaction temperature.[28–30] At low temperature (35°C) the reaction gave product with poor ee's of 27.3% and 10.0% in THF and toluene, respectively. When the reaction was carried out at refluxing temperature, 70.3% (in THF) and 40.5% (in toluene) ee values were achieved (Table 1, entries 3 and 8). These results also suggested that THF was better than toluene.

Increasing the catalyst loading is known to increase the asymmetric induction in some cases. The effect of catalyst loading on the enantioselectivity of the acetophenone reduction was revealed by using different amounts of the catalyst from 10 mol % to 0.1 mol %. When the reaction was carried out at reflux in THF using 10 mol % catalyst

TABLE 1. Enantioselective borane reduction of acetophenone[a]

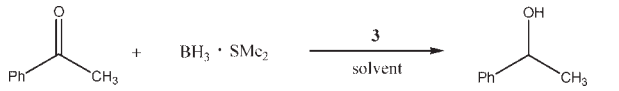

Entry	**3** (mol%)	Solvent	Temperature (°C)	Yield[b] (%)	ee[c] (%)	Config[d]
1	5	THF	35	85	27.3	*R*
2	5	THF	50	86	49.0	*R*
3	5	THF	refluxing	88	70.3	*R*
4	5	Toluene	35	90	10.0	*R*
5	5	Toluene	50	90	13.1	*R*
6	5	Toluene	66	87	33.1	*R*
7	5	Toluene	90	85	34.5	*R*
8	5	Toluene	refluxing	87	40.5	*R*
9	10	THF	refluxing	80	51.9	*R*
10	7.5	THF	refluxing	83	57.1	*R*
11	2.5	THF	refluxing	86	72.5	*R*
12	1	THF	refluxing	88	82.6	*R*
13	0.5	THF	refluxing	88	81.4	*R*
14	0.25	THF	refluxing	80	66.2	*R*
15	0.1	THF	refluxing	78	38.8	*R*

[a]Reaction was carried out on a 0.5-mmol scale, molar ratio of ketone: $BH_3{\cdot}Me_2S$ = 1:1.2.
[b]Isolated yield by column chromatography.
[c]ee values were determined by HPLC (Daicel Chiracel OD-H Column).
[d]The absolute configuration of the product was determined by comparison of the sign of the specific rotation to the literature data.[24–27]

loading, the corresponding secondary alcohol (*R*)-1-phenylethanol was obtained in 51.9% ee. A decrease in the catalyst loading from 10 to 1 mol % resulted in an increase in the enantioselectivity. When the catalyst loading was decreased from 1 to 0.5 mol %, ee decreased slightly. However, when the catalyst loading was further decreased from 0.5 to 0.25 or 0.1 mol %, obvious decrease of the enantiomeric excess was observed.

To understand the applicability of catalyst **3**, a variety of aromatic ketones were subjected to the conditions optimized for acetophenone (refluxing in THF 1 mol % catalyst loading). As the results summarized in Table 2 show, the enantioselectivities obtained for prochiral ketones containing electon-withdrawing groups were higher than that of electron-donating ones(Table 2, entries 2–6). The decrease in enantioselectivity for the reduction of the ketone 4-methyloxyacetophenone may be rationalized to the coordination of the heteroatom with the boron atom in the catalyst and borane.[31–33] Probably because of steric effects, ketones containing substitution at the *ortho* position and l-acetonaphthone gave lower enantioselectivities (Table 2, entries 7–9). The ee values of the corresponding product decreased with increasing size of alkyl group (Table 2, entries 1 and 10). A dramatic decrease in selectivity was observed in the case of the cyclic ketone (Table 2, entry 12), which probably results from its relatively rigid conformation.

Catalyst **3** was also employed as a ligand in the reduction of a variety of α-halo ketones (Table 3), ee value of up to 94.5% was obtained. From these results it can also be concluded that α-halo ketones provide higher enantioselectivities than simple aryl alkyl ketones.

Under the optimized reaction conditions (THF, refluxing, 10 mol % catalyst loading), catalyst **2** gave 81% (acetophenone), 54% (*n*-butyrophenone), and 84% (α-bromoacetophenone) enantioselectivities. Compared with **2**, ligand **3** increased the e.e. slightly when acetophenone was used as a substrate (Table 1, entry 12). As for *n*-butyrophenone and α-bromoacetophenone, more obvious increased ee (about 7%) was observed. In contrast, **3** provided lower enantioselectivity than **1**. Decrease of ee about 15% was observed when acetophenone and *n*-butyrophenone were used as substrates. However, when α-bromoacetophenone and l-acetonaphthone were used, the decrease of ee's was not so obvious (about 2%). Further studies to extend the scope for this catalyst are under way in our laboratory.

TABLE 2. Enantioselective reduction of aromatic ketones[a]

Entry	Ketone	Yield[b] (%)	ee[c] (%)	Config[e]
1	Acetophenone	88	82.6	*R*
2	4-Nitroacetophenone	89	86.8[d]	*R*
3	4-Fluorocetophenone	85	86.0[d]	*R*
4	4-Chloroacetophenone	85	82.3	*R*
5	4-Bromoacetophenone	88	79.1[d]	*R*
6	4-Methoxyacetophenone	86	51.2	*R*
7	2-Chloroacetophenone	86	63.5	*R*
8	2-Bromoacetophenone	87	69.1[d]	*R*
9	2-Methoxyacetophenone	82	56.9[d]	*R*
10	*n*-Butyrophenone	86	61.3	*R*
11	l-Acetonaphthone	85	35.7	*R*
12	α-Tetralone	80	36.6	*R*

[a]Reaction was carried out on a 0.5-mmol scale, molar ratio of ketone: $BH_3{\cdot}Me_2S$: **3** = 1: 1.2: 0.01.
[b]Isolated yield by column chromatography.
[c]ee values were determined by HPLC(Daicel Chiracel OD-H Column).
[d]ee values were determined by HPLC(Daicel Chiracel OB-H Column).
[e]The absolute configuration of the product was determined by comparison of the sign of the specific rotation to the literature data.[8–14,24–27]

TABLE 3. Asymmetric reduction of prochiral α-halo ketones[a]

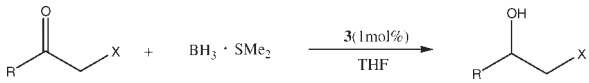

Entry	R	X	Yield[b] (%)	ee[c] (%)	Config[f]
1	Ph	Br	93	90.5	*S*
2	Ph	Cl	92	88.7	*S*
3	*p*-CH_3Ph	Br	90	91.5	*S*
4	*p*-CH_3Ph	Cl	92	94.5	*S*
5	*p*-BrPh	Br	93	91.2[d]	*S*
6	*p*-ClPh	Br	91	88.4[d]	*S*
7	*p*-NO_2Ph	Br	89	80.5[e]	*S*

[a]Reaction was carried out on a 0.5-mmol scale, molar ratio of ketone: $BH_3{\cdot}Me_2S$: **3** = 1: 1.2: 0.01.
[b]Isolated yield by column chromatography.
[c]ee values were determined by HPLC (Daicel Chiracel OD-H Column).
[d]ee values were determined by HPLC (Daicel Chiracel OJ-H Column).
[e]ee values were determined by HPLC (Daicel Chiracel OD-H Column) analysis of the corresponding acetate.
[f]The absolute configuration of the product was determined by comparison of the sign of the specific rotation to the literature data.[24–27]

LITERATURE CITED

1. Singh VK. Practical and useful methods for the enantioselective reduction of unsymmetrical ketones. Synthesis 1992;605–617.
2. Deloux L, Srebnik M. Asymmetric boron-catalyzed reactions. Chem Rev 1993;93:763–784.
3. Corey EJ, Helal CJ. Reduction of carbonyl compounds with chiral oxazaborolidine catalysis: a new paradigm for enantioselective catalysis and a powerful new synthetic method. Angew Chem Int Ed Engl 1998;37:1986–2012.
4. Hirao A, Itsuno S, Nakahama S, Yamazaki N. Asymmetric reduction of aromatic ketones with chiral alkoxy-amineborane complexes. J Chem Soc Chem Commun 1981;315–317.
5. Corey EJ, Bakshi RK, Shibata S. Highly enantioselective borane reduction of ketones catalyzed by chiral oxazaborolidines. Mechanism and synthetic implications. J Am Chem Soc 1987;109:5551–5553.
6. Corey EJ, Bakshi RK, Shibata S, Chen CP, Singh VK. A stable and easily prepared catalyst for the enantioselective reduction of ketones. Applications to multistep syntheses. J Am Chem Soc 1987;109:7925–7926.
7. Zhang Y-X, Du D-M, Chen X, Lü S-F, Hua W-T. Enantiospecific synthesis of pyridinylmethyl pyrrolidinemethanols and catalytic asymmetric borane reduction of prochiral ketones. Tetrahedron: Asymmetry 2004;15:177–182.
8. Gamble MP, Smith ARC, Wills M. A novel phosphinamide catalyst for the asymmetric reduction of ketones by borane. J Org Chem 1998;63:6068–6071.

9. Degni S, Wilén CE, Rosling A. Highly catalytic enantioselective reduction of aromatic ketones using chiral polymer-supported Corey, Bakshi, Shibata catalysts. Tetrahedron: Asymmetry 2004;15:1495–1499.
10. Zhou H-B, Zhang J, Lü S-M, Xie R-G, Zhou Z-Y, Choi MCK, Chan ASC, Yang TK. Design, synthesis and structure of new chiral squaric acid monoaminoalcohols and diaminoalcohols and their use as catalysts in asymmetric reduction of ketones and diketones. Tetrahedron 2001;57:9325–9333.
11. Du D-M, Fang T, Xu J-X, Zhang S-W. Structurally well-defined, recoverable C_3-aymmetric tris(β-hydroxy phosphoramide)-catalyzed enantioselective borane reduction of ketones. Org lett 2006;8:1327–1330.
12. Yang S-D, Shi Y, Sun Z-H, Zhao Y-B, Liang Y-M. Asymmeric borane reduction of prochiral ketones using imidazolium-tagged sulfonamide catalyst. Tetrahedron: Asymmetry 2006;17:1895–1900.
13. Fang T, Xu J-X, Du D-M. Highly enantioselective borane reduction of prochiral ketones catalyzed by C_3-symmetric tripodal β-hydrocy amides. Synlett 2006;1559–1563.
14. Wang G-Y, Liu X-Y, Zhao G. Synthesis of dendrimer-supported prolinols and their application in enantioselective reducrtion of ketones. Synlett 2006;1150–1154.
15. Jiang B, Feng Y. Enantioselective alkynylation of a prochiral ketone catalyzed by C_2-symmetric diamino diols. Tetrahedron Lett 2002;43:2975–2977.
16. Jiang B, Feng Y, Hang J-F. Catalytic enantioselective synthesis of secondary alcohols using C_2-symmetric diamino diol ligands. Tetrahedron: Asymmetry 2001;12:2323–2329.
17. Yang X-W, Shen J-H, Da C-S, Wang H-S, Su W, Liu D-X, Wang R, Michael CKC, Albert SCC. Highly enantioselective addition of diethylzinc to aldehydes catalyzed by a new chiral C_2-symmetric Ti–diol complex. Tetrahedron Lett 2001;42:6573–6575.
18. Garcia C, LaRochelle LK, Walsh PJ. A practical catalytic asymmetric addition of alkyl groups to ketones. J Am Chem Soc 2002;124:10970–10971.
19. Shi M, Jiang J-K. Chiral C_2-symmetric 2,4-disubstituted azetidines as chiral ligands in the addition of diethylzinc to aldehydes. Tetrahedron: Asymmetry 1999;10:1673–1679.
20. Chan T-H, Zheng G-Z. C_3-symmetric oxazolinyl ligand as catalyst in the enantioselective addition of diethylzinc to aldehydes. Can J Chem 1997;75:629–633.
21. Zhang R-F, Jordan R, Nuyken O. Preparation of poly(1,3,4-oxadiazole-2,5-diyl-1,2-vinylene) via anionic mechanism. Macromol Rapid Commun 2003;24:246–250.
22. Kanth JVB, Periasarny M. Convenient method for the synthesis of chiral α,α-diphenyl-2-pyrrolidinemethanol. Tetrahedron 1993;49:5127–5132.
23. Mathre DJ, Jones TK, Xavier LC, Blacklock TJ, Reamer RA, Mohan JJ, Jones ETT, Hoogsteen K, Baum MW, Grabowski EJJ. A practical enantioselective synthesis of .alpha.,.alpha.-diaryl-2-pyrrolidinemethanol. Preparation and chemistry of the corresponding oxazaborolidines. J Org Chem 1991;56:751–762.
24. Basavaiah D, Chandrashekar V, Das U, Reddy GJ. A study toward understanding the role of a phosphorus stereogenic center in (5S)-1,3-diaza-2-phospha-2-oxo-3-phenylbicyclo(3.3.0)octane derivatives as catalysts in the borane-mediated asymmetric reduction of prochiral ketones. Tetrahedron: Asymmetry 2005;16:3955–3962.
25. Basavaiah D, Reddy GJ, Chandrashekar V. A new chiral catalytic source with an N−P=O structural framework containing a proximal hydroxyl group for the borane-mediated asymmetric reduction of prochiral ketones. Tetrahedron: Asymmetry 2004;15:47–52.
26. Lin Y-M, Fu I-P, Uang B-J. Enantioselective borane reduction of aromatic ketones using chiral BINOL derivatives as ligands in an aluminum catalyst. Tetrahedron: Asymmetry 2001;12:3217–3221.
27. Basavaiah D, Rao KV, Reddy BS. (2S)-2-Anilinomethylpyrrolidine: an efficient in situ recyclable chiral catalytic source for the borane-mediated asymmetric reduction of prochiral ketones in refluxing toluene. Tetrahedron: Asymmetry 2006;17:1041–1044.
28. Stone GB. Oxazaborolidine catalyzed borane reduction of ketones: a significant effect of temperature on selectivity. Tetrahedron: Asymmetry 1994;5:465–472.
29. Xu J-X, Wei T-Z, Zhang Q-H. Effect of temperature on the enantioselectivity in the oxazaborolidine-catalyzed asymmetric reduction of ketones. Noncatalytic borane reduction, a nonneglectable factor in the reduction system. J Org Chem 2003;68:10146–10151.
30. Xu J-X, Wei T-Z, Zhang Q-H. Influences of electronic effects and anions on the enantioselectivity in the oxazaborolidine-catalyzed asymmetric borane reduction of ketone. J Org Chem 2004;69:6860–6866.
31. Xu J-X, Su X-B, Zhang Q-H. Preparation of highly enantiometically pure linear secondary alcohols via asymmetric reduction of prochiral ketones with borane. Tetrahedron: Asymmetry 2003;14:1781–1786.
32. Xu J-X, Lan Y, Wei T-Z, Zhang Q-H. Chiral oxazaborolidine-catalyzed asymmetric borane reduction of alkyl 4-dialkylaminophenyl ketones. Chin J Org Chem 2005;23:1457–1461.
33. Masuì M, Shioiri T. A practical method for asymmetric borane reduction of prochiral ketones using chiral amino alcohols and trimethyl borate. Synlett 1997;273–274.

CHIRALITY 20:115–118 (2008)

Candida rugosa Lipase-Catalysed Kinetic Resolution of 2-Substituted-Aryloxyacetic Esters with Dimethylsulfoxide and Isopropanol as Additives

ALESSANDRA AMMAZZALORSO, ROSA AMOROSO,* GIANCARLO BETTONI, BARBARA DE FILIPPIS, MARIALUIGIA FANTACUZZI, LETIZIA GIAMPIETRO, CRISTINA MACCALLINI, AND MARIA LUISA TRICCA

Department of Drug Sciences, University of Chieti "G. d'Annunzio", via dei Vestini, Chieti, Italy

ABSTRACT *Candida rugosa* lipase-catalysed hydrolysis of three different 2-substituted-aryloxyacetic esters was performed in aqueous buffer containing dimethyl sulphoxide and isopropanol from 0 to 80% v/v as additives, in order to obtain an enhancement of the enantioselectivity. For 2-(*p*-chlorophenoxy)acetic acid and 2-*n*-butyl-2-(*p*-chlorophenoxy)acetic acid ethyl esters, DMSO enhanced enzyme enantioselectivity more than IPA with an opposite enzymatic enantiopreference. The cosolvents moderately improved *Candida rugosa* lipase enantioselectivity for 2-phenyl-2-(*p*-chlorophenoxy)acetic acid ethyl ester. *Chirality 20:115–118, 2008.*

KEY WORDS: 2-substituted-aryloxyacetic acids; kinetic resolution; *Candida rugosa* lipase; dimethylsulphoxide; isopropanol

INTRODUCTION

Lipases are frequently used in enantiomeric discrimination because of their widely recognized potential for the production of enantiomerically pure compounds,[1] but their most common limitation is insufficient enantioselectivity. A strategy to obtain an enhancement of enzymatic enantioselectivity is the addition of additives to the reaction media[2]; it has been demonstrated that organic cosolvents or ionic liquids enhance the enantioselectivity of lipase-catalysed resolution of a wide range of compounds.[3,4] The inclusion of polar organic solvent changes the lipase conformation from the less hydrophobic closed form (the active site is covered by lid) to a more hydrophobic open form (the active site is open), favoring the binding of hydrophobic substrate to lipase.[5] Among various types of lipases, *Candida rugosa* lipase (CRL) is one of the most versatile and widely used enzymes for the resolution of esters and alcohols in both aqueous and organic media. In addition to stereoselective ester conversions, CRL can be used to perform regioselective and chemoselective acylations, deacylations and simple hydrolysis of esters under mild reaction conditions.[6]

The group of chiral 2-aryloxy acids includes compounds like Dichlorprop and Mecoprop, which are used as herbicides[7]; their racemic mixtures have been applied for many years. However, because only the (*R*)-forms have herbicidal properties, since the 1980s regulatory action prescribe the use of only pure active enantiomers.[8] Other chiral 2-aryloxy acids are the analogues of Clofibrate, that were found to exhibit antilipidemic activity; the role of enantioselectivity was demonstrated in the hypolipidemic action, human platelet function, chloride channel conductance, and peroxisome proliferation.[9] Several methods for the resolution of these racemic compounds were developed, including fractional crystallization, chromatographic enantioseparations on chiral stationary phases, dynamic kinetic resolution, and enzymatic kinetic resolution.[10–12]

Herein we report the CRL-catalysed hydrolysis of 2-substituted aryloxyacetic esters **1–3** (Fig. 1) in the presence of dimethyl sulphoxide (DMSO) and isopropanol (IPA) from 0 to 80% v/v as additives to the aqueous media, in an effort to improve enantioselectivity in the enzymatic synthesis of interesting herbicidal and antilipidemic compounds. Owing to the preliminary nature of this study, we began our work selecting DMSO and IPA according to published data regarding enzyme activation.[13,14] In particular, we directed our attention to the influence that the substituent at the stereogenic centre could exert upon the different enzymatic chiral recognition in the different media employed.

MATERIALS AND METHODS

General

Solvents (analytical grade) and buffers were used without further purification. A commercial preparation (Sigma) of lipase from *Candida rugosa* was used. Optical rotations were measured on a DIP 135 Jasco instrument. TLC was performed on silica gel plates (Merck 60 F254). Samples were analyzed by a HPLC device (Waters, model E600) equipped with a UV detector. A Chiracel IA (250 × 4.6

Contract grant sponsor: Italian MIUR
*Correspondence to: Rosa Amoroso, Department of Drug Sciences, University of Chieti "G. d'Annunzio", via dei Vestini, 66100 Chieti, Italy.
E-mail: ramoroso@unich.it
Received for publication 12 July 2007; Accepted 19 October 2007
DOI: 10.1002/chir.20505
Published online 11 December 2007 in Wiley InterScience (www.interscience.wiley.com).

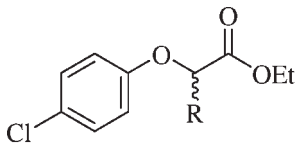

rac-**1** R = Me
rac-**2** R = *n*Bu
rac-**3** R = Ph

Fig. 1. 2-Substituted-aryloxyacetic esters used as CRL substrates.

mm, Daicel) chiral column was used at room temperature to determine both the conversion and the enantiomeric excess (ee_s) of the substrate.

Enzymatic Hydrolysis of Racemic Esters 1–3

Racemic ethyl esters **1–3** were synthesized by known procedures.[15] Each compound (0.025 mmol) was added to 0.01 M phosphate buffer pH = 7.4 (1 ml) containing DMSO or IPA (0–80 vol %), followed by ultrasonic dispersion (40 kHz). CRL (10 mg) was added and the reaction mixture was shaken at 37°C. At appropriate time intervals, 200 μl of the mixture was withdrawn and CH_3CN (0.5 ml) was added. After centrifugation (4500 rpm for 5 min), 5 μl of supernatant was analysed by HPLC.

HPLC Analysis

The mobile phase was *n*-hexane for compound **2**, and, for compounds **1** and **3**, *n*-hexane with the TFA 0.03 vol % or 0.05 vol %, respectively. Flow rate was 1 ml/min and detection was at 254 nm.

Stereochemistry of Unreacted Esters 1–3

Racemic **1**, **2**, and **3** (0.2 mmol) were suspended in phosphate buffer (8 ml) containing, respectively, 20, 40, and 0 vol % of DMSO; after ultrasonic dispersion (40 kHz), CRL (80 mg) was added (Table 1, entries 3, 11, and 13). The reaction mixtures were stirred at 37°C for 1 h, 4.5 h, and 48 h respectively, and then CH_3CN (5 ml) was added. After centrifugation (4500 rpm), the supernatant was filtered and concentrated in vacuum. The residue was resuspended in ether (5 ml) and washed with $NaHCO_3$ (7 ml). The organic layer was dried on Na_2SO_4 and evaporated under reduced pressure to give a pale oil containing the unreacted (*R*)- or (*S*)-enantiomer. Optical rotation of the residues were

1. $[\alpha]_D^{20}$: −90.0° (*c* 0.50, $CHCl_3$);

2. $[\alpha]_D^{20}$: +21.2° (*c* 0.50, $CHCl_3$);

3. $[\alpha]_D^{20}$:+ 63.3° (*c* 0.15, $CHCl_3$).

RESULTS AND DISCUSSION

In this work, the kinetic resolution of three 2-substituted-aryloxyacetic acids by CRL-catalyzed hydrolysis was investigated; reactions were carried on until no further improvement in enantiomeric excess of the substrate could be found upon monitoring by HPLC, injecting the sample on the chiral column at appropriate time intervals. Enantioselectivity of the kinetic resolution was estimated from the selectivity factor (*E* value), which is a convenient and often-used parameter for describing the efficiency of enzymatic resolution reactions.[16]

TABLE 1. Effects of addition of DMSO on the CRL-mediated hydrolysis of substrates 1–3 in aqueous buffer

Entry	Compd	DMSO % v/v	Time (h)	Conversion, *c* (%)	ee_s (%)	*E* value[a]
1	**1**	0	7	>90	0	–
2		10	2	50	58	4.8
3		20	1	55	96	>200
4		30	0.5	52	90	186.0
5		40	0.5	48	88	122.0
6		50	2	47	82	65.0
7		60–70	72	<20	0	–
8	**2**	0–10	24	>90	0	–
9		20	4.5	52	20	1.7
10		30	4.5	46	34	3.0
11		40	23	50	62	8.0
12		50–80	72	<15	0	–
13	**3**	0	48	72	90	5.6
14		10	72	60	49	3.0
15		20	48	70	76	4.1
16		30	48	49	48	4.7
17		40	48	42	40	4.9
18		50–80	72	<20	0	–

[a]Calculated by using following equation: $\ln[(1 - C)(1 - ee_s)]/[(1 - C)(1 + ee_s)]$.

Initially, the commercially available enzyme was screened with the *rac*-ethyl esters **1–3** in a reaction under standard conditions and then the CRL-mediated resolution of each racemic mixture was performed at 37°C in phosphate buffer (pH 7.4) containing DMSO or IPA up to 80% v/v (Scheme 1).

Effect of DMSO

Table 1 shows the extent of the conversion (*c*), the optical purity of the unreacted substrate expressed as enantiomeric excess (ee_s %), and the *E* value, for the hydrolysis of substrates **1–3** into the corresponding acids, using DMSO as cosolvent. For compound **1** (R = Me), hydrolysis with-

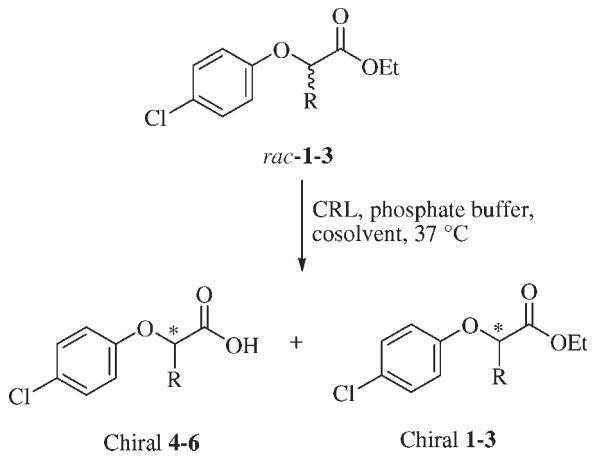

Scheme 1. Lipase-catalysed hydrolysis of *rac*-**1–3** with CRL.

TABLE 2. Effects of addition of IPA on the CRL-mediated hydrolysis of substrates 1–3 in aqueous buffer

Entry	Compd	IPA (%v/v)	Time (h)	Conversion (*c*) %	ee_s (%)	*E* value[a]
1	**1**	0	7	>90	0	–
2		10	1	52	71	10.2
3		20	2	60	72	6.0
4		30	0.5	44	74	74.0
5		40	0.5	41	16	1.8
6		50–80	2	<20	0	–
7	**2**	0	24	>90	0	–
8		10	48	50	58	6.5
9		20	44	49	10	1.3
10		30–80	72	<10	0	–
11	**3**	0	48	74	90	5.1
12		10	72	60	25	1.7
13		20	48	46	9	1.3
14		30–80	72	<20	0	–

[a]Calculated by using following equation: $\ln[(1 - C)(1 - ee_s)]/[(1 - C)(1 + ee_s)]$.

out cosolvent proceeded until 90% of substrate conversion, but no chiral discrimination was observed. The addition of DMSO to the reaction medium produced a dramatic enhancement of the enantioselectivity. In these conditions, the optimum DMSO amount was 20% v/v ($E > 200$). Good enantiomeric excesses were observed also when the cosolvent was between 30% and 50%, while an excess of DMSO (>50%) resulted in a loss of both enzymatic enantioselectivity and activity, probably due to an irreversible deformation of CRL.

Then we tested the effect of DMSO on the other substrates. Regarding compound **2** (R = *n*-Bu), in the absence of cosolvent, no substrate enantiomeric excess was observed up to 90% of substrate conversion, while addition of DMSO to the reaction medium gave a moderate increase to the enantioselectivity of the hydrolysis (*E* values between 1.7 and 8.0). The highest enantiomeric excess was reached after 23 h of reaction at 40% of cosolvent. Finally, for compound **3** (R = Ph), hydrolysis without addition of DMSO gave good enantiomeric excess of the unreacted substrate, although, after 48 h of reaction, conversion was quite high. Adding DMSO to the reaction media reduced both conversion and enantiomeric excesses with no substantial increase of the selectivity factor *E*. From the comparison of the earlier results, it appears that the DMSO-induced enantioselectivity was affected by the nature of the substituent at the stereogenic centre of the substrate; indeed, it was quite high for molecule **1**, moderate for substrate **2**, and negligible for compound **3**. The main finding that DMSO improves enantioselectivity for the compound **1** closely parallels that of Watanabe, who found similar results for the butyl ester analogue of **1**.[13]

Effect of IPA

Compared to DMSO, addition of IPA to the reaction medium resulted in a moderate improvement of the enantioselectivity, which was, also in this case, higher for substrate **1** than for esters **2** and **3**. Table 2 summarizes the results for the enantioselective hydrolysis of **1–3** using IPA as cosolvent. For compound **1**, adding 30% IPA to CRL showed the highest selectivity after 0.5 h ($E = 74$). For compound **2**, a small enhancement in enantioselectivity was reached only at 10% of IPA, while for compound **3** addition of the cosolvent made CRL selectivity worse.

Evaluation of the Enzymatic Enantiopreference

To establish which enantiomer was preferably hydrolyzed by CRL, we have performed preparative scale enzymatic hydrolysis of esters **1–3** in the presence of the optimum amount of DMSO (Table 1, entries 3, 11, and 13). Reaction mixtures were analyzed with HPLC and the chiral separation of unreacted substrates is shown in Figure 2. For evaluation of the enantiopreference of lipase, the optical rotation values of remaining chiral substrates were compared to $[\alpha]_D$ values from literature.[15] For compound **1**, (*S*)-enantiomer was found to be the unreacted optical

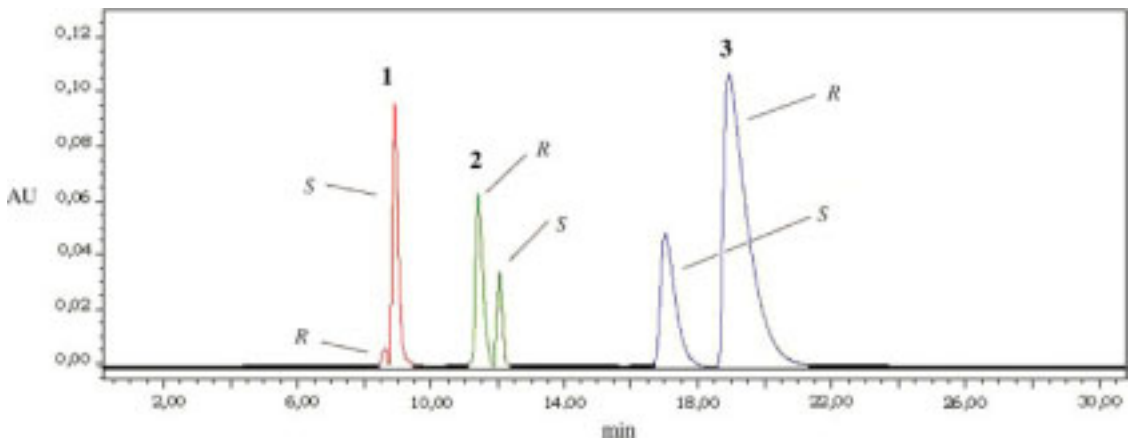

Fig. 2. HPLC enantioseparation of **1–3** esters after hydrolysis with CRL in the presence of optimum amount of DMSO. Conditions: column Diacel Chiralpak IA 0.46 cm × 25 cm, 5 μm; mobile phase *n*-hexane +0.03% TFA, 1 ml/min. [Color figure can be viewed in the online issue, which is available at www.interscience.wiley.com.]

TABLE 3. Enatiopreference of CRL in the hydrolysis of substrates 1–3

Entry	Compd	Experimental $[\alpha]_D^{20a}$	Absolute conf. of inalterate ester
1	**1**	−90.0° (*c* 0.5, $CHCl_3$)	*S*
2	**2**	+21.2° (*c* 0.5, $CHCl_3$)	*R*
3	**3**	+63.3° (*c* 0.15, $CHCl_3$)	*R*

[a]Evaluated from the unreacted residue after the preparative CRL-mediated hydrolysis.

antipode, while the opposite was observed for esters **2** and **3** (Table 3). So CRL preferentially hydrolyzed the (*R*)-enantiomer of compound **1** and the (*S*)-enantiomers of compounds **2** and **3**; these results are in agreement with the entantiopreference of the lipase expressed in exclusively aqueous media.[12]

In conclusion, we have reported the effect of two cosolvents in the enantioselectivity of CRL-catalysed hydrolysis of three 2-substituted-aryloxyacetic esters. The results obtained show that DMSO is a more efficacious cosolvent than IPA in enhancing enzyme selectivity when the substituent in 2-position is a methyl or a *n*-butyl group. When it is a phenyl group, addition of both DMSO or IPA does not increase CRL enantioselectivity. This preliminary work, that clearly calls for further detailed experimentation, suggests that small substituents allow better enantiomeric discrimination by the DMSO/IPA-modified CRL active site.

LITERATURE CITED

1. Jaeger K-E, Dijkstra BW, Reetz MT. Bacterial biocatalysts: molecular biology, three-dimensional structures and biotechnological applications of lipases. Annu Rev Microbiol 1999;53:315–351.
2. Theil F. Enhancement of selectivity and reactivity of lipases by additives. Tetrahedron 2000;56:2905–2919.
3. Koops BC, Verheij HM, Slotboom AJ, Egmond MR. Effect of chemical modification on the activity of lipases in organic solvents. Enzyme Microbial Technol 1999;25:622–631.
4. van Rantwijk F, Lau RM, Sheldon RA. Biocatalytic transformations in ionic liquids. Trends Biotechnol 2003;21:131–138.
5. Secundo F, Carrea G. Lipase activity and conformation in neat organic solvents. J Mol Catal B 2002;19-20:93–102.
6. Domınguez de Marıa P, Sanchez-Montero JM, Sinisterra JV, Alcantara AR. Understanding *Candida rugosa* lipases: an overview. Biotechnol Advances 2006;24:180–196.
7. Tomlin C, editor. The pesticide manual, 10th ed. Surrey, UK: British Crop Protection Council; 1994.
8. Williams A. Opportunities for chiral agrochemicals. Pestic Sci 1996;46:3–9.
9. Rangwala SM, O'Brien ML, Tortorella V, Longo A, Loiodice F, Noonan DJ, Feller DR. Stereoselective effects of chiral clofibric acid analogs on rat peroxisome proliferator-activated receptor α (rPPARα) activation and peroxisomal fatty acid β-oxidation. Chirality 1997;9: 93–97.
10. Fantacuzzi M, Bettoni G, D'Orazio G, Fanali S. Enantiomeric separation of some demethylated analogues of clofibric acid by capillary zone electrophoresis and nano-liquid chromatography. Electrophoresis 2006;27:1227–1236.
11. Ammazzalorso A, Amoroso R, Bettoni G, De Filippis B, Giampietro L, Maccallini C, Tricca ML. Dynamic kinetic resolution of α-bromoesters containing lactamides as chiral auxiliaries. Arkivoc 2004;375–381.
12. Chiaianoya F, Ferorelli S, Franchini C, Scilimati. A. *Candida cylindracea* lipase-mediated kinetic resolution of α-aryloxyacetic acid methyl esters. Il Farmaco 1996;51:293–296.
13. Watanabe K, Ueji S. Dimethyl sulfoxide as a co-solvent dramatically enhances the enantioselectivity in lipase-catalysed resolutions of 2-phenoxy-propionic acyl derivatives. J Chem Soc Perkin Trans 1 2001;1386–1390.
14. Colton IJ, Ahmed SN, Kazlauskas RJ. A 2-propanol treatment increases the enantioselectivity of *Candida rugosa* lipase toward esters of chiral carboxylic acids. J Org Chem 1995;60:212–217.
15. Bettoni G, Ferorelli S, Loiodice F, Tangari N, Tortorella V, Gasparrini F, Misiti D, Villani C. Chiral α-substituted α-aryloxyacetic acids: synthesis, absolute configuration, chemical resolution and direct separation by HPLC. Chirality 1992;4:193–203.
16. Chen C-S, Fujimoto Y, Girdaukas G, Sih C. Quantitative analyses of biochemical kinetic resolutions of enantiomers. J Am Chem Soc 1982;104:7294–7299.

CHIRALITY 20:119–124 (2008)

Comparative Studies on Pharmacokinetic Fates of Tetrahydropalmatine Enantiomers in Different Chemical Environments in Rats

ZHANYING HONG,[1] JIAN LE,[2] MEI LIN,[2] GUORONG FAN,[1]* YIFENG CHAI,[1] XUEPING YIN,[1] AND YUTIAN WU[1]

[1]*School of Pharmacy, Second Military Medical University, Shanghai Key Laboratory for Pharmaceutical Metabolites Research, Shanghai, People's Republic of China*

[2]*Shanghai Institute for Drug Control, Shanghai, People's Republic of China*

ABSTRACT Tetrahydropalmatine (THP) is the active component in *Rhizoma corydalis* and the medicine Yuanhu-Baizhi (YB), which consists of *Rhizoma corydalis* and *Radix angelicae dahuricae*. The aim of this work was to compare pharmacokinetic features of THP enantiomers in rats dosed with racemic THP (*rac*-THP), *Rhizoma corydalis*, or YB extracts. A single dose of *rac*-THP (5 mg kg^{-1}) or extracts of *Rhizoma corydalis* and YB (both equivalent to 5 mg kg^{-1} of *rac*-THP) was given orally to three groups of Sprague-Dawley rats, respectively. Blood samples were collected periodically and plasma concentrations of THP enantiomers were determined using an achiral–chiral high-performance liquid chromatographic (HPLC) method previously reported, with some modifications. The C_{max} ratio (−/+) of THP was 2.91, 1.38, and 1.19, and the $AUC_{0\sim\infty}$ ratio (−/+) of THP was 2.84, 1.50, and 1.35 in rats after dosed with *rac*-THP, extracts of *Rhizoma corydalis* and YB, respectively. The mean $AUC_{0\sim\infty}$ and C_{max} of (+)-THP dosed with YB extracts were 0.652 ± 0.30 μg h ml^{-1} and 0.148 ± 0.09 μg ml^{-1}, significantly higher ($P < 0.05$) than those dosed with *rac*-THP and *Rhizoma corydalis* extracts. The mean $AUC_{0\sim\infty}$ and T_{max} of *rac*-THP dosed with YB extracts were 1.500 ± 0.56 μg h ml^{-1} and 2.12 ± 1.1 h, significantly higher ($P < 0.05$) than those dosed with *rac*-THP or *Rhizoma corydalis* extracts. These findings suggested the stereoselectivity in pharmacokinetics of THP enantiomers in rats was decreased when dosed in plant form, while the $AUC_{0\sim\infty}$ of *rac*-THP increased when YB extracts were dosed, confirming the compatibility in drug combination of *Rhizoma corydalis* and *Radix angelicae dahuricae*. *Chirality 20:119–124, 2008.*

KEY WORDS: *Rhizoma corydalis* (Yuanhu); prescription Yuanhu-Baizhi extracts; tetrahydropalmatine enantiomers; pharmacokinetics

INTRODUCTION

Rhizoma corydalis, the dried tuber of *Corydalis yanhusuo* W.T. Wang, is a traditional Chinese medicine, named as Yuanhu in Chinese.[1] As a widely used medicinal herb to treat spastic pain, abdominal pain, and pain due to injuries, *Rhizoma corydalis* is known to be rich in alkaloids.[2–5] Among these alkaloids, tetrahydropalmatine (THP) is one of the most active ingredients with hypnotic and anodyne activities.[6] THP is used clinically as the racemic mixture. Pharmacological studies revealed that (−)-THP blocks dopamine receptor in central nervous system, accounting for most of analgesic activity, while (+)-THP acted as initiative substance of dopamine emptier.[7] In previous studies, we reported a sequential achiral–chiral high-performance liquid chromatographic (HPLC) method for the quantification of the two enantiomers of THP in dog plasma, and revealed the stereoselective disposition of THP in dogs, the $AUC_{0\sim\infty}$ and C_{max} of **(−)**-THP were significantly higher than that of (+)-THP.[8] The stereoselective disposition kinetics of THP was further demonstrated in rats, and *rac*-THP at 40 mg kg^{-1} and the **(−)**-THP at 20 mg kg^{-1} produced comparable plasma concentration–time profiles, C_{max}, $AUC_{0\sim\infty}$, and $t_{1/2}$ of the **(−)**-enantiomer, indicating no enantiomeric interaction for THP enantiomers in rats and dogs.[9]

Radix Angelicae dahuricae (Chinese name: Baizhi), the dried root of *Angelica dahurica* Benth. et Hook., has been used as a natural remedy since ancient times to treat common cold and headache, pain in supra-orbital ridge, toothache, swelling, and abscesses.[10] Its main active components include essential oils and coumarins.[11] Yuanhu-Baizhi (YB), a traditional Chinese prescription containing

Contract grant sponsor: National Natural Science Foundation of China; Contract grant numbers: 30271603, 30600815

*Correspondence to: Guorong Fan, School of Pharmacy, Second Military Medical University, No 325 Guohe Road, Shanghai 200433, People's Republic of China. E-mail: guorfan@yahoo.com.cn

Received for publication 18 June 2007; Accepted 19 October 2007
DOI: 10.1002/chir.20507
Published online 11 December 2007 in Wiley InterScience (www.interscience.wiley.com).

Rhizoma corydalis (Yuanhu) and *Radix angelicae dahuricae*, is officially recorded in the Chinese Pharmacopoeia.[12] Chinese medicine practitioners usually include both *Rhizoma corydalis* and *Radix angelica dahurica* in their prescriptions to treat various pains. This clinical practice suggests that there might be synergic effects between the herbs. Data obtained from pharmacokinetic studies on the active compounds of medicinal herbs could help to understand the complex action and compatibility of Chinese herbal medicines in combination and to predict efficacy and toxicity of herbs and herbal prescriptions.[13,14]

In the present study, the pharmacokinetic features of THP enantiomers given to rats in different chemical environments, i.e. dosed with *rac*-THP, extracts of *Rhizoma corydalis* or YB were investigated and compared. The results help to explore the synergic effects of YB and understand the compatibility in drug combination of *Rhizoma corydalis* and *Radix angelica dahurica* from the pharmacokinetic point of view.

MATERIALS AND METHODS

Herb Materials, Chemicals, and Reagents

Rhizoma corydalis (Yuanhu) and *Angelica dahurica* (Baizhi) were purchased from Lei-Yun-Shang Pharmaceutical (Shanghai, China) and were authenticated by Department of Pharmacognosy in our university.

Rac-THP (purity 99.5%) and its enantiomer, **(−)**-THP (optical purity 99.5%) were provided by Nanning Pharmaceuticals (Guangxi, China). HPLC-grade acetonitrile and ethanol were obtained from Merck Company (Darmstadt, Germany). Hexane, 2-propanol, triethylamine, sodium hydroxide, and phosphoric acid, of analytical reagent grade, were purchased from Shanghai Reagents Company (Shanghai, China). Double-distilled water was used for the preparation of all solutions and 0.45 μm pore size filters (Millipore, MA) was used to filter the solutions.

Animals

Sprague-Dawley rats weighing 280–320 g were obtained from the Laboratory Animal Center of Chinese Academy of Sciences (Shanghai, China). Animals were housed under normal conditions and allowed to acclimatize for at least 1 wk before initiation of studies. Water and standard laboratory food were given until 12 h before the experiments. Animal studies were approved by the Second Military Medical University Animal Ethics Committee. The experimental procedures were carried out in accordance with the Guidelines for Animal Experimentation of Second Military Medical University (Shanghai, China).

Apparatus and Chromatography

The HPLC system consisted of a LC-10 ATvp pump (Shimadzu, Kyoto, Japan), a Rheodyne injector with 100 μl loop (Rheodyne 7125, Cotati, CA), and a SPD-10 ATvp multiwavelength detector (Shimadzu, Kyoto, Japan). Achiral separation was performed on a C_{18} reversed-phase column (150 mm × 4.6 mm, 5 μm) (Kromasil, Akzo Nobel, Stockholm, Sweden) maintained at 25°C. The mobile phase (I) was comprised of acetonitrile-0.1% phosphoric acid solution, adjusted with triethylamine to pH 6.63 (47:53, v/v). Chiral separation of THP enantiomers was conducted on a chiral stationary phase (Chiralcel OJ-H, 250 mm × 4.6 mm, 5 μm), protected by a guard column (10 mm × 4 mm) packed with the same packing material (Daicel Chemicals, Japan). The mobile phase (II) was anhydrous ethanol, flow rate of 0.5 ml min^{-1} and temperature at 30°C. The detection wavelength was 230 nm.

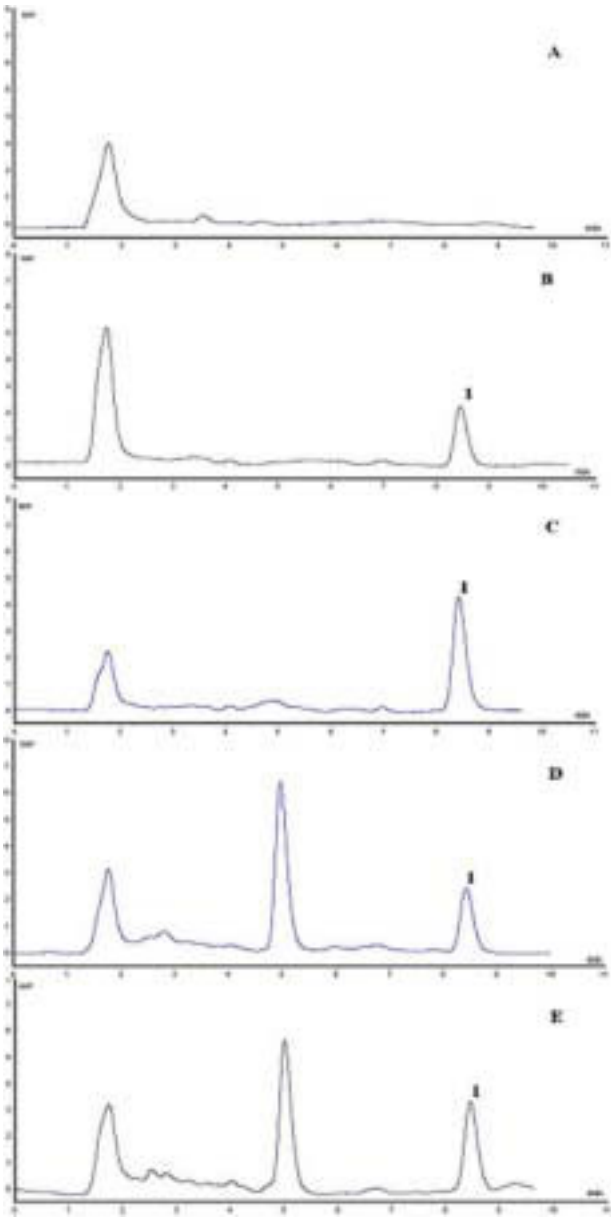

Fig. 1. Representative chromatograms of *rac*-THP on achiral system. (**A**) A blank plasma, (**B**) plasma spiked with *rac*-THP, and plasma samples after oral administration of *rac*-THP (**C**), extracts from *Rhizoma corydalis* (**D**) and YB (**E**), respectively. Chromatographic conditions: a C_{18} reversed-phase column (150 mm × 4.6 mm, 5 μm); mobile phase, acetonitrile-0.1% phosphoric acid solution (adjusted with triethylamine to pH 6.63, 47:53, v/v); flow rate, 1 ml min^{-1}; UV detection, 230 nm; column temperature, 25°C. Peak:1 = *rac*-THP. [Color figure can be viewed in the online issue, which is available at www.interscience.wiley.com.]

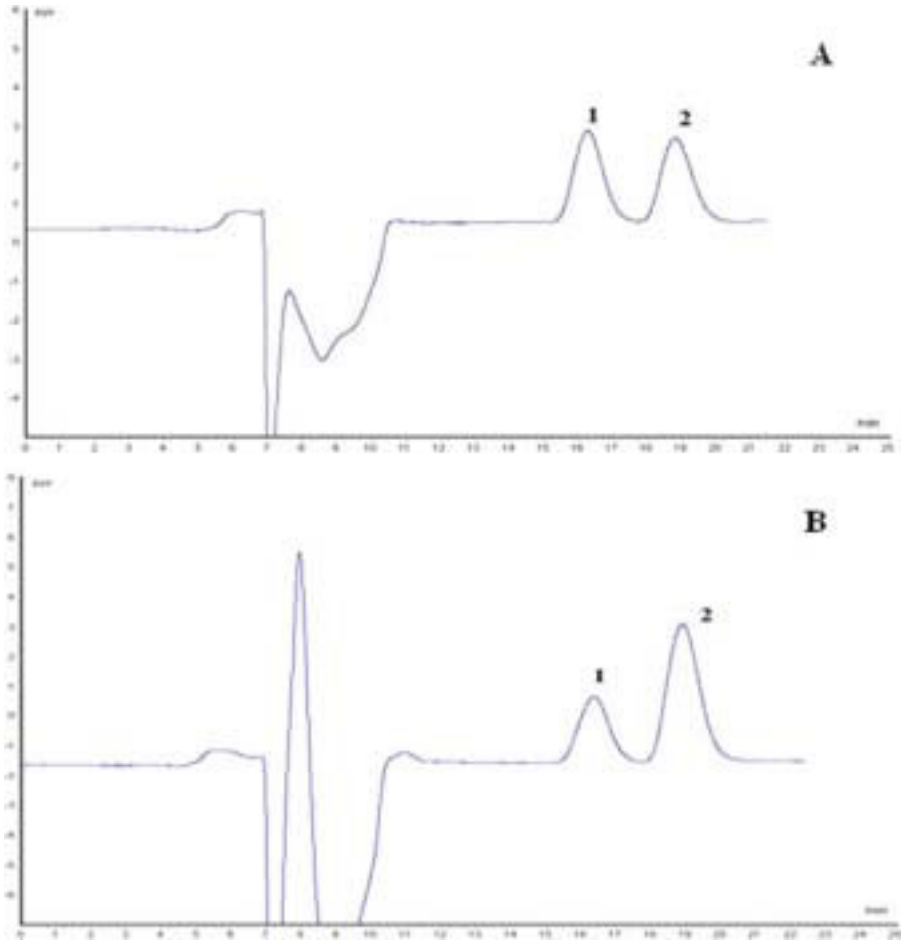

Fig. 2. Representative chromatograms of THP enantiomers obtained from chiral system. (**A**) Standard solution of *rac*-THP, (**B**) plasma sample after oral administration of *rac*-THP. Chiral separation conditions: Chiralcel OJ-H column (250 mm × 4.6 mm, 5 μm), protected by a guard column (10 mm × 4 mm); mobile phase, anhydrous ethanol; flow rate, 0.5 ml min^{-1}; column temperature, 30°C; UV detection, 230 nm. Peaks: 1, (+)-THP; 2, (−)-THP. [Color figure can be viewed in the online issue, which is available at www.interscience.wiley.com.]

Preparation of Rhizoma corydalis *and YB extracts*

The preparation of both kinds of extracts was based on the method in Chinese Pharmacopoeia.[12] Briefly, 200 g of *Rhizoma corydalis* was extracted with 2000 ml of 60% ethanol by refluxing on a water bath at 100°C for 3 h and then filtered. The extraction was repeated twice and the filtrates were combined. The filtrates were evaporated under reduced pressure and the reserved extract was stored at 4°C until administration to rats.

Rhizoma corydalis and *Radix angelica dahurica* were weighed and mixed in 2:1 ratio. The mixture was extracted with the same procedure as that of *Rhizoma corydalis*. The *rac*-THP content of *Rhizoma corydalis* and YB extracts was determined to be 2.15 mg g^{-1} and 1.84 mg g^{-1}, respectively, and was identified by LC-MS and quantified by HPLC.

Drug Administration and Blood Sampling

Sprague-Dawley rats were divided into three groups (30 rats per group) and received *rac*-THP at a dose of 5 mg kg^{-1} or *Rhizoma corydalis* extracts or its prescription YB extracts (both equivalent to 5 mg kg^{-1} of *rac*-THP) by gavage. Blood samples were collected at 0.083, 0.25, 0.5, 1, 1.5, 2, 3, 4, 6, and 8 h from the inner canthal vein (vena angularis) with a glass capillary (0.9 mm × 1.2 mm i.d.). Each group was subdivided into five subgroups of six rats for sampling, i.e. 0.083 and 2 h, 0.25 and 3 h, 0.5 and 4 h, 1 and 6 h, and 2 and 8 h. About 0.5 ml of blood was withdrawn each time. Plasma was separated by centrifugation at 3000 rpm for 10 min and stored at −20°C until analysis.

Determination of THP Enantiomers in Rat Plasma

The concentrations of THP enantiomers in rat plasma were determined by using a previously reported achiral–chiral HPLC method[9] with some modifications. Briefly, THP enantiomers were extracted from calibration standards, control solutions, or samples from dosed animals by liquid–liquid extraction. Aliquots (250 μl) of plasma were alkalinized with 50 μl of 1 M NaOH and extracted (2.0 ml) with a mixture of hexane and 2-propanol (95:5). After centrifugation (3500 rpm) for 10 min, an accurately measured volume (1.6 ml) of the organic layer was evaporated to dryness under a stream of nitrogen. The residue was reconstituted in 100 μl of the mobile phase (I), and 80 μl

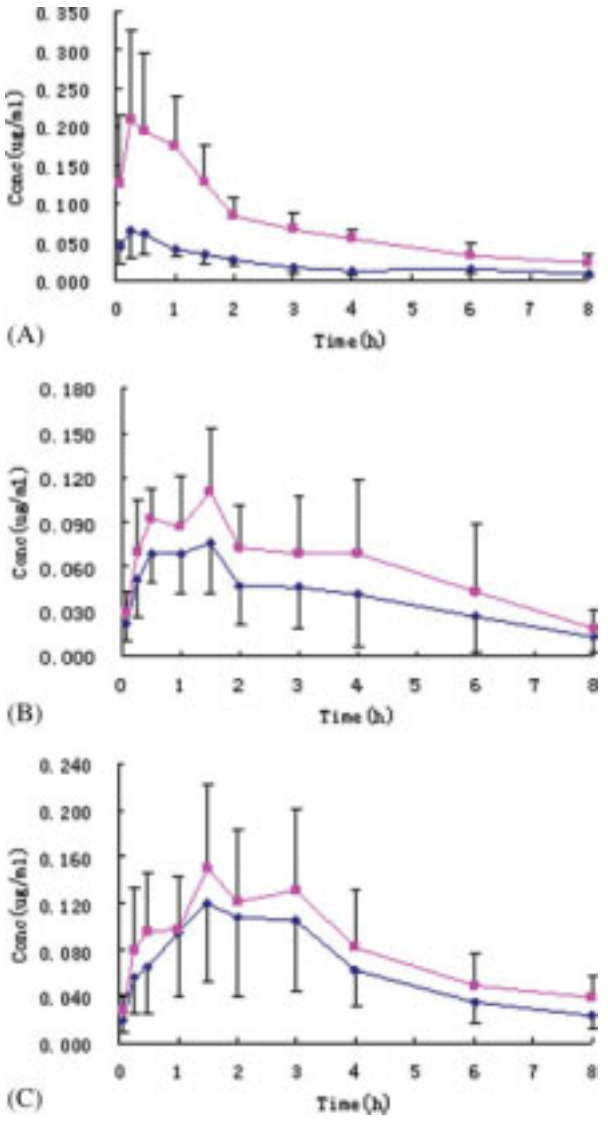

Fig. 3. Plasma concentration-time profiles for THP enantiomers in rats following oral administration of *rac*-THP (**A**), ethanol extracts from *Rhizoma corydalis* (**B**), and its prescription YB (**C**). (◆) (+)-THP, (■) (−)-THP. Each data point represents the mean values ± SD from six rats. [Color figure can be viewed in the online issue, which is available at www.interscience.wiley.com.]

aliquot of the sample was injected into the C_{18} column. The THP fraction (8.2–9.2 min) was collected and extracted with a mixture of hexane and 2-propanol (95:5). After evaporation, the residue was dissolved in 100 μl ethanol and 80 μl aliquot of the supernatant was directly injected into the same HPLC system fitted with the Chiralcel OJ-H column. Using this system, *rac*-THP can be separated and quantified as the mixture of (+) and (–)-THP using achiral C_{18}-column and the (−)/(+) ratio can be measured on the chiral column, and thus the concentration of each enantiomer was calculated.[9]

Assay validation was performed in rat plasma. Linearity of calibration curve was estimated for the peak area of *rac*-THP as a function of the analyte concentration in plasma over the range of 0.020–1.0 μg ml^{-1}, and the data were subjected to least squares regression analysis. The lower limit of quantification (LLOQ) was estimated at a signal-to-noise ratio of 10:1. The accuracy and precision of the method were determined over 5 days by replicate analysis of blank rat plasma spiked with *rac*-THP at three concentrations (0.040, 0.20, and 1.0 μg ml^{-1}). Each day, one calibration curve and 15 determinations of five quality controls at three concentrations were performed. The within-day (n = 5) and between-day (n = 5) results for accuracy and precision were expressed as deviation from the theoretical value (RE) and relative standard deviations (RSD). The extraction recovery was calculated by comparing the peak area of plasma-extracted standards versus that of neat standards.

Pharmacokinetic and Statistical Analyses

Pharmacokinetic parameters were determined using a noncompartment model and calculated with an in-house validated computer program. The maximum plasma concentration (C_{max}) and the time to reach maximal plasma concentration (T_{max}) were obtained by inspection of the concentration-time curves. The area under the plasma concentration-time curve (AUC) and the area under the first-moment time curve (AUMC) were calculated by the trapezoidal method, and were extrapolated to infinity using the last detectable plasma concentration and the terminal elimination rate constant. Mean residence time (MRT) was calculated using the equations MRT = AUMC/AUC. The terminal elimination half-life ($t_{1/2}$) was derived by linear regression analysis of the terminal phase of the plasma concentration-time curve.

All values are reported as means ± standard deviation. Differences between pharmacokinetic parameters for the two enantiomers were evaluated by the Paired *t*-test. Comparisons of administration of different extracts versus *rac*-THP were made by an independent measured *t*-test. A value of $P < 0.05$ was considered statistically significant.

RESULTS AND DISCUSSION

Assay Validation

Representative chromatograms of blank plasma and spiked plasma sample from the achiral system and the

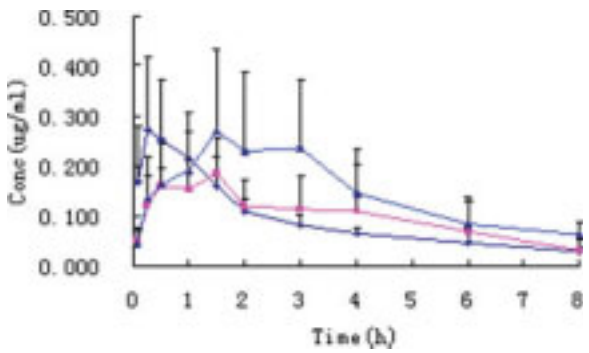

Fig. 4. Plasma concentration-time profiles for *rac*-THP in rats following oral administration of *rac*-THP (◆), ethanol extracts from *Rhizoma corydalis* (■) and its prescription YB (▲). Each data point represents the mean values ± SD from six rats. [Color figure can be viewed in the online issue, which is available at www.interscience.wiley.com.]

TABLE 1. Noncompartment pharmacokinetic parameters of THP enantiomers in rats after i.g. ethanol extracts from *Rhizoma corydalis* and YB (mean ± SD, $n = 6$)

	Rac-THP		*Rhizoma corydalis*		YB	
Parameter	(+)-THP	(−)-THP	(+)-THP	(−)-THP	(+)-THP	(−)-THP
C_{max} (μg ml^{-1})	0.077 ± 0.02	0.224 ± 0.10[a]	0.091 ± 0.03	0.126 ± 0.03	0.148 ± 0.09[b]	0.176 ± 0.07
T_{max} (h)	0.56 ± 0.56	0.71 ± 0.62	1.39 ± 1.2[c]	1.56 ± 1.0	2.02 ± 1.1[b]	1.83 ± 1.1
AUC_{0-t} (μg ml^{-1} h)	0.172 ± 0.04	0.587 ± 0.18[a]	0.323 ± 0.17	0.485 ± 0.23	0.523 ± 0.29[b]	0.666 ± 0.24
$AUC_{0-\infty}$ (μg ml^{-1} h)	0.246 ± 0.09	0.698 ± 0.24[a]	0.381 ± 0.20[c]	0.571 ± 0.27	0.652 ± 0.30[b]	0.877 ± 0.34
$T_{1/2}$ (h)	6.47 ± 4.5	3.10 ± 1.2[a]	3.01 ± 1.4[c]	2.94 ± 1.4	3.50 ± 2.9[b]	3.50 ± 1.7
MRT (h)	7.25 ± 5.3	4.07 ± 1.6[a]	4.48 ± 1.6	4.56 ± 1.6	5.70 ± 3.8	5.67 ± 2.2

[a]Significantly different from (+)-THP at $P < 0.05$.
[b]Significantly different from the results of (+)-THP dosed with *rac*-THP or *Rhizoma corydalis* extracts at $P < 0.05$.
[c]Significantly different from the results of (+)-THP dosed with *rac*-THP at $P < 0.05$.

chiral system are shown in Figures 1 and 2, respectively. In achiral system, the retention time of *rac*-THP was about 8.4 min. No endogenous interference at the retention times of peaks of interest was observed in chromatograms of blank rat plasma or plasma spiked with *rac*-THP. The chiral system was suitable for the separation of THP enantiomers and the retention times for (+)-THP and (−)-THP were about 16.3 and 19.1 min, respectively.

Calibration curves for *rac*-THP showed good linearity over the concentration range 0.020–1.0 μg ml^{-1} in rat plasma (r = 0.9995). The LLOQ estimated at a signal-to-noise ratio of 10:1 was 0.020 μg ml^{-1} for *rac*-THP and 0.010 μg ml^{-1} for (+)-THP or (−)-THP. The within-day ($n = 5$) and between-day ($n = 5$) results for accuracy (expressed as RE) and precision (expressed as RSD) were less than 10%. The extraction recoveries of *rac*-THP from rat plasma, determined at three concentrations (0.040, 0.20, and 1.0 μg ml^{-1}), were 90.1% ± 5.6%, 93.2% ± 4.3%, and 94.8% ± 6.1%, respectively. These results demonstrated that the assay was reproducible and accurate for quantification of *rac*-THP and its enantiomers in rat plasma samples.

Stereoselectivity of THP Enantiomers in Different Chemical Enviroment

Single doses of *rac*-THP (5 mg kg^{-1}) and extracts of *Rhizoma corydalis* and YB (both equivalent to 5 mg kg^{-1} of *rac*-THP) were given orally to three groups of Sprague-Dawley rats, respectively. Plasma concentration-time profiles of THP enantiomers are illustrated in Figure 3. For the group dosed with *rac*-THP, the maximum concentrations of (+)-THP and (−)-THP were found at approximately 0.25 h after administration. The concentration-time courses of individual THP enantiomers in plasma were distinctly different. The plasma concentration of (−)-THP, was higher than that of (+)-THP at each time point, as shown in Figure 3A. For the groups dosed with extracts of *Rhizoma corydalis* and YB, the maximum concentrations of (+)-THP and (−)-THP occurred approximately 1.5 h after administration, significantly later than after dosing with *rac*-THP. The plasma concentration of (−)-THP was higher than that of (+)-THP at most time points (as shown in Figs. 3B and 3C). However, the difference in concentration-time courses of individual THP enantiomers was reduced, especially for that dosed with YB extracts. The plasma concentrations of (+)-THP after dosing with YB extracts was higher than that of (+)-THP aftrer *rac*-THP or extracts of *Rhizoma corydalis*.

Pharmacokinetic parameters of THP enantiomers determined by noncompartmental method are summarized in Table 1. The C_{max} ratio (−/+) of THP was 2.91, 1.38, and 1.19, and the $AUC_{0\sim\infty}$ ratio (−/+) of THP was 2.84, 1.50, and 1.35 after *rac*-THP, extracts of *Rhizoma corydalis* and YB, respectively. For the group dosed with *rac*-THP, the C_{max} and $AUC_{0\sim\infty}$ of (−)-THP were about three times higher than those of (+)-THP, respectively, indicating significantly greater adsorption and distribution of (−)-THP. Similarly, the other pharmacokinetic parameters of the enantiomers were also significantly different. The stereoselectivity in the pharmacokinetics of THP enantiomers was evident after *rac*-THP. The above results were consistent with our previous report.[9] When the rats were given

TABLE 2. Noncompartment pharmacokinetic parameters of *rac*-THP in rats after i.g. ethanol extracts from *Rhizoma corydalis* and YB (mean ± SD, $n = 6$)

Parameter	Dosed with *rac*-THP	Dosed with extracts from *Rhizoma corydalis*	Dosed with extracts from YB
C_{max} (μg ml^{-1})	0.299 ± 0.12	0.210 ± 0.05	0.320 ± 0.16
T_{max} (h)	0.56 ± 0.56	1.25 ± 0.56[a]	2.12 ± 1.1[a]
AUC_{0-t} (μg ml^{-1} h)	0.760 ± 0.17	0.808 ± 0.39	1.190 ± 0.50
$AUC_{0-\infty}$ (μg ml^{-1} h)	0.915 ± 0.25	0.950 ± 0.47	1.500 ± 0.56[a]
$T_{1/2}$ (h)	3.41 ± 1.1	2.94 ± 1.4	3.35 ± 1.8
MRT (h)	4.27 ± 1.5	4.50 ± 1.6	5.47 ± 2.3

[a]Significantly different from the results dosed with *rac*-THP at $P < 0.05$.

extracts of *Rhizoma corydalis* or YB, which contained more components than *rac*-THP, C_{max}, and $AUC_{0\sim\infty}$ of (−)-THP were still greater, but not significantly than those of (+)-THP, when compared with those obtained after dosed with *rac*-THP.

Furthermore, the pharmacokinetic parameters of THP enantiomers dosed with YB extracts were compared to those dosed with *rac*-THP or *Rhizoma corydalis* extracts. The C_{max} and $AUC_{0\sim\infty}$ of (−)-THP dosed with YB extracts were not statistically different from that of (−)-THP when dosed with *rac*-THP ($P > 0.05$). However, the mean $AUC_{0\sim\infty}$ and C_{max} of (+)-THP after dosed with YB extracts were 0.652 ± 0.30 μg h ml^{-1} and 0.148 ± 0.09 μg ml^{-1}, significantly higher ($P < 0.05$) than after *rac*-THP or *Rhizoma corydalis* extracts. The results indicated greater absorption of (+)-THP after dosing with YB extracts, which might be affected by other components in the YB extracts. Thus, the difference in the stereoselective pharmacokinetics of THP enantiomers in rats was decreased as its chemical environment became more complex.

Compatibility of the Combination Use of Rhizoma corydalis *and* Radix angelica dahurica

Plasma concentration-time profiles of *rac*-THP are illustrated in Figure 4. Compared with the concentration-time course after *rac*-THP, slower absorption and elimination of *rac*-THP were observed after *Rhizoma corydalis* and YB extracts. The mean $AUC_{0\sim\infty}$ and T_{max} of *rac*-THP following YB extracts were 1.500 ± 0.56 μg h ml^{-1} and 2.12 ± 1.1 h, significantly higher ($P < 0.05$) than those dosed with *rac*-THP or *Rhizoma corydalis* extracts (Table 2). The C_{max} and MRT of *rac*-THP dosed with YB extracts were 0.320 ± 0.16 μg ml^{-1} and 5.47 ± 2.3 h, also greater than those dosed with *rac*-THP or *Rhizoma corydalis* extracts (Table 2). These results suggested that the combination use of *Rhizoma corydalis* and *Radix angelica dahurica* might improve the AUC of *rac*-THP.

Zhu and Yu[15] used the two mice analgesic test models, i.e. acetic acid tail-flick test and hot plate test, to compare the analgesic effect of YB extracts, *Rhizoma corydalis* extracts, and *Radix Angelica dahurica* extracts. The results showed that YB extracts had an analgesic effect, obviously stronger than *Rhizoma corydalis* and *Radix angelica dahurica* extracts, which suggests that *Rhizoma corydalis* and *Radix angelica dahurica* are synergistic in combination. The pharmacokinetic results in our study also support the combination use of *Rhizoma corydalis* and *Radix angelica dahurica*.

The active components of *Radix angelica dahurica* are coumarins, which have been reported to inhibit drug metabolism enzymes such as cytochrome P450s.[16–18] In this study, greater absorption of (+)-THP from YB extracts was observed, which might be affected by other components like coumarins in YB extracts. Further experiments focusing on the influence of coumarins on the metabolism of THP enantiomers are in progress.

LITERATURE CITED

1. Pharmacopoeia Commission of RPC. Chinese pharmacopoeia, Part I. Beijing: Chemical Industry Press; 2005. p 94.
2. Kaneko H, Naruto S. Studies on the constituents of *Corydalis* sp. alkaloids from *Chinese corydalis* and the identity of D-corydamine with D-corybulbine. J Org Chem 1969;34:2803–2805.
3. Fu XY, Liang WZ, Tu GT. Chemical studies on alkaloids in *Rhizoma corydalis* from Zhejiang Dongyang. Acta Pharm Sin 1986;21:447–453.
4. Wu TS, Leu YL, Kuoh CS, Lee KH. Cytotoxic principles from *Saussurea lappa* and Corydalis *turtshaninovii f.* yanhusuo. J Chin Chem Soc 1997;44:357–359.
5. Xiang H, Wang ZT, Yu GD, Ruan BF, Li J. Alkaloids from Rhizoma corydalis. J Chin Pharm Univ 2002;33:483–486.
6. Sha S. Assay methods for active components in Chinese herb medicines. Beijing: The People's Medical Publishing House; 1985. p 53–54.
7. Jin GZ. Advances in pharmacological study of (−)-tetrahydropalmatine and its analogs. Acta Pharm Sin 1987;22:472–474.
8. Hong ZY, Fan GR, Chai YF, Yin XP, Wen J, Wu YT. Chiral liquid chromatography resolution and stereoselective pharmacokinetic study of tetrahydropalmatine enantiomers in dogs. J Chromatogr B 2005;826:108–113.
9. Hong ZY, Fan GR, Chai YF, Yin XP, Wu YT. Stereoselective pharmacokinetics of tetrahydropalmatine after oral administration of (−)-enantiomer and the racemate. Chirality 2005;17:293–296.
10. Pharmacopoeia Commission of RPC. Chinese pharmacopoeia, Part I. Beijing: Chemical Industry Press; 2005. p 69–70.
11. Xu S, Hu JH, Quan SC. Review about the studies on the chemical constituents and clinical usage of *Radix Angelicae dahuricae.* Chin Pharm 2005;16:467–469.
12. Pharmacopoeia Commission of RPC. Chinese pharmacopoeia, Part I. Beijing: Chemical Industry Press; 2005. p 362.
13. De Smet PA, Brouwers JR. Pharmacokinetic evaluation of herbal remedies basic introduction, applicability, current status and regulatory needs. Clin Pharmacokinet 1997:32:426–427.
14. De Smet PA, River L. A general outlook on ethnopharmacology. J Ethnopharmacol 1989;25:127–138.
15. Zhu YY, Yu BY. Comparative studies on chemistry and pharmacodynamics of the compatibility of Yuanhu Zhitong prescription. J Chin Pharm Univ 2003;34:461–464.
16. Inhibara K, Kushida H, Yuzurihara M, Wakui Y, Yanagisawa T, Kamei H, Ohmori S, Kitada M. Interaction of drugs and Chinese herbs: pharmaco kinetic changes of tolbutamide and diazepam caused by extract of *Angelica daburica*. J Pharm Pharmacol 2000;52:1023–1029.
17. Guo LQ, Taniguchi M, Chen QY, Baba K, Yamazoe Y. Inhibitory potential of herbal medicines on human cytochrome P450-mediated oxidation: properties of umbelliferous of citrus crude drugs and their relative prescriptions. Jpn J Pharmacol 2001;85:399–408.
18. Guo LQ, Taniguchi M, Xiao YQ, Baba K, Ohta T, Yamazoe Y. Inhibitory effect of natural furanocumarins on human microsomal cytochrome P450. Jpn J Pharmacol 2000;82:122–129.

CHIRALITY 20:125–129 (2008)

Stereoselective Degradation of Benalaxyl in Tomato, Tobacco, Sugar Beet, Capsicum, and Soil

XU GU, PENG WANG, DONGHUI LIU, CHUNGUANG LV, YUELE LU, AND ZHIQIANG ZHOU*
Department of Applied Chemistry, China Agricultural University, Beijing, China

ABSTRACT The stereoselective degradation of the racemic benalaxyl in vegetables such as tomato, tobacco, sugar beet, capsicum, and the soil has been investigated. The two enantiomers of benalaxyl in the matrix were extracted by organic solvent and determined by validated chiral high-performance liquid chromatography with a cellulose-tris-(3, 5-dimethylphenylcarbamate)-based chiral column. *Rac*-benalaxyl was fortified into the soil and foliar applied to vegetables. The assay method was linear over a range of concentrations (0.5–50 μg ml^{-1}) and the mean recoveries in all the samples were more than 70% for the two enantiomers. The limit of detection for both enantiomers was 0.05 μg g^{-1}. The results in soil showed that *R*-(−)-enantiomer dissipated faster than *S*-(+)-enantiomer and the stereoselectivity might be caused by microorganisms. In tomato, tobacco, sugar, beet, and capsicum plants, there was significantly stereoselective metabolism. The preferential absorption and degradation of *S*-(+)-enantiomer resulted an enrichment of the *R*-(−)-enantiomer residue in all the vegetables. *Chirality 20:125–129, 2008.*

KEY WORDS: benalaxyl; stereoselectivity; tomato; tobacco; sugar beet; capsicum; soil

INTRODUCTION

Nowadays, more and more chiral pesticides, up to 25% of the total, have been introduced into environment in racemic form.[1] Chiral pesticides consist of at least two enantiomers or stereoisomers, which have identical physicochemical properties[2] but show differences in bioactivity, toxicity, metabolism, and excretion in asymmetrical matrices.[3,4]

Benalaxyl, methyl-*N*-phenylacetyl-*N*-2,6-xylyl alaninate, is a systemic fungicide with protective, curative, and eradicant action belonging to the acylalanine family.[5] It can be absorbed by the roots, stems, and leaves, with translocation acropetally to all parts of the plant. It can be used to control late blight of potatoes and tomatoes, downy mildew of hops, vines, tomato, sugar beet, onions, soya beans, tobacco, capsicum, and other crops. Benalaxyl has a chiral carbon and consists of two enantiomers. Its absolute configuration was confirmed with (−) rotation of the *R*-enantiomer and (+) rotation of the *S*-enantiomer (Fig. 1). The activity of this fungicide is mainly attributed to the *R*-(−)-enantiomer.[6] A number of methods have been reported for the determination of benalaxyl residues in various samples, such as enzyme-linked immunosorbent assay and gas chromatography. Determination of benalaxyl enantiomers in soil and water[5] was reported with (*R*, *R*) Whelk-O 1 as chiral stationary phase (CSP). The stereoselective degradation of benalaxyl in cucumber[3] and metabolism in rabbit plasma[7] was also reported.

In this contribution, we investigated the behavior of the two enantiomers of benalaxyl in vegetables (tobacco, tomato, sugar beet, and capsicum) and the soil. We also developed a high-performance liquid chromatography–chiral stationary phase (HPLC-CSP) technology[7] to determine the two enantiomers of benalaxyl and set up methods of extraction of benalaxyl from soil and plant matrices. These methods were then successfully applied to study the stereoselective bioaccumulation, degradation, and metabolism of *rac*-benalaxyl in four breeds of plant and soil.

MATERIALS AND METHODS

Chemicals

All analytical grade reagents were from Yili Fine Chemicals (Beijing, China). Mobile phase reagents such as 2-propanol and *n*-hexane were distilled and filtered through a 0.45-μm filter membrane before use. Water was purified by a Milli-Q system (Millipore Purification Systems). *Rac*-benalaxyl (purity, 98.0%) and benalaxyl-EC (20.0%) were obtained from Lianyungang Liben Agrochemical (Jiangsu Province, China). Stock solution of *rac*-benalaxyl was prepared in 2-propanol and stored at −20°C. Working standard solutions were prepared by dilutions of the stock solution with 2-propanol.

Contract grant sponsor: National Natural Science Foundation of China;
Contract grant number: 20377052
*Correspondence to: Prof. ZhiQiang Zhou, Department of Applied Chemistry, China Agricultural University, Beijing 100094, China.
E-mail: zqzhou@cau.edu.cn
Received for publication 8 August 2007; Accepted 19 October 2007
DOI: 10.1002/chir.20504
Published online 11 December 2007 in Wiley InterScience (www.interscience.wiley.com).

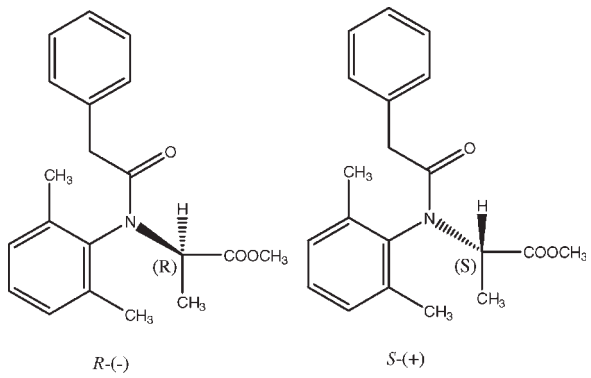

Fig. 1. Chemical structure of benalaxyl enantiomers.

Treatment of Soil

The test soil was from the region (0–15 cm horizon) where the plants were grown (Beijing, China). The region had not been treated with benalaxyl in the last 5 yr. The physical and chemical properties of the soil were: sand 52.5%, silt 39.8%, clay 7.7%, and organic matter 2.16% and pH 8.9 (suspension of soil in water, 1:2.5 v/v).

The soil was air-dried at room temperature and sieved through a 2.0-mm sieve; the moisture content of the soil adjusted to 25% and kept in the dark at 25 (±2)°C for 2 wk activation period. After that period, batches of 25 g soil (based on dry weight) were weighed into 250-ml conical flasks. One milliliter of solution was added to give equivalent to 5 mg kg^{-1} *rac*-benalaxyl for per gram soil. Finally, the flasks were sealed with cotton–wool plugs and stored at 25 (±2)°C in the dark and water added to maintain the initial moisture.

For aseptic experiment, soil was sterilized with an electrothermal autoclave (YXQG02, 0.14 MPa). Sterilized soil was treated the same as above except that the water added was sterilized and the experiment was conducted in an aseptic console.

Extraction Procedure of the Soil

Acetone (40 ml), silica gel (1 g), activated carbon (0.03 g), and sodium chloride (3 g) were added to the sample conical flask. After shaking for 30 min (machine), the soil was filtered through a Buchner funnel with glass fiber filter paper. Acetone (10 ml thrice) was used to rinse the homogenizer jar and the Buchner funnel to further extract the fungicide. The acetone was evaporated under reduced pressure the aqueous phase transferred with 40 ml distilled water to a 250-ml separation funnel. One gram sodium chloride was added and the mixture was extracted three times (30 ml + 15 ml + 15 ml) with dichloromethane. The organic phase was filtered through anhydrous sodium sulfate (15 g) and concentrated to 1 ml by vacuum rotary evaporator at 40°. The concentrate was dried under nitrogen and diluted to 1 ml with isopropanol. The sample was filtered (0.45-μm pore size).

Plant Care and Fungicide Application

The plant (tomato, tobacco, capsicum, and sugar beet) seeds were purchased from Beijing Vegetable Research Center. Benalaxyl-EC was used as foliar spray at rate of 0.3 kg a.i. ha^{-1} at 30 days (blossom stage) after sowing. Plant materials were sampled immediately after treatment and at 0, 1, 2, 4, 6, 8, 10, 15, 20, and 25 days after treatment (there was no natural rainfall during the study period). All samples were rinsed for 10 min with distilled water and stored at −20°C until analysis.

Extraction and Purification Procedure of Plants

Ten gram triturated plant sample was weighed in a 250-ml conical flask and 50 ml ethyl acetate, 10 g anhydrous sodium sulfate, and 3 g sodium chloride added. The mixture was filtered through fiberglass with glass fiber filter paper into a 250-ml evaporation flask. The conical flask and the filter were rinsed with ethyl acetate (10 ml). The ethyl acetate was removed under vacuum (40°C) to about 1 ml and evaporated under a stream of nitrogen. The evaporation flask was washed with 10 ml petroleum ether. The concentrate was then passed through a column of anhydrous Na_2SO_4/silica gel + activated carbon (2 g + 0.6 g)/anhydrous Na_2SO_4, which was prerinsed by 20 ml acetone and 20 ml petroleum ether. The extraction solution was transferred to the column with 15 ml petroleum ether and eluted with 40 ml petroleum ether: ethyl acetate (80:20 by volume). The first 15 ml eluate was discarded and the remainder was collected and dried.

High-Performance Liquid Chromatographic Analysis

The HPLC system used was an Agilent 1100 series HPLC equipped with a G1322A degasser, G1311A pump, G1316A column compartment, G1315B diode array detector (DAD), G1328B manual injector, and a 20 μl sample loop (Wilmington, DE). The signal was received and processed by an Agilent Chemstation.

The enantiomers of benalaxyl were separated on a cellulose tris-(3,5-dimethylphenyl-carbamate) (CDMPC) 250 × 4.6-mm^2 (i.d.) prepared by us.[7] The chromatographic separation was conducted at 20°C. The mobile phase used was a mixture of *n*-hexane and 2-propanol (90:10 for the soil and 98:2 for plant samples) flow rate of 1.0 ml min^{-1}, detection wavelength was 210 nm. The first eluted enantiomer was *R*-(−)-form and the second was *S*-(+)-form determined by the previous research work.[8]

Calibration Curves and Assay Validation

The series of *rac*-benalaxyl standard solutions (0.5, 5, 50, 100, and 125 mg l^{-1}) were prepared by diluted with 2-propanol. Injection volume was 20 μl.

Calibration curves were prepared by plotting peak area of each enantiomer versus the concentration. The standard deviation (S.D.) and the relative standard deviation (R.S.D.) (R.S.D. = S.D./mean × 100%) were calculated over the calibration range. Three concentration levels were investigated for recovery estimation. A given series of the racemate standard solutions were added in 25 g blank soil to give final concentrations equivalent to 0.5, 1,

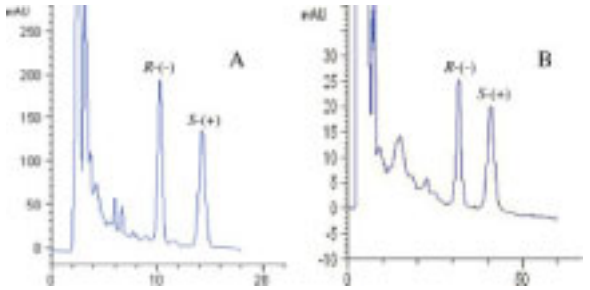

Fig. 2. Representative chromatograms of *rac*-benalaxyl, extract from soil fortified with *rac*-benalaxyl (5 μg g^{-1}) (**B**), extract from tomato leaves fortified with *rac*-benalaxyl (2μg g^{-1}) (n). [Color figure can be viewed in the online issue, which is available at www.interscience.wiley.com.]

and 5 mg kg^{-1}, respectively. The plant samples were prepared by adding the racemate standard solutions to 10 g plant to get final concentrations of 0.04, 0.20, and 2.00 mg kg^{-1}. The samples were extracted, cleaned, and determined as described. Recovery of the method was estimated by comparing the peak area of each enantiomer extracted from soil and plant to those of an equivalent amount of the standard solution. The lowest possible standard on the calibration curve was accepted as the limit of quantitation (LOQ). All the studies of calibration curves and recovery validations were performed in duplicate and repeated three times ($n = 3$).

Pharmacokinetic and Statistical Analysis

It was assumed that the degradation of the enantiomers in soil[9] and plant[2] accorded with first-order kinetics. From the linear range of semilogarithmic plots, corresponding rate constants k for the *R*-(−)- and *S*-(+)-enantiomer were determined, *R* and *S* versus time *t*, respectively.

$$C = C_0 e^{-kt} \quad (1)$$

$$T_{1/2} = \ln 2/\mathrm{k} = 0.693/k \quad (2)$$

The enantiomer fraction (EF) was used to measure the enantioselectivity of the degradation of enantiomers in the soil and plant samples. This ranged from 0 to 1 and the racemate represent EF = 0.5. EF was defined as follows:

$$\mathrm{EF} = \text{peak areas of the}(-)/[(-) + (+)] \quad (3)$$

RESULTS AND DISCUSSION

Calibration and Method Validation

S-(+) and *R*-(−)-benalaxyl were baseline separated. There were no endogenous interfering peaks eluted at the retention times of the two enantiomers. Typical chromatograms of samples fortified with *rac*-benalaxyl standard solution are shown in Figure 2. Good linear calibration curves were obtained over the range of 0.5–50 μg g^{-1} ($n = 5$) for both *R*-(−)-, ($y = 71.812x + 106.63$, $R^2 = 0.9998$) and *S*-(+)-enantiomers ($y = 73.004x + 56.326$, $R^2 = 0.9994$). The mean recoveries of the two enantiomers from soil and plant samples were determined at three levels and are summarized in Table 1. Recoveries from soil samples of *rac*-benalaxyl at 0.5, 1, and 5 μg g^{-1} ranged from 90.68% ± 3.51% to 99.22% ± 1.17%, and from plants at 0.04, 0.20, and 2.00 μg g^{-1} ranged from 71.62 ± 4.52 to 80.32 ± 3.27. The limit of detection (LOD) ($S/N > 3$) for both enantiomers, defined as the concentration, was 0.05 μg g^{-1} of soil and plant samples.

TABLE 1. Summary of recoveries (%) (± SE[a]) data for the enantiomers of benalaxyl in soil and plants ($n = 3$)

Test materials	*rac*-benalaxyl fortification (μg/g)	Recovery (%)	
		R-(−)-benalaxyl	*S*-(+)-benalaxyl
Soil	0.20	90.68 ± 3.51	92.81 ± 3.42
	1.00	94.71 ± 1.19	93.83 ± 2.29
	5.00	97.69 ± 1.08	99.22 ± 1.17
Tobacco	0.04	77.94 ± 4.03	74.82 ± 3.52
	0.20	78.91 ± 2.44	78.48 ± 2.65
	2.00	80.32 ± 3.27	78.69 ± 3.21
Tomato	0.04	71.95 ± 4.70	72.68 ± 4.25
	0.20	76.43 ± 4.33	75.71 ± 3.97
	2.00	74.16 ± 2.64	76.35 ± 3.08
Capsicum	0.04	77.64 ± 2.69	72.93 ± 3.15
	0.20	79.31 ± 2.12	76.85 ± 2.94
	2.00	80.23 ± 1.98	77.24 ± 2.36
Beet	0.04	71.62 ± 4.52	73.78 ± 3.57
	0.20	72.85 ± 3.97	72.46 ± 5.04
	2.00	75.49 ± 1.22	74.91 ± 2.93

Values represent the means ± SD.

Benalaxyl Degradation in Soil

Under laboratory conditions, the degradation of the two enantiomers in soil followed first-order kinetics. The degradation kinetics of *R*-(−)- and *S*-(+)-enantiomers are shown in Table 2. The half-life of the *S*-(+)-enantiomer was more than twice that of *R*-(−)-enantiomer. The EF value of benalaxyl in soil sample decreased from 0.497 to 0.031 (Fig. 4A) after 77 days.

TABLE 2. Regression functions for the metabolism of the enantiomers on benalaxyl in test plants

Plants	Enantiomer	Regressive functions[a]	R^2	Half-life (days)
Tobacco	*R*-(−)	$y = 981.83\ e^{-0.1505t}$	0.9973	4.60[b]
	S-(+)	$y = 1674.40\ e^{-0.2013t}$	0.9955	3.44[b]
Sugar beet	*R*-(−)	$y = 1051.00\ e^{-0.2753t}$	0.9730	2.52
	S-(+)	$y = 852.09\ e^{-0.3000t}$	0.9724	2.31
Capsicum	*R*-(−)	$y = 1138.50\ e^{-1.0926t}$	0.9973	0.63[b]
	S-(+)	$y = 2151.6\ e^{-1.5314t}$	1.0000	0.45[b]
Tomato	*R*-(−)	$y = 39.011\ e^{-0.2680t}$	0.9027	2.59[b]
	S-(+)	$y = 41.701\ e^{-0.8126t}$	0.9951	0.85[b]

[a]The regressive functions were obtained based on the mean value of three replicates.
[b]Significantly different from each other, $P < 0.05$ (Student's paired *t*-test).

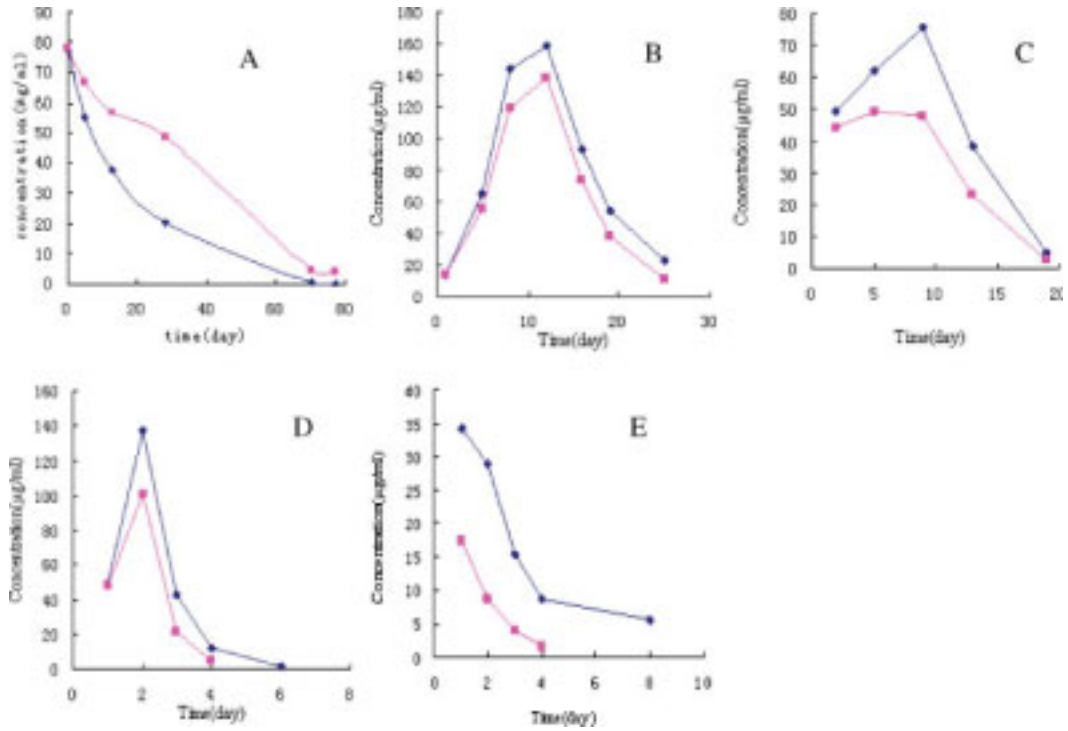

Fig. 3. Degradation curves (concentration vs. time curves) of benalaxyl enantiomers in soil (**A**), tobacco (**B**), sugar beet (**C**), capsicum (**D**), tomato (**E**) following use as foliar spray (□ *R*-(−)-enantiomer; ■ *S*-(+)-enantiomer). [Color figure can be viewed in the online issue, which is available at www.interscience.wiley.com.]

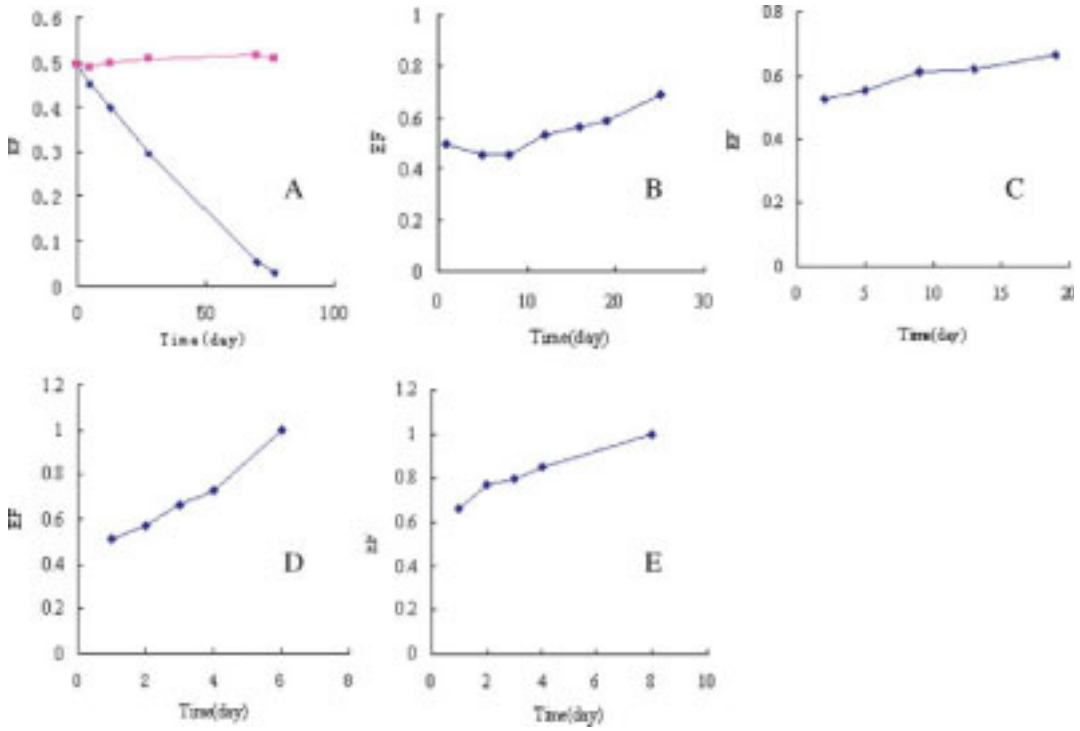

Fig. 4. EF value versus time curves of benalaxyl in soil (**A**) □ active soil, ■ sterilized soil, tobacco (**B**), sugar beet (**C**), capsicum (**D**), tomato (**E**) following used as foliar spray. [Color figure can be viewed in the online issue, which is available at www.interscience.wiley.com.]

Microorganisms in soil may play an important role in the stereoselective metabolism of many chiral compounds.[3,10–13] The two enantiomers of benalaxyl degraded very slowly in sterilized soil but there was no difference in degradation rates. The EF value of benalaxyl in the sterilized samples was unchanged (about 0.5) showing no stereoselectivity (Fig. 4A). This result implied that the stereoselectivity seen with the enantiomers of benalaxyl in test soil was caused by microorganisms. Organic matter, pH, and other properties of soil might also influence the degradation of the fungicide.[3,10]

Bioaccumulation and Biodegradation of Benalaxyl in Plants

Obvious stereoselective behavior was found in the test vegetables. Degradation in the test plants can be divided into first-order and pseudo first-order kinetics.

The degradation curve in tomato (Fig. 3E) showed that the degradation of both enantiomers followed first-order kinetics: the concentrations of the two enantiomers decreased gradually with time. The half-life of the *R*-(−)-enantiomer was nearly three times that of *S*-(+)-enantiomer. The EF value in tomato was 0.663 at first day after applying benalaxyl indicating selectivity. The EF value increased with time and reached to 0.852 at the 4th day (Fig. 4E). The *S*-(+)-enantiomer was preferentially metabolized and it could not be detected after 8 days.

From the degradation curves of tobacco, sugar beet, and capsicum (Figs. 3B–3D), the degradation followed pseudo first-order kinetics. The degradation rate constants are shown in Table 2. The concentrations of the two enantiomers in capsicum increased and reached the maximum value at the 2nd day, and then degraded gradually with the half-lives ($T_{1/2}$) for *R*-(−)-benalaxyl and *S*-(+)-benalaxyl of 0.63 day and 0.45 day, respectively. Figure 4D shows that the EF value in capsicum increased from 0.509 to 0.727 after 4 days. The *S*-(+)-enantiomer was not detected on the 6th day. The concentration of *R*-(−)-enantiomer was higher than that of *S*-(+)-enantiomer (Fig. 3D), and the *S*-(+)-enantiomer was preferentially metabolized by capsicum. The maximum concentration of the two enantiomers in tobacco and sugar beet occurred at about the 10th day. The EF value in tobacco decreased from 0.494 to 0.453 in the first 8 days and then increased to 0.687 after 17 days (Fig. 4B). The EF value in sugar beet rose slowly from 0.526 to 0.665 on day 19 (Fig. 4C). The data showed capsicum metabolized benalaxyl enantiomers faster than other plants. Greater stereoselectivity occurred in tobacco, capsicum, and tomato. The preferential absorption and degradation of the *S*-(+)-enantiomer resulted in an enriched residue of *R*-(−)-enantiomer in these vegetables. It was also found that benalaxyl degraded faster in the plants than in the soil.

LITERATURE CITED

1. Williams A. Opportunities for chiral agrichemicals. Pestic Sci 1996; 46:3–9.
2. Zadra C, Marucchini C, Zazzerini A. Behavior of metalaxyl and its pure *R*-enantiomer in sunflower plants. J Agric Food Chem 2002;50:5373–5377.
3. Wang XQ, Jia GF, Qiu J, Diao JL, Zhu WT, Lv CG, Zhou ZQ. Stereoselective degradation of fungicide benalaxyl in soils and cucumber plants. Chirality 2007;19:300–306.
4. Wang YS, Tai KT, Yen JH. Separation bioactivity and dissipation of enantiomers of the organophosphorus insecticide fenamiphos. Ecotoxicol Environ Saf 2004;57:346–353.
5. Liu DH, Wang P, Zhou WF, Gu X, Chen ZS, Zhou ZQ. Direct chiral resolution and its application to the determination of fungicide benalaxyl in soil and water by high-performance liquid chromatography. Anal Chem Acta 2006;555:210–216.
6. http://www.alanwood.net/pesticides/index_cn_frame.
7. Zhou ZQ, Qiu J, Yang XL, Jiang SR. HPLC separation of metalaxyl and metalaxyl intermediate enantiomers on cellulose-based sorbent. Anal Lett 2004;37:167–173.
8. Qiu J, Wang QX, Zhu WT, Jia G.F, Wang XQ, Zhou ZQ. Stereoselective determination of benalaxyl in plasma by chiral high-performance liquid chromatography with diode array detector and application to pharmacokinetic study in rabbits. Chirality 2007;9:51–55.
9. Buerge I, Thomaspoiger M. Enantioselective degradation of metalaxyl in soils: chiral preference changes with soil pH. Environ Sci Technol 2003;37:2668–2674.
10. Monkiedje A, Spiteller M, Bester K. Degradation of racemic and enantiopure metalxyl in tropical and temperate soils. Environ Sci Technol 2003;37:707–712.
11. Vetter WR, Bartha SG, Tomy G. Enantioselective determination of two persistent chlorobornane congeners in sediment from a toxaphene-treated Yukon Lake. Environ Toxicol Chem 1999;18:2775–2781.
12. Liu WP, Gan JP, Daniel S, William AJ. Enatioselectivity in environmental safety of current chiral insecticide. Environ Sci Technol 2005;102:701–706.
13. Meijer SN, Halsall CJ, Harner T, Peters AJ, Ockenden WA, Johnston AE, Jones KC. Organochlorine pesticide residues in archived UK soil. Environ Sci Technol 2001;35:1989–1995.

CHIRALITY 20:130–138 (2008)

Separation and Aquatic Toxicity of Enantiomers of 1-(Substituted Phenoxyacetoxy)alkylphosphonate Herbicides

LING LI,[1] SHANSHAN ZHOU,[2] MEIRONG ZHAO,[1] ANPING ZHANG,[1] HAO PENG,[3] XIAOSONG TAN,[3] CHUNMIAN LIN,[1]* AND HONGWU HE[3]*

[1]*Research Center of Environmental Science, College of Biological and Environmental Engineering, Zhejiang University of Technology, Hangzhou 310032, China*

[2]*Institute of Environmental Science, Zhejiang University, Hangzhou 310027, China*

[3]*Key Laboratory of Pesticides and Chemical Biology, Ministry of Education, College of Chemistry, Central China Normal University, Wuhan 430079, China*

ABSTRACT A series of organophosphorous compounds (OPs), 1-(substituted phenoxyacetoxy)alkylphosphonates containing a chiral carbon atom, show notable herbicidal activities. In this study, the enantioselective separation and biological toxicity of all these compounds were investigated. The enantioselective separation on the columns of Chiralpak AD, Chiralpak AS, Chiralcel OD, and Chiralcel OJ were compared under various chromatographic conditions. All the analytes investigated obtained baseline resolution (Rs > 1.5) on Chiralpak AD column, which showed best chiral separation capacity. Further investigation was carried out on Chiralpak AD to evaluate the influence of the mobile phase composition and column temperature. The effect of the structural features on discrimination was also examined. The resolved enantiomers were distinguished by their signs of circular dichroism. The acute aquatic toxicity of enantiomers and racemate to *Daphnia magna* (*D. magna*) were assessed. The in vivo assays showed that compound **3** was about 2-148.5 times more toxic than the other four analogues to *D. magna*. The racemates of compounds **3** and **5** showed intermediate toxicity compare to their enantiomers, while those of compounds **1**, **2,** and **4** showed synergistic or antagonistic effect. These results suggest that the biological toxicity of chiral OPs to nontarget organisms is enantioselective and therefore should be evaluated with their pure enantiomers. *Chirality 20:130–138, 2008.*

KEY WORDS: organophosphorous compounds; enantiomeric separation; enantioselective toxicity

INTRODUCTION

About 25% of current-use pesticides are chiral, and this ratio is yet increasing as compounds with more complex structures are introduced.[1] Organophosphorous compounds (OPs) are one of the most important classes of agricultural insecticides used to protect crops and livestock in the past 60 years.[2] Chirality can be commonly found in OPs. Numerous OPs are chiral and their potential biological effects may be enantioselective.[3] Nowadays, all chiral OPs are still applied in their racemic forms, as equimolar mixtures of enantiomers.

Chiral OPs can be divided into two main classes: compounds with asymmetric phosphorus and those with an asymmetric carbon atom. The significance has long been recognized in regard to enantiomeric selectivity in biological activities such as toxicity,[3,4] endocrine disruption[5,6] and fate in the environment for individual enantiomers of natural and synthetic compounds. For instance, toward some chiral OPs, only one enantiomer has biological effects on target organisms, with other enantiomers being less effective or even completely inactive. Therefore, it is imperative to assess the environmental safety of chiral OPs in their enantiopure forms. However, synthesis and purification of enantiomers are challenging. Search for new and effective chiral selectors capable of separating a wide variety of enantiomeric compounds is an ongoing process. With the development of chiral separation technology, semipreparation of enantiomer standards has been gradually made possible. Studies on chiral separation of OPs by high performance liquid chromatography (HPLC) with specific mobile phase on different chiral stationary

Contract grant sponsor: National Basic Research Program of China, Contract grant number: 2003CB114400.
Contract grant sponsor: Program for Changjiang Scholars and Innovative Research Teams, China; Contract grant number: IRT 0653.
Contract grant sponsor: Natural Science Foundation of Zhejiang Province, China, Contract grant number: Z506070.
*Correspondence to: C. Lin, Research Center of Environmental Science, College of Biological and Environmental Engineering, Zhejiang University of Technology, Hangzhou 310032, China. E-mail: lcm@zjut.edu.cn and H. He, Key Laboratory of Pesticides and Chemical Biology, Ministry of Education, College of Chemistry, Central China Normal University, Wuhan 430079, China. E-mail: He1208@mail.ccnu.edu.cn.
Received for publication 17 July 2007; Accepted 24 October 2007
DOI: 10.1002/chir.20511
Published online 11 December 2007 in Wiley InterScience (www.interscience.wiley.com).

TABLE 1. Chemical structures of the compounds investigated in this study

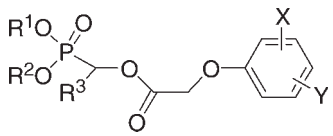

Compound	R^1	R^2	R^3	X	Y
1	C_2H_5	C_2H_5	CH_3	2-Cl	4-Cl
2	CH_3	CH_3	C_2H_5	2-Cl	4-Cl
3	CH_3	CH_3	CH_3	–	4-Cl
4	CH_3	CH_3	CH_3	2-Cl	–
5	CH_3	CH_3	CH_3	–	4-F

phases (CSPs) have been reported and these methods are becoming increasingly available. A series of 14 *O*-ethyl *O*-phenyl *N*-isopropyl phosphoroamidothioate enantiomers containing a phosphorus atom as a chiral center have been separated by HPLC on a Prikle model chiral stationary phase.[7]Chiral resolution of 12 OPs such as malathion, isofenphos, and fonofos was conducted on several polysaccharide chiral stationary phases and achieved almost baseline resolution.[8] Capillary electrophoresis was also used for enantiomeric separation of OPs.[9,10]

In the past few years, the enantioselective aquatic toxicity of chiral OPs has also received increasing attention. Lin et al. reported that the (+)-enantiomer of methamidophos was 7.0 times more toxic than its (−)-enantiomer to *D. magna* in 48-h tests.[11] The acute aquatic toxicity of trichloronate to *D. magna* was also found to be selective that the (−)-form was 8–11 times more toxic than its (+)-form, while the racemate showed intermediate toxicity.[12]

A series of 1-(substituted phenoxyacetoxy)alkylphosphonate herbicides have been synthesized. They possess notable herbicidal activities,[13-16] some of which are the inhibitors of PDHc E1.[17,18] While OPs have an asymmetric carbon atom, the stereoisomeric separation and aquatic toxicity of their racemates and enantiomers have not been well tested. In this study, we evaluated the HPLC separation of enantiomers of five 1-(substituted phenoxyacetoxy) alkylphosphonates on CSPs. The chiral resolution was compared among four chiral columns, Chiralpak AD, Chiralpak AS, Chiralcel OD, and Chiralcel OJ. Separation of the enantiomers of the five OPs was further investigated on Chiralpak AD and Chiralcel OD in order to evaluate the effects of mobile phase composition and temperature. CD detector was used to distinguish between the resolved enantiomers. The biological toxicity of the resolved enantiomers and racemates were assayed by in vivo acute aquatic toxicity to *D. magna* under static conditions. As that these chiral OPs are used as herbicides in racemate forms, the knowledge of the acute aquatic toxicity of analogous derivatives and individual enantiomers will play an important role in assessing their environmental safety.

MATERIALS AND METHODS

Chemicals

Analytical standards of racemic *O,O*-diethyl-1-(2,4-dichlorophenoxyacetoxy)ethylphosphonate (compound **1**, 97%), *O,O*-dimethyl-1-(2,4-dichlorophenoxyacetoxy)propylphosphonate (compound **2**, 98%), *O,O*-dimethyl-1-(4-chlorophenoxyacetoxy)ethylphosphonate (compound **3**, 97%); *O,O*-dimethyl-1-(2-chlorophenoxyacetoxy)ethylphosphonate (compound **4**, 97%), *O,O*-dimethyl-1-(4-fluorophenoxyacetoxy)ethylphosphonate (compound **5**, 94%) were synthesized and purified according to the methods described in the literature.[13-18] General structures of these five herbicides are listed in Table 1. Other solvents and chemicals used in this study were of analytical or HPLC grade.

Apparatus

Chiral separation was performed on a Jasco LC-2000 series HPLC system (Jasco, Tokyo, Japan). This chromatographic system consists of a PU-2089 quaternary gradient pump, a mobile phase vacuum degasser, an AS-2055 intelligent sampler with a 100-μL loop, a CO-2060 column thermostat, a UV-2075 detector, a variable-wavelength CD-2095 circular dichroism (CD), and an LC-NetII/ADC data collector. Chromatographic data were acquired and processed with computer-based ChromPass software (version 1.7.403.1, Jasco). The injection volume was 20 μl.

Chromatographic Conditions

Four commercial HPLC columns were evaluated in this study: Chiralpak AD [amylase tris-(3, 5-dimethylphenylcarbamate)], Chiralpak AS [amylase tris-((S)-1-methylphenyl-carbamate)], Chiralpak OD [cellulose tris-(3, 5-dimethylphenyl-carbamate)] and Chiralcel OJ [cellulose tris-(4-methylbenzoate)]. All the columns, purchased from Daicel Chemical Industries (Tokyo, Japan), were 250 × 4.6 mm i.d. with the enantioselective phase coated onto a 5-μm silica gel substrate.

The mobile phase was a normal-phase eluent of hexane as the apolar solvent and ethanol or isopropanol as the polar modifier. The analysis was investigated on different columns with hexane/isopropanol = 90/10 for the initial test. The percentage or type of polar modifier was changed if the resolution obtained under the initial conditions was not satisfactory. These reagents were filtered through a 0.45-μm filter and degassed in vacuum prior to use. Column temperature, flow-rate and detection wavelength were 25°C, 1 ml/min and 220 nm, respectively. The effect of temperature was evaluated in the range of 10–40°C under the pre-determined optimal mobile phase condition.

Chiroptical Detection

Although absolute configurations of the enantiomers in this study were not determined, they were differentiated based on the CD signs due to the differences in absorbing right and left circularly polarized lights. CD signals are intrinsically stable during temperature and solvent changes, making it gradient compatible. The sign of (+) or (−) in this article indicates the CD signal, and is used

to compare the order of elution between columns since the chromatographic conditions were equivalent.

CD spectra were recorded by stop-flow technique in the chromatogram peaks as well as using the "wavelength mode" in the spectral range of 220–420 nm, a resolution of 0.2 nm, 10 × accumulation, a set of fast response and a scan speed of 50 nm min^{-1}. The Chromatogram evaluation and data handling were performed using BORWIN 1.50 for Window.

Chromatographic Characterization

The chromatographic parameters, including retention factor (k'), separation factor (α), and resolution factor (R_s) for resolved enantiomers were calculated using the following formulas, which were subsequently used to evaluate the enantioselectivity of the CSPs. The retention foctor *k'* for each enantiomer was calculated as:

$$k' = \frac{t_R - t_0}{t_0}$$

where t_R is the average retention time of the analyte taken at peak maximum and t_0 is the column void time determined by recording the first baseline perturbation. The selectivity was then be expressed as the ratio:

$$\alpha = \frac{k'_2}{k'_1}$$

where k'_1 and k'_2 are the respective retention factors for the less retained and more retained enantiomer peaks. The resolution factor R_s was calculated as:

$$R_s = 2 \times \frac{t_2 - t_1}{w_1 + w_2}$$

where t_1 and t_2 represent the respective peak retention times of the first and second eluted enantiomers, and w_1 and w_2 are the peak widths measured at the peak bases of the less and more retained peaks, respectively.

Aquatic Toxicity Assays

The resolved stereoisomers for subsequent bioassays were manually collected at the column outlet. They were evaporated to dryness under a nitrogen stream and redissolved in acetone. The concentrations of enantiomers were determined by assuming the same response factor for enantiomers as for the racemate and also by analyzing an aliquot on a gas chromatograph coupled with a nitrogen-phosphorus detector (GC-NPD). Each enantiomer with the purity of more than 98% was obtained under its best HPLC separation conditions.

Enantioselectivity in aquatic toxicity was evaluated through 48-h acute toxicity assays using *D. magna* as the test species. The test organisms were obtained from continuous culture maintained at 22° ± 1°C in M4 culture medium[19] with photoperiod of 12 h/day and a density of <50 animals per liter. The medium was renewed three times a week, and *D. magna* were fed daily with the alga *Scenedesmus obliquus*, which were cultured in the laboratory using a nutrient medium. Stock organisms were originally obtained from the Chinese Academy of Protection and Medical Science (Beijing, China). Prior to testing, a sensitive test for *D. magna* to potassium dichromate ($K_2Cr_2O_7$) was performed as a positive control, and the LC50 (24-h) value was in the range of 0.6–1.7 mg l^{-1}.[11] The overall testing procedures followed the EPA guidelines.[20] Briefly, test solutions containing a given enantiomer or racemate with a range of concentrations were prepared (by dilution) from the resolved enantiomers using M4. The maximum content of acetone in the final test solutions was <0.2% (by volume). Twenty milliliter of the prepared solutions were transferred to 50 ml glass beakers, and four replicates were prepared for each concentration level. Five active *D. magna* aged 6–24 h were added into each beaker. The test organisms were fed with *Scenedesmus obliquus* 6 h prior to the exposure. All beakers were monitored at 24-h intervals until reaching 48 h of exposure. The concentration that caused 50% morality of the test population, or LC_{50} (mg l^{-1}), was determined by probit analysis (ToxCalc™ v5.0, Tidepool Scientific Software, McKinleycille, CA).

RESULTS AND DISCUSSION

Evaluation of Enantioselective Columns

The five chiral organophosphorous compounds in Table 1 all have a chiral carbon directly bonded to phosphorus, with only slight distinction in other positions. This diversity would seem to require equally divergent enantioselective separation mechanisms in enantioselective HPLC columns. The best separation data on each column were summarized in Table 2. In the present investigation, the main aim was to develop a HPLC method for enantioselective separation.

These four CSPs of derivative cellulose and amylase are reported to separate a wide range of racemic compounds.[8,20,21] It is believed that the higher order structure of the CSP greatly influences its enantioselective ability. For all the compounds tested, successful enantiomeric separation were obtained on Chiralpak AD with proper mobile phase compositions. Less or no separation was obtained for compounds **2**, **3,** and **5** on Chiralcel OD, for compound **2** on Chiralcel OJ, and for compound **5** on Chiralpak AS. Typical chromatograms of these five herbicides are shown in Figure 1.

Although Chiralcel OD had the same D-glucose constituents as chiral absorbing sites as Chiralpak AD (the same chiral selector), it only gave partial resolution of compounds **2**, **3**, and **5**. The different chiral recognition mechanisms could be attributed to the higher order structures arising from their different arrangements of the glucose units (Fig. 2). The analyte-CSP interactions leading to the formation of hydrogen bonding, π–π, dipole–dipole, dipole-induced dipole and inclusion, may be distinctive. Chiralpak AS also showed an excellent selectivity toward the four compounds. Their separation factor α and resolution obtained were substantially greater than on Chiralpak AD, Chiralcel OD, and Chiralcel OJ, and the elution times

TABLE 2. Separation of 1-(substituted phenoxyacetoxy)alkylphosphonate herbicides on polysaccharide chiral stationary phases, 25°C, 1 ml min^{-1}

Chiral column	Compound	Hexane/isopropanol	k_1	k_2	α	R_s	CD pk1/pk2
Chiralpak AD	**1**	90/10[a]	1.88	2.53	1.34	4.75	−/+
	2	90/10	3.03	3.76	1.24	2.65	+/−
	3	90/10	3.93	4.49	1.14	1.60	−/+
	4	95/5	11.38	12.36	1.09	1.59	−/+
	5	95/5	7.07	7.98	1.13	2.37	−/+
Chiralpak AS	**1**	90/10	1.72	4.06	2.36	8.53	−/+
	2	90/10	2.36	3.22	1.37	2.33	−/+
	3	90/10	4.99	6.70	1.34	3.23	−/+
	4	90/10	11.72	20.55	1.75	5.88	−/+
	5	90/10[a]	1.87	2.07	1.10	1.10	−/+
Chiralcel OD	**1**	90/10	2.96	3.46	1.17	1.50	−/+
	2	95/5	6.46	6.70	1.04	0.56	+/−
	3	90/10	4.06	4.50	1.11	1.12	−/+
	4	95/5	1.51	2.00	1.33	2.32	−/+
	5	90/10[a]	4.15	4.15	1.00	0	n.r
Chiracel OJ	**1**	90/10	2.33	2.86	1.23	1.93	+/−
	2	90/10[a]	4.89	4.89	1.00	0	n.r
	3	90/10	12.09	12.86	1.06	1.66	+/−
	4	90/10	22.60	28.28	1.25	2.09	+/−
	5	90/10[a]	6.29	7.15	1.14	1.73	−/+

[a]Hexane/Ethanol.

were relatively short. Baseline resolution of four compounds in test, except compound **5**, was easily obtained under the initial chromatographic conditions (hexane/isopropanol = 90:10) on Chiralpak AS. Another chiral column involved was Chiralcel OJ. Although four compounds achieved baseline resolution ($R_s > 1.5$), their retention times were too long, which would prevent a semipreparative application, as shown in Table 2. In general, the complexity of chiral recognition mechanisms resulted in different enantioselectivity among different CSPs. It was difficult to elucidate which models were involved, but may be attributed to the following several mechanisms. First, all the 1-(substituted phenoxyacetoxy)alkylphosphonates studied contain carbonyl (C=O) group. The C=O can directly interact through dipole–dipole contact with the C=O group on each column tested, and form hydrogen bonding with NH group on Chiralpak AD, Chiralpak AS, Chiralcel OD (no NH group in Chiralcel OJ) (Fig. 2). Second, different stability of the transient diastereomeric complexes between enantiomers and CSPs may be formed. Moreover, the degree of steric fit into the chiral cavities of CSPs may also play an important role in chiral recognition and the chiral cavities of different CSPs may have different accessibilities for the compounds.

Overall, the columns Chiralpak AD and Chiralpak AS performed better in separation than the columns Chiralcel OJ and Chiralcel OD for these five compounds, although Chiralcel OJ was slightly better than Chiralcel OD. Chiralpak AD was chosen for more specific tests.

Influence of Mobile Phase Composition

Isopropanol and ethanol were used as the polar modifiers in order to search for the best enantiomeric selectivity for the five analytes. It is known that changing the polarity of mobile phase by varying the percentage or the type of polar modifier can greatly influence the elution time and resolution.[22,23] The effect of mobile phase composition on the elution time and selectivity for the enantiomers of five compounds was investigated on Chiralpak AD by varying the isopropanol content from 5 to 15% (by volume). The chromatographic results shown in Figure 3 revealed that an increase in the content of isopropanol decreased the retention. This was observed for all the analytes investigated. The increase of isopropanol content showed a dramatic decrease in retention, indicating that hydrogen bonding was the dominant interaction for retention.[24] The hydrogen bonding between the C=O of the analyte and NH group of the CSP could be the dominant interaction for the retention. With increasing the polarity of the mobile phase, the hydrogen bonding interaction could be disturbed.[25] In other words, due to the decrease in solvent polarity, the ability of the solvent to displace the solute from CSP decreased.[26,27]

For the separation factor α, however, the change did not follow a specific trend when the polarity of the mobile phase was altered (Fig. 4). As expected for the normal-phase behavior of these CSPs, the α value generally decreased with increasing the content of isopropanol (compound **2**). It may be due to the competition of the alcohol for the chiral bonding sites with chiral solutes. However, long retention time was needed if no isopropanol or ethanol was added to the mobile phase. Sometimes no resolution was obtained if the polarity of mobile phase was too weak. For instance, a slight increase in α value was observed for compound **1** when the polarity of the mobile phase was increased. It is suggested that alcohol in the mobile phase can alter the steric environment of the chiral cavities on CSPs by bonding to achiral sites at or

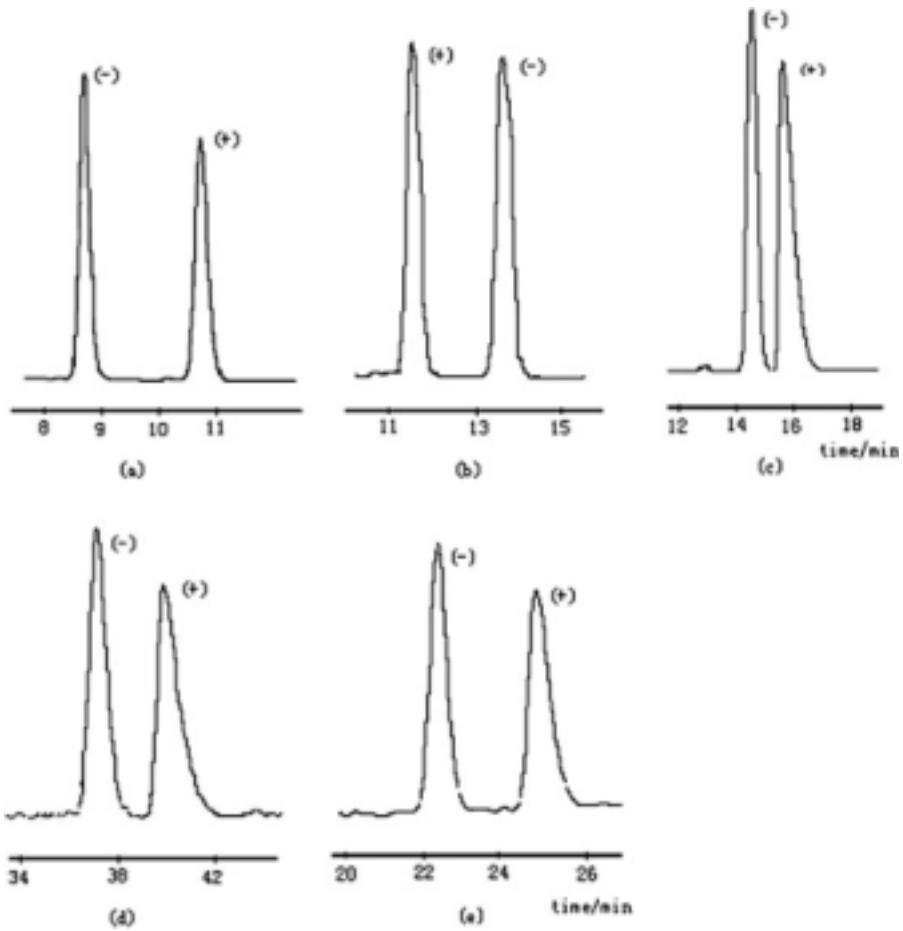

Fig. 1. HPLC chromatograms of chiral 1-(substituted phenoxyacetoxy) alkylphosphonate herbicides using Chiralpak AD column: (**a**) compound 1, (**b**) compound 2, (**c**) compound 3, (**d**) compound 4, (**e**) compound 5; mobile phase: (a), Hexane/Ethanol = 90/10 (v/v), (b) and (c), hexane/isopropanol = 90/10 (v/v), (d) and (e), hexane/isopropanol = 95/5 (v/v).

near the chiral cavity. Consequently, appropriate alcohol content is beneficial for chiral separation. For some compounds, the α values were affected little by the concentration of organic modifier.[28] This may be explained that there was no competition between the analyte and the organic modifier for the active sites of CSPs.

In general, the resolution is determined by the polarity of the mobile phase. Sometimes, it is additionally affected by the type of the mobile phase. According to the R_s value (4.75), the separation of compound **1** on Chiralpak AD at 90/10 hexane/ethanol was excellent. By comparison, no baseline resolution was obtained when isopropanol was used in place of ethanol as organic modifier. The resolution varied from 0.69 to 0.55 to 0.57 when the content of isopropanol was changed from 10 to 5 to 2%. For compound **5** on Chiralpak AD, ethanol was also a better organic modifier. For the same compound on different columns, in fact, solvents performed differently. With isopropanol, the separation of compound **1** on three columns was better than on column AD, in contrast to the separation with ethanol on the latter column. The results were due likely to the steric differences between the two solvent molecules, leading to quite different chiral surfaces on the stationary phases.[27,29]

From these results, we concluded that the addition of a polar additive was essential to obtain satisfactory enantioselectivity for OPs and the selection of the additive depended not only on the compound tested but also on the column used.

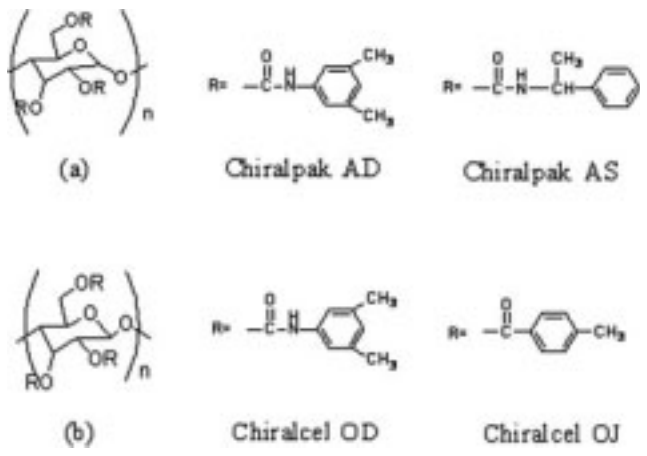

Fig. 2. Structures of derivatized polysaccharide CSPs: (**a**) Amylose-O-R, Chiralpak AD and Chiralpak AS; (**b**) Cellulose-O-R, Chiralcel OD and Chiralcel OJ.

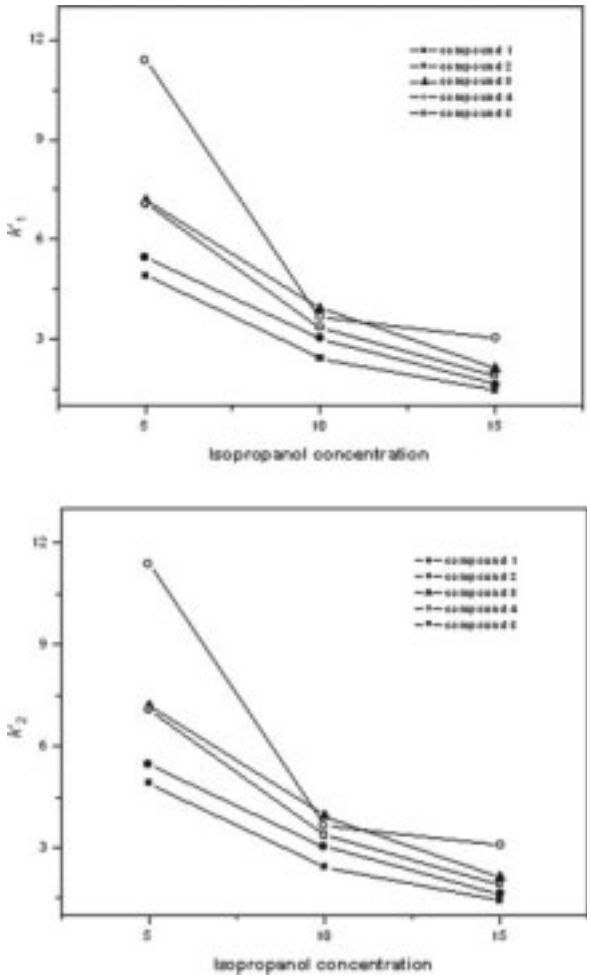

Fig. 3. Influence of isopropanol percentage in the mobile phase on k'_1 and k'_2.

Effect of Chemical Structures of the Analytes

The characteristics of a chiral analyte (e.g., position, number, and size of substituents) are often critical to the chiral recognition. Interactions between analytes and the derivatives of polysaccharides have been proposed to include hydrogen bonding, dipole–dipole, π–π interactions and inclusion. In this work, Chiralpak AD and Chiralcel OD were compared to determine the effects of chemical structures of analytes with hexane/isopropanol = 90/10 (v/v). From the differences in the chiral separation between compounds **1** and **2**, it was observed that the substitution of ethyl for methyl on asymmetric carbon atom and the substitution of methoxyl for ethoxyl on phosphorus resulted in a good baseline resolution on Chiralpak AD. On Chiralcel OD, the result was completely opposite (Fig. 5). The inconsistency in the resolution of compounds **1** and **2** indicates that higher steric hindrance of ethyl or methoxyl than methyl or ethoxyl in fitting into the chiral cavities of Chiralpak AD, and that methyl or ethoxyl was more difficult than ethyl or methoxyl in fitting into the chiral cavities of Chiralcel OD column. In addition, the selectivity (α) of compounds **3** and **4** which contain the same

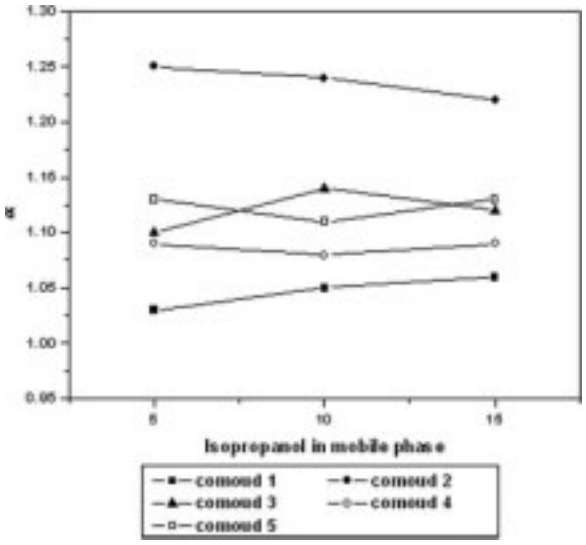

Fig. 4. Influence of isopropanol percentage in the mobile phase on selectivity (|Á).

substituent at different positions on the aromatic ring changed to a certain extent on both Chiralpak AD and Chiralcel OD under the same chromatographic conditions (hexane/isopropanol = 90/10, v/v), as shown in Table 3. On Chiralpak AD, the separation factor α value of para-substituent analog **3** was higher than that of the ortho-

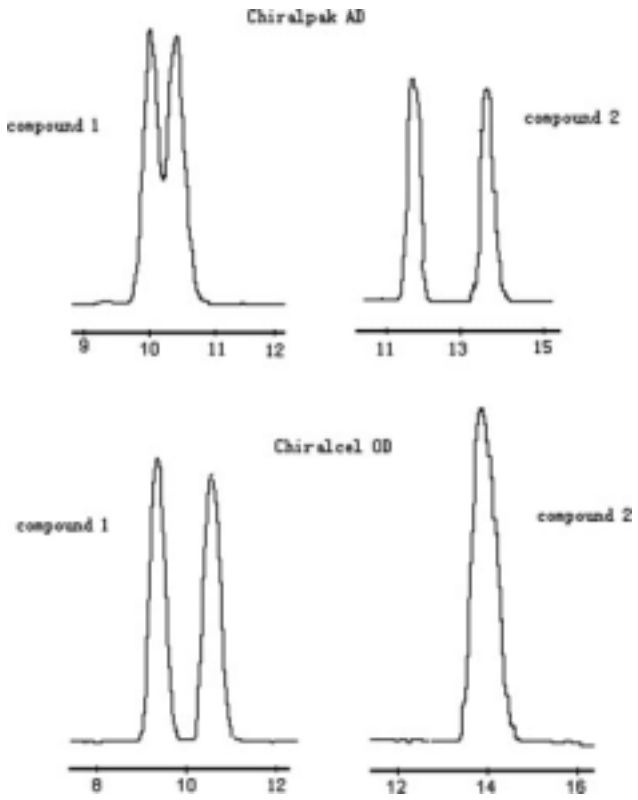

Fig. 5. HPLC chromatograms of compounds 1 and 2 using Chiralpak AD column and Chiralcel OD column. Hexane/isopropanol = 90/10 (v/v) at the flow rate of 1.0 ml min^{-1}.

TABLE 3. Separation of 1-(substituted phenoxyacetoxy)alkylphosphonate herbicides on Chiralcel OD and Chiralpak AD using hexane/isopropanol = 90/10 (v/v), 25°C, 1 ml min^{-1}

	Column									
	Chiralpak OD					Chialcel AD				
Compound	k_1	k_2	α	R_s	CD pk1/pk2	k_1	k_2	α	R_s	CD pk1/pk2
1	2.96	3.46	1.17	1.50	−/+	2.43	2.55	1.05	0.69	−/+
2	3.46	3.46	1.00	0	n.r	3.03	3.76	1.24	2.65	+/−
3	4.06	4.50	1.11	1.12	−/+	3.93	4.49	1.14	1.60	−/+
4	4.71	5.14	1.09	0.86	−/+	3.66	3.94	1.08	0.55	−/+
5	4.15	4.15	1.00	0	n.r	3.36	3.73	1.11	1.44	−/+

substituent analog **4**. On Chiralcel OD, the α value of para-substituent analog **3** was 1.11, while that of *ortho*-substituent analog **4** was 1.09. The para-position was apparently better than the ortho-position on both Chiralpak AD and Chiralcel OD. From the chromatographic data for compounds **3** and **5** bearing different halogen substituents at the same position, it was interesting to note that their separation factors were higher for the chloro- than for the fluoro-substituted. On Chiralcel OD, the α values of chloro- and fluoro-substituted analogs were 1.11 and 1.00, respectively. The existence of smaller groups involves the formation of a π–π complex between phenyl of the CSP and the aryl substituent of the organic phosphours compound as well as the hydrogen bonding of the amino tethering group of CSP with the halogen atom of the aromatic ring of the analyte. It seems that the π–π and H-bonding effects are favorable when electron-donating atom (halogen) is in the para position on both Chiralpak AD and Chiralcel OD columns. Furthermore, compared to fluorine atom, the π–π and H-bonding effects are more favorable when chlorine atom is in para position. In the study by Róbert Berkecz et al., the H-bonding effect was favorable when electron-donating atoms were in the meta or para position, and unfavorable when electron-donating atoms were in the ortho position.[22]

Effect of Column Temperature

The effect of temperature was investigated on Chiralpak AD in the range of 10–40°C using the mobile phase composition of hexane/isopropanol (90/10, v/v) at the flow rate of 1.0 ml min^{-1}. The calculated parameters including retention factor (*k'*), separation factor (α), and resolution (R_s) are summarized in Table 4. As a potential factor, temperature can affect chiral separation at least in two ways. One is the effect of viscosity and diffusion coefficient of solute. The other is the thermodynamic effect that changes the separation factor (α).[30] Generally, the former is often negligible, while the latter is more important and can be investigated using the following two equations:

$$\Delta G^\circ = -RT \ln\left(\frac{k'}{\phi}\right) \quad (1)$$

where k' is a retention factor, R is the gas constant, ϕ is the column phase ratio (stationary phase volume over the mobile phase volume) and T is the temperature in K.

$$\ln k' = -\frac{\Delta H^\circ}{RT} + \frac{\Delta S^\circ}{R} + \ln \phi \quad (2)$$

where ΔH° and ΔS° are the standard transfer enthalpy and entropy of the analyte from the mobile phase to the stationary phase. They are obtained from the slope and intercept of the straight line from eq. 2, respectively. The corresponding $\Delta\Delta H^\circ$ and $\Delta\Delta S^\circ$ values can be obtained as the differences ($\Delta H_2^\circ - \Delta H_1^\circ$) and ($\Delta S_2^\circ - \Delta S_1^\circ$), or can be estimated from the selectivity factor (α) if the temperature range investigated is sufficiently small that the plots of lnα vs. $1/T$ can be fitted by a straight line (eq. 3). The Gibbs free energy change $\Delta\Delta G^\circ$ for the separation also can be obtained (eq. 3). All the data from this study are presented in Table 4.

$$\Delta\Delta G^\circ = -RT \ln \alpha = \Delta\Delta H^\circ - T\Delta\Delta S^\circ \quad (3)$$

In the present study, all the plots of natural logarithms of retention factors (ln k) of enantiomers as a function of the inverse of temperature ($1/T$) could be fitted by straight

TABLE 4. Effect of temperature on the separation of five 1-(substituted phenoxyacetoxy) alkylphosphonate herbicides on Chiralpak AD column

Column	Compound																			
AD	**1**				**2**				**3**				**4**				**5**			
T (°C)	k_1	k_2	α	R_s	k_1	k_2	α	R_s	k_1	k_2	α	R_s	k_1	k_2	α	R_s	k_1	k_2	α	R_s
10	2.91	3.07	1.06	0.56	3.26	4.35	1.33	4.49	4.47	5.24	1.17	2.22	7.00	7.98	1.14	1.78	4.09	4.80	1.17	2.12
20	2.38	2.49	1.05	0.59	2.72	3.36	1.24	3.50	3.75	4.29	1.14	2.17	5.54	6.23	1.13	1.79	3.27	3.76	1.15	2.19
30	2.00	2.10	1.05	0.69	2.27	2.64	1.16	2.53	3.15	3.66	1.16	2.57	4.56	5.14	1.13	1.96	2.77	3.17	1.14	2.27
40	1.68	1.80	1.07	1.00	1.98	2.18	1.10	1.64	2.74	3.26	1.19	3.22	4.01	4.92	1.23	3.00	2.44	2.95	1.21	3.22

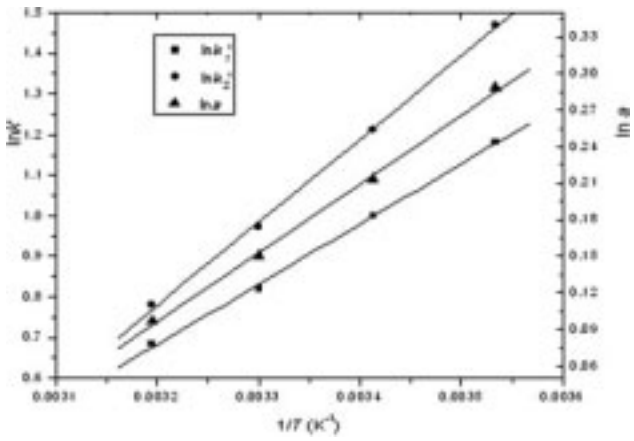

Fig. 6. The van't Hoff plots of k' and |Á for the enantiomers of compound 2. Chromatographic conditions: Chiralpak AD column, and hexane/isopropanol (90/10, v/v) at the flow rate of 1.0 ml min^{-1}.

lines. Only the variation of compound **2** in ln α versus $1/T$, according to the van't Hoff model, showed a linear relationship in the range of 10–40°C. The result can be explained that the temperature range was not appropriate for the other four investigated compounds that the relationship between lnα and $1/T$ went beyond the linear range.[26] The parameters such as $\Delta\Delta H^\circ$ and $\Delta\Delta S^\circ$ of compound **2** can be obtained from Figure 6, and they were -4.8 kJ mol^{-1} and -14.5 kJ mol^{-1}, respectively. The negative values of $\Delta\Delta H^\circ$ suggest that better enantioselectivity of compound **2** on Chiralpak AD may be achieved at a lower temperature. In this case, a decrease in temperature, along with a decrease in flow-rate in some cases, increased the enantioselectivity and resolution R_s which increased from 1.64 to 4.49 when the temperature decreased from 40 to 10°C. Similar phenomenon has been reported by A. Péter et al.[31]

Enantioselectivity in Aquatic Toxicity

Acute aquatic toxicities were measured for the racemates and individual enantiomers of the five 1-(substituted phenoxyacetoxy)alkylphosphonates using a 24-h and 48-h static test to *D. magna*. The LC_{50} values are listed in Table 5. From the LC_{50} values for the five derivatives, significant differences were observed among these compounds, although they have similar chemical structures. Especially, compound **3** which possesses outstanding toxicity against *D.magna* was 2-148.5 times more toxic than the others. There was also a significant difference in LC50 between the two enantiomers of compound **3**, with the (+)-form enantiomer being 8.08 times more toxic than the (−)-form. It was revealed that the (+)-enantiomer of compound **3** showed higher toxicity than its (−)-form and racemic form. From the LC50 values measured for the individual enantiomers, it can be calculated that the (+)-enantiomer of compound **3** contributed about 91% to its activity against *D. magna* in the racemate. According to Table 5, enantioselective toxicities of the other four compounds also can be obtained. Although the difference between the enantiomers was not remarkable (1.2–4.2 folds), it also can be inferred that the toxicities of most chial OPs are enantioselective. Similar to our finding (compounds **3** and **5**), the in vivo toxicities of fenamiophos,[32] leptophos,[33] and methanmidophos[11]to *D. magna* arose primarily from their (+)-enantiomer. In contrast, the toxicity to *D. magna* of the other three chiral OPs, fonofos, profenofos[4] and trichoronate,[12] was primarily from their (−)-enantiomers.

TABLE 5. LC_{50} (48 h mg l^{-1}) for racemate and enantiomers of 1-(substituted phenoxyacetoxy)alkylphosphonate herbicides to *D. magna*

Compound	(±)	(+)	(−)
1	0.24 ± 0.06	0.18 ± 0.03	0.14 ± 0.08
2	1.14 ± 0.32	1.87 ± 0.15	1.41 ± 0.05
3	0.020 ± 0.003	0.012 ± 0.008	0.097 ± 0.007
4	2.97 ± 0.28	1.99 ± 0.44	2.72 ± 0.35
5	2.54 ± 0.42	2.30 ± 0.36	9.77 ± 0.88

The toxicities of these OPs were enantioselective. For compound **2**, it was interesting to note that the toxicity of racemate was slightly higher than that of individual enantiomers. By comparing compound **1** with compound **4**, we observed that their racemates showed lowest toxicity, while compounds **3** and **5** showed intermediate toxicity. These results indicate that the toxicological effects of racemate or equimolar mixture of enantiomers cannot be predicted as the simple addition of the effects of the individual enantiomer. Since OPs are widely applied in their racemic forms in modern agriculture and sometimes only one of the two enantiomers contributes primarily to the activity of the racemate, further investigations on the enantioselective environmental behavior of chiral OPs are needed. Moreover, the synergistic and antagonistic interactions between enantiomers may exist in biological processes and must be taken into consideration in pesticide risk assessment.

CONCLUSIONS

This study demonstrated that Chiralpak AD Column can be used for the determination of a series of five 1-(substituted phenoxyacetoxy) alkylphosphonate derivatives containing a chiral carbon atom, as compared to Chiralpak AS, Chiralcel OD and Chiralcel OJ columns. Mobile phase composition, column temperature and chemical structure all together affect the separation. This work also revealed that the biological toxicity of these five compounds to *D. magna* is stereospecific. The significant enantioselectivity of these compounds in aquatic toxicity suggests that enantiomers and racemate need to be individually assessed for the environmental safety to evaluate the overall toxicity of chiral OPs. Because most chiral pesticides are still used in racemic forms, more comprehensive studies are needed to evaluate their enantioselective environmental behaviors and ecological risks.

LITERATURE CITED

1. Williams A. Opportunities for chiral chemicals. Pestic Sci 1996;46:3–9.
2. John EC, Gary BQ. Organophosphate toxicology: safety aspects of nonacetylcholinesrerase secondary targets. Chem Res Toxicol 2004; 17:983–998.

3. Zhou SS, Lin KD, Yang HY, Li L, Liu WP, Li J. Sereoisomeric separation and toxicity of a new organophosphorus insecticide chloramidophos. Chem Res Toxicol 2007;20:400–405.
4. Liu WP, Gan JY, Schlenk D, Jury WA. Enantioselectivity in environmental safety of current chiral insecticides. Proc Natl Acad Sci USA 2005;102:701–706.
5. Castañeda OL, Kraak GVD, Canul RR, Gold G. Endocrine disruption mechanism of o,p'-DDT in mature male tilapia (Oreochromis niloticus). Toxicol Appl Pharm 2007;221:158–167.
6. Hoekstra PF, Burnison BK, Neheli T, Muir DCG. Enantiomer-specific activity of o,p'-DDT with the human estrogen receptor. Toxicol Lett 2001;125:75–81.
7. Gao RY, Yang GS, Yang HZ, Chen ZY, Wang QS. Enantioseparation of fourteen O-ethyl O-phenyl N-isopropyl phosphoroamiddothioates by high-performance liguid chromatography on a chiral stationary phase. J Chromatogr A 1997;763:125–128.
8. Ellington JJ, Evans JJ, Prickett KB, Champion WL. High-performance liquid chromatographic separation of the enantiomers of organophosphorus pesticides on polysaccharide chiral stationary phase. J Chromatogr A 2001;928:145–154.
9. Ruiz CG, Lamas GA, Puerta A, Blanco E, Medel AS, Marina ML. Enantiomeric separarion of organophosphorus pesticides by capillary electrophoresis. Analytica Chimica Acta 2005;543:77–83.
10. Zhu WH, Wu FY, Raushel FM, Vigh GA. Capillary electrophoretic separation of the enantiomers of organophosphates with a phosphorus stereogenic center using the sodium salt of octakis (2,3-diacetyl-6-sulfo)-γ-cyclodextrin as resolving agent. J Chromatogr A 2000;895: 247–254.
11. Lin KD, Zhou SS, Xu C, Liu WP. Enantiomeric resolution and biotoxicity of methamidophos. J Agric Food Chem 2006;54:8134–8138.
12. Liu WP, Lin KD, Gan JY. Separation and aquatic toxicity of enantiomers of the organophophorus insecticide trichloronate. Chirarity 2006;18:713–716.
13. Chen T, Shen P, Li YJ, He HW. Synthesis and herbicidal activity of O,O-dialkyl phenoxyacetoxyalkylphosphonates containing fluorine. J Fluorine Chem 2006;127:291–295.
14. He HW, Wang T, Li YJ, Shen P, Chen T, Liao GH, Mo WY. CN 1685825A, 2005.
15. He HW, Wang T, Yuan JL. Synthesis and herbicidal activities of methyl-1(2, 4-dichlorophenoxyacetoxy)alkylphosphonate monosalts. J Organomet Chem 2005;690:2608–2613.
16. Peng H, Wang T, Xie T, Chen T, He HW, Wan J. Molecular docking and three-dimensional quantitative structure-activity relationship studies on the binding modes of herbicidal 1-(substituted phenoxyacetoxy) alkylphosphonates to the E1 component of pyruvate dehydrogenase. J Agric Food Chem 2007;55:1871–1880.
17. He HW, Liu ZJ. Progresses in research of R-oxophosphonic acid derivatives with herbicidal activity. Chin J Org Chem 2001;21:878–883.
18. Wang T, He HW, Yuan JL. Peng DH. A new reacting target for herbicide. Chin J Appl Chem 2003;20:613–617.
19. Organization for Economic Cooperation and development (OECD). Report of the Final Ring Test of the Daphnia magna Reproduction Study; 1995.
20. Weber CI. Methods for measuring the acute toxicity of effluents and receiving waters to freshwater and marine organisms. Cincinnati, OH: US Environmental Protection Agency; 1995.
21. Calabrò ML, Raneri D, Tommasini S. Enantioselective recognition of 2, 3-benzodiazepin-4-one derivatives with anticonvulsant activity on several polysaccharide chiralstationary phases. J Chromatogr B 2006;838:56–62.
22. Berkecz R, Ivaov AS, Ilisz I, Forró E, Fülöp F, Hyun MH, Péter A. High-performance liquid chromatographic enantioseparation of β-amino acid stereoisomers on a (+)-(18-crown-6)-2, 3, 11, 12-tetracarboxylic acid-based chiral stationary phase. J Chromatogr A 2006;1125: 138–143.
23. Yang LM, Xie YF, Chen HZ, Lu Y. Diastereomeric and enantiomeric high-performance liquid chromatographic separation of synthetic anisodamine. J Pharmceut Biomed 2007;43:905–909.
24. O'Brien T, Crocker L, Thompson R, Thompson K, Toma PH, Conlon DA, Feibush B, Moeder C, Bicker G., Grinberg N. Mechanistic aspects of chiral discrimination on modified cellulose. Anal Chem 1997;69:1999–2007.
25. Liu WP, Gan JY, Qin SJ. Isolation, identification and aqueous toxicity of enantiomers of cypermethrin and cyfluthrin. Chirality 2005;17: S127–S133.
26. Daicel Chemical Industries. Instruction manual for Chiralcel OD-H, Instruction for Chiralcel OJ, Baker France.
27. Rao RN, Nagaraju D, Raju AN. Enantiomeric resolution of doxazosin mesylate and its process-related substances on polysaccharide chiral stationary phases. J Pharmaceut Biomed 2006;41:766–773.
28. Caccamese S, Scivoli G, Bianca S, L'opez-Romero JM, Ortiz-L'opez FJ. Chiral high-performance liquid chromatographic separation and circular dichroism spectra of the enantiomers of cytotoxic aristocularine alkaloids. J Chromatogr A 2006;1129:140–144.
29. Kunath A, Theil F, Wagner J. Diastereomeric and enantiomeric separation of monoesters prepared from meso-cyclopentanediols and racemic carboxylic acids acids on a silica phase and on amylose and cellulose chiral stationary phases. J Chromatogr A 1994;684:162–167.
30. Péter A, Vékes E, Armstrong DW. Effects of temperature on retention of chiral compounds on a ristocetin A chiral stationary phase. J Chromatogr A 2002;958:89–107.
31. Péter A, Lázár L, Fülöp F, Armtrong DW. High-performance liquid chromatographic enantioseparation of β-amino acids. J Chromatogr A 2001;926:229–238.
32. Wang YS, Tai KT, Yen JH. Separation, bioactivity, and dissisopropanoltion of enantiomers of the organophosphorous insecticide fenamiphos. Ecotoxicol Environ Saf 2004;57:346–353.
33. Yen JH, Tsai CC, Wang YS. Separation and toxicity of enatiomers of organophosphorus insecticide leptophos. Ecotoxicol Environ Saf 2003;55:236–242.

CHIRALITY 20:139–146 (2008)

The Application of Preparative Batch HPLC, Supercritical Fluid Chromatography, Steady-State Recycling, and Simulated Moving Bed for the Resolution of a Racemic Pharmaceutical Intermediate

TONY Q. YAN,[1]* CARLOS ORIHUELA,[1] AND DAVID SWANSON[2]

[1]*Separation Group, Process Analytical Science, Chemical Process Research and Development, Amgen, Inc., Amgen One Center Dr., Thousand Oaks, California*

[2]*Johnson Matthey Pharma Services, 25 Patton Road, Devens, Massachusetts*

ABSTRACT This article discusses the chromatographic resolution of a racemic pharmaceutical intermediate. Preparative batch high performance liquid chromatography (HPLC), supercritical fluid chromatography (SFC), steady-state recycling (SSR), and simulated moving bed (SMB) were used to resolve a total of 12.2 kg of a racemic pharmaceutical intermediate. In this study, a first batch of 0.8 kg of racemate was separated on the preparative batch HPLC and SFC, and subsequently another 5.9 kg of racemate was separated on the SSR. Lastly, a third batch of 5.5 kg was separated on the SMB. The separation conditions and results of these techniques are discussed. The productivities and solvent costs of SFC versus HPLC are compared. The productivities and solvent costs of SMB, SSR, and HPLC are also compared. The analytical method development and process optimization of these processes are also discussed in this article. *Chirality 20:139–146, 2008.* © 2007 Wiley-Liss, Inc.

KEY WORDS: chiral separation; preparative chromatography; pharmaceutical intermediate

INTRODUCTION

Enantiomer separation is one of the most important types of binary separations in the pharmaceutical industry. Enantiomers have been demonstrated to have different biological activities. Therefore, it is essential to test the toxicity and efficacy of the individual enantiomer in the early stages of drug development. There are two ways to get enantiomerically pure pharmaceutical intermediates, asymmetric synthesis of the desired enantiomer or resolution of a racemic mixture into individual enantiomers. In the early stages of pharmaceutical research and development, the resolution of the racemic mixtures is the preferred choice because development time is of the utmost priority. Therefore, preparative chromatographic resolution of racemates is being used increasingly in the pharmaceutical industry for rapidly accessing enantiomerically pure materials.[1–5] Most frequently used modes of preparative chromatography for chiral resolution include simulated moving bed (SMB), steady-state recycling (SSR), batch high performance liquid chromatography (HPLC), and supercritical fluid chromatography (SFC). SMB is a continuous process and almost always requires less solvent to separate a given quantity of racemate. SMB or other multicolumn chromatography is predominating at large scale (>20-kg scale). At this scale, SMB process is often less expensive than batch HPLC process having higher productivity and less solvent consumption. In the past a few years, SMB for enantiomeric separations has been used at manufacturing scale (>100 kg) by numerous pharmaceutical companies.[6–8] In addition, SMB gives a better production rate for a separation with low separation factor. The major disadvantage of SMB is capital cost. SMB systems are significantly more expensive than batch HPLC systems. A relatively new technique, SSR, has shown promise in approaching the performance of SMB for medium to large scale (0.5–20 kg) separations. When compared with SMB, this SSR technique incorporates a relatively simple design, low cost, and relatively high efficiency.[9,10] SSR is a chromatographic technique for the separation of binary components, especially good for separations with low selectivity. SSR only uses one column and one mobile phase pump. The capital costs of an SSR system are marginally higher than those of the batch HPLC system, but they are substantially lower than those of an SMB system. The simplicity of SSR process makes it a "phase appropriate" technology for the early development support.[11] However, the SSR separation efficiency is lower than SMB. The efficiency of the SSR process is only ~50% that of an SMB process. The SSR process is only able to compare with a nonoptimized SMB process.[12] Batch HPLC has been often used for small quantity of chiral resolution due to its rapid

*Correspondence to: Tony Q. Yan, Separation Group, Process Analytical Science, Chemical Process Research and Development, Amgen, Inc., Amgen One Center Dr., Thousand Oaks, California 91320, USA.
E-mail: qiy@amgen.com

Received for publication 22 May 2007; Accepted 23 October 2007
DOI: 10.1002/chir.20512
Published online 11 December 2007 in Wiley InterScience (www.interscience.wiley.com).

turn around time (a few grams to several hundreds grams of racemate). This method requires good selectivity and uses large quantity of solvent. To achieve high purity and yield of both enantiomers, a baseline separation is normally desired for the batch HPLC separation. In this mode, only a portion of the column bed is utilized, therefore the separation efficiency is usually low. SFC has been proven to be a very efficient tool for separation of small amounts of chiral compounds.[13–15] It has been widely used to support discovery chemists in the pharmaceutical industry. The low viscosity and high diffusivity of the supercritical fluid allow the SFC to work at higher linear velocity through the column. Therefore, SFC separations are usually fast and also allow the use of more efficient media such as 5-μm stationary phase. SFC also has its unique selectivity, which often offers an alternative way to HPLC separations. However, for the large-scale chiral separations, the capital and facility costs to use SFC can be substantial.[16] Moreover, SFC systems currently conduct separations in batch mode only. The separation efficiency at the large scale is limited when compared with a continuous chromatography process such as SFC–SMB. Prototype SFC–SMB systems have been described by Novasep[17] and Johannsen et al.[18] These SFC–SMB systems show some promise for separations at industrial scale, and offer a more efficient approach for chiral separations. An SMC–SFC system was described by Zhang et al. SMC uses two or three short columns connected in series, and enables the unresolved enantiomers to separate repeatedly and exclusively through each of the columns until sufficient resolution is attained.[19] SMC–SFC increases the number of SMC cycles with significantly less band broadening compared with HPLC.[20] A new SFC tandem column screening tool was discussed by Welch et al. This instrument is a useful tool for facilitating the screening of tandem column arrangements for separation of complex mixtures of stereoisomers or other multicomponent mixtures. In this article, we used batch HPLC, SFC, SSR, and SMB techniques for an enantiomeric resolution of a pharmaceutical intermediate. We will discuss the separation conditions, the purity and yield, the productivity and the solvent consumption for the separations of 12.2 kg of racemate using these four techniques. The racemate was used as an intermediate for the toxicity batches. This racemate was made in three batches. The first batch (0.8 kg) was used for a 14-day toxicity study, the second batch (5.9 kg) was used for a 28-day toxicity study, and a third batch (5.2 kg) was used for a GLP toxicity study. By isolating the racemate mixture, the drug development time was shortened while allowed more time for the synthetic chemists to optimize the drug development process.

EXPERIMENTAL

Material

The racemate to be separated was a pharmaceutical intermediate belonging to and synthesized at Amgen pharmaceuticals (Thousand Oaks, CA). The compound contains an aliphatic cyclic group and an amine group at the asymmetric center. The partial structure can be described as follows:

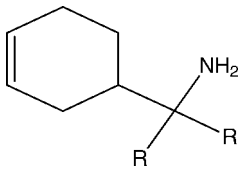

The mobile phase used was reagent grade methanol from a variety of sources. The chiral stationary phase (CSP) was ChiralPAK-AD and was obtained from Chiral Technologies (Exton, PA). The bulk material (20 μm) was used for preparative HPLC purification. The prepacked column (5 μm) from Chiral Technologies also was used for preparative SFC separation.

Preparative Batch HPLC

The preparative batch chromatographic system was a prep-star system from Varian (Wakefield, RI). The preparative HPLC run was performed using a MODCOL spring loaded column from Grace (Hesperia, CA) with an inner diameter of 10.3 cm and was packed to a length of ~40 cm with 2.0 kg of CSP. The column was jacketed and the mobile phase passed through a heat exchanger before entering the column. The heat exchange fluid was thermostated at 30°C. The mobile phase was 100% methanol. The flow rate was 400 ml/min. The racemate was dissolved in methanol. The concentration was 25 mg racemate/ml. The sample solution was filtered through a 30–50-μm sintered glass funnel before injecting into the system.

Preparative SFC

The preparative SFC system was a Supersep 30/50 from Novasep (Wakefield, PA). The flow rate was 180 g CO_2/min. The operating pressure was 100 bars. The SFC run was performed using a pre-packed column (3 cm i.d. × 25 cm length containing of ~100 g of ChiralPAK-AD-H, 5 μm, Chiral Technology). The column was placed in an oven, which was thermoset at 40°C. Methanol was used as a cosolvent. The percentage of the methanol was varied from 10 to 20% in supercritical fluid CO_2. The racemate was dissolved in methanol. The concentration was 25 mg racemate/ml. The sample solution was also filtered through a 30–50-μm sintered glass funnel before injecting into the system.

SSR

The SSR experiments were performed at Amgen using a steady cycle system from Hitachi (San Jose, CA). The instrument consists of four 20-ml injection loops, which were connected in series to give the desired injection volume. SSR process was developed by using three conventional recycle methods. Recycled data from the first cycle and second cycle were graphically overlaid using Microsoft Excel to determine the approximate position for isomer fraction cuts and midpoint of the profile for injection of racemate. The preparative SSR run was performed

TABLE 1. Performance of the six selected columns for SMB study

Columns	K1	K2	N1	N2	α
1	0.18	0.39	1501	1322	2.01
2	0.17	0.40	1630	1401	2.03
3	0.18	0.38	1585	1388	2.02
4	0.18	0.39	1705	1459	2.03
5	0.19	0.41	1648	1420	2.01
6	0.17	0.41	1698	1448	2.02
Mean	0.19	0.42	1619	1407	2.02
RSD	4.85	4.23	4.08	4.51	0.78

using a MODCOL spring loaded column with an inner diameter of 10.3 cm and was packed to a length of ~20 cm with 1.0 kg of CSP. The column was also jacketed and the mobile phase and column were thermostated to 30°C using a heat exchanger. The mobile phase was 100% methanol. The flow rate was 400 ml/min. The racemate was dissolved in methanol at a concentration of 25 mg racemate/ml. The sample solution was also filtered through a 30–50 μm sintered glass funnel before injecting into the system.

SMB

Process development of SMB. A small-scale SMB system was used for the process development of the SMB separation. This unit uses six column configurations. Six columns (1 cm i.d. × 10 cm length) were packed using the slurry method with ChiralPAK-AD as CSP, 20 μm. Isopropanol and heptane at a ratio of 50:50 were used as slurry solvent. Each column contained ~5.1 g of CSP for a total of 30.6 g. The performance of the six columns was tested. A sufficient reproducibility from column to column was achieved. Repacking would have been necessary if the reproducibility was not satisfied. The test results of these columns are listed in Table 1. These six columns were then used for the process development. The small unit and columns are used at this stage to eliminate unnecessary solvent waste and to minimize the amount of target compound consumed. The separation parameters are initially estimated based on the data obtained from the analytical chromatograms and sample loading studies. The unit is operated and the final separation parameters are obtained from the instrument based on the feed throughput (productivity) and purity of both the raffinate and the extract.

SMB separation. After the process development from the small SMB unit, the separation was scaled to the pilot SMB system. Six column configurations were also used on this system. Six columns (5 cm i.d. × 10 cm length) were each packed with ~132 g ChiralPAK AD under a pressure of ~60 bars using 50/50 heptane/isopropyl alcohol as a packing solvent. The columns were then flushed and equilibrated with methanol. The column performance was tested. The reproducibility of each column was then ensured. Separation parameters were estimated using the data obtained on the process development unit. The SMB parameters were optimized based on the final productivity and purity required. Because the parameters scale quite readily from the smaller unit, the process is much less time consuming at this point. The instrument only needs small manipulations to obtain the final parameters needed to produce material within specifications. At this stage, because of the high flow rates, the solvent and feed usages are much greater than that consumed during the process optimization on the smaller unit.

The experimental conditions of the four different processes are summarized in Table 2.

RESULTS AND DISCUSSIONS

Batch HPLC and SFC Separations

The first batch of ~800 g of racemate was used for a 14-day toxicity study. This batch was separated by using both batch HPLC and SFC. Because only a small SFC column (3 cm i.d. × 25 cm length) was available, the timeline to process 800 g of racemate was not acceptable. Therefore, both batch HPLC and SFC were used for the separation of the first 800 g of racemate. Approximately 600 g of racemate was purified using batch HPLC and ~200 g of racemate was purified on SFC. For HPLC analytical method development, various CSPs (ChiralPAK-AD, ChiralPAK-AS, ChiralPAK-IA, Chiralcel-OD, Chiralcel-OJ, Kromasil TBB, Whelk-O, RR, and Whelk-O, SS) and solvents (methanol, acetonitrile, ethanol, IPA, and mixture of IPA and heptane) were evaluated. The best separation on the HPLC analytical column was achieved using ChiralPAK-AD with a mobile phase of 100% methanol. The analytical HPLC chromatogram is shown in Figure 1. The best separation condition was chosen based upon the selectivity, the retention time, the solubility, and viscosity. The sample solubility was estimated by weighing small amount of sample into vials. A certain amount of selected solvents were added into the vials to make concentrations of solution at 10, 20, 30, 50, 100, and 150 mg/ml. The contents in the vials were subsequently stirred for at least 30 min at a temperature of 30°C. The sample solubility was estimated

TABLE 2. Summary of the experimental conditions for batch, SFC, SSR, and SMB processes

Processes	Stationary phase	Mobile phase	Number of columns	Flow rate (ml/min)	Temperature (°C)
Batch HPLC	AD	100% Methanol	1	400	30
SFC	AD	20% Methanol	1	~220[a]	40
SSR	AD	100% Methanol	1	400	30
SMB	AD	100% Methanol	6	~240	25

[a]Combined flow rate of supercritical fluid and co-solvent.

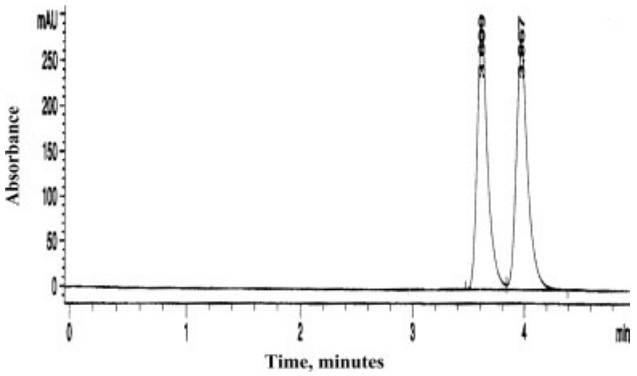

Fig. 1. Analytical HPLC separation. Analysis conducted on ChiralPAK-AD column (250 mm × 4.6 mm i.d.), detection at 230 nm. Mobile phase: 100% methanol, flow rate: 1 ml/min.

to be ~30 mg/ml in methanol. The temperature of 30°C was chosen on the basis of sample solubility and stability. The preparative batch HPLC separation was carried out with a conventional recycling method to minimize the solvent usage and improve the resolution of enantiomers. The HPLC chromatogram is shown in Figure 2. The profile was recycled once and then the pure enantiomers were collected on the second cycle. Approximately 2.0 g of racemate was loaded on the column each cycle at a cycle time of ~16.5 min. A total of ~300 cycles were performed for the separation of the first 600 g of racemate. To ascertain the purities of the both enantiomers, a small overlap fraction was collected at the valley between the peak-1 and the peak-2. This overlap fraction was reprocessed at the end of the separation. The productivity for this process was estimated at 110 g racemate per kilogram stationary phase per day (55 g product per kilogram stationary phase per day) using a racemate concentration of 25 mg/ml. The separation results from batch HPLC in terms of productivity and solvent usage were compared with the SFC process.

For SFC analytical method development, various CSPs (ChiralPAK-AD, ChiralPAK-AS, ChiralPAK-IA, Chiralcel-OD, Chiralcel-OJ, and Whelk-O, SS) and solvents (methanol, acetonitrile, and IPA) were evaluated. ChiralPAK-AD-H column with a mobile phase of 20% methanol as co-solvent showed a very promising of separation on SFC. The analytical HPLC chromatogram is shown in Figure 3. This analytical condition was then scaled up to the preparative condition. The preparative SFC separation was optimized based on the flow rate, the column pressure and the amounts of the co-solvent. For a 5-μm preparative SFC column, due to the back pressure limitation, the flow rate and column pressure should normally operate at their full capacities as the system allows. The speed of the separation is dependent on the flow rate and the column pressure. Therefore, a flow rate of 180 g CO_2/min and column pressure of 100 bars were chosen based on this consideration. The productivity and solvent usage were also related to the amounts of co-solvent. At 20% co-solvent, the cycle time was very short, the productivity was higher, but, the solvent usage was also higher. The effects of the amounts of co-solvent on the productivity and the solvent usage were studied. The results are listed in Table 3. From Table 3, we can see that the solvent usage is reduced to half by using 10% methanol as co-solvent, but, the productivity was also slightly lower due to the longer cycle time. The preparative SFC chromatogram with 20% co-solvent is shown in Figure 4. From Figure 4, the two enantiomer peaks are well separated. Approximately 25 mg of racemate was loaded on the SFC column each cycle at a cycle time of ~1.0 min. The desired purity of 98% ee (enan-

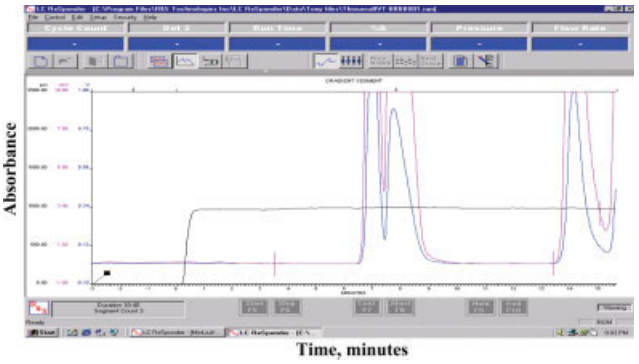

Fig. 2. Preparative batch HPLC chromatogram. Experiment conducted at a flow rate: 400 ml/min, wavelength: 230 nm, mobile phase: 100% methanol. [Color figure can be viewed in the online issue, which is available at www.interscience.wiley.com.]

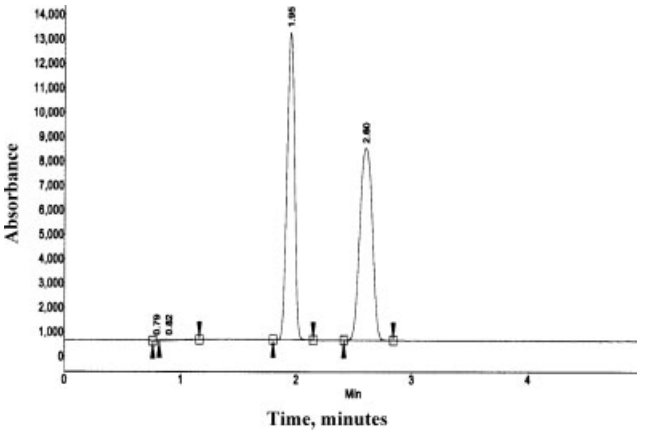

Fig. 3. Analytical SFC separation. Analysis conducted on ChiralPAK-AD-H column (250 mm × 4.6 mm i.d.), detection at 230 nm. Mobile phase: 20% methanol as co-solvent, flow rate: 3 g CO_2/min. Pressure: 100 bar. Temperature: 40°C.

TABLE 3. Productivity and solvent usage of SFC and batch HPLC processes

	Productivity (g racemate/ kg CSP/day)	Solvent consumption (l/g racemate)
SFC, at 10% methanol	329	0.76
SFC, at 15% methanol	345	1.14
SFC, at 20% methanol	362	1.52
Batch HPLC	110	2.10

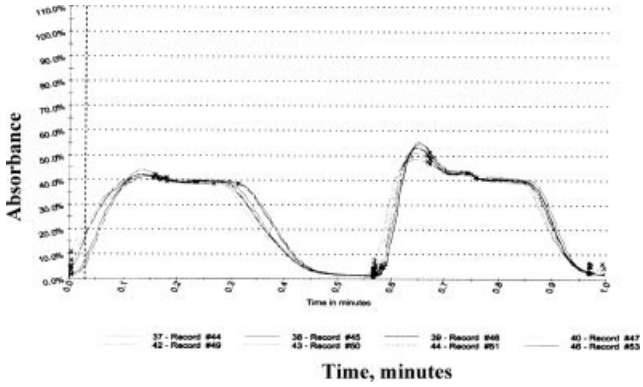

Fig. 4. Preparative SFC chromatogram. Experiment conducted at a flow rate: 180 g CO_2/min, co-solvent: 20% methanol, pressure: 100 bar, temperature: 40°C.

tiomer excess) was achieved on both enantiomers. Approximately 27 mg sample loading per cycle was also performed on the same SFC column, but, the purities of both enantiomers were below the specification (98% ee). The productivity for the SFC process is estimated to be 362 g racemate per kilogram stationary phase per day (181 g product per kilogram stationary phase per day) using a racemate feed concentration of 25 mg/ml with 20% co-solvent. These results of SFC purification were compared with the batch HPLC separation. The results are also listed in Table 3. From this table, the SFC productivity increases more than three times whereas the solvent usage is reduced to more than two times when it compares with the batch HPLC process.

SSR Separation

The second batch of 5.9 kg of racemate was used for a 28-day toxicity study and a formulation study. This batch was separated with an SSR process. The SSR method development was started with conventional recycling. The sample loading tests were performed on the three conventional recycle processes. Three cycles were normally performed to obtain the best estimation for the cycle time. The best sample loading can be estimated by observing a ~2/3 peak valley on the first cycle and a close to baseline separation in the third cycle. The three conventional cycle process are described in Figure 5 and the overlay graphic from first cycle to second cycle is described in Figure 6. From Figures 5 and 6, the cycle time, the peak collection time and the injection time of SSR process are estimated. Once these time events were obtained, the steady-state recycling process was then started. It took ~10 cycles to reach the steady state. The material, generated before a steady state, is often below the specification. We normally recombined it into the crude racemate for reprocessing. The steady-state recycle profile is shown in Figure 7. A detector signal (ascending height) of ~2% of the full scale was used as a trigger point to start a timer, the times of peak-1 and peak-2 collection time and injection time were then defined relative to this trigger time. In this separation, ~40 sec of clean fraction of peak-1 was collected and followed by ~2.0 min of recycling the middle overlap profile back to the column and then ~70 sec of clean fraction of peak-2 was collected at the end of the profile. The cycle time was ~4.2 min. Approximately 1.1 g of racemate was

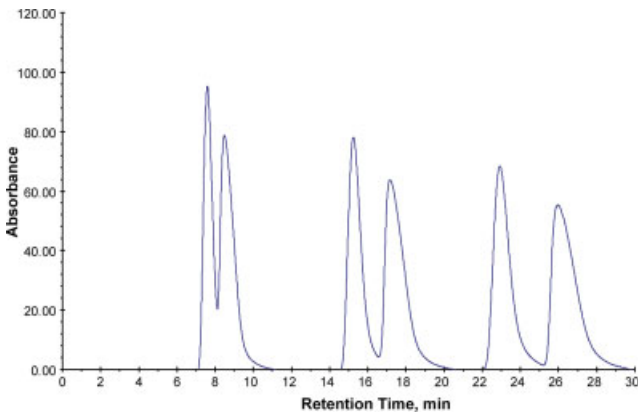

Fig. 5. SSR method development—three initial cycles. Experiment conducted at a flow rate: 400 ml/min, wavelength: 230 nm, mobile phase: 100% methanol. [Color figure can be viewed in the online issue, which is available at www.interscience.wiley.com.]

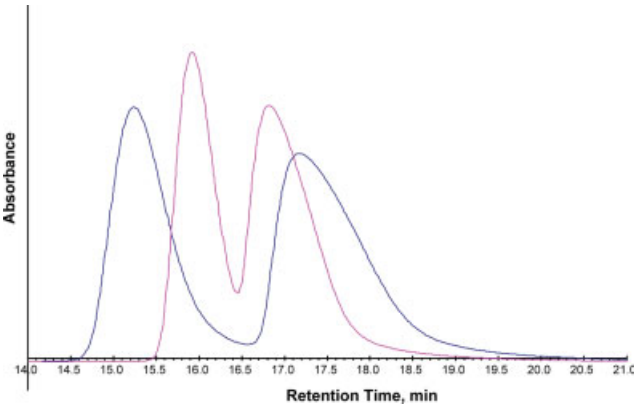

Fig. 6. SSR method development—overlay profile. Experiment conducted at a flow rate: 400 ml/min, wavelength: 230 nm, mobile phase: 100% methanol. [Color figure can be viewed in the online issue, which is available at www.interscience.wiley.com.]

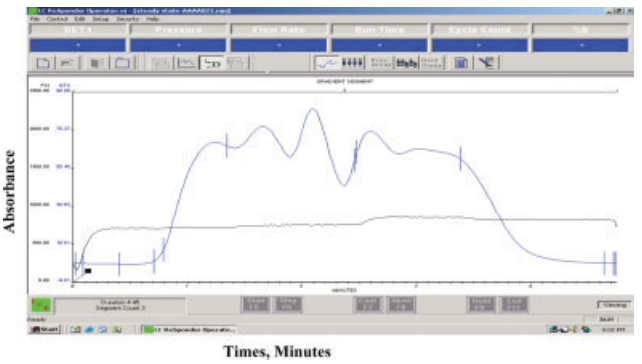

Fig. 7. SSR steady state profile. Experiment conducted at a flow rate: 400 ml/min, wavelength: 230 nm, mobile phase: 100% methanol. [Color figure can be viewed in the online issue, which is available at www.interscience.wiley.com.]

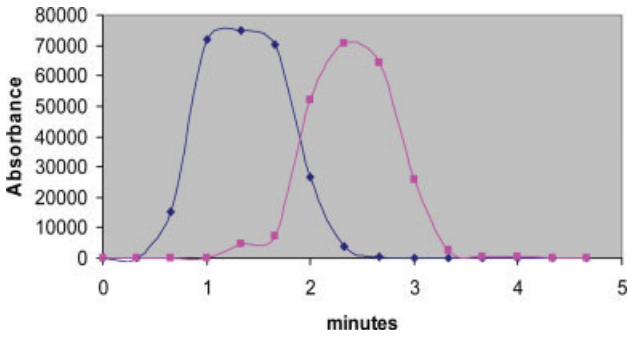

Fig. 8. SSR internal profile. Analysis conducted on ChiralPAK-AD column (250 mm × 4.6 mm i.d.), detection at 230 nm. Mobile phase: 100% methanol, flow rate: 1 ml/min. [Color figure can be viewed in the online issue, which is available at www.interscience.wiley.com.]

loaded on the column at each cycle. The desired high purity was achieved on the both peak-1 and peak-2 at >98% ee. At the end of the separation, the fractions were collected across the profile every ~0.3 min to understand the distribution of the enantiomers within the steady-state profile. Each fraction was then analyzed by analytical HPLC. The results are shown in Figure 8. As shown in Figure 8, the fractions are collected for peak-1 and peak-2 are essentially pure, the peak-1 was collected before the enantiomer-2 appears and the concentration of enantiomer-2 having decreased nearly to zero at the end of cycle. Approximately 5000 cycles were performed for the separation of 5.9 kg of racemate. The total purification time for the 5.9-kg racemate was ~190 h. The solvent usage was ~800 l/kg racemate. A total of ~2708 g of the desired enantiomer was recovered, thus, the yield was estimated to be ~95.2%. This yield was defined as the desired enantiomer yield [(the amount of the desired enantiomer recovered after the purification/the amount of the desired enantiomer present in the original batch) × 100%]. The productivity of SSR process is estimated to be 358 g racemate per kilogram stationary phase per day (179 g product per kilogram stationary phase per day) using a racemate feed concentration of 25 mg/ml. The separation results from SSR purification in terms of productivity and solvent usage were compared with the batch and SMB processes. The purification results are listed in Table 4.

SMB Separation

The third batch of 5.5 kg of racemate was used for a GLP toxicity study. This batch was separated using SMB.

TABLE 4. Productivity, solvent usage, purity, and yield of SMB, SSR, and batch HPLC processes

	Productivity (g racemate/ kg CSP/day)	Solvent consumption (l/g racemate)	Purity (ee %)	Yield (desired enantiomer %)
SMB	500	0.55	~99	~91.7
SFC	362	0.76	~99	>95
SSR	358	0.80	~99	~95.2
Batch HPLC	110	2.10	99	~97.5

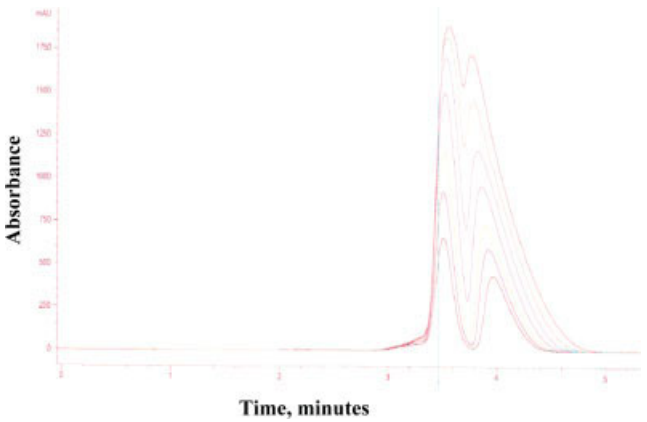

Fig. 9. Sample loading chromatograms of SMB process. Analysis conducted on ChiralPAK-AD column (250 mm × 4.6 mm i.d.), detection at 230 nm. Mobile phase: 100% methanol, flow rate: 1 ml/min. [Color figure can be viewed in the online issue, which is available at www.interscience.wiley.com.]

From the solubility study, a racemate concentration of 28 mg/ml was used as the feed solution. A loading study was carried out using this feed solution with an isocratic method used 100% methanol as mobile phase and ChiralPAK-AD as the CSP (column: 0.46 cm i.d. × 25 cm L, 20 μm; flow rate: 1.0 ml/min and temperature: 30°C). The results are shown in Figure 9. The data from the loading study were used for the estimation of isotherm parameters. The in-house software was used to determine SMB parameters (external flow rate and switch time). The calculated parameters for small-scale SMB unit include the various flow rates, switch time and the production rate, and solvent usage. These initial SMB parameters were used for the experimental runs. After the steady-state was reached, samples at the extract and raffinate streams were collected and analyzed on an analytical HPLC system. From these analytical results, the raffinate was at over 99% ee, whereas the extract stream was at ~90% ee. The optimization started by increasing the switch time to improve

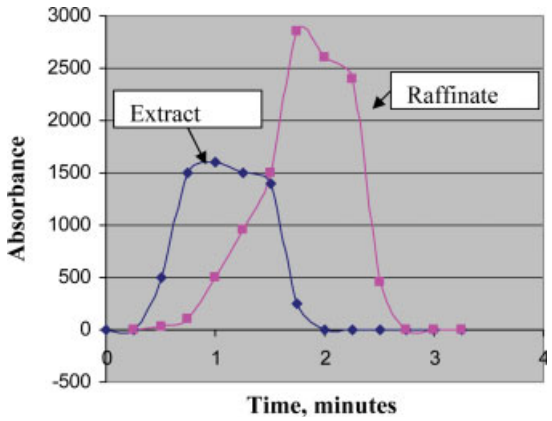

Fig. 10. Internal profile of SMB process. Analysis conducted on ChiralPAK-AD column (250 mm × 4.6 mm i.d.), detection at 230 nm. Mobile phase: 100% methanol, flow rate: 1 ml/min. [Color figure can be viewed in the online issue, which is available at www.interscience.wiley.com.]

the purity at extract stream. For the further optimization, in terms of operating pressure, an overall increase of the external flow rate was also carried out. The results of the optimization on the small SMB unit are listed in Table 5. It shows the optimized separation parameters experimentally determined after process development for a feed composition of 28 mg/ml racemate in 100% methanol. Productivity was estimated to be 505 g racemate per kilogram stationary phase per day (253 g product per kilogram stationary phase per day) using a racemate feed concentration of 28 mg/ml. This method scaled well to the larger pilot SMB system. Table 6 shows the optimized separation parameters experimentally determined after final scale-up and process development for a feed composition of 28 mg/ml racemate in 100% methanol. The productivity at this scale was 500 g racemate per kilogram stationary phase per day (250 g product per kilogram stationary phase per day) using a racemate feed concentration of 28 mg/ml. The solvent usage was estimated at ~550 l per kilogram of racemate. The recovered extract and raffinate were then analyzed and dried down by rotovaping. The purities of both extract and raffinate are in specification. Overall, about 5.5 kg of feed were processed. The product was determined to be over 2.5 kg. The yield of the desired enantiomer after the purification was ~91.7%. The yield loss was attributed to an early SMB system malfunction. The material generated during the malfunction was not reprocessed. During the last cycle of the production run, fractions were collected using an "on-line" loop, once at the beginning of a switch and once in the middle of it for a total of 16 fractions. From the analysis of such fractions the internal concentration profile was obtained. The profile is shown in Figure 10. This profile shows that the separation is running in stable conditions and is as highly loaded as possible.

The separation results of SMB were compared with the SSR and batch HPLC purifications. The results are also listed in Table 3. The productivity of the SMB process was the highest whereas the solvent usage was the lowest in Table 4. However, the SMB process required more material for the process development. The column packing and testing were also time consuming. A relatively low yield of SMB process was observed because the off specification material was not recovered from the process development. The SSR process significantly improved the productivity and solvent usage when compared it with the batch HPLC process. The process development time for SSR was less than a day. However, the separation efficiency of SSR process was lower than the efficiency of SMB process. The efficiency of the separation processes can be arranged in this order: SMB > SFC > SSR > Batch HPLC.

TABLE 5. Optimized separation parameters for process development SMB unit

SMB parameters	Description	Value
Number and size of columns	To the SMB valve module	6; 10 mm × 100 mm
Column configuration	Column in each zone	1–2–2–1
Cycle time	Time for one complete cycle	5.5 min
Feed flow	Flow rate of feed	0.5 ml/min
Mobile phase flow	Flow rate of eluent	17.5 ml/min
Raffinate flow	Flow rate of raffinate	9 ml/min
Recycle flow	Flow rate of recycle	2.5 ml/min
Extract flow	Flow rate of extract	9 ml/min

TABLE 6. Optimized separation parameters for scale-up SMB unit

SMB parameters	Description	Value
Number and size of columns	To the SMB valve module	6; 50 mm × 100 mm
Column configuration	Column in each zone	1–2–2–1
Cycle time	Time for one complete cycle	10 min
Feed flow	Flow rate of feed	0.6 l/h
Mobile phase flow	Flow rate of eluent	14.2 l/h
Raffinate flow	Flow rate of raffinate	9.1 l/h
Recycle flow	Flow rate of recycle	1.5 l/h
Extract flow	Flow rate of extract	4.2 l/h

CONCLUSIONS

Batch HPLC, SFC, SSR, and SMB chromatography were utilized for the chromatographic resolution of 12.2 kg of racemate. SMB, SSR, and SFC are more efficient processes and use much less solvent than batch HPLC. Higher productivities and lower solvent usage were observed with SMB relative to the SFC, SSR, and batch HPLC chromatography. The SFC improved the separation efficiency when compared with batch HPLC. The productivity and solvent consumption of SFC separation was also related to the amount of co-solvent usage. At 10% co-solvent, the solvent usage of SFC was reduced to half amount compared with that of 20% co-solvent. However, the productivity was also reduced due to the longer cycle time.

ACKNOWLEDGMENTS

The authors thank Victor Rivera from LC support for his assistance and George Moniz and Jeff Adams for supplying the multiple batches of the racemates.

LITERATURE CITED

1. Miller L, Grill CM, Yan TQ, Dapremont O, Huthmann E, Juza M. Batch and simulated moving bed chromatographic resolution of a pharmaceutical racemate. J Chromatogr A 2003;1006:267.
2. Terfloth GJ. Enantioseparations in super- and subcritical fluid chromatography. J. Chromatogr A 2001;906:301.
3. Zhao Y, Pritts WA. Chiral separation of selected proline derivatives using a polysaccharide type stationary phase by high-performance liquid chromatography. J Chromatogr A 2007;1156:228.
4. Yan TQ, Orihuela C. Rapid and high throughput separation technologies—Steady state recycling and supercritical fluid chromatography

for chiral resolution of pharmaceutical intermediates. J Chromatogr A 2007;1156:220.

5. Schramm H, Kaspereit M, Kienle A, Seidel-Mogenstern A. Improved operation of simulated moving bed processes through cyclic modulation of feed flow and feed concentration. Chem Eng Sci 2003;58:5217.
6. Francotte E, Leutert T, La Vecchia L, Ossola F, Richert P, Schmidt A. Preparative resolution of the enantiomers of *tert*-leucine derivatives by simulated moving bed chromatography. Chirality 2002;14:313.
7. Zhang Z, Mazzotti M, Morbidelli M. Power feed operation of simulated moving bed units: changing flow-rates during the switching interval. J Chromatogr A 2003;1006:87.
8. Strube J, Jupke A, Epping A, Schmidt-Traub H, Sculte M, Devant R. Design, optimization, and operation of SMB chromatography in the production of enantiomerically pure pharmaceuticals. Chirality 1999;11:440.
9. Grill CM. Closed-loop recycling with periodic intra-profile injection: a new binary preparative chromatographic technique. J Chromatogr A 1998;796:101.
10. Grill CM, Miller L. Separation of a racemic pharmaceutical intermediate using closed-loop steady state recycling. J Chromatogr A 1998;827:359.
11. Kennedy JH, Bevo MD, Sharp VS, Williams JD. Comparison of separation efficiency of early phase active pharmaceutical intermediates by steady state recycle and batch chromatographic techniques. J Chromatogr A 2004;1026:101.
12. Grill CM, Miller L, Yan TQ. Resolution of a racemic pharmaceutical intermediate: a comparison of preparative HPLC, steady state recycling, and simulated moving bed. J Chromatogr A 2004;1046:55.
13. Villeneuve MS, Anderegg RJ. Analytical supercritical fluid chromatography using fully automated column and modifier selection valves for the rapid development of chiral separations. J Chromatogr A 1998;826:217.
14. Karanam BV, Welch CJ, Reddy VG, Chllenski J, Biba M, Vincert S. Species differential stereoselective oxidation of a methylsulfide metabolite of Mk-0767, a peroxisome proliferator-activated receptor dual agonist. Drug Metab Dispos 2004;22:1061.
15. Liu Y, Berthod A, Mitchell CR, Xiao TL, Zhang B, Armstrong DW. Super/subcritical fluid chromatography chiral separations with macrocyclic glycopeptide stationary phases. J Chromatogr A 2002;978:185.
16. Jusforgues P. Instrument design and separation in large scale industrial supercritical fluid chromatography. J High Res Chromatogr 1995;4:153.
17. Blehaut J, Nicoud RM. Recent aspects in simulated moving bed. Analusis 1998;26:M60.
18. Johannsen M, Peper S, Depta A. Simulated moving bed chromatography with supercritical fluids for the resolution of bi-naphthol enantiomers and phytol isomers. J Biochem Biophys Methods 2002;54:85.
19. Zhang Y, McConnell O. Simulated moving columns technique for chiral liquid chromatography. J Chromatogr A 2004;1028:227.
20. Zhang Y, Dai J, Wang-Iverson DB, Tymiak AA. Simulated moving columns technique for enantioselective supercritical fluid chromatography. Chirality 2007;9:683.
21. Welch CJ, Biba M, Gouker JR, Kath G, Augustine P, Hosek P. Solving multicomponent chiral separation challenges using a new SFC tandem column screening tool. Chirality 2007;3:184.

CHIRALITY 20:147–150 (2008)

Enantioseparation of 2-aryl-1,3-dicarbonyl analogues by High Performance Liquid Chromatography Using Polysaccharide Type Chiral Stationary Phase

ZHE XU,[1,2] ZUODING DING,[1] XU XU,[1]* AND XIAOAN XIE[3]

[1]*Shanghai Institute of Organic Chemistry, Chinese Academy of Sciences, Shanghai 200032, China*
[2]*Graduate University of Chinese Academy of Sciences, Beijing 100039, China*
[3]*Department of Chemistry, Fudan University, Shanghai 200433, China*

ABSTRACT The HPLC chiral separation of 21 kinds of 2-aryl-1,3-dicarbonyl analogues was investigated in normal phase mode with amylose tris(3,5-dimethylphenylcarbamate), amylose tris((*S*)-1-phenylethylcarbamate), cellulose tris(3,5-dimethylphenylcarbamate), and cellulose tris(4-methylbenzoate) chiral stationary phases, respectively. The whole set of 2-aryl-1,3-dicarbonyl analogues shows better enantioselectivity and enantioseparation on amylose tris(3,5-dimethylphenyl carbamate) (Chiralpak AD-H). The temperature dependence of enantioselectivity was studied to improve the enantioseparation. In addition, efforts are made to relate analyte structure with the quality of the achieved chiral separation. *Chirality 20:147–150, 2008.*

KEY WORDS: enantiomer separation; 2-aryl-1,3-dicarbonyl analogues; polysaccharide chiral stationary phases

INTRODUCTION

Liquid chromatographic separation of the enantiomers using chiral stationary phases (CSPs) has had a great impact on the pharmaceutical industry as well as such fields as asymmetric synthesis and biochemistry. At present there are many chiral stationary phase (CSP) high-performance liquid chromatography (HPLC) columns available that can directly separate enantiomers.[1-3] Among these CSPs, polysaccharide derivative CSPs have shown excellent enantiomeric recognition because of their versatility, durability, and in particular, loadability.[1,4] These materials are very useful both for analytical[5] and preparative[6] purpose. Polysaccharide-type CSPs not only effectively recognize enantiomers of a wide variety of chiral analytes but also may be used in combination with various mobile phases such as normal-phase alcohol-hydrocarbon mixtures,[7] reversed-phase buffered and unbuffered aqueous-organic mobile phase[8] and pure polar organic solvents.[9] As a result, a number of CSPs based upon cellulose and amylose have been developed and are well known as the commercially available Chiralcel OD, Chiralcel OJ, Chiralpak AD and Chiralpak AS columns, etc.

1,3-dicarbonyl structures can be used as building blocks for the preparation of natural and modified (unnatural) biologically active compounds.[10] In consequence of the wide-ranging utility of these compounds, much attention has been paid to their enantioselective synthesis,[11-13] which requires analytical methods to control the chiral purity of the final products.

This article describes the HPLC separation of a series of 2-aryl-1,3-dicarbonyl analogues on different chiral stationary phases of polysaccharide-based: cellulose (Chiralcel OD and OJ) and amylose (Chiralpak AD-H and AS). Separation of the enantiomers of some 2-aryl-1,3-dicarbonyl analogues was investigated further on Chiralpak AD-H column. It turned out that Chiralpak AD-H was the most suitable for resolving the enantiomers of 2-aryl-1,3-dicarbonyl analogues. In this work, the contributions of various functional groups of the chiral analytes to binding affinity and chiral recognition of the enantiomers of selected chiral 2-aryl-1,3-dicarbonyl analogues were studied.

EXPERIMENTAL

Equipment

HPLC system consisted of a Waters 515 pump, a 2487 dual λ absorbance detector (Milford, MA) and a Rheodyne Model 7725i injector (Cotati, CA). Chromatograms acquisition and processing was performed by Junrui SrAdv software package (China). Generally, the analyses were carried out at 15°C, with UV detection at 230 nm. Flow rate of a mobile phase was 0.5 or 1.0 ml min^{-1}. Any other conditions are indicated. The column temperature was regulated and controlled by a HCT-360 HPLC column thermostat (Quandao, Shanghai, China).The dead-time (t_0) of the column was determined by injecting 5 μl of a 1.0 mg ml^{-1} solution of Tri-*tert*-butylbenzene (Acros, Geel, Belgium). The following HPLC columns (Daicel Chemical Industries,

*Correspondence to: X. Xu, Shanghai Institute of Organic Chemistry, Chinese Academy of Sciences, Shanghai 200032, China.
E-mail: xuxu@mail.sioc.ac.cn
Received for publication 12 April 2007; Accepted 23 October 2007
DOI: 10.1002/chir.20513
Published online 11 December 2007 in Wiley InterScience (www.interscience.wiley.com).

Tokyo, Japan) were used: Chiralpak AD-H [amylose tris(3,5-dimethylphenylcarbamate), 150 mm × 4.6 mm I.D., 5 μm], Chiralpak AS [amylose tris((*S*)-1-phenylethylcarbamate), 250 mm × 4.6 mm I.D., 10 μm], Chiralcel OD [cellulose tris(3,5-dimethylphenylcarbamate), 250 mm × 4.6 mm I.D., 10 μm], Chiralcel OJ [cellulose tris(4-methylbenzoate), 250 mm × 4.6 mm I.D., 10 μm].

Chemicals and Reagents

Analytical-grade *n*-hexane (hex), 2-propanol (IPA) and ethanol (EtOH) were made in China.

Compounds **1**-**21** were synthesized in our laboratory. The structures of the compounds studied are presented in Figure 1. The sample solutions of the investigated analytes (0.1–1.0 mg ml^{-1}) were prepared in mobile phase and injected after filtration on a 0.45 μm Millipore filter.

RESULTS AND DISCUSSTION

Chiral Separation with Various CSPs

A series of 21 2-aryl-1,3-dicarbonyl analogues were chromatographed on four polysaccharide CSPs, using a *n*-hexane-alcohol mobile phase. Each analogue has a chiral center at the α-position of the aromatic ring. To simplify the presentation, only the chromatographic results that gave the best resolution on different columns are presented in the tables. The results relating to the separation of 2-aryl-1,3-dicarbonyl enantiomers on polysaccharide-based columns were to be seen in Table 1.

Of 21 chiral analytes investigated in this study, baseline enantioseparations were observed for 16 compounds and only one was not resolved at all. Representative chromatograms of some analytes were demonstrated in Figure 2. Many compounds could be separated on more than one CSP (e.g. compound **13** racemate was separated on the Chiralpak AD-H (Table 1) and on the Chiralcel OJ (Fig. 2)). However, it could be found that Chiralpak AD-H is a effective column resolving a wide range of 2-aryl-1,3-dicarbonyl racemates. About 75% of all analytes presented in Figure 1 were separated on this column.

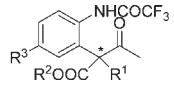

1 R^1 = Me, R^2 = Et, R^3 = Me
2 R^1 = Me, R^2 = Et, R^3 = COMe
3 R^1 = Et, R^2 = $C(CH_3)_2Bn$, R^3 = H
4 R^1 = Me, R^2 = Et, R^3 = COOMe
5 R^1 = Me, R^2 = Et, R^3 = H
6 R^1 = Me, R^2 = $C(CH_3)_2Bn$, R^3 = H
7 R^1 = Me, R^2 = cyclohexyl, R^3 = H
8 R^1 = Et, R^2 = $C(CH_3)_2Bn$, R^3 = COMe
9 R^1 = Me, R^2 = $C(CH_3)_2Bn$, R^3 = COOMe
10 R^1 = Me, R^2 = Bn, R^3 = H
11 R^1 = Et, R^2 = Et, R^3 = H
12 R^1 = Et, R^2 = Bu^i, R^3 = H
13 R^1 = allyl, R^2 = Et, R^3 = H
14 R^1 = Et, R^2 = $C(CH_3)_2Bn$, R^3 = COOMe
15 R^1 = allyl, R^2 = $C(CH_3)_2Bn$, R^3 = H
16 R^1 = Bu^n, R^2 = Et, R^3 = H
17 R^1 = Me, R^2 = Pr^i, R^3 = H
18 R^1 = allyl, R^2 = Bu^t, R^3 = H
19 R^1 = Me, R^2 = Ph, R^3 = H

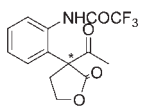

20

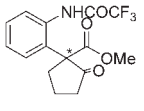

21

Fig. 1. Structures of chiral 2-aryl-1,3-dicarbonyl analogues. The chiral center is marked with an asterisk.

TABLE 1. Enantioseparation of 2-aryl-1,3-dicarbonyl analogues on polysaccharide-based columns in normal-phase mode

Compound	CSP	Eluent (v/v)	k'_1	α	R_S
1	AS	90/10[b,d]	1.391	1.245	2.212
2	AD-H	95/5[a,e]	0.985	1.295	3.261
3	OD	100/1[a,d]	3.520	1.391	2.001
4	AD-H	95/5[a,e]	2.506	1.188	2.769
5	AD-H	90/10[b,e]	0.782	1.205	2.358
6	AD-H	95/5[a,e]	1.116	1.176	1.553
7	AD-H	95/5[b,e]	0.809	1.361	3.697
8	AD-H	90/10[a,e]	1.132	1.157	1.436
9	AD-H	90/10[b,e]	0.884	1.114	1.160
10	AD-H	80/20[b,e]	1.097	2.016	5.738
11	AD-H	100/1[a,c]	1.754	1.290	1.768
12	AD-H	100/1[a,c]	1.755	1.035	1.288
13	AD-H	100/1[a,e]	5.519	1.187	1.606
14	AD-H	95/5[b,e]	0.959	1.321	1.499
15	AD-H	95/5[a,e]	1.640	1.248	3.432
16	OJ	90/10[a,d]	0.933	1.405	1.897
17	OJ	100/1[a,d]	3.418	1.591	2.014
18	OD	100/1[a,e]	2.979	1.216	1.024
19	OD	90/10[a,d]	0.917	1	NR
20	AD-H	95/5[a,e]	7.090	1.090	1.628
21	AD-H	95/5[b,e]	3.867	1.233	3.670

NR means no separations were obtained on four columns.
Chromatographic conditions: Mobile phase: [a]hex/IPA; [b]hex/EtOH; Flow-rate: [c]1.0 ml min^{-1}; [d]0.7 ml min^{-1}; [e]0.5 ml min^{-1}; Detection: 230 nm; 15°C.

The effect of mobile phase composition on the selectivity of the Chiralpak AD-H column of the enantiomers of **2**, **4**-**15,** and **20**-**21**, was investigated by decreasing the alcohol (IPA or EtOH) concentration from 20 to 1% by volume. An increase in the amount of alcoholic modifier in the mobile phase gave a decrease of *k*' values for all compounds.

It was apparent from early observations, that temperature was an important parameter to control in HPLC.[14-19] It is suggested that at least two different effects of temperature can affect chiral separation.[20] One is a kinetic effect that influences the viscosity and diffusion coefficient of the solute. Another is the thermodynamic effect that changes the separation factor. Mostly, a higher temperature leads to a decrease in retention factors, selectivity and resolution. In few cases, the enantioselectivity α of 4 compounds (compounds **5**, **8,** and **20**-**21**) increased when the column temperature rose.

Effect of the Analyte Structures

Particular attention was paid to the mechanism of chiral discrimination of 21 2-aryl-1,3-dicarbonyl enantiomers. One of the interesting effects observed was the influence of the substituents on the aryl ring (electron-withdrawing vs. electron-donating) on the enantioseparation characteristics. Comparing the different substituted analogues (compounds **1**, **2**, **4**, **5,** Table 2), compound **1**, with an aryl ring substituted by electron-donating group (R^3 = –Me), was not baseline separated on Chiralpak AD-H.

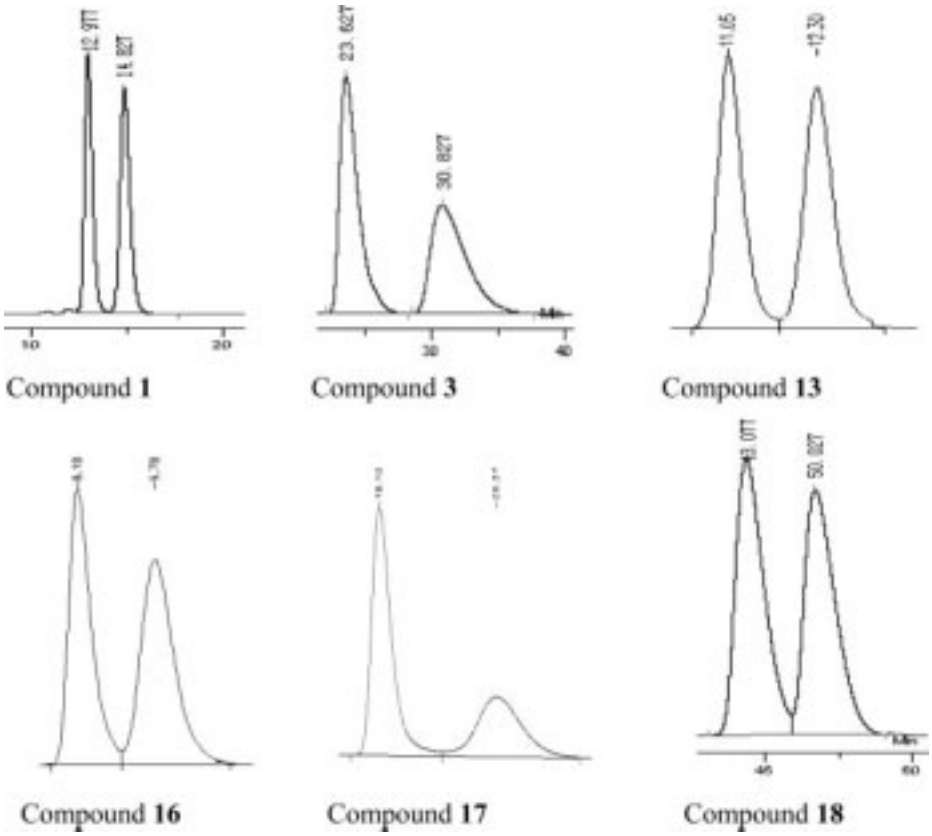

Fig. 2. Representative chromatograms of Compounds **1**, **3**, **10**, **13**, **16-18**. Chromatographic condition: Compound **1**: Chiralpak AS, hex/EtOH 90/10 (v/v), 0.7 ml min^{-1}; Compound **3**: Chiralcel OD, hex/IPA = 100/1 (v/v), 0.7 ml min^{-1}; Compound **13**: Chiralcel OJ, hex/EtOH = 95/5 (v/v), 0.7 ml min^{-1}; Compound **16**: Chiralcel OJ, hex/IPA = 90/10 (v/v), 0.7 ml min^{-1}; Compound **17**: Chiralcel OJ, hex/IPA = 100/1 (v/v), 0.7 ml min^{-1}; Compound **18**: Chiralcel OD, hex/IPA = 100/1 (v/v), 0.5 ml min^{-1}.

Replacement of the methyl group with electron-deficient group (R^3 = —COMe and —COOMe for compounds **2** and **4**, respectively) led to larger selectivity factor (α-value of 1.37 and 1.20, respectively) (Table 2). Compound **5** (R^3 = H) showed an α-value of 1.07 with a baseline separation. It seemed that, when the substituents on the aryl ring were more electron deficient, the column produced increased separation efficiency (Table 2). We presume that this is a result of a hydrogen bonding and/or π–π interaction between analytes and amylose-type CSP.

Compounds **5-7**, **10** and **19** have different esteratic site adjacent to chiral center. Compound **19**, with a —COOPh substituent, cannot achieve resolution on four polysaccharide CSPs. This might be due to its larger steric hindrance produced by phenyl group in its interaction with the CSP. While the sterically less hindered R^2 group in compounds **5-7**, leads to a baseline separation. On the other hand, alkyl group adjacent to chiral carbon has an effect to some extent on the separation factor (α) and resolution (R_S). The methyl substituted compound **5** was separated with the largest R_S-value (3.058) on Chiralpak AD-H, whereas the *n*-butyl derivative compound **16** was not separated and the ethyl derivative compound **11** displayed a smaller R_S-value of 1.768.

TABLE 2. Effect of substituent on the aryl ring on enantioselectivity on Chiralpak AD-H

Comp.	k'_1	α	R_S	Comp.	k'_1	α	R_S
1	4.17	1.06	1.045	**4**	2.50	1.20	2.833
2	1.61	1.37	4.389	**5**	1.67	1.07	2.833

Mobile Phase: hex/IPA (95/5) with a flow-rate of 0.5 ml min^{-1}; UV detection: 230 nm; Injection volume: 5 μl; 10°C.

CONCLUSIONS

In the present study 21 variously substituted chiral 2-aryl-1,3-dicarbonyl analogues were separated by direct enantioselective HPLC employing four different polysaccharide columns. In all but one (compound **19**) full or partial separation of enantimers was achieved with at least one of the four polysaccharide CSPs. The influences of the mobile phase composition and column temperature on the resolution on the Chiralpak AD-H column were studied.

LITERATURE CITED

1. Ghanem A, Hoenen H, Aboul-Enein HY. Application and comparison of immobilized and coated amylose tris-(3,5-dimethylphenylcarbamate) chiral stationary phases for the enantioselective separation of β-blockers enantiomers by liquid chromatography. Talanta 2006;68:606–609.

2. Maier NM, Franco P, Lindner W. Separation of enantiomers: needs challenges, perspectives. J Chromatogr A 2001;906:3–33.
3. Subrananian G. A practical approach to chiral separations by liquid chromatography. Weinheim: Wiley-VCH; 1994.
4. Yashima E. Polysaccaride-based chiral stationary phases for high-performance liquid chromatographic enantioseparation. J Chromatogr A 2001;906:105–125.
5. Okamoto Y, Yashima E. Polysaccharide derivatives for chromatographic separation of enantiomers. Angew Chem Int Ed 1998;37:1020–1043.
6. Schulte M, Strube J. Preparative enantioseparation by simulated moving bed chromatography. J Chromatogr A 2001;906:399–416.
7. Toribio L, del Nozal MJ, Bernal JL, Alonso C, Jimenez JJ. Comparative study of the enantioselective separation of several antiulcer drugs by high-performance liquid chromatography and supercritical fluid chromatography. J Chromatogr A 2005;1091:118–123.
8. Tachibana K, Ohnishi A. Reversed-phase liquid chromatographic separation of enantiomers on polysaccharide type chiral stationary phases. J Chromatogr A 2001;906:127–154.
9. Chankvetadze B, Kartozia I, Yamamoto C, Okamoto Y. Comparative enantioseparation of selected chiral drugs on four different polysaccharide-type chiral stationary phases using polar organic mobile phases. J Pharm Biomed Anal 2002;27:467–478.
10. Blanc-Delmas E, Lebegue N, Wallez V, Leclerc V, Yous S, Carato P, Farce A, Bennejean C, Renard P, Caignard DH, Audinot-Bouchez V, Chomarat P, Boutin J, Hennuyer N, Louche K, Carmona MC, Staels B, Pénicaud L, Casteilla L, Lonchampt M, Dacquet C, Chavatte P, Berthelot P, Lesieur D. Novel 1,3-dicarbonyl compounds having 2(3H)-benzazolonic heterocycles as PPARr agonists. Bioorg Med Chem 2006;14:7377–7391.
11. Bartoli G, Bosco M, Carlone A, Cavalli A, Locatelli M, Mazzanti A, Ricci P, Sambri L, Melchiorre P. Organocatalytic asymmetric conjugate addition of 1,3-dicarbonyl compounds to maleimides. Angew Chem Int Ed 2006;45:4966–4970.
12. Xie X, Cai G, Ma D. CuI/L-proline-catalyzed coupling reactions of aryl halides with activated methylene compounds. Org Lett 2005;7:4693–4695.
13. Frantz R, Hintermann L, Perseghini M, Broggini D, Togni A. Titanium-catalyzed stereoselective geminal heterodihalogenation of β-ketoesters. Org Lett 2003;5:1709–1712.
14. Berthod A, He BL, Beesley TE. Temperature and enantioseparation by macrocyclic glycopeptide chiral stationary phases. J Chromatogr A 2004;1060:205–214.
15. Peyrin E, Guillaume YC, Guinchard C. Interactions between dansyl amino acids and human serum albumin using high-performance liquid chromatography: mobile-phase pH and temperature considerations. Anal Chem 1997;69:4979–4984.
16. Morin N, Guillaume YC, Peyrin E, Rouland JC. Retention mechanism study of imidazole derivatives on a beta-cyclodextrin-bonded stationary phase. Thermal analysis contributions. Anal Chem 1998;70:2819–2826.
17. Ravelet C, Michaud M, Ravel A, Grosset C, Villet A, Peyrin E. Streptavidin chiral stationary phase for the separation of adenosine enantiomers. J Chromatogr A 2004;1036:155–160.
18. Peter A, Torok G, Armstrong DW, Toth G, Tourwe D. Effect of temperature on retention of enantiomers of beta-methyl amino acids on a teicoplanin chiral stationary phase. J Chromatogr A 1998;828:177–190.
19. Berkecz R, Ilisz I, Forro E, Fulop F, Armstrong DW, Peter A. LC enantioseparation of aryl-substituted-lactams using variable-temperature conditions. Chromatographia 2006;63(Suppl):S29–S35.
20. Ma L, Luo H, Dai J, Carr PW. Development of acid stable, hypercrosslinked, silica-based reversed-phase liquid chromatography supports for the separation of organic bases. J Chromatogr A 2006;1114:21–28.

CHIRALITY 20:151–158 (2008)

Synthesis and Characterization of Novel Chiral Ionic Liquids and Investigation of their Enantiomeric Recognition Properties

DAVID K. BWAMBOK,[1] HADI M. MARWANI,[1] VIVIAN E. FERNAND,[1] SAYO O. FAKAYODE,[2] MARK LOWRY,[1] IOAN NEGULESCU,[1] ROBERT M. STRONGIN,[3] AND ISIAH M. WARNER[1]*

[1]*Department of Chemistry, Louisiana State University, Baton Rouge, Louisiana*
[2]*Department of Chemistry, Winston-Salem State University, Winston-Salem, North Carolina*
[3]*Department of Chemistry, Portland State University, Portland, Oregon*

ABSTRACT We report the synthesis and characterization of amino acid ester based chiral ionic liquids, derived from L- and D-alanine *tert* butyl ester chloride. The synthesis was accomplished via an anion metathesis reaction between commercially available L- and D-alanine *tert* butyl ester chloride using a variety of counterions such as lithium bis (trifluoromethane) sulfonimide, silver nitrate, silver lactate, and silver tetrafluoroborate. Both enantiomeric forms were obtained as confirmed by bands of opposite sign in the circular dichroism spectra. The L- and D-alanine *tert* butyl ester bis (trifluoromethane) sulfonimide were obtained as liquids at room temperature and intriguingly exhibited the highest thermal stability (up to 263°C). In addition, the ionic liquids demonstrated enantiomeric recognition ability as evidenced by splitting of racemic Mosher's sodium salt signal using a liquid state ^{19}F nuclear magnetic resonance (NMR) and fluorescence spectroscopy. The L- and D-alanine *tert* butyl ester chloride resulted in solid salts with nitrate, lactate, and tetrafluoroborate anions. This illustrates the previously observed tunability of ionic liquid synthesis, resulting in ionic liquids of varying properties as a function of varying the anion. *Chirality 20:151–158, 2008.*

KEY WORDS: chiral ionic liquids; chiral selectors; synthesis; chiral recognition

INTRODUCTION

Ionic liquids (ILs), commonly termed room temperature ionic liquids (RTILs), are a class of organic salts. These molecules typically contain an organic cation with delocalized charge and a bulky inorganic anion. Interest in RTILs continues to grow because of their potential as greener solvent alternatives to conventional environmentally damaging organic solvents.[1] In addition, ILs have unique properties such as lack of measurable vapor pressure, high thermal stability, and recyclability.[1–5] Such environmental-friendly properties make ILs relatively benign solvents for cleaner processes to minimize toxic chemical wastes which have become a priority for chemical industries.[6] Room temperature ILs have been used in various applications such as replacing conventional organic solvents in organic synthesis,[7] solvent extractions,[8] electrochemical reactions,[9,10] liquid–liquid extractions,[11] and in enzymatic reactions.[12] In addition, analytical applications of ILs such as their use as buffers in capillary electrophoresis,[13] as stationary phases in gas chromatography[14,15] as well as high performance liquid chromatography,[16] and enhancement of sensitivity in thermal lens measurement have also been investigated.[17] A review of several analytical applications of ILs has been reported by Baker et al.[18] In addition, Baker et al. have developed an optical sensor based on an ionic liquid.[19]

Analysis of chiral molecules is very important since different enantiomers of a chiral racemic drug may display different properties.[20] For example, one enantiomer of a chiral drug may have the desired medicinal properties, while the other enantiomer may be harmful. Various chiral selectors, such as cyclodextrins, molecular micelles, antibody, and crown ethers have been widely used because of their chiral recognition abilities.[21–24] However, the use of many current chiral selectors is often limited because of low solubility, difficult organic syntheses, instability at high temperature, as well as high cost. In addition, many currently available chiral selectors require the use of another solvent and sometimes more than one solvent system if the analyte and the chiral selector are not soluble in the same solvent. Therefore, there is a need for the development of new chiral selectors that can be used simultaneously as solvent and chiral selector. Thus, the use of chiral ILs have gained popularity since they can be used as chiral solvents for asymmetric induction in synthesis.[25] Chiral ILs can also serve as chiral stationary phases in

Contract grant sponsors: National Science Foundation, Phillip West Endowment.
*Correspondence to: Isiah M. Warner, Department of Chemistry, 436 Choppin Hall, Louisiana State University, Baton Rouge, LA 70803, USA. E-mail: iwarner@lsu.edu
Received for publication 14 August 2007; Accepted 30 October 2007
DOI: 10.1002/chir.20517
Published online 11 December 2007 in Wiley InterScience (www.interscience.wiley.com).

chromatography as demonstrated by Ding and Armstrong in capillary electrophoresis.[26] Tran and coworkers have also recently used chiral ILs for determining the enantiomeric composition of pharmaceutical products.[27,28]

To our knowledge, the first chiral ionic liquid, 1-butyl-3-methyl imidazolium lactate was reported by Seddon and his coworkers in 1999.[29] This chiral ionic liquid, with a chiral anion, was prepared via anion metathesis using 1-butyl-3-methyl imidazolium chloride and sodium (*S*)-2-hydroxypropionate. This ionic liquid also afforded good endo/exo selectivity in a Diels-Alder reaction. Recently, ILs with chiral carboxylates have been synthesized by Allen et al.[30] This synthesis was achieved in water by reacting tetrabutylammonium hydroxide with the corresponding amino acids or chiral carboxylic acids. In 2002, Wasserscheid et al. synthesized chiral ILs from chiral starting materials affording many different chiral ILs in good yields.[31] A novel imidazolium based chiral ionic liquid with planar chirality was synthesized by Saigo and coworkers in 2002.[32] However, this ionic liquid could only be obtained as a racemic mixture and required further separation of the enantiomers before investigating its applications. Other chiral ILs based on imidazolium,[33,34] ephedrinium,[35] and pyridinium[36] cations have been synthesized.[33–36] However, chiral precursors for ILs are often used in a multistep synthesis. A detailed review of chiral ionic liquid synthesis has been reported.[37] Tao et al. have also successfully prepared chiral ILs from amino acids and their corresponding methyl and ethyl esters.[38] These chiral ILs from amino acid esters had low melting points compared with those derived from amino acids. Other interesting amino acid derived chiral ILs have also been synthesized recently.[39–41] Ding et al. have successfully synthesized chiral ILs via a simple anion exchange between a commercially available halide salt with *N*-lithiotrifluoromethanesulfonimide.[42] This approach provides an attractive one step synthesis with a chiral precursor, while allowing the product to be easily purified by washing with water. The same approach was employed by Tran and Oliveira to prepare chiral ILs.[27] The variety and applications of these ILs suggest that other chiral ILs need to be explored in order to obtain ILs for different applications.

Natural materials are often used as precursors for preparing chiral ILs in multiple step synthesis. As an example, the use of amino acids for preparation of imidazolium cations is clear evidence of such use.[33] Chiral induction in some reactions may be required to afford chiral ILs, mostly in one enantiomeric form. In addition, the few commercially available chiral ILs are often very expensive. The high cost, combined with the difficulty in chiral ionic liquid synthesis, has limited their extensive study and applications.

The primary objective of this study was to synthesize and characterize both enantiomeric forms of new chiral ILs from commercially available amino acid ester chlorides. The presence of a chiral center in the precursor further simplifies the synthesis, alleviating the need for asymmetric induction. In addition, esterification reduces hydrogen bonding of amino acids affording low melting point ILs.[38] By varying the anions, the synthesis of ILs can be tailored, resulting in ILs of different properties that may be used for various applications. In addition, this study reports an investigation of the enantiomeric recognition ability of a variety of chiral amino acid ester based ILs. The synthesis of chiral ILs was accomplished via a simple anion metathesis reaction and characterization was performed using nuclear magnetic resonance (NMR), thermal gravimetric analysis (TGA), differential scanning calorimetry (DSC), circular dichroism (CD), and elemental microanalysis. The relatively simple synthetic procedure and the presence of chiral centers in the precursors is a tremendous advantage for our approach. Finally, the chiral recognition ability of L- and D-alanine *tert*-butyl ester bis (trifluoromethane) sulfonimide ionic liquid was evaluated using ^{19}F NMR with a racemic Mosher's sodium salt substrate and fluorescence spectroscopy with some chiral fluorescent analytes.

EXPERIMENTAL PROCEDURES

Chemicals and Materials

L- and D-alanine *tert* butyl ester hydrochloride [L- and D-AlaC_4Cl)], bis(trifluoromethane) sulfonimide lithium salt ($LiNTf_2$), silver tetrafluoroborate ($AgBF_4$), silver lactate (AgLac), silver nitrate ($AgNO_3$), 2-methoxy-2-(trifluoromethyl) phenylacetic acid (Mosher's acid), and methanol (ACS certified) were purchased from Sigma Aldrich Chemicals (Milwaukee, WI). In addition, enantiomerically pure *R*- and *S*-enantiomers of warfarin, naproxen and 2,2,2-trifluoroanthrylethanol (TFAE) were purchased from Sigma Aldrich Chemicals (Milwaukee, WI). All chemicals were used as received.

General Instrumental Methods

The NMR spectra were recorded in d_6-DMSO on a Bruker-250 MHz instrument with tetramethyl silane (TMS) as an internal standard. Melting point (T_m) was determined by differential scanning calorimeter using a thermal analysis instrument TA SDT2960 at a scanning rate of 5°C min^{-1}. Thermal decomposition temperature (T_{dec}) of ILs was determined with a thermal analysis instrument 2950 TGA HR V6.1A (module TGA 1000°C). The heating rate for TGA was 5°C min^{-1} under nitrogen from 25 to 300°C. A Jasco-710 spectropolarimeter was used to obtain the CD spectra of our ILs. Steady-state fluorescence measurements were recorded at room temperature by use of a Spex Fluorolog-3 spectrofluorimeter (model FL3-22TAU3; Jobin Yvon, Edison, NJ) equipped with a 450-W xenon lamp and R928P photomultiplier tube (PMT) emission detector. Fluorescence emission spectra were collected in a 4-mm quartz fluorescence cuvet with slit widths set for entrance exit bandwidths of 4 nm on both excitation and emission monochromators for warfarin, 2 nm for TFAE, and 1.5 nm for naproxen, respectively. Fluorescence for warfarin, TFAE, and naproxen were respectively monitored at excitation wavelengths of 306, 365, and 280 nm. In addition, all fluorescence spectra were blank subtracted before data analysis.

^{19}F NMR Experiment

Racemic Mosher's sodium salt was prepared from Mosher's acid by reacting with an equivalent of sodium hydroxide in water and the salt was dried under vacuum before ^{19}F NMR measurement. The racemic Mosher's sodium salt (8.38 mg, 0.03 mmol) and 129.07 mg (0.3 mmol) of L- or D-$AlaC_4NTf_2$ were dissolved in 0.75 ml of d_6 DMSO. The mixture was shaken vigorously for 10 min on an orbital shaker before recording ^{19}F NMR spectra.

Synthesis of L- and D-Alanine tert *Butyl Ester Bis (trifluoromethane) Sulfonimide $AlaC_4NTf_2$*

0.5 g (2.75 mmol) of L- or D-alanine *tert* butyl ester chloride was dissolved in water. An equimolar amount (0.79 g, 2.75 mmol) of bis (trifluoromethane) sulfonimide lithium salt was dissolved separately in water. The two solutions were mixed and stirred for 2 h at room temperature. The mixture resulted in two layers, of which the lower layer was separated and dried under vacuum overnight. This resulted in 0.94 g (79% yield) of colorless ionic liquid. The decomposition temperature (T_{dec}) of this ionic liquid was found to be 263°C by use of TGA measurements. ^{1}H NMR (250 MHz, d_6 DMSO) δ (ppm) 8.19 (s, 3H), 3.97 (q, 1H), 1.45 (s, 9H), 1.36 (d, J = 7.0 Hz, 3H). ^{13}C NMR δ (ppm) 170.12, 83.66, 49.19, 28.32, 16.69. Anal. Calcd. for $C_9H_{16}N_2O_6S_2F_6$: C, 25.35; H, 3.78; N, 6.57. Found: C, 25.07; H, 3.98; N, 6.52.

Synthesis of L- and D-Alanine tert *Butyl Ester of Nitrate, Tetrafluoroborate, and Lactate*

Representative procedure: Synthesis of L-alanine tert butyl ester nitrate. 0.1 g (0.55 mmol) of L-AlaBuCl was dissolved in methanol. An equimolar amount of silver nitrate (0.0935 g, 0.55 mmol) was suspended separately in methanol. The two solutions were mixed and stirred, and the precipitate was then filtered. The product was evaporated *in vacuo* and purified by crystallizing in methanol/ether to obtain 0.08 g (77% yield) of the product L-$AlaC_4NO_3$ as white crystals (T_m, 104°C). This ionic liquid was thermally stable up to 130°C. ^{1}H NMR (250 MHz, d_6 DMSO) δ (ppm) 8.36 (s, 3H), 3.92 (q, 1H), 1.44 (s, 9H), 1.35 (d, J = 7.0 Hz, 3H). ^{13}C NMR δ (ppm) 170.05, 83.51, 49.18, 28.36. Anal Calcd. for $C_7H_{16}N_2O_5$: C, 40.38; H, 7.75; N, 13.45. Found: C, 44.97; H, 8.53; N, 9.03.

L-alanine *tert* butyl ester tetrafluoroborate. Yield: 80%. T_m, 93°C; T_{dec}, 125°C. ^{1}H NMR (250 MHz, d_6 DMSO) δ (ppm) 8.18 (s, 3H), 3.94 (q,1H) 1.45 (s,9H), 1.36 (d, J = 7Hz, 3H). ^{13}C NMR δ (ppm) 170.13, 83.68, 49.19, 28.38, 16.74. Anal. Calcd. for $C_7H_{16}NO_2BF_4$: C, 36.08; H, 6.92; N, 6.01. Found: C, 35.71; H, 7.31; N, 6.13.

L-alanine *tert* butyl ester lactate. Yield: 86%. T_m, 114°C; T_{dec}, 132°C. ^{1}H NMR (250 MHz, d_6 DMSO) δ (ppm) 5.53 (s, 3H), 3.79 (q, 1H), 3.62 (q, 1H), 1.40 (s, 9H), 1.25 (d, J = 7 Hz, 3H) 1.15 (d, J = 6.75, 3H). ^{13}C NMR δ (ppm) 209.50, 178.31, 173.10, 110.00, 81.97, 67.28, 49.91, 28.46, 21.87, 18.98. Anal Calcd. for $C_{10}H_{21}NO_5$: C, 51.05; H, 8.99; N, 5.95. Found: C, 50.85; H, 8.96; N, 5.96.

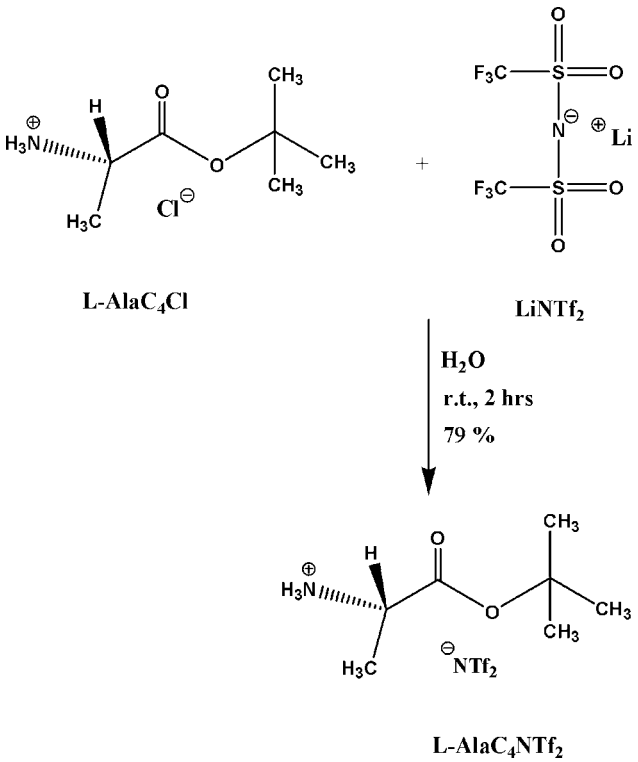

Scheme 1. Synthesis of L-$AlaC_4NTf_2$.

RESULTS AND DISCUSSION

Synthesis and Characterization of a New Amino Acid Ester Chiral Ionic Liquid (L- or D-$AlaC_4NTf_2$)

The synthesis of both enantiomeric forms of alanine *tert*-butyl ester bis (trifluoromethane) sulfonimide was accomplished via anion metathesis reaction of the corresponding amino acid ester chloride and bis (trifluoromethyl) sulfonylimide lithium salt (Scheme 1). The reaction proceeded well in water with good yield (79%) of L- or D-alanine *tert*-butyl ester bis (trifluoromethyl) sulfonylimide (L- or D-$AlaC_4NTf_2$). The ^{1}H NMR (Fig. 1) and ^{13}C NMR (see Fig. 2) of the ionic liquid was consistent with the chemical structure of $AlaC_4NTf_2$. The NMR spectra obtained for other ILs were very similar to that of $AlaC_4NTf_2$. The similarity in NMR spectra was expected since only the anions were varied. The alanine tert-butyl ester bis (trifluoromethyl) sulfonylimide ionic liquid was found to be a desirable liquid at room temperature and stable up to 263°C, as indicated by thermal gravimetric analysis (TGA) measurement (Fig. 3A).

The ionic liquid L-$AlaC_4NTf_2$ was also heated at 225°C for 2 h to verify and confirm whether decomposition occurs at a lower temperature. From Figure 3B, it seems that at this isothermal plateau (225°C), there is a constant rate loss of 0.42%/min for the span of 120 min. The constancy of the weight loss rate might be an indication that a physical phenomenon (e.g. evaporation), rather than a chemical decomposition process, is occurring. The rather low decomposition temperature for the BF_4 salt (125°C), is

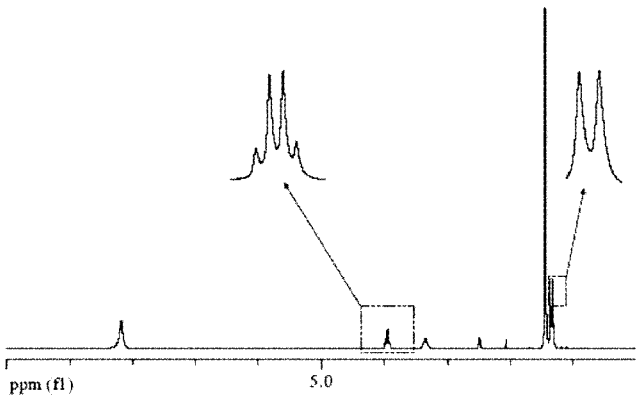

Fig. 1. Proton (^{1}H) NMR spectrum of L-AlaC_4NTf_2 in d_6 DMSO with tetramethyl silane (TMS) as an internal standard at room temperature.

still uncertain and may not be solely due to the cation instability upon moderate heating. This is because as much as the cation might not be very stable at moderate heating, the same cation had relatively higher stability (263°C) with the NTf_2 anion.

The high thermal stability of alanine *tert*-butyl ester bis (trifluoromethyl) sulfonylimide makes it a preferred chiral selector and chiral solvent for reactions at high temperature or as a coating in gas chromatography. It is indeed extremely important that the chiral center in the precursor be retained in the final ionic liquid product. According to Jodry and Mikami, some imidazolium based chiral ILs will sometimes undergo racemization after synthesis.[34] The possibility of racemization in the synthesized ILs was investigated by use of circular dichroism (CD) measurements of the ionic liquid products and their precursors. Examples of the CD bands obtained for both enantiomeric forms of the ILs are as shown in Figure 4. As expected, the CD bands of the precursors were in the same direction as those of the ionic liquid products, confirming retention of configuration. In addition, the opposite CD bands confirmed that the L-and D-configurations of the ILs had been retained (see Fig. 4).

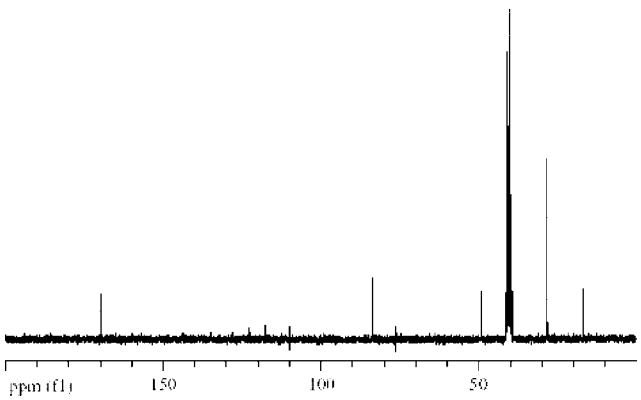

Fig. 2. Carbon-13 (^{13}C) NMR spectrum of L-AlaC_4NTf_2 in d_6 DMSO with tetramethyl silane (TMS) as an internal standard at room temperature.

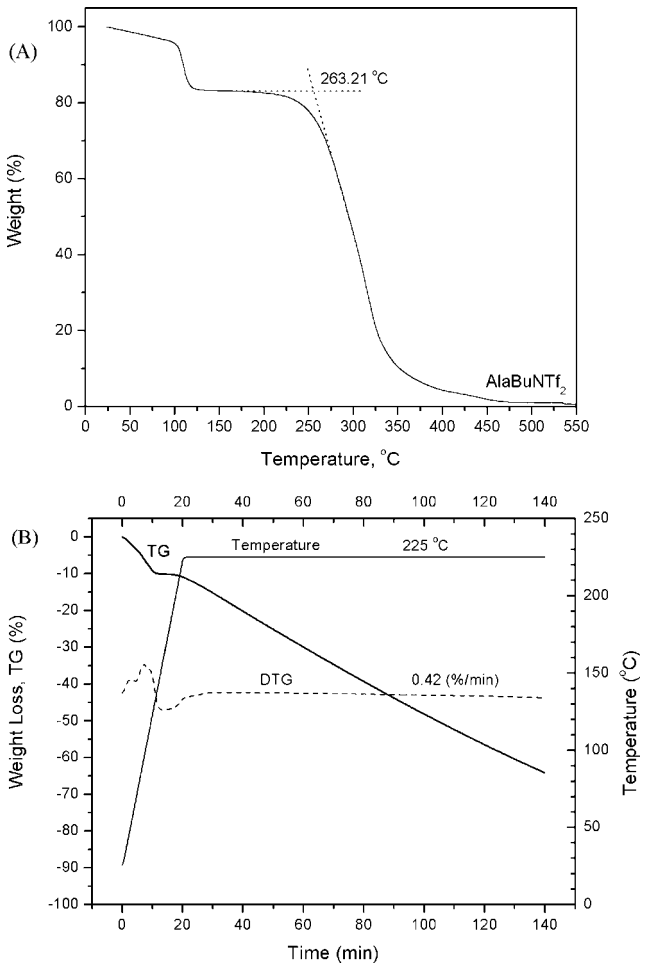

Fig. 3. Thermal gravimetric analysis of L-AlaC_4NTf_2 with a heating rate of 5°C min^{-1} under nitrogen (**A**) from 25 to 300°C, and (**B**) from 25 to 225°C, then isothermally at 225°C for 2 h.

Chiral Recognition Study of ILs Using ^{19}F NMR

As previously noted, L- and D-alanine *tert*-butyl ester bis (trifluoromethane) sulfonimide are liquids at room temperature. It was therefore interesting to investigate their ability to act both as solvent and chiral selector. The chiral recognition ability of L- and D-alanine *tert*-butyl ester bis (trifluoromethane) sulfonimide was investigated by use of ^{19}F NMR and racemic Mosher's sodium salt. In this experiment, various solvents such as methylene chloride, deuterium oxide, dimethyl sulfoxide (DMSO) as well as chloroform were examined. However, d_6-DMSO demonstrated good solubility as compared with other solvents investigated. The results of the ^{19}F NMR study for enantiomeric recognition ability of L- and D-alanine *tert*-butyl ester bis (trifluoromethane) sulfonimide are shown in Figure 5. The diastereomeric interactions lead to a shift in the ^{19}F NMR signal of the racemic Mosher's sodium salt. In addition, the ^{19}F NMR signal of the racemic substrate was split by both enantiomeric forms of the ionic liquid demonstrating their enantiomeric recognition (see Fig. 5). This confirms that this ionic liquid can be a suitable chiral selector

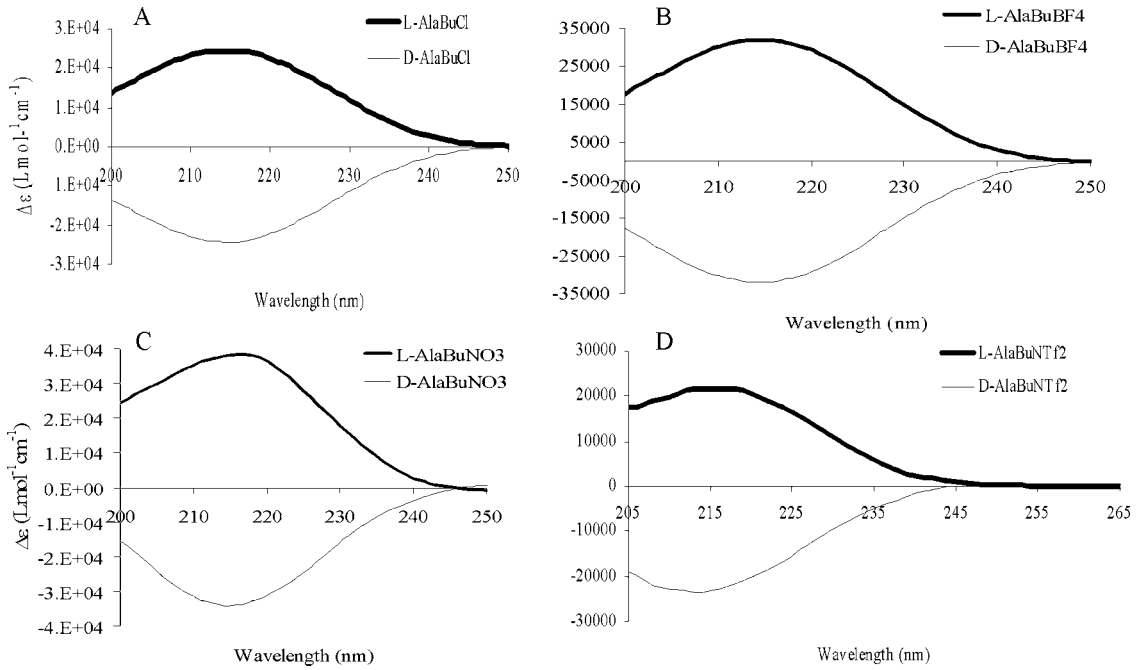

Fig. 4. Circular dichroism spectra of L- and D- (**A**) AlaBuCl, (**B**) AlaBuBF$_4$, (**C**) AlaBuNO$_3$, and (**D**) AlaBuNTf$_2$ at room temperature.

for various applications such as determination of enantiomeric composition of chiral molecules of pharmaceutical, biomedical, and environmental interest.

Chiral Recognition of ILs Using Fluorescence Spectroscopy

Steady-state fluorescence spectroscopy was further used to evaluate the chiral recognition ability and enantio-selectivity of the chiral ILs on 2,2,2-trifluoroanthrylethanol (TFAE), warfarin, and naproxen chiral analytes. The choice of these chiral analytes in this study was due to their fluorescence properties; furthermore, they are of environmental and pharmaceutical interest. For instance, warfarin is an anticoagulant drug used for the treatment of thromboembolic diseases and is also generally used as a pesticide, while naproxen is used as an anti-infammatory drug.

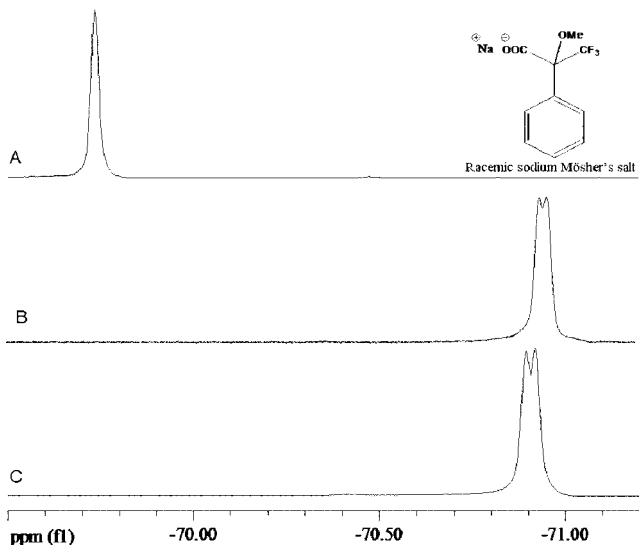

Fig. 5. ^{19}F NMR spectra of (**A**) racemic sodium Mösher's salt; and a mixture of the racemic sodium Mösher's salt with (**B**) D-AlaC$_4$NTf$_2$, and (**C**) L-AlaC$_4$NTf$_2$ at room temperature.

The emission spectra of the 10 μM *R*- and *S*-enantiomers of TFAE, warfarin, and naproxen analytes in the presence of L-AlaC$_4$NTf$_2$ chiral ILs are, respectively, shown in Figures 6A1, B1, and C1. The intensity of emission of the *R*-enantiomers obtained in the presence of ionic liquid solvent and chiral selector is noted to be higher than that of the *S*-enantiomers for all three analytes investigated. A difference in emission intensity of *R*- and *S*-enantiomers in the presence of chiral selectors is due to different diastereomeric interactions between the enantiomers and the IL chiral selectors. Such spectral shifts have been widely reported and associated with enantioselectivity of chiral selectors as a result of diastereomeric complexes.[43–45]

Finally, a mean-centered plot of emission spectra was used to gain better insight into the enantiomeric selectivity and chiral recognition ability of the chiral ILs. The mean centered plot of the emission spectra depicted in Figures 6A1, B1, and C1 are shown in Figure 6A2, B2, and C2, respectively. The spectra were obtained by subtracting the spectrum of *R*- and *S*-enantiomer in the presence of chiral selectors from the *R*- and *S*-mean spectra. It is of great importance to note that *R*- and *S*- enantiomers have opposite mean spectra, further demonstrating the chiral recognition ability and enantio-selectivity of the ionic liquid chiral selector.

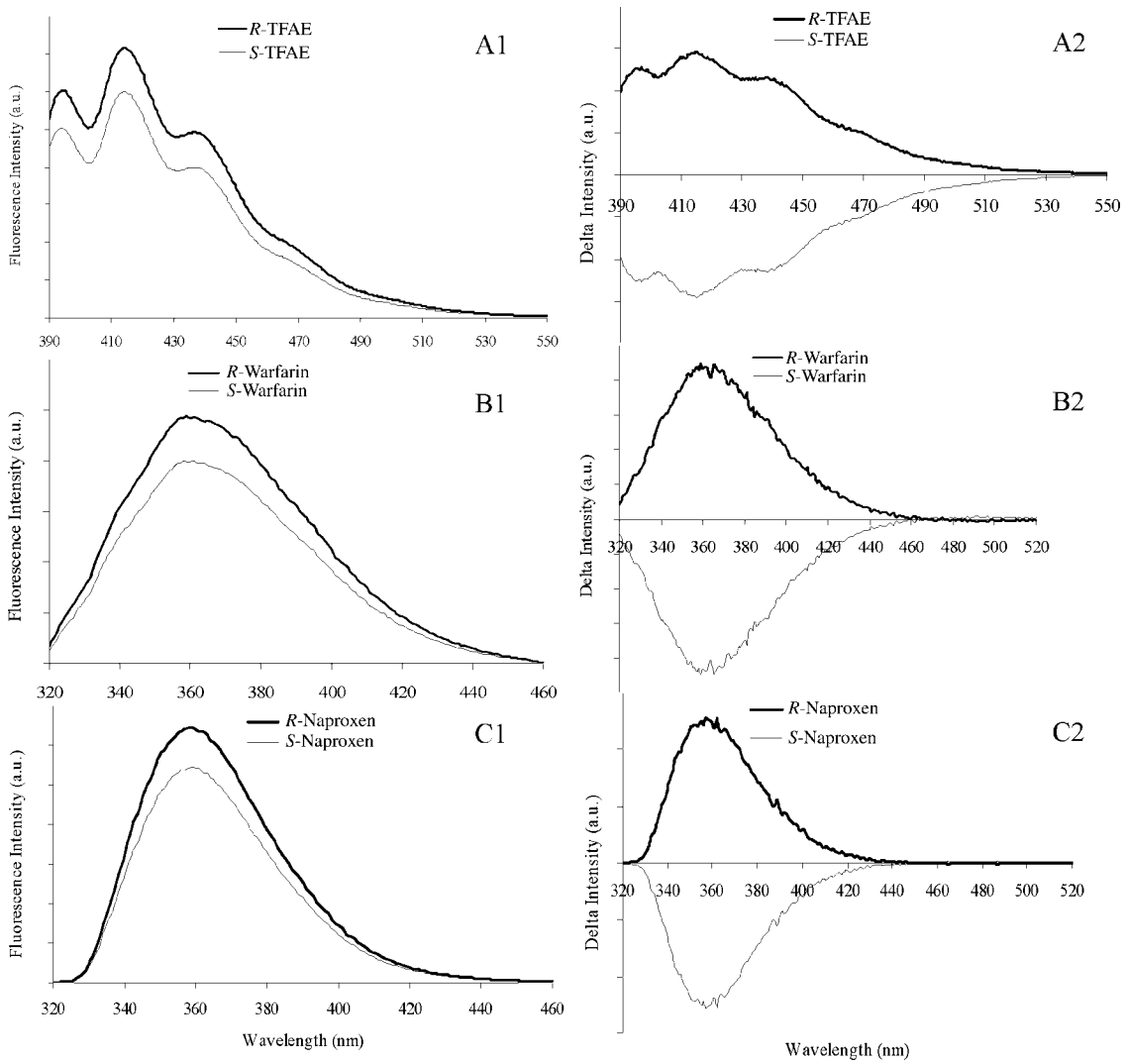

Fig. 6. Fluorescence emission and mean centered spectral plots of 10 μM *R*- and *S*- (**A**) TFAE, (**B**) warfarin, and (**C**) naproxen enantiomers in the presence of L-$AlaC_4NTf_2$ chiral ionic liquid. The emission spectra of TFAE, warfarin, and naproxen were monitored at excitation wavelength of 365, 306, and 280 nm, respectively, at room temperature.

Synthesis and Characterization of Novel Amino Acid Ester Chiral ILs (L- or D-$AlaC_4NO_3$, $AlaC_4BF_4$, $AlaC_4Lac$)

A similar anion metathesis reaction used for the synthesis of $AlaC_4NTf_2$ was employed for the synthesis of $AlaC_4NO_3$, $AlaC_4BF_4$, and $AlaC_4Lac$. However, the reaction was performed in methanol at a shorter time of 5 min (Scheme 2). The silver chloride precipitate was filtered off in each case affording good yields of the respective chiral ILs after removing methanol *in vacuo*.

Alanine *tert*-butyl ester nitrate ($AlaC_4NO_3$) crystallized to form a white solid at room temperature. $AlaC_4BF_4$ was obtained as a colorless greasy solid, whereas $AlaC_4Lac$

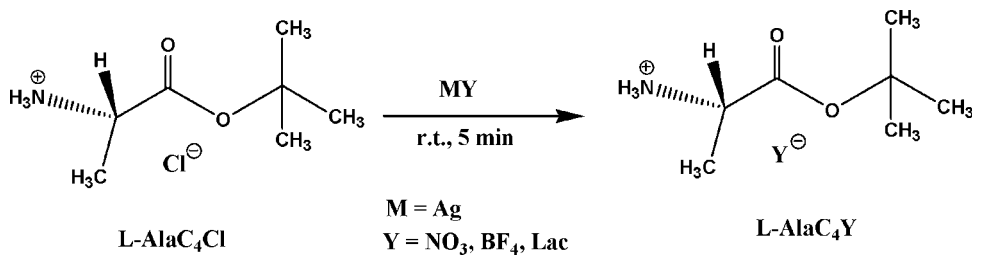

Scheme 2. Synthesis of $AlaC_4NO_3$, $AlaC_4BF_4$, $AlaC_4Lac$.

forms clear needle-like crystals at room temperature. The fact that solid ILs were obtained upon changing the anion demonstrates the tunability of the ILs synthesized in this study. By varying the anion or cation, different ILs with different properties is obtained for various applications. These results illustrate that bis (trifluoromethane) sulfonimide is probably a poorly coordinating anion with an alanine *tert* butyl ester cation. The poor crystal packing between the anion and cation results in ionic liquid. Del Po' polo describes this as frustrated packing between a bulky inorganic anion and cation leading to lower melting point ILs.[46] Their findings are in agreement with our results that bis (trifluoromethane) sulfonimide being the largest of the anions yielded an ionic liquid product that was liquid at room temperature. The other smaller anions such as nitrate afforded ILs that was solid at room temperature.

CONCLUSION

In summary, we have successfully synthesized a series of new chiral ILs in both enantiomeric forms using a simple metathesis reaction between the chiral chloride ester salt and the corresponding anion sources. Alanine *tert*-butyl ester bis (trifluoromethane) sulfonylimide is desirably liquid at room temperature and is thermally stable up to 263°C. It can therefore be used in high temperature reactions or as a chiral selector in gas chromatography. Furthermore, the ILs presented here has the same chiral configuration as the chloride salt precursors indicating that enantiomeric salts were obtained upon anion metathesis. Both enantiomeric forms of alanine *tert*-butyl ester bis (trifluoromethane) sulfonylimide ionic liquid demonstrated enantiomeric recognition of racemic Mosher's sodium salt. This is an advantage since the ionic liquid can serve both as solvent and chiral selector, alleviating the need for use of environmentally damaging solvents to dissolve the analyte. As an example, this compound could probably be used to provide chiral selectivity in the determination of enantiomeric composition of pharmaceutical products and in chiral separations. While the solid ILs could not be used for this purpose, we believe that their synthesis and characterization is a step towards exploring their potential applications.

ACKNOWLEDGMENTS

The authors acknowledge Dr. Gary Baker for helpful discussions.

LITERATURE CITED

1. Welton T. Room-temperature ionic liquids. Solvents for synthesis and catalysis. Chem Rev 1999;99:2071–2083.
2. Levillain J, Dubant G, Abrunhosa I, Gulea M, Gaumont AC. Synthesis and properties of thiazoline based ionic liquids derived from the chiral pool. Chem Commun 2003:2914–2915.
3. Tran CD, Lacerda SHP. Determination of binding constants of cyclodextrins in room-temperature ionic liquids by near-infrared spectrometry. Anal Chem 2002;74:5337–5341.
4. Tran CD, Lacerda SHP, Oliveira D. Absorption of water by room-temperature ionic liquids: effect of anions on concentration and state of water. Appl Spectrosc 2003;57:152–157.
5. Mele A, Tran CD, Lacerda SHP. The structure of a room-temperature ionic liquid with and without trace amounts of water: the role of C_H···O and C_H···F interactions in 1-*n*-butyl-3-methylimidazolium tetrafluoroborate. Angew Chem Int Ed Engl 2003;42:4364–4366.
6. Huddleston JG, Willauer HD, Swatloski RP, Rogers RD. Room temperature ionic liquids as novel media for 'clean' liquid–liquid extraction. Chem Commun 1998:1765–1766.
7. Dupont J, de Souza RF, Suarez PAZ. Ionic liquid (molten salt) phase organometallic catalysis. Chem Rev 2002;102:3667–3692.
8. Dietz ML, Dzielawa JA. Ion-exchange as a mode of cation transfer into room-temperature ionic liquids containing crown ethers: implications for the 'greenness' of ionic liquids as diluents in liquid–liquid extraction. Chem Commun 2001:2124–2125.
9. Compton DL, Laszlo JA. Direct electrochemical reduction of hemin in imidazolium-based ionic liquids. J Electroanal Chem 2002;520:71–78.
10. Quinn BM, Ding Z, Moulton R, Bard AJ. Novel electrochemical studies of ionic liquids. Langmuir 2002;18:1734–1742.
11. Kazarian SG, Briscoe BJ, Welton T. Combining ionic liquids and supercritical fluids: *in situ* ATR-IR study of CO_2 dissolved in two ionic liquids at high pressures. Chem Commun 2000:2047–2048.
12. Laszlo JA, Compton DL. α-Chymotrypsin catalysis in imidazolium-based ionic liquids. Biotechnol Bioeng 2001;75:181–186.
13. Mwongela SM, Numan A, Gill NL, Agbaria RA, Warner IM. Separation of achiral and chiral analytes using polymeric surfactants with ionic liquids as modifiers in micellar electrokinetic chromatography. Anal Chem 2003;75:6089–6096.
14. Armstrong DW, He L, Liu YS. Examination of ionic liquids and their interaction with molecules, when used as stationary phases in gas chromatography. Anal Chem 1999;71:3873–3876.
15. Anderson JL, Armstrong DW. High-stability ionic liquids. A new class of stationary phases for gas chromatography. Anal Chem 2003;75:4851–4858.
16. Wang Q, Baker GA, Baker SN, Colon LA. Surface confined ionic liquid as a stationary phase for HPLC. Analyst 2006;131:1000–1005.
17. Tran CD, Challa S, Franko M. Ionic liquids as an attractive alternative solvent for thermal lens measurements. Anal Chem 2005;77:7442–7447.
18. Baker GA, Baker SN, Padey S, Bright F. An analytical view of ionic liquids. Analyst 2005;130:800–808.
19. Baker GA, Baker SN, McClensky TM. Noncontact two-color luminescence thermometry based on intramolecular luminophore cyclization within an ionic liquid. Chem Commun 2003:2932–2933.
20. Caldwell J. Importance of stereospecific bioanalytical monitoring in drug development. J Chromatogr A 1996;719:3–13.
21. Fanali S. Enantioselective determination by capillary electrophoresis with cyclodextrins as chiral selectors. J Chromatogr A 2000;875:89–122.
22. Desiderio C, Fanali S. Chiral analysis by capillary electrophoresis using antibiotics as chiral selector. J Chromatogr A 1998;807:37–56.
23. Hyun MH, Jin JS, Lee W. Liquid chromatographic resolution of racemic amino acids and their derivatives on a new chiral stationary phase based on crown ether. J Chromatogr A 1998;822:155–161.
24. Fakayode SO, Williams AA, Busch MA, Busch KW, Warner IM. The use of poly(sodium *N*-undecanoyl-L-leucylvalinate), poly(sodium *N*-undecanoyl-L-leucinate) and poly(sodium *N*-undecanoyl-L-valinate) surfactants as chiral selectors for determination of enantiomeric composition of samples by multivariate regression modeling of fluorescence spectral data. J Fluoresc 2006;16:659–670.
25. Baudequin C, Baudoux J, Levillain J, Cahard D, Gaumont A-C, Plaquevent JC. Ionic liquids and chirality: opportunities and challenges. Tetrahedron: Asymmetry 2003;14:3081–3093.
26. Ding J, Armstrong W. Chiral ionic liquids as stationary phases in gas chromatography. Anal Chem 2004;76:6819–6822.
27. Tran CD, Oliveira D, Yu S. Chiral ionic liquid that functions as both solvent and chiral selector for the determination of enantiomeric compositions of pharmaceutical products. Anal Chem 2006;78:1349–1356.
28. Tran CD, Oliveira D. Fluorescence determination of enantiomeric composition of pharmaceuticals via use of ionic liquid that serves as both solvent and chiral selector. Anal Biochem 2006;356:51–58.

29. Earle MJ, McCormac PB, Seddon KR. Diels-Alder reactions in ionic liquids. Green Chem 1999;1:23–25.
30. Allen CR, Richard PL, Ward AJ, van de Water LGA, Masters AF, Maschmeyer T. Facile synthesis of ionic liquids possessing chiral carboxylates. Tetrahedron Lett 2006;47:7367–7370.
31. Wasserscheid P, Bősmann A, Bolm C. Synthesis and properties of ionic liquids derived from the 'chiral pool.' Chem Commun 2002:200–201.
32. Ishida Y, Miyauchi H, Saigo K. Design and synthesis of a novel imidazolium-based ionic liquid with planar chirality. Chem Commun 2002: 2240–2241.
33. Bao WL, Wang ZM, Li YX. Synthesis of chiral ionic liquids from natural amino acids. J Org Chem 2003;68:591–593.
34. Jodry JJ, Mikami K. New chiral imidazolium ionic liquids: 3D-network of hydrogen bonding. Tetrahedron Lett 2004;45:4429–4431.
35. Vo-Thanh G, Pegot B, Loupy A. Solvent-free microwave-assisted preparation of chiral ionic liquids from (−)-*N*-methylephedrine. Eur J Org Chem 2004:1112–1116.
36. Patrascu C, Sugisaki C, Mintogaud C, Marty JD, Génisson Y, Viguerie NL. New pyridinium chiral ionic liquids. Heterocycles 2004;63:2033–2041.
37. Ding J, Armstrong W. Chiral ionic liquids: synthesis and applications. Chirality 2005;17:281–292.
38. Tao G-H, He L, Sun N, Kou Y. New generation ionic liquids: cations derived from amino acids. Chem Commun 2005:3562–3564.
39. Ni B, Garre S, Headley AD. Design and synthesis of fused-ring chiral ionic liquids from amino acid derivatives. Tetrahedron Lett 2007;48: 1999–2002.
40. Ni B, Headley AD. Novel imidazolium chiral ionic liquids that contain a urea functionality. Tetrahedron Lett 2006;47:7331–7334.
41. Luo S-P, Xu D-Q, Yue H-D, Wang L-P, Yang W-L, Xu Z-H. Synthesis and properties of novel chiral-amine-functionalized ionic liquids. Tetrahedron: Asymmetry 2006;17:2028–2033.
42. Ding J, Desikan V, Han X, Xiao TL, Ding R, Jenks WS, Armstrong DW. Use of chiral ionic liquids as solvents for the enantioselective photoisomerization of dibenzobicyclo [2.2.2] octatrienes. Org Lett 2005;7:335–337.
43. Smith VK, Ndou TT, Warner IM. Spectroscopic study of the interaction of catechin with α-, β-, and γ-cyclodextrins. J Phys Chem 1994;98:8627–8631.
44. Dotsikas Y, Kontopanou E, Allagiannis C, Loukas YL. Interaction of 6-*p*-toluidinylnaphthalene-2-sulphonate with β-cyclodextrin. J Pharm Biomed Anal 2000;23:997–1003.
45. Macdonald SA, Hieftje GM. Use of shift reagents to determine enantiomers by near-infrared analysis. Appl Spectrosc 1996;50:1161–1164.
46. Del Po'polo MG, Voth GA. On the structure and dynamics of ionic liquids. J Phys Chem B 2004;108:1744–1752.

CHIRALITY 20:159–165 (2008)

Modulatory Effect of Chiral Nonsteroidal Anti-inflammatory Drugs on Apoptosis of Human Neutrophils

MAŁGORZATA ZIELIŃSKA-PRZYJEMSKA,[1]* FRANCISZEK K. GŁÓWKA,[2] AND JOANNA KLACZYŃSKA[1]
[1]*Department of Pharmaceutical Biochemistry, Poznań University of Medical Sciences, Poznań, Poland*
[2]*Department of Physical Pharmacy and Pharmacokinetics, Poznań University of Medical Sciences, Poznań, Poland*

ABSTRACT Polymorphonuclear neutrophils (PMNs) are short-lived leukocytes that die by apoptosis. Although PMNs are crucial in the defense against infection, they have been implicated in the pathogenesis of tissue injury observed in inflammatory diseases. The induction or prevention of PMN apoptosis is currently discussed as a key event in the control of inflammation. Caspase-3 activation is the first step in the execution phase of apoptosis. In the study, effect of racemic mixtures and enantiomers of 2-arylpropionic acid derivatives: ketoprofen, flurbiprofen (FBP), and (+)-*S*-naproxen and 2-arylbutyric acid: indobufen on apoptosis activation via caspase-3 and phosphatidylserine (PS) translocation (annexin-V binding) in human neutrophils in vitro has been investigated. Caspase-3 activation was detected by Western blotting, fluorometric assay of DEVD-AMC cleavage, and flow cytometry with carboxyfluorescein (FAM) labeled caspase inhibitor. PMNs were isolated and cultured up to 24 h. The chiral nonsteroidal anti-inflammatory drugs (NSAIDs) were found to modulate human PMN apoptosis in a dose- and time-dependent manner. The greater activation of caspase was found at 75–150 μg/ml concentration of racemates as well enantiomers, especially for FBP, whereas NSAIDs at smaller quantities (15 μg/ml) were inactive. At concentration of 75 μg/ml, NSAIDs increased the rate of PS externalization in PMA-stimulated and non-stimulated neutrophils. Additionally, no cytotoxic effect of the NSAIDs was observed at concentration up to 75 μg/ml that induce apoptosis. Regulation of caspase activity by NSAIDs may represent a potent target to trigger apoptosis and resolve inflammatory disorders. *Chirality 20:159–165, 2008.*

KEY WORDS: 2-arylpropionic acid derivatives; 2-arylbutyric acid; racemic mixtures; enantiomers; polymorphonuclear neutrophils; reactive oxygen species; PMN oxidative burst

INTRODUCTION

Polymorphonuclear neutrophils (PMNs) play a crucial role in host response to injury and infection. Upon activation, PMNs produce and release various mediators and enzymes as well as reactive oxygen species (ROS), which are some of the most toxic mediators, with the resultant development of inflammation. Microorganisms are equipped with an extensive defense system against toxic oxygen metabolites. However, under certain pathophysiological conditions, this defense system is insufficient to prevent oxidative damage to tissues or cells.[1] Injuries and inflammatory reactions can initiate and promote carcinogenesis because of the peroxidative activity of ROS, which are generated mainly by activated PMNs infiltrating the inflammation site. The oxidative lesions in the DNA of the nearby cells can cause mutagenic and/or carcinogenic changes.[2]

Under normal conditions, apoptosis is a crucial way of removing PMNs from the site of inflammation.[3,4] Activated PMNs alter their volume and shape and are then recognized by macrophages and undergo phagocytosis. Clearance of dead cells precludes release of noxious cellular contents, thus allowing for extensive cell death without eliciting tissue disruption or inflammation.[5] A common recognition signal for phagocytes is the loss of phospholipid asymmetry and attendant externalization of phosphatidylserine (PS) on the outer leaflet of the plasma membrane of apoptotic cells.[5] Neutrophil apoptosis is modulated by diversified factors, e.g. bacterial lipopolysaccharide or TNF-α, which can affect proteins engaged directly in cell death.[6] Caspases play a central role in apoptotic cell death by degradation of regulatory and structural proteins essential for cell survival. Activated nucleases and caspase-3 are considered to be important mediators of apoptosis.[7]

Recent reports have shown that nonsteroidal anti-inflammatory drugs (NSAIDs) can induce apoptosis.[8–10] NSAIDs are an integral part of therapy of rheumatoid arthritis (RA) and other inflammatory diseases.[11] An increasing number of NSAIDs has become available recently, most of which

*Correspondence to: M. Zielińska-Przyjemska, Department of Pharmaceutical Biochemistry, Poznań University of Medical Sciences, Święcickiego 4, 60-781 Poznań, Poland. E-mail: mzielin@amp.edu.pl
Received for publication 16 February 2007; Accepted 29 October 2007
DOI: 10.1002/chir.20516
Published online 11 December 2007 in Wiley InterScience (www.interscience.wiley.com).

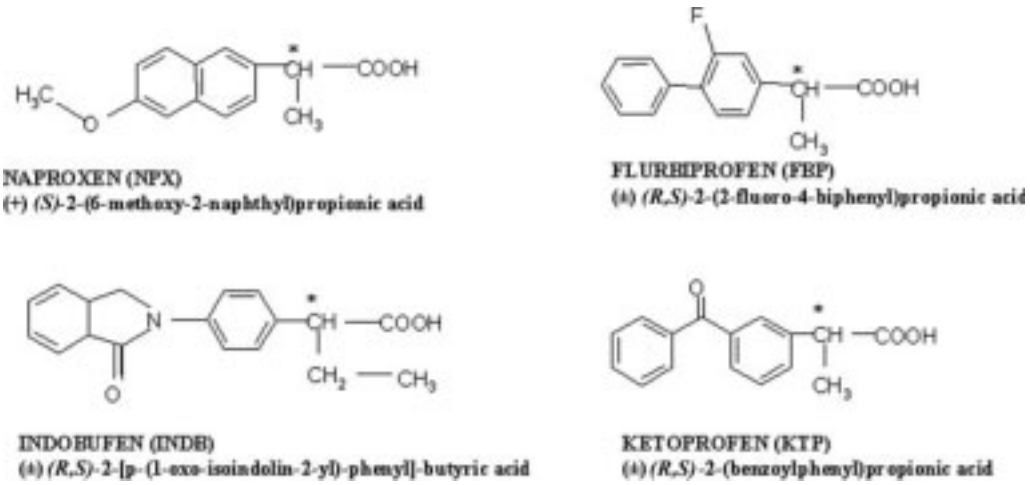

Fig. 1. Chemical structure of NSAID investigated.

are as effective as aspirin, but with lower adverse effects.[8] 2-Arylpropionic acid (2-APA) and 2-arylbutyric acid (2-ABA) derivatives possess an asymmetric α-carbon and occur as (+)-*S* and (−)-*R* enantiomers. In vivo, the (−)-*R*-enantiomer of some 2-APA derivatives undergoes a unindirectional bioinversion to the active (+)-*S*-enantiomer via the formation of their acyl CoA thioesters. The rate and extent of inversion varies from species to species, and it is significant for ibuprofen (IBP), fenoprofen, and benoxaprofen but is insignificant for flurbiprofen (FBP), indoprofen, and ketoprofen (KTP). Although their pharmacological activity, inhibition of cyclooxygenases-1 and -2 (COX-1 and COX-2), resides principally in the (+)-*S* enantiomer, they have been used in medical treatment as racemates, except for naproxen (NPX).[12,13] IBP and KTP are also marketed as the (+)-enantiomer formulations. However, published investigations indicate that the (−)-*R* enantiomers are not devoid of pharmacodynamic activity. It contributes to the analgesic activity of the racemic KTP.[14] Moreover, the (−)-*R* enantiomer of IBP and FBP may inhibit synthesis of β-amyloid related to Alzheimer's disease.[15]

Thus, the aim of the present study was the assessment of the influence of the racemic mixtures (*rac*-) and enantiomers of the 2-arylpropionic acid derivatives: KTP, FBP, (+)-*S*-NPX, and the 2-ABA:indobufen (INDB; Fig. 1) on caspase-3 activation and plasma membrane translocation of PS in human PMNs in vitro.

MATERIALS AND METHODS

Chemicals

NSAIDs [Fig. 1; *rac*-KTP and (+)-*S*-KTP (optical purity (o.p.) 99.0%; S:R was 99:1%], *rac*-FBP, and (+)-*S*-FBP (o.p. 98.0%), and (+)-*S*-NPX (o.p. 98%)) were purchased from Sigma Chemical Co. (St. Louis, MO). *rac*-INDB and (+)-*S*-INDB (o.p. 99.6%) were obtained from Pharmacia & Upjohn (Milan, Italy). Stock solutions of NSAIDs were prepared in dimethyl sulfoxide (DMSO) and diluted in phosphate buffered saline (PBS). The final concentration of DMSO was always 0.2% (v/v).

Density gradient medium for the neutrophil isolation, Gradisol G (dextran and uropoline mixture, d = 1.115 g/ml), was supplied by Aqua-Medica, Poland. DMSO, diphenylene iodonium (DPI), fetal bovine serum, L-glutamine, *n*-2-hydroxyethylpiperazyne-*N*′-2-ethanesulfonic acid (HEPES), penicillin, phorbol 12-myristate 13-acetate (PMA), RPMI 1640 medium, streptomycin, and trypan blue were provided by Sigma Chemical Co. Other reagents of the highest available grade were obtained from common chemical suppliers.

Isolation and Culture of Human Neutrophils

Peripheral venous blood from healthy volunteers, anticoagulated with heparin (10 U/ml blood), was layered on Gradisol G and centrifuged at 500*g* for 30 min. PMNs were collected and washed in PBS.[16] The population obtained consisted of ∼96% neutrophils. Freshly isolated PMNs (2×10^6 cells) were maintained in RPMI 1640 medium (supplemented with 10% heat-inactivated fetal bovine serum, 2 mM L-glutamine, 100 units/ml penicillin and 100 μg/ml streptomycin, and 5 mM HEPES) in 40-mm culture dishes. Cells were preincubated for 1 h with PBS alone (controls) or various concentrations of NSAIDs, and then incubated in the presence or absence of PMA (200 nM), the protein kinase C activator, or DPI (10 μM), an inhibitor of the NADPH oxidase, at 37°C in a humidified atmosphere containing 5% CO_2. Three culture dishes were used for each experiment. After 2 or 24 h of incubation with NSAIDs, a 1% trypsin solution was used to detach adherent cells.

Western Blotting

The cleavage of procaspase-3 was determined by Western blotting. Whole cell lysates were obtained by extracting 2×10^6 PMNs in RIPA buffer. Sixty micrograms of protein was resuspended in sample buffer and separated on 12% Tris-glycine gel using SDS-polyacrylamide gel electrophoresis (SDS-PAGE). Proteins were transferred from the gel to nitrocellulose membrane (0.2 μm; Sigma), which was blocked with 5% milk in Tris buffered saline/

Tween. The immunodetection was performed with 1:1000 diluted polyclonal rabbit antihuman caspase-3 antibodies (Santa Cruz Biotechnology), which recognize both inactive procaspase-3 and its cleavage product. Thereafter, the blots were incubated for 1 h with goat anti-rabbit IgG-HRP conjugated (HRP-horseradish peroxide) antibody (Santa Cruz Biotechnology). The membranes were reblotted with anti-actin HRP-conjugated antibodies (Santa Cruz Biotechnology) to ensure equal protein loading of the lanes. Bands were revealed using Lumi-Light western Blotting kit (Roche) and Hyperfilm ECL Amersham (Piscataway, NJ).

Determination of Ac-DEVD-AMC Cleavage

Caspase-3 activity was measured using a caspase-3 fluorogenic substrate Ac-DEVD-AMC Caspase-3 assay kit (BD Bioscience Pharmingen, San Diego, CA). Briefly, cultured cells were washed with ice-cold PBS (pH 7.4) and lysed in buffer provided by the kit [10 mM Tris-HCl; 10 mM NaH_2PO_4/Na_2HPO_4 (pH 7.5); 130 mM NaCl; 1% Triton®-X-100; 10 mM $NaPP_i$ (sodium pyrophosphate)] for 30 min on ice, and protein concentration was determined according to the method of Lowry et al.[17] Cell lysates (containing ~100 μg of protein) and substrate Ac-DEVD-AMC (20 μM) were combined in a standard reaction buffer (20 mM HEPES pH 7.5; 10% glycerol; 2 mM DTT). After 1-h incubation at 37°C, fluorescence of AMC liberated from Ac-DEVD-AMC was determined in a Hitachi F-2500 spectrofluorimeter (λ_{ex} = 388 nm, λ_{em} = 450 nm). The activity of caspase-3 was expressed in AMC fluorescence units. The competitive inhibitor DEVD-CHO completely blocked the activity of caspase-3, which demonstrated the specificity of the assay. Blanks were measured in the absence of cell lysate to determine background fluorescence.

Flow Cytometry Detection for Caspase-3 Activity

Detection of active caspase-3 in live cell cultures was performed using an ApoFluor® carboxyfluorescein (FAM) caspase detection kit (ICN Biomedicals). The kit detects active caspases in living cells through the use of a FAM-labeled DEVD fluoromethyl ketone (FMK) caspase inhibitor, which irreversibly binds to active caspase-3.[18] The inhibitor is cell-permeable and noncytotoxic. FAM-DEVD-FMK binds to the other caspases participating in apoptosis with lesser affinity: caspase-8 > caspase-7 > caspase-10 > caspase-6 in the order of decreasing binding affinity.[19] The kit was used as recommended by the manufacturer. Briefly, 10 μl of 30× working dilution FAM-Peptide-FMK was added to 300 μl of cell culture medium (2×10^6 cell) after 2 h or 24 h of incubation with NSAIDs. Cells were incubated for 1 h at 37°C under 5% CO_2, protected from light. Then the cells were centrifuged and washed twice with 1× working dilution wash buffer. The resuspended cell pellets in 400 μl of wash buffer were then labeled with 2 μl PI for 15 min at RT. The green (caspase-positive cells) and red (PI) fluorescent signal of individual cells was determined by flow cytometry (Cytoron Absolute, Ortho) at 488-nm excitation wavelength and standard setting of the emission filters.

Annexin-V Staining of Externalized PS

PS exposure was determined by flow cytometric detection of annexin-V using the protocol outlined in Annexin-V-FLUOS Staining Kit (Roche Diagnostics GmbH, Germany). Neutrophils were treated with or without PMA (200 nM) and incubated with NSAIDs (75 μg/ml). After 4 h, cells were stained with 2 μl Annexin-V-Fluos labeling reagent and 2 μl propidium iodide for 15 min in the dark. Fluorescence of cell surface- (AV) or DNA-bound (PI) markers was analyzed with flow cytometry (Cytoron Absolute, Ortho) at 488 nm (excitation).

MTT Assay for Cell Viability

Cell viability was determined with the Cell Proliferation Kit I [3-[4,5-dimethylthiazol-2-yl]-2,5-diphenyltetrazolium bromide (MTT); Roche Diagnostics GmbH, Germany]. This colorimetric assay is based on the absorbance of the formazan dye which is produced only in live cells by reductive cleavage of the tetrazolium salt MTT.[20] PMNs (1×10^6 cells/well) were treated with different concentrations of each NSAID (up to a final concentration of 150 μg/ml) for 24 h at 37°C, together with untreated control samples. Cells were subsequently incubated in a 96-well plate with MTT solution for a further 4 h. The water-insoluble formazan dye was solubilized overnight at 37°C before measurement of absorbance using an ELISA reader at 570 nm, with a reference wavelength of 690 nm.

Statistical Analysis

Differences between the means of treatment were compared after analysis of variance by the Student *t*-test. Differences were considered significant if $P \leq 0.05$.

RESULTS AND DISCUSSION

NSAIDs are widely used in the treatment of chronic inflammation.[11] In addition, they show promise for the prevention and therapy of cancer.[21–23] The mechanism for this response is not clear, but it might result from accumu-

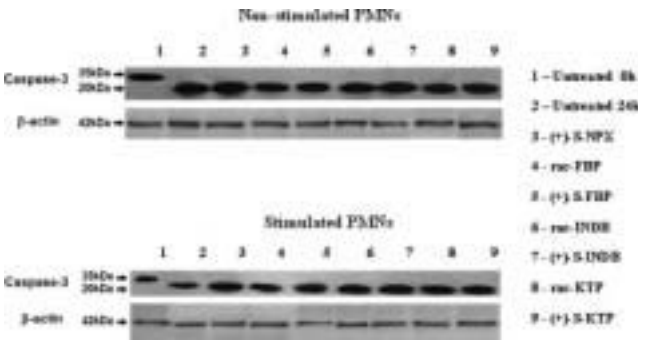

Fig. 2. Western blot analysis of procaspase-3 cleavage in PMNs. PMNs were cultured 24 h in the absence (nonstimulated PMNs) or in the presence of PMA (200 nM) (stimulated PMNs) and NSAIDs (75 μg/ml). Then whole cell lysates were subjected to SDS-PAGE, and Western blot was performed with a caspase-3 polyclonal antibody. In PMA-stimulated and nonstimulated PMNs incubated with NSAIDs, procaspase-3 was cleaved, and a 20 kDa cleavage product appeared. β-Actin bands were as the internal control. Results are representative of three independent experiments.

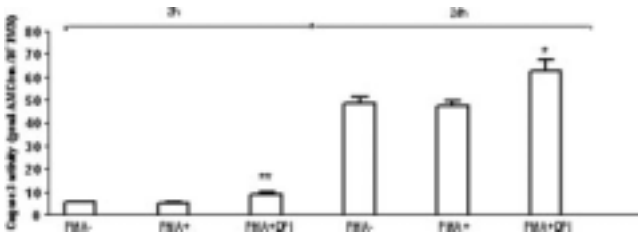

Fig. 3. Caspase-3 activity in neutrophils from healthy people undergoing spontaneous and PMA-stimulated or PMA-stimulated apoptosis in the presence of DPI (10 μmol/L), after 2 and 24 h in culture, as measured by cleavage of specific fluorogenic substrate DEVD-AMC. Results are expressed as mean ± SE of five independent experiments. Significantly different from the unstimulated control: $*P \leq 0.05$; $**P \leq 0.01$.

lation of the substrate arachidonic acid, the absence of prostaglandin product, or diversion of the substrate into another pathway.[24]

The apoptosis of neutrophils is one existing mechanisms known to limit inflammatory reactions. Delayed recognition and removal of activated neutrophils which contain aggressive proinflammatory mediators is responsible for the prolongation of the inflammation of joints.[3,5] Therefore, controlled cell death prevents damage to healthy tissues and is necessary for the resolution of inflammation.[25] It is widely emphasized that neutrophils contribute to inflammatory diseases[25] and they are significant in the etiology of malignancy, RA, reperfusion injury, and arteriosclerosis.[2]

The aim of this study was to estimate apoptosis of neutrophils treated with the racemic mixtures and enantiomers of KTP, FBP, INDB, and (+)-*S*-NPX. We studied caspase-3 processing during spontaneous and PMA-stimulated apoptosis by Western blotting. Upon PMA activation, nonmitochondrial oxygen uptake is initiated by the PMNs, resulting in the production of ROS. This process, known as the oxidative burst, is the result of the assembly of the multienzyme NADPH-oxidase system that promotes the one-electron reduction of oxygen to superoxide anion.[2] Caspase-3 is expressed in normal PMNs as a 32-kDa inactive precursor (Fig. 2, lane 1), which is proteolytically cleaved into an active form on mediation of apoptosis.[26] This cleavage generates a large (17–20 kDa) and a small (3–12 kDa) subunit. Neutrophils aged for 24 h showed loss of caspase-3 precursor and a band of an ~20-kDa cleavage product (Fig. 2, lane 2); in contrast, the amount of β-actin remained constant. The expression of the 20-kDa active form was substantially increased in the presence of NSAIDs when compared with PMA-stimulated control cells after 24 h (Fig. 2, lanes 3–9).

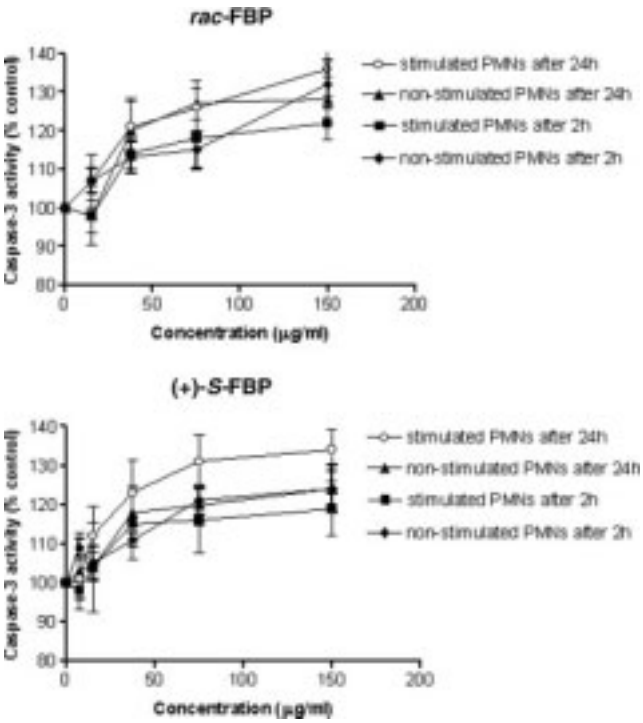

Fig. 4. Caspase-3 activity in neutrophils from healthy people undergoing spontaneous and PMA-stimulated apoptosis after 2 and 24 h of racemic mixture and (+)-*S*-enantiomer of flurbiprofen treatment, as measured by cleavage of specific fluorogenic substrate DEVD-AMC. Data are presented as mean ± SE ($n = 5$).

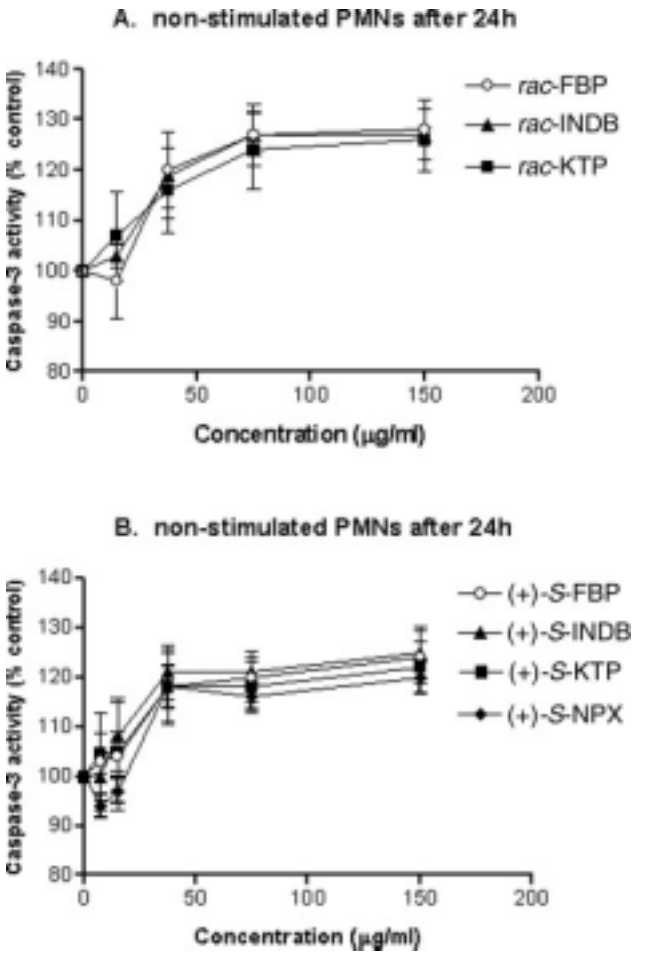

Fig. 5. Caspase-3 activity in nonstimulated PMNs after 24 h exposure to racemic mixture (**A**) and (+)-*S*-enantiomer (**B**) of NSAIDs.

To confirm this result, the enzymatic activity of caspase-3 was measured in the cell lysates obtained from nonstimulated control cells as well as from PMA-stimulated cells. Using a fluorogenic substrate bearing the caspase-3-specific cleavage site DEVD,[27] caspase activity was detected as early as 2 and 24 h of culture in nonstimulated control cells. Treatment with PMA, either for 2 or 24 h, did not significantly change the caspase-3 activity in comparison with the nonstimulated cells (Fig. 3), suggesting that the products of neutrophil oxidative burst prevented caspase-3 from acting. This observation corroborates the finding of Fadeel et al.,[28] who compared the apoptotic reactions in resting and stimulated PMNs and found that under stimulation of neutrophils and subsequent NADPH oxidase activation and resulting ROS production, there was no apoptosis. Importance of NADPH oxidase activity in the caspase-3 regulation was also found in a separate set of experiments, where PMNs were incubated with DPI (NADPH oxidase inhibitor) prior to phorbol stimulation (Fig. 3).

Fadeel et al.[28] concluded that elevated concentrations of ROS suppress caspase-3 action in neutrophils. Similar suggestions emerge from the work of Arroyo et al.,[29] who showed that, in neutrophils present in inflamed tissues, two concurrent pathways may appear: ROS-mediated inactivation of caspase-3 and delay of apoptosis and, in the presence of NADPH oxidase inhibitors/ROS scavengers, caspase-3 activation occurs and leads to apoptosis. This may be the case in our experiments, where in the isolated human PMNs pretreated with FBP, in the concentration range of 37.5–150 μg/ml, there was a time- and dose-dependent induction of caspase activity (Fig. 4). The highest activity of caspase-3 was observed in stimulated PMNs cultured for 24 h.

The NSAID racemic mixtures and enantiomers at concentrations 37.5–150 μg/ml also induced cell death in comparison to control samples. FBP was the most efficacious, but the differences between the drugs are not statistically significant. Figures 5 and 6 present caspase-3 activity as a function of dose in nonstimulated and stimulated cells pretreated with NSAIDs for 24 h.

A significant increase of caspase-3 activity was observed at higher concentrations of NSAIDs (75–150 μg/ml) (Fig. 7). This shows that the modulatory role of the NSAIDs on the processing of the procaspase corresponded to the enzymatic activity of caspase-3 in the cell lysates.

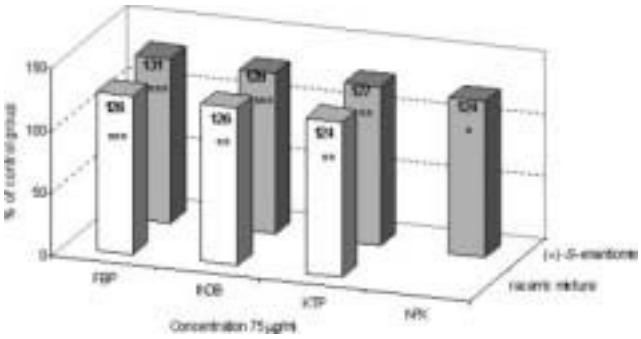

Fig. 7. Influence of NSAIDs at concentration of 75 μg/ml on caspase-3 activity in stimulated PMNs after 24-h exposure. Data are mean ± SE from five independent experiments. Significantly different from control: $^{*}P < 0.05$; $^{**}P < 0.01$; $^{***}P < 0.001$; unpaired t test.

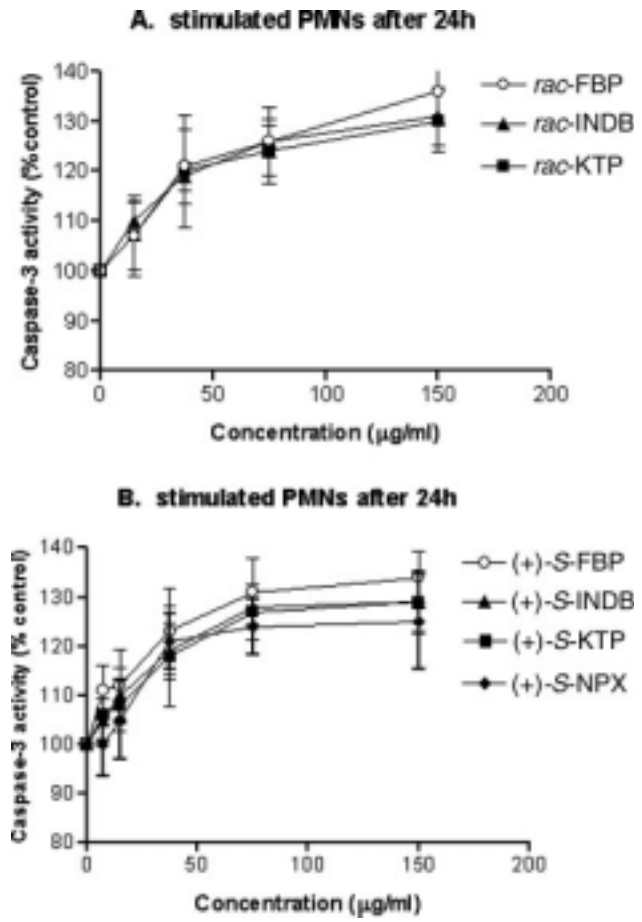

Fig. 6. Caspase-3 activity in stimulated PMNs after 24 h exposure to racemic mixture (**A**) and (+)-*S*-enantiomer (**B**) of NSAIDs.

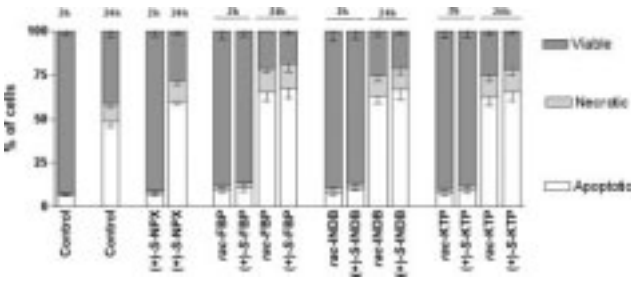

Fig. 8. Simultaneous detection of caspase-3 activation and nonviable cells in cultured human neutrophils after 2- and 24-h incubation with 75 μg/ml of NSAIDs. Detection of active caspase-3 was performed in live cell cultures using a FAM-labeled DEVD fluoromethyl ketone (FMK) caspase inhibitor, which irreversibly binds to active caspase-3. The percentage of neutrophils undergoing primary apoptosis in the presence of NSAIDs is significantly increased at 24 h compared to control. $^{a}P < 0.05$. Values are means ± SE of three experiments.

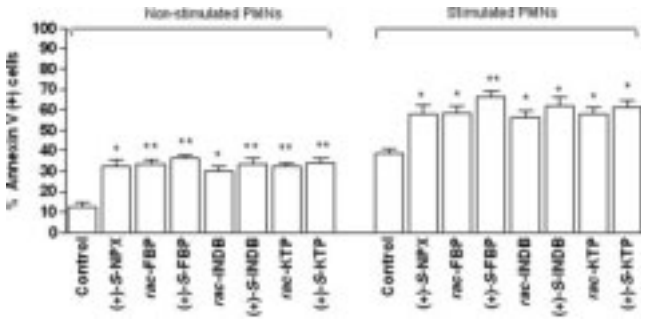

Fig. 9. Phosphatidylserine externalisation measured by annexin-V binding assay in PMA-stimulated and nonstimulated neutrophils after 4-h incubation with 75 μg/ml of NSAIDs. Values are means ± SE of three experiments. Differences statistically significant between control and treated cells: $*P < 0.05$; $**P < 0.01$.

The presence of caspase-3 substrate-specific fluorescence in NSAID-treated samples, where the PMA-induced oxidative burst leads to the indirect conclusion that these compounds interfere with NADPH oxidase and/or ROS and promote apoptosis. This result agrees with the suggestions of Arroyo et al.[29] and Wilkie et al.[30] on the oxidative inhibition of caspase-3 activity in stimulated PMNs.

Next, to visualize of active caspase-3 directly in living cells, a FAM-labeled peptide caspase inhibitor (FAM-DEVD-FMK) was employed (see Materials and Methods). Caspase-3-positive neutrophils were detected after 2 and 24 h culture of PMNs with NSAIDs at a concentration of 75 μg/ml. PMNs cultured for 2 and 24 h without stimulation undergo spontaneous apoptosis, 6.62% ± 0.32% and 48.50% ± 3.30%, at 2 and 24 h, respectively (Fig. 8). After 24 h treatment of PMNs with NSAIDs, apoptosis was significantly increased when compared with control incubations. In the presence of both the racemate and enantiomers of FBP, apoptosis was maximal (65.30% ± 5.08% and 67.42% ± 5.69%, respectively) (Fig. 8).

Caspase activation was compared with a relatively early apoptosis marker, plasma membrane translocation of PS as monitored by annexin-V binding. Freshly isolated PMNs contained 95.8% ± 2.1% live cells, which were negative for both annexin-V and PI (data not shown). However, PS translocation was evident at 4 h and was markedly accelerated after PMA-stimulation compared with untreated neutrophils (untreated cells:12.65 ± 2.20; PMA-treated cells: 38.50 ± 2.40; mean ± SE; $n = 3$; Fig. 9), demonstrating that changes similar to those observed in apoptotic cells are taking place. Increased annexin-V binding on the cell's surface was observed after 4-h treatment with NSAIDs (75 μg/ml) in both stimulated and nonstimulated neutrophils (Fig. 9).

The results allow us to state that both the racemates and enantiomers of the NSAIDs examined induce apoptosis of polymorphonuclear leukocytes. It might be supposed that the restoration of balance in tissues through stimulation of apoptosis at neutrophils could be a new, effective strategy of treatment of chronic inflammatory diseases. However, the highest concentration of NSAIDs used, i.e. 150 μg/ml, turned out to be toxic for cells, what corresponds to the data of Raz,[31] who observed an inhibition of cell proliferation and/or a stimulation of apoptosis/necrosis by NSAIDs at concentrations 10–250 times higher than those needed to inhibit COX. Hence some investigators suggest that the antiproliferative effects of NSAIDs are independent of inhibition of COX inhibition. The results from cell culture studies confirm the necessity of using very high, often toxic concentrations of NSAIDs (piroxicam at 900 μM, indomethacin at 300 μM, NPX at 200 μM, aspirin at 1 mM) with the aim of inhibiting neoplastic transformation. As proapoptotic effects are independent of COX inhibition, they are seen in both cells that contain COX enzymes and cells that are devoid of them.[31] The viability of PMNs pretreated for 24 h with the examined NSAIDs in concentration of 37.5–75 μg/ml exceeded 90%, indicating that none of the compounds displayed any toxicity up to 75 μg/ml (Table 1).

In the present research we did not record statistically significant differences between the effect of racemates and their enantiomers. In view of the trend to introduce pure enantiomers instead of racemic drugs, it is important to carry out studies leading to the accurate explanation of mechanisms of NSAID action. Hence, the present observations are to be treated as initial results, which must be confirmed with respect to the (−)-*R*-enantiomers in particular.

TABLE 1. Cytotoxicity of NSAIDs measured by the MTT incorporation to polymorphonuclear neutrophils [a,b]

NSAID concentration (μg/ml)	Incorporated MTT (% of control)						
	(+)-*S*-NPX	*rac*-FBP	(+)-*S*-FBP	*rac*-INDB	(+)*S*-INDB	*rac*-KTP	(+)-*S*-KTP
150.0	66.2 ± 6.1*	66.1 ± 5.9*	70.9 ± 2.9*	78.0 ± 7.4**	79.9 ± 7.3**	65.3 ± 9.6**	84.7 ± 9.6
75.0	85.2 ± 10.3	79.7 ± 4.7**	80.7 ± 2.7*	91.3 ± 10.2	92.4 ± 14.7	84.7 ± 4.9**	90.7 ± 7.0
37.5	94.5 ± 9.5	90.1 ± 8.6	94.0 ± 4.9	92.3 ± 4.9	93.7 ± 4.9	91.7 ± 8.6	95.8 ± 4.9
15.0	101.0 ± 12.1	99.0 ± 4.3	100.0 ± 7.0	101.0 ± 9.6	98.8 ± 7.0	97.0 ± 2.7	98.1 ± 3.0

[a]Results are expressed as mean ± SE of percent control for $n = 3$ independent experiments. More then 90% viable cells were considered to be unaffected by NSAIDs. 80–90% as modestly affected, and values of less than 80% viable cells were ascribed to cytotoxic effect of the compounds. Absorbance value of control PMNs was 0.119.
[b]Significantly different from the untreated control.
$*P < 0.01$; $**P < 0.05$.

ACKNOWLEDGMENTS

Authors thank Michał Łuczak from Department of Biochemistry and Molecular Biology, Poznań University of Medical Sciences, for his assistance in Western blotting studies.

LITERATURE CITED

1. Marshall JC, Malam Z, Jia S. Modulating neutrophil apoptosis. Novartis Found Symp 2007;280:53–66.
2. Babior BM. Phagocytes and oxidative stress. Am J Med 2000;109:33–44.
3. Rossi AG, Hallett JM, Sawatzky DA, Teixeira MM, Haslett C. Modulation of granulocyte apoptosis can influence the resolution of inflammation. Biochem Soc Trans. 2007;35:288–291.
4. Hofman P. Molecular regulation of neutrophil apoptosis and potential targets for therapeutic strategy against the inflammatory process. Curr Drug Targets Inflamm Allergy 2004;3:1–9.
5. Maianski NA, Maianski AN, Kuijpers TW, Roos D. Apoptosis of neutrophils. Acta Haematol 2004;111:56–66.
6. Akgul C, Moulding DA, Edwards SW. Molecular control of neutrophil apoptosis. FEBS Lett 2001;487:318–322.
7. Vaughan AT, Betti CJ, Villalobos MJ. Surviving apoptosis. Apoptosis 2002;7:173–177.
8. Grodzicky T, Elkon KB. Apoptosis in rheumatic disease. Am J Med 2000;108:73–82.
9. Adachi M, Sakamoto H, Kawamura R, Wang W, Imai K, Shinomura Y. Nonsteroidal anti-inflammatory drugs and oxidative stress in cancer cells. Histol Histopathol 2007;22:437–442.
10. Swierkot J, Międzybrodzki R, Szymaniec S, Szechinski J. Activation-dependent apoptosis of peripheral blood mononuclear cells from patients with rheumatoid arthritis treated with methotrexate. Ann Rheum Dis 2004;63:599–600.
11. Harris RC, Breyer MD. Update on cyclooxygenase-2 inhibitors. Clin J Am Soc Nephrol 2006;1:236–245.
12. Jamali F. Research methodology in NSAID monitoring: plasma concentrations of chiral drugs. J Rheumatol 1988;15:71–74.
13. Hutt AJ, Caldwell J. The metabolic chiral inversion of 2-arylprpionic acids: a novel route with pharmacological consequences. J Pharm Pharmacol 1983;35:693–704.
14. Cooper SA, Reynolds DC, Reynolds B, Hersh EV. Analgesic efficacy and safety of (*R*)-ketoprofen in postoperative dental pain. J Clin Pharmacol 1998;38:11S–18S.
15. Morihara T, Chu T, Ubeda O, Beech W, Cole GM. Selective inhibition of Abeta42 production by NSAID *R*-enantiomers. J Neurochem 2002;83:1009–1012.
16. Ferrante H, Thong YH. A rapid one-step procedure for purification of mononuclear and polymorphonuclear leukocytes from human blood using a modification of the Hypaque-Ficoll technique. J Immunol Methods 1978;24:389–393.
17. Lowry OH, Rosenbrough NJ, Farr AL, Randall RJ. Protein measurement with the Folin phenol reagent. J Biol Chem 1951;193:265–275.
18. Amstad PA, Johnson GL, Lee BW, Dhawan S. An in situ marker for the detection of activated caspases. Biotechnol Lab 2000;18:52–56.
19. Carcia-Calvo ME, Peterson B, Leiting R, Nicholson D. Thornberry N. Inhibition of human caspases by peptide-based and macromolecular inhibitors. J Biol Chem 1998;273:32608–32613.
20. Mosman T. Rapid colorimetric assay for cellular growth and cytotoxicity assay. J Immunol Methods 1983;65:55–63.
21. Fratelli M, Minto M, Crespi A, Erba E, Vandenabeele P, Del Soldato P, Ghezzi P. Inhibition of nuclear factor-κB by a nitro-derivative of flurbiprofen: a possible mechanism for anti-inflammatory and antiproliferative effect. Antioxid Redox Signal 2003;5:229–235.
22. Dempke W, Rie C, Grothey A, Schmoll HJ. Cyclooxygenase-2: a novel target for cancer chemiotherapy? J Cancer Res Clin Oncol 2001; 127:411–417.
23. Chan TA. Nonsteroidal anti-inflammatory drugs, apoptosis, and colon-cancer chemoprevention. Lancet Oncol 2002;3:166–174.
24. Cao Y, Pearman AT, Zimmerman GA, McIntyre TM, Prescott SM. Intracellular unestrified arachidonic acid signals apoptosis. Proc Natl Acad Sci USA 2000;97:11280–11285.
25. Kabayashi SD, Voyuich JM, Deleo FR. Regulations of the neutrophil-mediated inflammatory response to infection. Microbes Infect 2003; 5:1337–1344.
26. Yamashita K, Takahashi A, Kobayashi S, Hirata H, Mesner PW Jr, Kaufmann SH, Yonehara S, Yamamoto K, Uchiyama T, Sasada M. Caspases mediate tumor nectrosis factor-α-induced neutrophil apoptosis and downregulation of reactive oxygen production. Blood 1999;93: 674–685.
27. Nicholson DW, Ali A, Thornberry NA, Vaillancourt JP, Ding CK, Gallant M, Gareau Y, Griffin PR, Labelle M, Lazebnik YA, Munday NA, Raju SM, Smulson ME, Yamin TT, Yu VL, Miller DK. Identification and inhibition of the ICE/CED-3 protease necessary for mammalian apoptosis. Nature 1995;376:37–43.
28. Fadeel B, Ahlin A, Henter JI, Orrenius S, Hampton MB. Involvement of caspases in neutrophil apoptosis: regulation by reactive oxygen species. Blood 1998;92:4808–4818.
29. Arroyo A, Modriansky M, Serinkan FB, Bello RI, Matsura T, Jiang J, Tyurin VA, Tyurina YY, Fadeel B, Kagan VE. NADPH-oxidase-dependent oxidation and externalization of phosphatidylserine during apoptosis in Me_2SO-differentiated HL-60 cells. J Biol Chem 2002;277: 49965–49975.
30. Wilkie RP, Vissers MC, Dragunow M, Hampton MB. A functional NADPH oxidase prevents caspase involvement in the clearance of phagocytic neutrophils. Infect Immun 2007;75:3256–3263.
31. Raz A. Is inhibition of cyclooxygenase required for the anti-tumorigenic effects of nonsteroidal, anti-inflammatory drugs (NSAIDs)? In vitro versus in vivo results and the relevance for the prevention and treatment of cancer. Biochem Pharmacol 2002;63:343–347.